

Université de Montréal

**Reconsidérer les interactions entre l'écoulement, le  
transport de sédiments en charge de fond et la  
morphologie en rivière à lit de graviers :  
approches, échelles et analyses**

par  
Geneviève Marquis

Département de géographie  
Faculté des arts et sciences

Thèse présentée à la Faculté des études supérieures et postdoctorales  
en vue de l'obtention du grade de Philosophiæ Doctor (Ph. D.)  
en géographie

Août 2012

© Geneviève Marquis, 2012



Université de Montréal  
Faculté des études supérieures et postdoctorales

Cette thèse intitulée :

Reconsidérer les interactions entre l'écoulement, le transport de sédiments en charge de fond et la morphologie en rivière à lit de graviers : approches, échelles et analyses

Présentée par :  
Geneviève Marquis

a été évaluée par un jury composé des personnes suivantes :

François Courchesne, président-rapporteur  
André G. Roy, directeur de recherche  
Pascale Biron, membre du jury  
Lynne Frostick, examinateur externe  
Alain Vincent, représentant du doyen de la FES



## RÉSUMÉ

---

L'objectif ultime en géomorphologie fluviale est d'expliquer les formes des cours d'eau et leur évolution temporelle et spatiale. La multiplication des études nous a mené à la réalisation que les systèmes géomorphologiques sont complexes. Les formes observées sont plus que la somme des processus individuels qui les régissent en raison d'interactions et de rétroactions non-linéaires à de multiples échelles spatiales et temporelles. Dans ce contexte, le but général de la thèse est de proposer et de tester de nouvelles avenues de recherche afin de mieux appréhender la complexité des dynamiques fluviales en utilisant des approches méthodologiques et analytiques mettant l'accent sur les interactions entre l'écoulement, le transport de sédiments en charge fond et la morphologie du lit en rivière graveleuse. Cette orientation découle du constat que les paradigmes actuels en géomorphologie fluviale n'arrivent pas à expliquer adéquatement la variabilité naturelle du transport en charge de fond ainsi que des formes du lit qui en résultent. Cinq pistes de réflexion sont développées sous forme d'articles basés sur des études de cas :

1. L'intégration des échelles de variation de l'écoulement permet d'insérer la notion de structures turbulentes dans des pulsations de plus grande échelle et d'améliorer la compréhension de la variabilité du transport de sédiments.
2. La quantification des taux de changement de l'écoulement (accélération /décélération) au cours d'une crue permet d'expliquer la variabilité des flux de transport en charge fond autant que la magnitude de l'écoulement.
3. L'utilisation de techniques de mesures complémentaires révèle une nouvelle dynamique du lit des rivières graveleuses, la dilatation et la contraction du lit suite à une crue.
4. La remise en cause du fait généralement accepté que le transport en charge de fond est corrélé positivement à l'intensité des modifications morphologiques en raison d'un problème associé aux échelles différentes des processus en cause.
5. L'approche systémique des dynamiques fluviales par l'utilisation d'analyses multivariées permet d'appréhender la complexité des dynamiques de rétroactions linéaires et non-linéaires dans l'évolution d'un chenal et d'illustrer l'importance de l'historique récent des changements géomorphologiques en réponse aux crues.

Cette thèse se veut une avancée conceptuelle issue d'une profonde réflexion sur les approches classiques que l'on utilise en géomorphologie fluviale depuis plusieurs décennies. Elle est basée sur un jeu de données unique récolté lors du suivi intensif de 21 événements de crue dans un petit cours d'eau à lit de graviers, le ruisseau Béard (Québec). Le protocole expérimental axé sur la simultanéité des mesures de l'écoulement, de la morphologie du lit et du transport de sédiments en charge de fond a permis de centrer la recherche directement sur les interactions entre les processus plutôt que sur les processus individuels, une approche rarement utilisée en géomorphologie fluviale. Chacun des chapitres illustre un nouveau concept ou une nouvelle approche permettant de résoudre certaines des impasses rencontrées actuellement en géomorphologie fluviale. Ces travaux ont des implications importantes pour la compréhension de la dynamique des lits de rivières et des habitats fluviaux et servent de point de départ pour de nouveaux développements.

**Mots-clés :** Géomorphologie fluviale, Échelles, Rivières à lit de graviers, Écoulement, Crues, Transport de sédiments en charge de fond, Formes du lit

## ABSTRACT

---

The overarching objective in fluvial geomorphology is to explain river morphology and its temporal and spatial evolution. The multiplication of studies led to the realization that geomorphic systems are complex and difficult to understand. The observed river morphology is more than the sum of the individual processes which govern them because of the superimposition of process interactions and non-linear feedback loops at multiple scales. In this context, the goal of this thesis is to explore new avenues of research in order to comprehend more accurately the complexity of gravel-bed river dynamics by using methodological and analytical approaches focusing on the interactions between the flow, transport of sediments as bedload and the bed morphology. This orientation of the thesis is in line with the fact that current paradigms in fluvial geomorphology have not succeeded in explaining adequately the natural variability of the sediment transport and its consequences on the river bedforms. Five avenues are developed in the form of articles based on case studies:

1. The study of the scales of variation of the flow allows us to integrate the turbulent flow structures into flow pulsations at larger scales and to potentially improve our understanding comprehension of bedload sediment transport variability.
2. The quantification of the rates of change of the flow magnitude (acceleration /deceleration) during a flood explains as much the variability of bedload transport fluxes as the flow intensity itself.
3. The use of complementary measurement techniques of bedload processes can reveal new river bed dynamics in gravel-bed rivers: the dilation and contraction of the bed resulting from a flood.
4. The investigation of the generally accepted fact that bedload sediment transport is correlated with the intensity of the morphological changes reveals that the two processes do not relate directly due to their different characteristic scales.
5. The systemic approach of river dynamics based on the use of multivariate analytical techniques is better suited for the study of complex linear and non-linear interactions and feedbacks in the evolution of a river channel. This analysis has shown the importance of the recent history of the morphological changes in response to a flood.

The conceptual orientation of this thesis results from a deep reflection on the traditional approaches previously used for several decades in fluvial geomorphology. It is based on a single very extensive data set collected during 21 flood events in a small gravel-bed river, Béard creek (Quebec). The experimental protocol aimed at the simultaneity of processes measurements in order to focus the analysis on the interactions between the flow, the channel morphology and the bedload sediment transport rather than on the individual processes, an approach seldom used in fluvial geomorphology. Each chapter reports on a new concept or a new approach making it possible to resolve some of the issues met in fluvial geomorphology. This work has important implications for the understanding of river bed dynamics and fluvial habitats and is a starting point for new developments.

**Keywords :** Fluvial geomorphology, Scales, Gravel-bed rivers, Flow, Flood, Bedload transport, Bed morphology

## TABLE DES MATIÈRES

---

RÉSUMÉ.....	I
ABSTRACT .....	III
TABLE DES MATIÈRES .....	V
LISTE DES TABLEAUX .....	IX
LISTE DES FIGURES .....	XI
LISTE DES SYMBOLES.....	XIX
REMERCIEMENTS .....	XXV
<b>CHAPITRE 1. INTRODUCTION : CONSIDÉRATIONS SCIENTIFIQUES ET MÉTHODOLOGIQUES.....</b>	<b>1</b>
1.1. Introduction générale .....	1
1.2. Perspectives sur la recherche en géomorphologie fluviale .....	2
1.2.1. Contexte historique .....	2
1.2.2. Contexte contemporain.....	7
1.2.3. Directions futures .....	10
1.3. Problématique et objectifs.....	13
1.4. Contexte scientifique .....	18
1.5. Considérations méthodologiques .....	22
1.5.1. Choix du site .....	22
1.5.2. Stratégie d'échantillonnage.....	23
1.5.3. Jeu de données .....	30
<b>CHAPITRE 2. IMBRICATION D'ÉCHELLES : IMPACT DE LA MORPHOLOGIE SUR L'ÉCOULEMENT .....</b>	<b>37</b>
2.1. Contexte .....	37
2.2. Bridging the gap between turbulence and larger scales of flow motions in rivers.....	39
2.2.1. Abstract.....	39
2.2.2. Introduction.....	39
2.2.3. Methods and analysis .....	41
2.2.4. Results and discussion .....	44
2.2.5. Conclusion .....	49
2.3. From turbulent coherent flow structures to flow pulsations in gravel-bed rivers .....	50
2.3.1. Abstract.....	50
2.3.2. Introduction and research context.....	50

2.3.3. Methods .....	54
2.3.3.1. Data sampling.....	54
2.3.3.2. Data analysis .....	57
2.3.4. Results .....	60
2.3.4.1. Main flow characteristics .....	60
2.3.4.2. Flow pulsation characteristics .....	61
2.3.4.3. Flow pulsations length .....	63
2.3.5. Discussion.....	65
2.3.6. Implications and conclusions .....	67
<b>2.4. Paragraphe de liaison, chapitres 2-3.....</b>	<b>69</b>
<b>CHAPITRE 3. GRADIENTS DE CHANGEMENT : IMPACT DE L'ACCÉLÉRATION SUR LE TRANSPORT DE SÉDIMENTS .....</b>	<b>71</b>
<b>3.1. Fluid acceleration and deceleration during flood hydrographs as drivers of bedload sediment transport .....</b>	<b>71</b>
3.1.1. Abstract .....	71
3.1.2. Context .....	71
3.1.3. Research question and hypothesis .....	73
3.1.4. Data sampling and transformations.....	74
3.1.5. Results and discussion.....	76
3.1.6. Perspectives .....	79
<b>3.2. Paragraphe de liaison, chapitres 3-4.....</b>	<b>81</b>
<b>CHAPITRE 4. COMBINAISON DE MÉTHODES : VERS L'IDENTIFICATION D'UNE NOUVELLE DYNAMIQUE MORPHOLOGIQUE.....</b>	<b>83</b>
<b>4.1. Using multiple bedload measurements: towards the identification of bed dilation and contraction in gravel-bed rivers .....</b>	<b>83</b>
4.1.1. Abstract .....	83
4.1.2. Introduction .....	83
4.1.3. Field site & data collection .....	86
4.1.4. Analyses.....	91
4.1.5. Results .....	93
4.1.5.1. Data inspection and validation.....	93
4.1.5.2. Morphological response of the bed to a bedload event.....	99
4.1.5.3. Dilation and contraction effect on topographical data .....	101
4.1.5.4. Conditions leading to dilation and contraction.....	103
4.1.5.5. Effects of dilation and contraction on fluvial processes .....	106
4.1.6. Discussion.....	108
4.1.6.1. Possible causes of dilation and contraction .....	108
4.1.6.2. Dilation and contraction of the bed at Béard Creek .....	111
4.1.6.3. Perspectives .....	112
4.1.7. Conclusions .....	113
<b>4.2. Paragraphe de liaison, chapitres 4-5-6.....</b>	<b>116</b>

<b>CHAPITRE 5. TRANSFERTS D'ÉCHELLE : DU TRANSPORT DE SÉDIMENTS À LA RÉPONSE MORPHOLOGIQUE .....</b>	<b>119</b>
<b>5.1. Morphodynamics of gravel-bed rivers. A- Morphology and bedload transport responses .</b>	<b>119</b>
5.1.1. Abstract.....	119
5.1.2. Introduction .....	119
5.1.2.1. General context .....	119
5.1.2.2. Bedload transport and morphology interactions in gravel-bed rivers .....	122
5.1.3. Methods.....	125
5.1.3.1. Field site and data collection .....	125
5.1.3.2. Data set.....	128
5.1.3.3. Bedload and morphology variables .....	130
5.1.3.4. Data analysis.....	133
5.1.4. Results.....	136
5.1.5. Discussion .....	143
5.1.6. Conclusion .....	147
<b>CHAPITRE 6. APPROCHE SYSTÉMIQUE : LA RÉPONSE D'UN COURS D'EAU À UN ÉVÈNEMENT DE CRUE .....</b>	<b>149</b>
<b>6.1. Morphodynamics of gravel-bed rivers. B-The effects of flow, flood history and initial conditions.....</b>	<b>149</b>
6.1.1. Abstract.....	149
6.1.2. Introduction .....	149
6.1.2.1. General context .....	149
6.1.2.2. Factors of bedload transport and morphological variability .....	150
6.1.2.3. Objectives .....	154
6.1.3. Methods.....	154
6.1.3.1. Field site and data collection .....	154
6.1.3.2. Bedload, morphological and explanatory variables pre-processing.....	157
6.1.3.3. Quantitative analyses .....	158
6.1.4. Results.....	162
6.1.4.1. Data set description.....	162
6.1.4.2. Comparisons of the results among the different analytical schemes .....	164
6.1.4.3. A global analysis.....	170
6.1.5. Discussion .....	172
6.1.6. Conclusion .....	178
<b>CHAPITRE 7. CONCLUSION GÉNÉRALE.....</b>	<b>181</b>
<b>7.1. Principales découvertes et avancées conceptuelles .....</b>	<b>181</b>
<b>7.2. Modification de la trinité fluviale en une tétralogie fluviale .....</b>	<b>185</b>
<b>7.3. Recherche future .....</b>	<b>188</b>
<b>BIBLIOGRAPHIE .....</b>	<b>191</b>



## LISTE DES TABLEAUX

---

<b>Tableau 1.1</b> Informations sur les caractéristiques et les données disponibles de chaque évènement de crue échantillonné au ruisseau Béard.....	32
<b>Table 2.1</b> Sampling location characteristics.....	43
<b>Table 2.2</b> Characteristics of the surveyed reaches.....	55
<b>Table 2.3</b> Field time series characteristics (shown for $0.5H$ except when mentioned). .....	56
<b>Table 2.4</b> Flume time series characteristics.....	57
<b>Table 4.1</b> Principal characteristics of the surveyed bedload events listed in chronological order. Basic information about flow (peak discharge and average stream power), bedload transport (duration, quantity and size) and morphological changes (active bed surface from the bed tag surveys, volumes of erosion and deposition from the DEMs of difference) are presented for each surveyed section of Béard creek. ....	90
<b>Table 4.2</b> Standardized coefficients for each explanatory variable and the total coefficient of determination ( $R^2$ ) of the multiple regression models for the contraction and dilation areas for floods where the bed active area was less than 60 %. ....	104
<b>Table 5.1</b> Bedload and morphology response variables.....	130
<b>Table 6.1</b> Flow magnitude, hydrograph shape, morphological initial conditions and antecedent flow history explanatory variables.....	158
<b>Table 6.2</b> Relationships between explanatory variables and stream response variables detected by the four quantitative analysis (LR: linear regression, MR: Multiple regression, DA: discriminant analysis, CT: classification tree). ....	168



## LISTE DES FIGURES

---

<b>Figure 1.1</b> Interactions et rétroactions entre la couche-limite turbulente, le transport de sédiments et le développement des formes du lit (dans Best (1993), modifié de Leeder (1983)).....	13
<b>Figure 1.2</b> Spectre de puissance temporel de la vitesse schématisé dans les rivières à lit de graviers représentant les échelles de variabilité de l'écoulement pour différentes échelles caractéristiques (Nikora, 2007) .....	14
<b>Figure 1.3</b> Cadre conceptuel de la thèse situant les cinq chapitres de résultats ainsi que les considérations conceptuelles traitées dans chacune des études de cas au sein de la trinité fluviale, modifiée de Leeder (1983) et Best (1993). .....	16
<b>Figure 1.4</b> Compilation des références citées dans les chapitres de résultats. (a) Nombre de références par chapitre selon le thème traité. (b) Nombre de références uniques à chacun des chapitres et partagées par plusieurs chapitres représentées selon l'année de publication. (c) Nombre de références par thème et selon l'origine des données. Voir le texte pour des explications sur le classement des références.....	19
<b>Figure 1.5</b> (a) Localisation et topographie du bassin versant du ruisseau Béard. (b) Photo du bassin versant du ruisseau Béard prise vers le Sud-ouest. (c) Photo du bassin versant du ruisseau Béard prise vers le Sud.....	24
<b>Figure 1.6</b> Emplacement des instruments automatisés et topographie du tronçon d'étude d'après l'interpolation des élévations résiduelles du lit (sans la pente du tronçon). Les classes d'élévation représentent un pourcentage de la distribution des élévations résiduelles de la section dont l'étendue est de 1.15 m. L'emplacement des sections est identifié par les encadrés le long du tronçon et leur allure générale est visible sur les photos. ....	25
<b>Figure 1.7</b> Photos des diverses composantes des boîtes à sédiments installées au ruisseau Béard. (a) Extérieur de la boîte avec le couvercle. (B) Intérieur de la boîte sans le couvercle et sans le boîtier interne. (c) Appareil de répartition du poids qui s'insère au fond de la boîte à sédiments. (d) La cellule de charge. (e) La cellule de charge dans son compartiment permettant la répartition du poids. (f) La boîte à sédiments de la section aval. Notez que le boîtier interne amovible est accessible lorsque le couvercle est retiré.....	28
<b>Figure 2.1</b> Schematized velocity spectra in gravel-bed rivers in the frequency domain, from Nikora (2007) .....	41

<b>Figure 2.2</b> Field site location in Southern Québec (Canada) on the left side and a downstream view during the recording in pool B joined with an underwater picture of the ECM's on the right side. ....	42
<b>Figure 2.3</b> (a, b) Velocity time series. (c, d) Cumulative curves of the velocity fluctuations. (e, f, g, h) Zoom of the cumulative curves, location show with the box on the previous curve. All data are presented for ECM located at 0.14 m above the bed for both velocity measurements in pools A (left) and B (right). ....	45
<b>Figure 2.4</b> Representations of the dominance of ejections and sweeps over time windows of 1, 12 and 120 seconds. (a, b) Dominance by duration of the turbulent structures. (c, d) Dominance by the magnitude of the Reynolds shear stress during the passage of the turbulent events. All data are presented for ECM located at 0.14 m above the bed for both velocity measurements in pools A (left) and B (right).....	47
<b>Figure 2.5</b> Study reaches with the photos taken looking upstream and the interpolated maps of the morphological surveys. The white star represents the location of the time series measurements.....	54
<b>Figure 2.6</b> Raw time series (a) and transformed times series (b to e) for the low flow stage measurements at Béard Creek and the run A3 in the flume. The examples were chosen for their similar flow depth and average velocity. ....	58
<b>Figure 2.7</b> Comparisons of the flow pulsation amplitudes for different analyses between the field time series, the flume time series and random time series (generated based of the characteristics of the flume time series). .....	63
<b>Figure 2.8</b> Relations between the pulsation cycle length and the mean flow velocity for (a) the flume data set and (b) the field data set. The grey vertical lines represent the range of values between the percentiles 25 and 75 of the pulsation lengths. ....	64
<b>Figure 2.9</b> Relations between the pulsation cycle lengths measured in the field and (a) the pool spacing, (b) the channel flow width, (c) the mean flow depth of the reach and (d) the relative roughness of the reach. The grey vertical lines represent the range of values between the percentiles 25 and 75 of the pulsation lengths. The horizontal grey lines in (a) represent the range of pool spacing upstream of the measurement point. ....	64
<b>Figure 2.10</b> Relation between the pulsation cycle lengths measured in the field and the pool spacing. The size of the data points is proportional to the riffle relative roughness. The outliers are identified by grey circles instead of white. ....	67

<b>Figure 3.1</b> Possible flow conditions during a flood even. In space, the configuration of the river bed combined with the slope of the water surface determines if the flow is locally uniform (the bed and water surface slope are parallel), in expansion and decelerating (the bed slope is steeper than the water surface slope) or in constriction and accelerating (the water surface slope is steeper than the bed slope). In time, the rate of increase or decrease in flow depth during the rising and falling limb determined if the flow is steady, in acceleration or deceleration. Note that the spatial and temporal flow conditions can be combined with each other.....	73
<b>Figure 3.2</b> (a) Upstream view of the study section at Béard creek (Montérégie, Québec, Canada). (b) Unit bedload flux rate computed for periods of five minutes against average discharge during the same period estimated using a flow stage rating curve. For the remaining analyses in the paper, we used the standardized bedload rate residuals of the regression presented here. The color coding designates individual floods ranked in an ascendant order of the value median of the bedload rate residuals.....	74
<b>Figure 3.3</b> (abcd) The distributions of the variables used in the analysis for each flood event. (fghi) The distributions of the variables by flow condition groups defined through a regression tree model analysis. (e) Individual data points membership to flow condition groups for each flood event, the group colors are the same as in Figure 3.3g-i. (j) Individual data points membership to flood events for each flow condition group, the flood colors are the same as in Figure 3.2b and Figure 3.3a-d. In (a) and (f), the number of individual data points for a flood or a flow condition group is indicated.....	77
<b>Figure 4.1</b> (a) Location of Béard Creek and the study reach in the Eastern Townships, Québec, Canada. (b) Downstream views of both study sections. (c) Contour maps (generated from DEMs) of the initial topographic elevation of both study sections.....	87
<b>Figure 4.2</b> Case scenarios of morphological changes following a bedload event when combining information from the DoDs and the bed tag surveys. Diagrams are in the cross-sectional plane of the stream bed. Case 1A: Bed elevation did not change and the bed was inactive, thus the bed was similar to the initial state. Case 1B: Bed elevation did not change but the bed was active, suggesting that scour compensated fill during the event. Case 2A & 3A: The grains did not move during the event but the bed elevation changed. Case 2B & 3B: The bed was active and the bed elevation changed. ....	93
<b>Figure 4.3</b> Error estimation among five repeated morphological surveys of the upstream section using a total station. (a) Distribution of the DEM elevation differences of all possible pairs of the five repeated surveys. (b) Classification of the bed tag survey between the six different case scenarios using the DoDs between the five successive surveys and the survey following the flood of 24 October 2009. (c) Binary representation of the spatial distribution of the maximal absolute error between the five repeated surveys (95 % of errors are in the range 0 to 0.03m). .....	95

<b>Figure 4.4</b> Bedload estimates from three different sampling methods for the upstream and downstream sections of Béard Creek. Each dot represents one flood event. Unit stream power ( $\omega$ ) is averaged over the period when the bedload transport was active. Bedload rate is calculated as submerged material. ....	98
<b>Figure 4.5</b> Examples of the classification of the DoDs into increased, decreased or stable elevation using the minimal level of detection $\pm 0.03$ m. The color dots are the locations of three morphological scenarios that cannot be identified when using only the DoDs derived from the morphological surveys. Examples were chosen to illustrate the typical spatial distribution of large dilated or contracted bed areas for each section. ....	98
<b>Figure 4.6</b> Proportion of each of the six case scenarios of morphological changes after each of the 20 bedload events in the data set. Data are presented in percentage of the section area in chronological order. All flood events are successive except for the winter period for which no data are available. The peak discharge is also represented to put the morphological response into context. ....	100
<b>Figure 4.7</b> Bed volume changes in relation to total bedload yield for each bedload event for both sections. Bed volume changes corresponded to the addition of the absolute erosion and accumulation estimated from the DoDs. (a) Raw bed volume changes estimated using only the DoDs. (b) Bed volume changes after the subtraction of the dilation and contraction areas elevation changes as these areas did not experience local bedload transport. (c) Bed volume changes corrected for dilation and contraction volumes and to which an estimated volume for the active areas without elevation change is added. The total bedload rate is estimated for the width of the section and for the period when bedload was active during the flood. ....	101
<b>Figure 4.8</b> Comparisons of the active bed areas estimated using the morphological and bed tag surveys for each bedload event for both sections. In principle, the areas should be identical and the dots all on the 1:1 line. (a) Raw data. (b) The dilation and contraction areas are subtracted from the active areas estimated from the DoDs. (c) The dilation, contraction and active areas without elevation change are subtracted from the active areas estimated from the DoDs. ....	102

<b>Figure 4.9</b> Morphological response sequences for local bed dilation and contraction (i.e. locations of the bed tags). For every occurrence of bed dilation and contraction in both study sections, previous and following local bed states are compiled. (a) Probability of observing a specific morphological state before contraction, after contraction, before dilation and after dilation at a particular location of the bed. The probability of occurrence of all morphological responses for the whole data set is shown for comparison. (b) To appreciate the differences between the general probability of occurrence of one morphological scenario ( $p_{\text{all}}$ ) and the probability of occurrence before or after a specific morphological scenario ( $p_i$ ), we show the ratio $p_i / p_{\text{all}}$ . If the ratio is greater than one, this means that this succession of morphological responses is more likely to occur.....	105
<b>Figure 4.10</b> Bedload and morphological variables that are likely to be affected by the occurrence of bed areas where contraction or dilation occurred during the previous flood, thus changing the initial conditions of the bed. Erosion volumes are corrected for dilation and contraction areas. Each dot represents one flood event and its size is proportional to the contracted or dilated areas of the previous flood. Unit stream power ( $\omega$ ) is averaged over the period when the bedload transport was active.....	107
<b>Figure 5.1</b> Field site location.....	125
<b>Figure 5.2</b> Detrended initial morphology of the surveyed sections and instruments location.....	126
<b>Figure 5.3</b> Cumulative particle size distributions. The bedload curve is for average distribution events below bankfull discharge $Q_{\text{bf}}$ . Surface pebble counts are based on 400 particles measured at each section. Bulk sampling is based on the sieving of about 40 kg samples.....	126
<b>Figure 5.4</b> Pictures looking upstream for various discharges at the upstream section. The white dot serves as a reference point from picture to picture. Note that the bankfull discharge is $2.5 \text{ m}^3 \text{s}^{-1}$ .....	129
<b>Figure 5.5</b> Thalweg profile, slope $S$ and elevation $E$ evolution through time. The profiles were surveyed between each flood mobilising particles as bedload, no data was collected during winter. See text for explanation on the estimation of the data.....	132
<b>Figure 5.6</b> Distributions of bedload and morphology response for both sections and separated for floods below and above bankfull discharge. Boxplots over a shaded gray area indicate data that are not used in further analyses because of their inaccuracy due to estimation or incomplete flood record. We show that data only for general information.....	136

<b>Figure 5.7</b> Correlation matrices (Pearson's $r$ ) of bedload (black names) and morphological response (grey names) variables for both sections and for each section separately. Note that only floods below bankfull discharge are used for $i_b^*$ , $D_{50}^*$ and $MOB$ .....	138
<b>Figure 5.8</b> Distributions of all variables for groups of low, medium and high values or decrease, stable and increase values of each variable. Group limits were zscores values -0.5 and 0.5 of the normalized (if needed) and standardized distributions of each variable. Each row of subplots represents the grouping of the data points according to the distribution of one variable. Each column of subplots shows the distribution of the variables according to a specific grouping. The subplots in shaded gray highlight that at least one group is different according to an ANOVA test ( $p < 0.1$ ). Note that only floods below bankfull discharge are used for $i_b^*$ , $D_{50}^*$ and $MOB$ ( $n = 22$ ). For the other variables, all floods with sediment transport are used ( $n=36$ ). Bedload variable names are in black and morphological variable names in grey. See Figure 5.6 for boxplot legend. ....	140
<b>Figure 5.9</b> Principal component analysis of all bedload (names in black) and morphological response (names in grey) variables for flood events (dots) below bankfull discharge. The first four PCAs represent 78% of the variance of the whole data set and their individual variance exceeds 12.5%, the value of the variance if all axes were equal. All variables were standardized so that the variance was equal to 1 for each variable. Biplots of principal components (PC) 1 to 4 are drawn to see how the variables (arrows) correlate in the orthogonal space of the PCA, as the projection used preserves the correlation between the variables. ....	141
<b>Figure 5.10</b> Fraction of variance for the first four PCs for each variable and all variables together (left) and for each individual flood event and average for each section (right). As in Figure 10, only flood events below bankfull discharge are used....	142
<b>Figure 6.1</b> (a) Field site morphology and study sections picture (interpolated detrended elevations range is 1.15 m). (b) Longitudinal profile evolution during the study period.....	155
<b>Figure 6.2</b> Discharge time series during the study period and identification of bedload transport events. ....	156
<b>Figure 6.3</b> Correlation matrix (Pearson's $r$ ) of explanatory variables. ....	161
<b>Figure 6.4</b> Average dimensionless bedload transport rate as a function of the dimensionless flood peak discharge. Note that $i_b^*$ for floods above bankfull is partly estimated; see Marquis and Roy (2012) for further details.....	162

<b>Figure 6.5</b> Distributions of flow, flood history, initial conditions, bedload and morphology responses for both sections and separated for floods below and above the bankfull discharge. Note that $i_b^*$ , $D_{50}^*$ <i>MOB</i> of floods above bankfull (boxplots over shaded gray area) will not be further analysed as the recorded data were incomplete.....	163
<b>Figure 6.6</b> Explained variance or classification ratio for each of the four quantitative analyses applied to each response variable. Note that for the linear regression, the $r^2$ of the variable explaining the highest proportion of variance was chosen.....	164
<b>Figure 6.7</b> Proportion of variance explained for the linear and multiple regressions between all explanatory variables and all response variables. Variance partitionning of the unique contribution per explanatory variable and total variance explained by the multiple regression for each response variables. Note that only floods below the bankfull discharge are used for $i_b^*$ , $D_{50}^*$ and <i>MOB</i> .....	165
<b>Figure 6.8</b> Discriminant analysis of the groups of low, medium and high values or decrease, stable and increase values of each response variable. Group limits were zscores values -0.5 and 0.5 of the normalized (if needed) and standardized distributions of each variable. Note that only floods below the bankfull discharge are used for $i_b^*$ , $D_{50}^*$ and <i>MOB</i> . Note that when the coefficients of a variable were near zero, the variable is not represented.....	166
<b>Figure 6.9</b> Classification trees of the groups of low, medium and high values or decrease, stable and increase values of each response variable. Group limits were zscores values -0.5 and 0.5 of the normalized (if needed) and standardized distributions of each variable. Note that only floods below the bankfull discharge are used for $i_b^*$ , $D_{50}^*$ and <i>MOB</i> . .....	167
<b>Figure 6.10</b> Kmeans cluster analysis performed on the response variables and quantitative analysis of the explanatory variables in relation to the groups. Note that only floods below the bankfull discharge are used for the cluster analysis. The symbol (*) denotes that at least one group mean is significantly different according to an analysis of variance ( $p < 0.1$ ). See Figure 6.5 for boxplot legend. ....	171
<b>Figure 6.11</b> Discriminant analysis and classification tree analysis of the four groups based on Kmeans cluster analysis. Note that only floods below the bankfull discharge are used for the cluster analysis. The color coding of the groups is the same as in Figure 6.10. ....	171

**Figure 6.12** Interactions among the variables measured in this study. The interactions represented are shown in for Table 3. Note that the five variables that are both predictor and response variables were represented as a single element for simplification. To interpret correctly the figure, an arrow departing from a variable indicates a predictor while an arrow directed toward a variable is a response. For example, the initial slope controls the initial threshold for motion but the change of slope after a flood is influenced by the initial microform roughness.....175

**Figure 7.1** *Trinité fluviale* modifée en *tétralogie fluviale* suite à l'intégration conceptuelle des résultats de la thèse. Pour faire le lien avec la Figure 1.3, les numéros des chapitres et les principales découvertes et avancées sont placés selon les interactions étudiées.....186

## LISTE DES SYMBOLES

---

### Constantes

$g$	accélération gravitationnelle / gravitational acceleration
$\kappa$	constante de Von Karman / Von Karman constant
$\rho$	densité massique de l'eau / water density
$\rho_s$	densité massique des particules / particle density

### Variables

$D$	longueur de l'axe $b$ d'une particule / $b$ axis length of a particle
$D_f$	dimension fractale / fractal dimension
$D_x$	longueur de l'axe $b$ du percentile $x$ d'un ensemble de particules / $b$ axis length of the $x^{\text{th}}$ percentile of a group of particles
$D_{50}^*$	axe $b$ médian des particules transportées sans dimension / dimensionless median $b$ axis of transported particles
$E$	élévation moyenne du lit / mean bed elevation
$H$	Profondeur d'eau moyenne à un point / mean flow depth at a point
$HE$	exposant de Hurst / Hurst exponent
$h$	profondeur d'eau à un point / flow depth at a point
$h'$	fluctuation de la profondeur d'eau à un point / flow depth fluctuation at a point
$h_0$	hauteur où la vitesse de l'écoulement est nulle / height where flow velocity equal zero
$h_i$	hauteur au-dessus du lit / height above bed
$i_b$	taux de transport en charge de fond / bedload transport rate
$\hat{i}_b$	résidus des taux de transport en charge de fond / bedload transport rate residuals
$i_b^*$	taux de transport en charge de fond sans dimension / dimensionless bedload transport rate
$MOB$	surface active/mobilisée du lit / active/mobilised bed surface
$PF-v$	variable $v$ lors de l'évènement de crue précédent / previous flood variable $v$
$Q$	débit moyen pour une certaine période / mean discharge during a period of time
$Q_{bf}$	débit plein bord / bankfull discharge
$Q_{pk}$	débit de pointe / peak discharge
$Rn_{\text{falling}}$	proportion du ruissellement d'une crue durant la décrue / proportion of a flood runoff on the falling limb
$S$	pente du lit / bed slope

$S_w$	pente de la surface de l'eau / water surface slope
$T$	durée d'une période ou d'une fenêtre de calcul / period or calculation window duration
$T_b$	durée de la période de <i>bursting</i> / bursting period
$U$	vitesse moyenne de l'écoulement / mean flow velocity
$u$	vitesse longitudinale de l'écoulement / streamwise flow velocity
$u^*$	vitesse de friction / friction velocity
$u'$	fluctuation de la vitesse longitudinale / streamwise velocity fluctuation
$v$	vitesse verticale de l'écoulement / vertical flow velocity
$v'$	fluctuation de la vitesse verticale / vertical velocity fluctuation
$W$	largeur du chenal mouillé / wetted channel width
$Y$	profondeur moyenne d'une coupe transversale ou d'une section / mean flow depth of a cross section or a reach
$Y_p$	profondeur moyenne d'une mouille / mean flow depth of a pool
$Y_r$	profondeur moyenne d'un seuil / mean flow depth of a riffle
$\delta$	épaisseur de la couche-limite / boundary layer thickness
$\theta_{ci}$	seuil critique d'entraînement / critical entrainment threshold
$\theta_{ci}^*$	seuil critique d'entraînement sans dimension / dimensionless critical entrainment threshold
$\tau$	contrainte de cisaillement / shear stress
$\tau'$	fluctuation de la contrainte de cisaillement / shear stress fluctuation
$\tau_f''$	rugosité des micro-formes sans dimension / dimensionless microform roughness
$\tau_g'$	rugosité des macro-formes sans dimension / dimensionless macroform roughness
$\Phi$	tailles de particules selon une échelle logarithmique / particle sizes on a logarithmic scale
$\omega$	puissance spécifique / unit stream power
$\omega_{\text{mean}}$	puissance spécifique moyenne / mean unit stream power

## Analyses

$k$	seuil utilisé dans la méthode de détection des structures turbulentes <i>U</i> -level / threshold used in the U-level turbulent flow structure detection analysis
$n$	nombre d'éléments d'un échantillon / number of elements in a sample
$p$	probabilité d'accepter l'hypothèse nulle d'un test statistique / probability of accepting the null hypothesis in a statistical test
$p_i$	probabilité d'occurrence d'un événement $i$ / probability of occurrence of an event $i$
$r$	coefficient de corrélation / correlation coefficient

$R^2$	coefficient de détermination d'une régression / determination coefficient of a regression
$RMSv$	écart-type d'une variable $v$ / standard deviation of a variable $v$
$z$ -score	valeur normalisée / normalised value
$\alpha$	probabilité d'une erreur de type I dans un test statistique / probability of a type I error in a statistical test
$\Delta v$	différence entre deux valeurs consécutives d'une variable $v$ / difference between two consecutive values of a variable $v$
$\lambda$	Exposant de la transformation Box Cox / exponent of the Box-Cox transformation

## Abbréviations

ANOVA	analyse de variance / analysis of variance
CFS	structure turbulente cohérente / coherent flow structure
DEM	Modèle d'élévation numérique / digital elevation model
DoD	différence de DEMs / DEMs of difference
ECM	courantomètre électromagnétique / electromagnetic current meter
HF	haut niveau d'eau / high flow stage
LF	bas niveau d'eau / low flow stage
LSM	structure turbulent cohérente à grande échelle / large scale motion coherent flow structure
PC	composante principale / principal component
PCA	analyse en composante principale / principal component analysis
Q1, Q2, Q3, Q4	types de structures turbulentes détectées par l'analyse des quadrants / types of turbulent flow structures detected using the quadrant scheme analysis
VLF	très bas niveau d'eau / very low flow stage
VLSM	structure turbulent cohérente à très grande échelle / very large scale motion coherent flow structure



*«The important thing in science is not so much to obtain new facts as to discover new ways of thinking about them.»*

Sir William Bragg



## REMERCIEMENTS

---

Lorsque j'ai commencé cette thèse, je ne soupçonnais pas qu'il me faudrait presque sept années pour la compléter. Durant ces années, mes proches et mes collègues m'ont toujours supporté admirablement autant dans les moments creux que lors des mes réussites. Je n'aurai jamais fait un doctorat sans André Roy, mon directeur. C'est lui qui a décelé très tôt dans mon cheminement universitaire mon potentiel à mener un tel projet. Il m'a fourni tous les outils nécessaires à la réalisation du projet mais surtout il a toujours su trouver le bon mot lors de mes remises en question. Je crois que ce qui me permet de déposer cette thèse avec fierté c'est la confiance absolue qu'il a toujours eu en mes capacités et la liberté qu'il m'a laissé dans le cadre du projet. Cette thèse ne serait rien sans les discussions conceptuelles imprévues à la fin d'une journée découlant d'une question anodine. André a réellement su me transmettre sa passion pour la recherche et la science en général.

Le succès de la thèse dépendait fortement du choix du site de recherche. Pour leur enthousiasme et leur intérêt face à mon projet, je suis reconnaissante à Monsieur et Madame Cloutier qui m'ont laissé accéder à leur terrain afin que je puisse étudier le ruisseau Béard, qui correspondait à tous mes critères de recherche. Souvent, ils m'ont tenu au courant de l'état du ruisseau et des instruments lorsque j'étais dans l'impossibilité de m'y rendre pour vérifier moi-même l'état des lieux. J'ai aussi eu le support inestimable de Martin Lambert et Jean-François Myre de l'atelier du Département de Chimie de l'Université de Montréal lors de la conception et la fabrication des boîtes à sédiments. Ils ont fait preuve d'ouverture d'esprit face à ce projet peu commun et ont relevé le défi avec brio. J'ai aussi apprécié leur aide bénévole pour les ajustements nécessaires et leur accueil toujours réceptif face à mes demandes.

Sur le terrain, une multitude d'étudiants, collègues et amis se sont succédés au fil des ans pour m'aider et je les remercie tous chaleureusement : Jean-François Brodeur, Christine Bergeron-Verville, Vincent Cardin-Tremblay, Laurence Chaput-Desrochers, Sylvio Demers, Claude Gibeault, Hélène Lamarre, Olivier Lalonde, Kevin Partington, Mathilde Péloquin-Guay, Mathieu Roy, Marylène Savoie, Katherine Sicotte, Rachel Thériault, Julie Therrien et Michèle Tremblay. J'aimerais remercier tout particulièrement Katherine Sicotte et Rachel Thériault pour leur énergie et leur initiative lors de l'installation des instruments et leur patience face à mon processus d'essais et erreurs.

Au département, je remercie tous les membres de la Chaire de Recherche en géomorphologie fluviale et tous les autres étudiants de cycles supérieurs que j'ai côtoyés. Particulièrement, j'aimerais exprimer ma reconnaissance à mes deux complices de bureau, Geneviève Ali pour sa persévérance et son assurance et Mathieu Roy pour nos innombrables discussions, nos joies et déprimes doctorales partagées, à Hélène Lamarre pour son humour sans pareil, à Laurence Chaput-Desrochers pour sa relève exceptionnelle au ruisseau Béard et à Mathilde Péloguin-Guay pour son enthousiasme face à ses premiers pas en recherche qui a eu l'effet d'une bouffée de fraîcheur lors de ma fin de parcours. Du laboratoire de pédologie, je salue le professionnalisme et le support indéfectible de Marie-Claude Turmel. Du comité doctoral, j'aimerais souligner l'apport majeur des questions posées tout au long de mon cheminement par Pascale Biron et François Courchesne qui ont fortement contribué à l'orientation de ma thèse.

Cette thèse a notamment été financée par le Conseil de Recherche National en Science et Génie (CRSNG), le Fonds Québécois de la recherche sur la nature et les technologies (FQRNT), le Fonds Canadien pour l'Innovation (FCI), la Chaire de recherche du Canada en dynamique fluviale, la Faculté des Études Supérieures et le Département de Géographie de l'Université de Montréal. Les bourses que j'ai reçues tout au long de mes études m'ont permis de me consacrer entièrement à la réalisation de cette thèse.

Enfin, je ne peux passer sous silence l'appui quotidien et inconditionnel de ma famille immédiate et élargie, des mes amis et de mon amoureux. Claire et Émile, merci de n'avoir jamais douté de ma capacité à terminer mon doctorat, même si j'ai dit pendant deux ans que j'étais sur le point de finir ! Je ne remercierai jamais assez ma mère Claire pour la relecture de mes textes en français comme en anglais même si parfois ils étaient probablement bien étranges pour une non initiée... Et je suis aussi reconnaissante à mon père Émile l'ingénieur d'être devenu le défenseur des géographes ! J'aimerais aussi mentionner l'intérêt et la curiosité de mes grands parents, oncles, tantes et cousins pour mon parcours scolaire particulier. Quant à mes amis, ils m'ont permis de relativiser lors de mes moments plus difficiles et ils m'ont donné l'énergie de continuer et d'aller jusqu'au bout. Finalement, j'admirerai à jamais la patience et la compréhension de mon amoureux, Pierre-Michel, qui est entré dans ma vie au moment où la fin m'apparaissait si loin. Il m'a supporté de toutes les manières possibles afin que je puisse enfin terminer ce fameux doctorat, une étape importante de ma vie.

# **CHAPITRE 1. INTRODUCTION :**

## **CONSIDÉRATIONS SCIENTIFIQUES ET MÉTHODOLOGIQUES**

---

### **1.1. Introduction générale**

Cette thèse basée sur un jeu de données unique est issue d'une réflexion sur la recherche en géomorphologie fluviale qui repose principalement sur des études intensives de cas. Chacun des chapitres de résultats formant le cœur de cette thèse a des implications sur les approches conceptuelles, méthodologiques et analytiques dans le but d'améliorer la compréhension des dynamiques fluviales en rivière graveleuse. La thèse met l'accent sur les interactions entre l'écoulement, le transport de sédiments en charge de fond et la morphologie du lit à diverses échelles spatiales et temporelles. Ce chapitre introductif vise donc à situer cette étude contemporaine par rapport à l'évolution de la discipline de la géomorphologie, fluviale en particulier, et aux défis actuels et futurs qui se présentent aux chercheurs. Suite à la présentation du contexte historique et des enjeux contemporains, la problématique de recherche de la thèse sera exposée afin d'introduire les objectifs spécifiques de la thèse. Une synthèse de la littérature scientifique servira à mettre en lumière la diversité des thèmes et approches couverts tout au long de la thèse. La méthodologie employée sera résumée brièvement afin de mettre en lumière les diverses considérations méthodologiques qui ont permis de mettre en place un protocole de recherche original ainsi que la construction d'un jeu de données unique. Les résultats présentés aux chapitres 2 à 6 correspondent à chacun des objectifs spécifiques de cette thèse. Ils sont rédigés sous la forme d'articles scientifiques dont deux sont publiés, un a été soumis pour faire partie d'un livre suite à une conférence internationale et les autres seront soumis suite au dépôt de la thèse. Ma contribution à ces articles en tant qu'auteur principal est majeure. J'ai mené toutes les étapes de l'élaboration de chacun des articles, de la récolte de données à la rédaction des manuscrits. Une conclusion générale dresse un bilan des connaissances acquises et de la portée et des impacts des résultats pour l'évolution de la géomorphologie fluviale.

## 1.2. Perspectives sur la recherche en géomorphologie fluviale

### 1.2.1. Contexte historique

La géomorphologie fluviale s'intéresse au rôle des cours d'eau comme agents de l'évolution des formes terrestres. Cet aspect était central dans la théorie évolutive du cycle de l'érosion développée par William Morris Davis à la fin du 19<sup>e</sup> siècle où le cours d'eau était le convoyeur du matériel terrestre de la montagne vers la mer (Gregory, 2000). Le modèle *davisien* de l'évolution des formes du paysage préconisait une évolution progressive et inéluctable du relief, formé suite à un soulèvement isostatique rapide, vers la pénéplaine par des processus de dénudation. La compréhension des formes contemporaines était essentiellement une approche d'interprétation historique (Church, 2010). Ce modèle publié en 1884 a dominé la discipline durant trois générations en tant que paradigme, malgré l'existence parallèle d'autres approches, notamment celle du géologue Grove Karl Gilbert. Ce chercheur a eu peu d'impact sur ses contemporains probablement par un manque de rayonnement de ses travaux en dehors de ses proches collaborateurs (Orme, 2002). Première en géomorphologie, Gilbert a intégré les travaux de mathématiciens et de physiciens à l'étude expérimentale des processus fluviaux dès la fin du 19<sup>e</sup> siècle. Ses travaux n'ont toutefois pas eu de répercussions majeures dans les courants de pensées avant les années 1950 (Baker et Pyne, 1978). À cette époque, le modèle de Davis fait l'objet de plusieurs critiques officiellement publiées, entre autres à propos de l'évolution unidirectionnelle du paysage et de l'absence de pouvoir prédictif quantitatif (Rudwick, 2008). En fait, la géomorphologie axée sur la mesure des processus est en partie née d'une réaction aux théories de Davies, comme souligné par Leighly en 1940, lors d'un symposium de l'AAG (Von Engeln, 1940, p.215):

"Davis's great mistake was the assumption that we knew the processes involved in the development of the landforms, we don't ; and until we do we shall be ignorant of the general course of their development."

Bien que des recherches basées sur la mécanique des processus dans la lignée de Gilbert étaient poursuivie par quelques uns comme par exemple Leighly (1934) et Bagnold (1941), la plupart des scientifiques ignoraient les processus fondamentaux de leur discipline (Orme, 2002). Le changement de paradigme dans la façon d'envisager le problème de l'évolution du paysage, de la description à la quantification des processus, s'est réellement produit lors de publications sur les réseaux de drainage par Horton (1945), sur les bases

dynamiques de la géomorphologie par Strahler (1952) et sur la géométrie hydraulique (Leopold et Maddock, 1953). Ces travaux, largement inspirés par des disciplines pratiques de l'ingénierie, tel que l'hydraulique et la mécanique des sols, sont aussi le produit d'une nouvelle philosophie de la science qui prône une démarche scientifique rigoureuse basée sur l'hypothèse de recherche (Doyle et Julian, 2005). Cette nouvelle ère de la géomorphologie, la révolution quantitative, basée sur la mesure du paysage et la quantification de relations mécanistiques entre les processus devient définitivement la pensée dominante avec la publication du livre *Fluvial Processes in Geomorphology* par Leopold, Wolman et Miller (1964) qui sera appelé à devenir un classique dans l'enseignement des bases de la géomorphologie. Ce changement de paradigme trouve réellement sa source dans les travaux de Gilbert qui ont été redécouverts dans les années 1950 (Orme, 2002). L'approche de Gilbert pour comprendre le paysage est résumée de manière simple par Pyne (1980, p.134) :

“...as he [Gilbert] argued by his own example, no topic was so trivial or refractory that it could not be expressed according to the laws and logic of physics, and no physical law was so inviolate that it could exist meaningfully outside of a specific context in the facts of physical geography”.

L'émergence d'une géomorphologie plus quantitative est aussi fortement liée au développement technologique suite à le deuxième guerre mondiale, comme l'imagerie aérienne et les méthodes de relevés topographiques (Church, 2010). Le changement d'approche a mené à un ajustement nécessaire des échelles d'étude par rapport à l'époque *davisiennne* où on s'intéressait à l'évolution du paysage à l'échelle globale, autant dans le temps que dans l'espace. La mesure des processus nécessite la mise en place de protocoles d'échantillonnage sur de petites superficies et des échelles de temps beaucoup plus courtes. La conséquence directe de cette nouvelle façon de faire est l'abandon presque complet de la notion historique (à l'exception des études Quaternaires) dans le courant dominant de la discipline moderne (Church, 2010). La géomorphologie des années 1960 à 1990 est donc largement dominée par une approche réductionniste basée sur les équilibres de forces de type Newtonien et l'appropriation des méthodes d'observation et d'analyse empruntées à l'ingénierie (Smith et al., 2002). Un exemple illustrant clairement cette tendance est le développement du concept de l'équilibre dynamique, énoncé très tôt par Gilbert (1877). L'équilibre dynamique est une condition par laquelle les formes du paysage sont maintenues dans le temps suite à un ajustement des processus internes aux forces externes

(Strahler, 1952; Schumm et Lichy, 1965). Dans les rivières, l'équilibre dynamique se concrétise principalement par le concept du régime fluvial qui correspond à une forme de chenal adaptée à un écoulement dominant et à un apport en sédiments donné.

Ainsi, l'objectif ultime en géomorphologie est d'expliquer et de comprendre l'évolution des formes du paysage en tenant compte de l'histoire de ces formes pour éventuellement développer des modèles prédictifs. Dans le contexte de l'évolution d'un chenal, le transport en charge de fond, en particulier, est le processus clé qui relie la morphologie du lit et l'écoulement qui y circule (Gomez, 1991) et il fait l'objet de nombreuses études car il détermine l'évolution de la morphologie du chenal (Church, 2006a). Le transport en charge de fond représente une faible fraction du débit solide total d'un cours d'eau en raison des forces élevées nécessaires pour le mouvement des particules grossières (Bravard et Petit, 1997). Bien que variées, les sources de sédiments grossiers se trouvent majoritairement dans le chenal dans le cas des rivières dont le lit est principalement composé de graviers. Ceci représente une occasion d'étudier les processus physiques dans un lieu relativement circonscrit (Johnson et Warburton, 2002). Avec la multiplication des études sur les processus fluviaux dont l'objectif était de construire des théories et des modèles afin de généraliser les processus observés, on a mis en évidence une gamme de réponses géomorphologiques complexes. Par exemple, des articles synthèses publiés dans la revue *Progress in Physical Geography* traitent de thèmes tels que la structure du lit en rivière à lit de graviers (Richards et Clifford, 1991) et les diverses échelles du transport de sédiments (Hoey, 1992; Nicholas et al., 1995).

Il devient évident que le transport en charge fond ne varie pas uniquement en fonction de la magnitude de l'écoulement (Gomez et al., 1989; Hoey, 1992). Le transport en charge de fond reste variable même pour des particules rondes de taille uniforme sous un écoulement constant (Charru et al., 2004). Cette variabilité est exacerbée en milieu naturel par la présence d'une gamme de tailles et de formes de particules dont l'agencement varie en fonction de l'historique des crues et de l'apport en sédiments. Malgré des dizaines, voire des centaines d'études, l'explication des conditions favorisant le transport de sédiments n'est toujours pas satisfaisante (Dietrich et al., 2003; Church, 2010; Jerolmack, 2011). La prédiction des taux de transport reste largement empirique et les erreurs associées aux modèles prédictifs sont de plusieurs ordres de grandeur (Gomez et al., 1989; Dietrich et al., 2003; Recking, 2010). Dans une compilation des articles portant sur la géomorphologie

fluviale publiées en 2008-2009 dans la revue *Earth Surface Processes and Landforms*, le transport de sédiments en milieu fluvial demeurerait toujours le thème le plus récurrent (Stott, 2011).

L'ensemble de ces études a mené à l'appréciation de la variabilité des processus en jeu dans la transformation des paysages et à la conclusion du besoin de mettre en place des programmes de mesure d'envergure afin de comprendre cette variabilité (Church, 2010). Avec le développement de la technologie à partir des années 1980, ces programmes ont enfin pu être développés. Malgré la multiplication des mesures, la variabilité des phénomènes reste en grande partie insaisissable et le besoin pour un nouveau cadre théorique se fait sentir comme le souligne le titre d'articles conceptuels comme *Fluvial geomorphology : less uncertainty and more practical application ?* (Gregory, 1982). L'ajout de plus en plus d'informations, le développement de la capacité de calcul des ordinateurs autorisant l'analyse de jeux de données de plus en plus volumineux et l'élaboration de modèles numériques complexes ont mené à la reconnaissance de la géomorphologie comme une science des systèmes, dans le sillon d'idées énoncées conceptuellement par Chorley et Kennedy (1971). Cette approche systémique recherche l'explication des phénomènes en intégrant de multiples aspects et processus qui interagissent dans le temps et l'espace (Werner, 1999). Dans un article intitulé *The trajectory of geomorphology*, Church (2010) identifie cinq aspects majeurs des systèmes géomorphologiques que la recherche des années 1960 jusqu'aux années 1990 a permis d'identifier :

1. Différents processus physiques se juxtaposent au même lieu et au même moment de telle façon qu'un changement observable du paysage est le produit d'un certain nombre de processus en synergie et/ou en compétition.
2. Les processus se déroulent selon une gamme d'échelles spatiales et temporelles de telle façon que l'effet à un point dans l'espace est le résultat d'interactions complexes d'effets à différentes échelles.
3. La formation de zones de stockage de sédiments (souvent désignées comme des unités distinctes du paysage) implique que l'évolution du système géomorphologique est toujours influencée par la précédente histoire du système.

4. L'existence de seuils et de limites imposés par les propriétés du matériel (soit par l'énergie nécessaire à l'entraînement ou pour des considérations d'échelles) entraîne l'occurrence de changements abrupts dans le comportement du système.
5. Différentes forces externes influencent le système à de multiples échelles.

Ces caractéristiques des systèmes morphologiques ont des conséquences importantes pour l'avancement des connaissances. Des notions comme la non-linéarité, la complexité, la sensibilité aux conditions initiales et externes, le chaos, l'autosimilarité, la hiérarchie et l'équilibre ont été abondamment discutées (Phillips, 1992; Phillips, 2003; Phillips, 2006; Huggett, 2007; Nicholas et Quine, 2007; Murray et al., 2009; Phillips, 2009; Keiler, 2011). On constate que le problème de la forme des chenaux alluviaux n'est toujours pas résolu (Eaton et al., 2004). En fait, certains vont jusqu'à avancer que la notion de l'équilibre dynamique entre l'écoulement, la capacité de transport et les apports en sédiments n'est qu'un sous produit émergent de principes physiques fondamentaux (Mayer, 1992; Phillips, 2010). Les systèmes seraient plutôt en perpétuel déséquilibre en réponse à des forces qui changent continuellement à diverses échelles de temps (Bracken et Wainwright, 2006). Mis à part le développement de modèles numériques basés sur l'approche systémique (Werner, 1999), la prise en considération explicite de la complexité lors de mesures sur le terrain, ou même en laboratoire, reste difficile et donc l'interprétation des résultats selon une approche systémique demeure largement philosophique ou conceptuelle. En effet, la juxtaposition des processus signifie qu'il devient très difficile d'en isoler un seul afin de comprendre sa variabilité de manière expérimentale, tel que requis par l'approche réductionniste. De plus, c'est en étudiant ces multiples relations entre les processus, qu'elles soient simplement additives ou aient un effet amplificateur, qu'on arrive à une compréhension globale du système. Aussi, l'existence de processus caractérisant le fonctionnement du système variant d'une échelle à l'autre entraîne le développement des modèles conceptuels, théoriques ou numériques spécifiques à une échelle donnée. Finalement, les processus de forçage externes au système interagissent avec les processus internes et peuvent compliquer l'interprétation de l'histoire, ou de la trajectoire du système, pourtant essentielle à la compréhension globale.

### 1.2.2. Contexte contemporain

Ainsi, nous assistons présentement non pas à un changement de paradigme mais plutôt à un élargissement des approches (Murray et al., 2009). En effet, la géomorphologie fluviale a évolué de l'approche où une seule réponse, une seule direction est possible pour un système à la reconnaissance de la multiplicité des réponses où plusieurs trajectoires sont possibles pour une même forme du paysage. Cette perspective sur l'évolution des systèmes peut être résumée par les quatre R : la Réponse (délais de réaction et de relaxation), la Résistance (par rapport aux facteurs de changements), la Résilience (capacité de récupération, basée sur la dynamique de la stabilité) et la Rétroaction (positive ou négative) (Phillips, 2009). Murray et al. (2009) ont proposé une liste de cinq caractéristiques empruntées à la science des systèmes complexes qui s'appliquent en géomorphologie et dont les conséquences sont majeures pour l'explication des phénomènes :

1. Les processus déterministes interagissent localement de façon non-linéaire en produisant une réponse spatialement distribuée si complexe qu'elle est au mieux chaotique, même si certains patrons caractéristiques peuvent être identifiés.
2. L'auto-organisation crée des structures locales issues d'interactions entre des éléments locaux du système.
3. Les comportements temporels autogènes, y compris les changements soudains, surviennent sans forçage externe apparent.
4. Les éléments caractéristiques des grandes échelles (autrement dit les formes du paysage) sont des propriétés émergentes, c'est-à-dire qu'ils ne sont pas explicables par la décomposition en ses éléments plus petits, un obstacle majeur en regard de l'approche réductionniste.
5. L'autosimilarité est une caractéristique des systèmes géomorphologiques à travers une gamme d'échelles spatiales et temporelles.

Toutes ces considérations se font à un niveau fondamental mais elles répondent aussi à la demande accrue du savoir géomorphologique dans la restauration et la planification environnementale (Thorndycraft et al., 2008). En effet, la connaissance de l'interaction des processus dans l'évolution du paysage amène le développement d'une discipline pratique de la géomorphologie où il faut développer des outils afin de caractériser et prédire la réponse des systèmes à des perturbations anthropiques et

environnementales (Downs et Gregory, 2004). Ces développements récents sont en grande partie survenus suite à la réalisation de l'importance de la dynamique des habitats pour les organismes vivants (Murray et al., 2009).

À travers toutes ces interrogations, la notion d'échelle reste au cœur de la réflexion en géomorphologie fluviale (Schumm et Lichaty, 1965; Lane et Richards, 1997; Church, 2006b; Nikora, 2007). L'écoulement, le moteur de la rivière, est hautement variable dans le temps, du centième de seconde à la dizaine, voir la centaine d'années. La connexion entre l'échelle de la variabilité hydrologique et l'échelle de la turbulence reste un défi de taille, d'autant plus que la variabilité de l'échelle intermédiaire de l'ordre de quelques minutes à quelques jours est mal définie (Nikora, 2007). L'étude des phénomènes à différentes échelles reste cruciale afin de comprendre l'agencement des conditions qui conduisent à l'émergence des formes fluviales (Kocurek et al., 2010). En effet, les formes du lit seraient des patrons émergents résultant de l'interaction de processus dans des conditions spécifiques puisque chaque forme est unique, même s'il y a des similarités entre elles (Werner, 1999). Il s'agit de déterminer à quel point la compréhension du mouvement individuel des particules, un phénomène de petite échelle, permet de comprendre l'organisation des formes des lits alluviaux à plus grande échelle. Certains vont même jusqu'à avancer que l'approche réductionniste qui vise à examiner les relations entre les formes et les processus de manière isolée est le problème fondamental qui empêche de comprendre les formes du paysage en raison de leurs échelles spatio-temporelles différentes (Harrison, 2001). Ainsi, il y a un besoin grandissant pour des mesures de haute résolution temporelle et spatiale qui permettent d'apprécier les dynamiques à différentes échelles et de vérifier l'applicabilité du transfert des processus entre les échelles (Lane et Richards, 1998; Lawler et Fairchild, 2010).

Malgré cet appel à l'acquisition de données probantes, il faut aussi s'interroger sur la façon de les récolter, les utiliser et les analyser sur le plan philosophique. L'élaboration de théories scientifiques passe par la construction de modèles causaux entre des variables d'intérêt en se basant sur des hypothèses. Bien que l'élaboration des expériences et protocoles de mesure réponde généralement à l'objectif de confirmer ou d'infirmer une hypothèse, le contrôle des conditions expérimentales favorise l'observation de résultats inattendus (Dunbar et Fugelsang, 2005a). En effet, environ 50 % des découvertes scientifiques surviendraient par hasard (Dunbar et Fugelsang, 2005b). Toutefois, c'est lors

de l'interprétation des résultats inattendus que l'ouverture d'esprit est nécessaire pour reconnaître la découverte (Dunbar et Fugelsang, 2005a). En mettant l'accent sur l'infirmité ou la confirmation d'hypothèse, il y a inévitablement une simplification des situations qui peut amener à sous-estimer l'importance de certains phénomènes inattendus (Rhoads, 1999).

En utilisant des exemples de recherche, Richards (1996) souligne qu'un des héritages de l'approche réductionniste et de l'approche hypothético-déductive qui en résulte est la collecte de données similaires pour un grand nombre de cas afin de pouvoir utiliser l'inférence statistique pour généraliser les résultats de manière empirique. Cette approche exhaustive est dominante au début de la révolution quantitative en géomorphologie mais elle a été remplacée de plus en plus par des mesures intensives à quelques sites d'études afin d'obtenir des informations plus détaillées sur les processus. Cette approche ne bénéficie toutefois pas du même crédit quant à son potentiel de généralisation. Afin de permettre une forme de généralisation, elle se base sur un raisonnement théorique d'interprétation des phénomènes. L'approche théorique a aussi été largement utilisée pour les expériences avec des modèles réduits où on a pu remettre l'inférence statistique de l'avant en utilisant des répliques d'expériences. Toutefois, comme les modèles réduits demeurent une simplification de la réalité, le besoin de mesurer intensivement les processus sur le terrain est toujours présent.

Alors que la sélection des sites pour une étude exhaustive est généralement fondée sur des règles d'échantillonnage statistiques acceptées, le choix d'un nombre limité de sites, voire même d'un seul, n'est guidé ou contraint par aucune règle. Souvent le choix est guidé par des raisons logistiques. Ainsi, les études intensives basées sur un nombre restreint de sites sont souvent jugées comme limitée quant à leur potentiel de généralisation à cause de l'impossibilité d'utiliser l'inférence statistique. Or, Richards (1996) prétend qu'au contraire, les études de cas ont le potentiel d'offrir une explication scientifique théorique, par opposition aux explications empiriques des études extensives. En effet, la multiplication des études de cas par plusieurs chercheurs indépendants permet la création d'une pensée latérale sur les facteurs interreliés. Les études de cas se développent souvent pour tester des idées à propos de mécanismes. Selon Richards (1996), les meilleures expériences sont éclectiques et elles portent à mettre l'effort sur la multiplication des approches à un problème plutôt que sur la multiplication des sites. Les études en profondeur d'un nombre

restreint de cas permettent de remettre l'accent sur ce qui rend un site unique en fonction des conditions locales et de ramener la notion ‘historique’ dans la géomorphologie, c'est-à-dire d'intégrer les trajectoires particulières de l'évolution des formes du paysage. Ce type d'approche nécessite toutefois de s'éloigner des tests d'hypothèses classiques puisque les résultats obtenus sont rarement prévisibles, surtout en milieu naturel.

### 1.2.3. Directions futures

Dans un symposium nommé *Geomorphology : a 2020 Vision*, qui a fait l'objet d'un numéro spécial dans *Earth Surface Processes and Landforms* les organisateurs nous mettent au défi d'être capable de produire des prévisions géomorphologiques, au même titre que les prévisions météorologiques, comme par exemple un bulletin détaillant les taux d'érosion pour les prochains 48 heures (Lawler et Fairchild, 2010). La compréhension du transfert des sédiments et des changements morphologiques a typiquement été approchée par l'étude de causes et d'effets individuels, plutôt que sur la chaîne d'interactions de processus, en incluant des rétroactions complexes (Raven et al., 2010). Il existe assurément un besoin en recherche pour dépasser l'étude des processus individuellement afin de mettre l'accent sur l'étude des interactions des phénomènes à l'échelle locale. Il s'agit d'un objectif louable mais difficile à réaliser notamment pour des raisons logistiques (Richards et Clifford, 2008). Dans ce contexte, Church (2010) a dressé un bilan des questions contemporaines et des directions futures de la recherche en géomorphologie sur le plan conceptuel :

1. La transformation du paysage passe par le transport du matériel sur les versants et dans les chenaux. Or, malgré des tentatives multiples pour comprendre les flux de matériel et le développement d'équations prédictives au cours du dernier siècle (Dietrich et al., 2003), il n'existe toujours aucune loi du transport de sédiments qui soit entièrement satisfaisante. Les approches à ce problème devront se multiplier car il est impératif de comprendre le transfert des sédiments dans le paysage.
2. Il faut réconcilier l'information géomorphologique et la représentation des processus à différentes échelles. Premièrement, il faut résoudre les questions reliées à l'extrapolation de l'information à l'échelle du paysage. Par exemple, les modèles réduits simplifiés à l'extrême peuvent-ils vraiment représenter les processus dominants ? Deuxièmement, il faut se pencher sur la réconciliation entre les théories

et modèles à différentes échelles de représentation. Ici, il s'agit d'arriver à un niveau de généralisation et de simplification adéquats pour permettre de réconcilier par exemple, le modèle d'évolution d'un chenal avec le modèle d'évolution d'une orogénie.

3. On doit développer de nouvelles approches afin d'inclure les dynamiques complexes des systèmes, tel que la non-linéarité, l'auto-organisation, l'autosimilarité, les propriétés émergentes et les comportements autogènes afin d'améliorer notre compréhension et notre capacité de prédiction.
4. Les plantes et les animaux jouent un rôle majeur dans les changements morphologiques et peu d'attention à ce jour y a été porté, et ce particulièrement dans l'étude de la dynamique fluviale. L'exemple des écrevisses est assez évocateur : dans une expérience en chenal expérimental, le déplacement des particules du lit par un écrevisse a provoqué un taux de transport deux fois plus important que celui observé en l'absence d'écrevisse (Johnson et al., 2011).
5. Il faut investiguer le rôle du climat en géomorphologie. À court et moyen terme, les changements climatiques influencent le cycle hydrologique ce qui aura des conséquences sur les systèmes géomorphologiques. Par exemple, il y a un besoin de comprendre les effets d'un changement dans le régime annuel des précipitations sur les processus géomorphologiques.
6. Considérant que l'humain est l'agent géomorphologique dominant sur la planète (Hooke, 2000), l'intégration des effets anthropiques dans notre compréhension des systèmes doit dépasser la simple étude de cas. Les géomorphologues font face au besoin urgent de trouver un nouveau paradigme qui investiguera l'intersection entre les processus géomorphologiques et l'humanité, mais aussi par rapport au monde vivant et au climat.

Il existe donc une dichotomie dans la géomorphologie contemporaine. D'un côté, une géomorphologie globale du système terrestre dans le contexte des changements environnementaux et anthropiques émerge. Il y a un appel au développement d'une science unifiée des systèmes terrestres en recouvrant l'hydrologie, la géomorphologie, la géochimie et l'écologie (Paola et al., 2006). D'un autre côté, l'héritage de l'approche réductionniste est toujours présent dans la volonté de développer des lois, notamment celles du transport des sédiments qui gouvernent la redistribution du matériel à la surface de la terre, dans

l'espoir que l'identification de ces lois permettra de comprendre la complexité des formes du paysage. Cette orientation exige la maîtrise d'une panoplie de méthodes de mesures et une solide connaissance mathématique et analytique afin de déterminer le niveau approprié de réductionnisme à appliquer à un problème de recherche. Ces deux visions de la géomorphologie sont unies par la volonté de comprendre les paysages, soit dans ses éléments fondamentaux, soit globalement. Cette thèse s'inscrit dans la deuxième approche dont l'objectif est l'appréciation de la complexité des processus géomorphologiques en interactions.

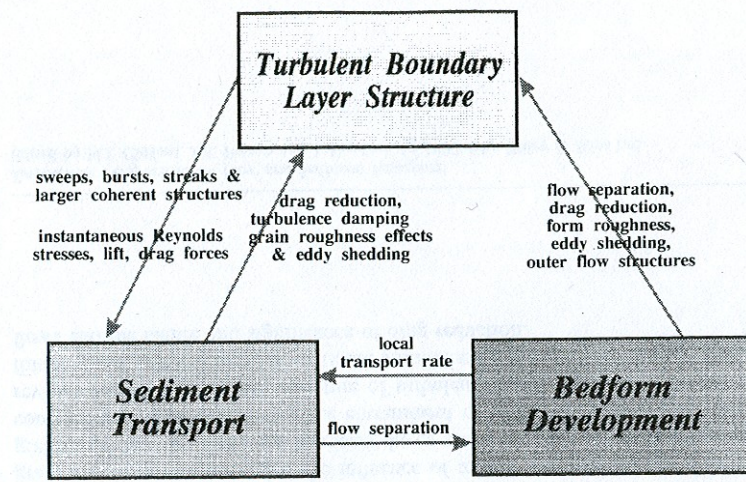


Figure 1.1 Interactions et rétroactions entre la couche-limite turbulente, le transport de sédiments et le développement des formes du lit (dans Best (1993), modifié de Leeder (1983)).

### 1.3. Problématique et objectifs

Cette thèse découle directement des questions philosophiques contemporaines en géomorphologie et son orientation est essentiellement conceptuelle en ce que l'objectif global est d'ouvrir de nouvelles pistes de réflexion pour mieux comprendre l'évolution des formes fluviales en misant sur l'étude des interactions et rétroactions entre les processus. Afin d'appréhender la complexité du système fluvial, une approche fondée sur le terrain est privilégiée puisque les expériences en laboratoire et les modèles numériques doivent nécessairement simplifier la réalité, ce qui est opposé à l'objectif général de la thèse. Le contexte utilisé est celui de la *trinité fluviale*, un cadre conceptuel qui représente les interactions et rétroactions entre la couche-limite turbulente, le transport de sédiments et les formes du lit dans un chenal (Figure 1.1). Ce schéma a été proposé par Leeder (1983) et plus tard actualisé par Best (1993). D'abord élaboré suite à des expériences en chenal en lit sablonneux, ce cadre conceptuel a vite été appliqué aux rivières graveleuses, où l'accent a été mis sur les interactions entre la couche-limite turbulente, les éléments de rugosité comme les amas de galets et le transport de sédiments en charge de fond (Brayshaw et al., 1983). D'abord élaboré pour des échelles fines, le concept a ensuite été élargi aux processus couvrant une section de cours d'eau comme par exemple dans les rivières tressées (Goff et Ashmore, 1994) ou encore en laboratoire (Hoey et Sutherland, 1991; Bennett et Bridge,

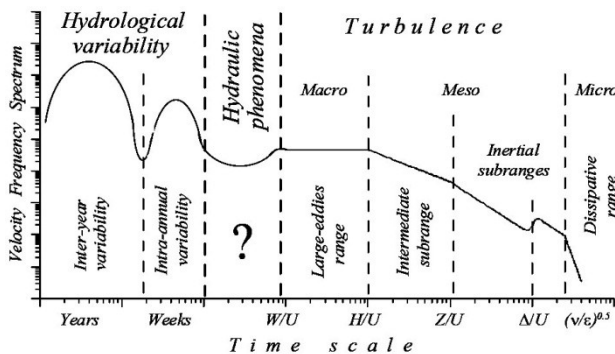


Figure 1.2 Spectre de puissance temporel de la vitesse schématisé dans les rivières à lit de graviers représentant les échelles de variabilité de l’écoulement pour différentes échelles caractéristiques (Nikora, 2007).

1995a; b). À l’origine, Leeder (1983) a souligné l’importance d’approcher la dynamique fluviale comme un tout et nous prévient contre les dangers d’étudier une portion isolée. Or, sur le plan logistique, mesurer simultanément plusieurs processus fluviaux durant une crue demeure un défi considérable, malgré les avancées technologiques (Powell et al., 2001) alors que c’est probablement l’étude explicite des interactions qui nous permet de mieux comprendre les systèmes géomorphologiques (Raven et al., 2010).

Dans cette optique, la thèse mettra l’accent sur les interactions et rétroactions entre les processus dans un cours d’eau à lit de graviers en milieu naturel (Figure 1.1). Les échelles de temps étudiées se démarquent de celle de l’ordre de la turbulence utilisée par Leeder (1983) et Best (1993) en ce que l’échelle temporelle de prédilection est celle de la crue et l’échelle spatiale de base est celle de la section de cours d’eau. Le choix de l’échelle temporelle ajoute un défi supplémentaire, puisque la variabilité de l’écoulement durant les crues reste relativement méconnue et peu de connaissances nous permettent de relier cette échelle de variabilité à la variabilité due à la turbulence ou celle liée aux variations interannuelles du débit comme l’illustre la Figure 1.2. Les mesures à l’échelle de la crue en temps continu permettent de connaître les conditions initiales et aussi les forces en jeu avant chaque évènement de crue. Chaque chapitre présentant les résultats est basé sur un objectif traitant spécifiquement des interactions dans la *trinité fluviale* (Figure 1.3). Particulièrement, c’est l’explication de la variabilité du transport de sédiments en charge de fond qui est au cœur de la thèse, que ce soit par la mesure directe de ce processus ou par la mesure indirecte de facteurs qui jouent sur le transport. Parallèlement, chaque étude de cas

est traitée selon un des problèmes contemporains en géomorphologie comme nous l'avons montré précédemment (Figure 1.3) :

**Chapitre 2.** Problème : L'imbrication des échelles.

Interaction : Écoulement et formes du lit.

Objectifs : 1) Caractériser les échelles de fluctuations de vitesse de l'écoulement pour une gamme d'échelles allant du dixième de seconde à plusieurs heures pour des écoulements stables et constants ; 2) tester leur relations avec des échelles morphologiques caractéristiques et 3) discuter du potentiel de ces échelles de fluctuations de l'écoulement sur le transport de sédiments en charge de fond.

**Chapitre 3.** Problème : L'absence d'équilibre due à des forces changeantes.

Interaction : Écoulement et transport de sédiments en charge de fond.

Objectif : Évaluer le rôle de l'accélération et la décélération de l'écoulement à l'échelle de la minute sur le transport de sédiments en charge de fond au cours d'une crue.

**Chapitre 4.** Problème : La mesure des processus complexes en milieu naturel.

Interaction : Transport de sédiments en charge de fond et formes du lit.

Objectif : Évaluer le potentiel de l'utilisation simultanée de différentes méthodes de mesures du transport en charge de fond afin de mieux comprendre les interactions et rétroactions avec les formes du lit.

**Chapitre 5.** Problème : Transfert d'échelles et réponses multiples.

Interaction : Transport de sédiments en charge de fond et formes du lit.

Objectif : Définir quels aspects du transport en charge de fond interagissent avec différentes échelles de changements morphologiques suite à une crue.

**Chapitre 6.** Problème : Approche systémique, détection de relations non-linéaires.

Interactions : Écoulement, transport de sédiments en charge de fond et formes du lit.

Objectif : Développer de nouvelles approches analytiques qui permettent de mieux cerner les dynamiques complexes entre l'écoulement, le transport de sédiments en charge de fond et les changements morphologiques en incluant explicitement la notion d'histoire du système et celle des conditions initiales.

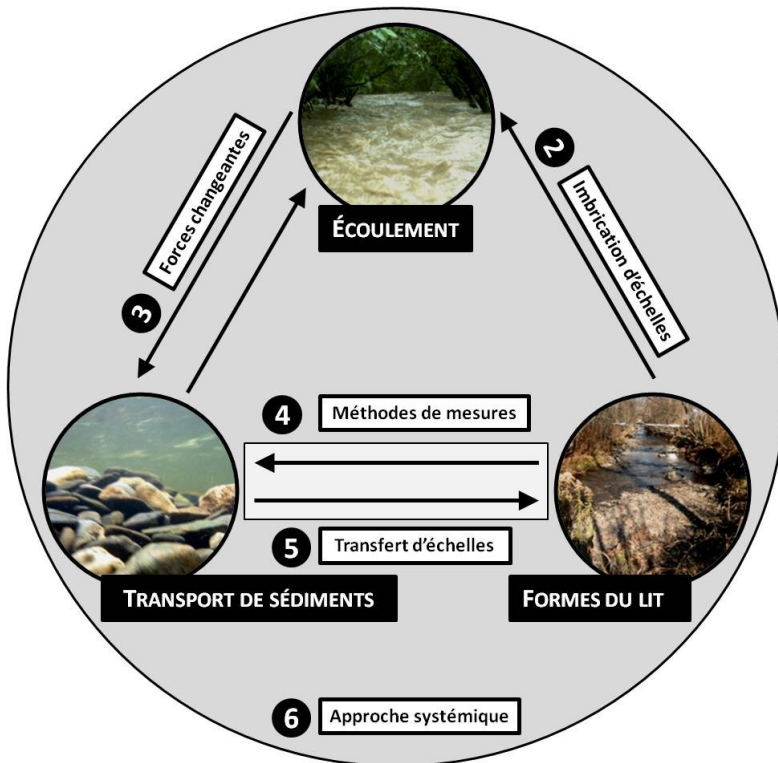


Figure 1.3 Cadre conceptuel de la thèse situant les cinq chapitres de résultats ainsi que les considérations conceptuelles traitées dans chacune des études de cas au sein de la trinité fluviale, modifiée de Leeder (1983) et Best (1993).

Les objectifs spécifiques de la thèse s'inscrivent donc dans la perspective de développer les idées qui ont cours en géomorphologie contemporaine et de les rendre plus concrètes en utilisant une étude de cas. La thèse se veut une proposition de réflexions où des approches méthodologiques renouvelées et des analyses adaptées aux réponses complexes des systèmes morphologiques sont explorées. Les objectifs sont pour la plupart exploratoires à l'exception des deux premiers, qui découlent d'hypothèses liées à des recherches récentes en rivière. Dans les deux cas, elles sont partiellement confirmées et une interprétation des résultats plus raffinée découle de l'exploration du jeu de données. Dans le cas de tous les objectifs, c'est l'approche exploratoire qui a permis de générer les conclusions les plus intéressantes. Bien que risquée, cette approche semble être la mieux adaptée au contexte actuel où l'on constate que l'approche réductionniste a ses limites et que l'étude intensive d'un site a le potentiel de générer de nouvelles connaissances. Cette thèse confirme que les études détaillées d'observations sur le terrain sont d'une importance

cruciale pour comprendre la nature complexe des rivières, et particulièrement les relations non-linéaires qui ont cours entre les processus.

La structure de la thèse comporte donc deux gradients de complexité. Dans un premier temps, au fur et à mesure que progresse la thèse de plus en plus d'éléments de la dynamique fluviale sont étudiés et dans un deuxième temps, l'aspect complexe des processus et des comportements de la rivière est de plus en plus considérés explicitement. Cette recherche est par conséquent basée sur une panoplie de méthodes de mesures simultanées qui a permis de générer une quantité de variables et d'indicateurs des dynamiques fluviales. Autant des données abondantes sont souhaitables pour comprendre les dynamiques complexes des rivières, autant elles peuvent être si nombreuses qu'il devient difficile de trouver les tendances recherchées. Dans cette optique, la thèse pose aussi une réflexion sur le type d'analyses employées en géomorphologie. L'héritage réductionniste de la discipline et la construction des théories à partir d'équilibre de forces ont pour conséquence l'utilisation majoritaire des régressions linéaires à deux variables. En multipliant le nombre de variables il devient évident que cette approche atteint ses limites rapidement. C'est pourquoi quatre des cinq chapitres introduisent les analyses multivariées comme une approche dont le potentiel est très grand pour comprendre les géosystèmes, surtout lorsque les données ont été récoltées en milieu naturel, en l'absence de contrôle expérimental.

## 1.4. Contexte scientifique

Le sujet de la thèse étant très vaste, il est préférable de revoir les éléments clés de la littérature lié aux processus d'intérêt en introduction de chapitre. En effet, faire une synthèse des connaissances de tous les processus fluviaux considérés ici pour une gamme d'échelles ne servirait pas adéquatement le propos, c'est-à-dire d'explorer de nouvelles avenues afin d'appréhender les dynamiques complexes des systèmes fluviaux. Par ailleurs, pour le bénéfice du lecteur, nous dressons ici un portrait général des études recensées dans les chapitres de résultats. Chacun des chapitres fait référence à plus de 50 articles scientifiques, livres ou actes de conférences (Figure 1.4a). Au total ce sont plus de 200 références uniques qui sont utilisées, dont seulement le quart se retrouve dans plus d'un chapitre (Figure 1.4b). En effet, environ 30 références par chapitre sont uniques à ce chapitre, ce qui illustre la variété des thèmes traités dans cette thèse. Les chapitres qui partagent le plus de références sont les chapitres 5 et 6 en raison de l'utilisation du même jeu de données dans le but de les soumettre en tant qu'articles compagnons. On peut constater qu'environ la moitié des références citées ont été publiées après l'année 2000. Toutefois, la décennie des années 90 a produit une multitude de travaux traitant de la variabilité des processus fluviaux et beaucoup de ces recherches servent de point de départ à la réflexion proposée dans la thèse, ce qui explique qu'ils occupent environ le tiers du total. Quand aux articles plus anciens, ce sont souvent des articles majeurs qui ont établi les bases de la discipline. Au-delà de la répartition entre les chapitres et de leurs années de publication, chacune des références a été classée selon deux critères afin de mieux comprendre la structure de la thèse : selon le thème principalement traité et selon l'approche méthodologique utilisée.

Les thèmes choisis recoupent le schéma conceptuel de la Figure 1.3. D'abord, il y a les articles qui traitent exclusivement d'une des trois pointes du triangle, soit l'écoulement, le transport de sédiments en charge de fond ou la morphologie. Souvent ces articles discutent des implications des conclusions de l'étude sur la dynamique fluviale en général mais sans avoir mesuré ou considéré explicitement d'autres aspects dans le plan d'échantillonnage. Ensuite, il y a les articles qui traitent des interactions entre deux pointes du triangle, soit les interactions entre l'écoulement et le transport de sédiments, entre l'écoulement et la morphologie ainsi qu'entre le transport de sédiments et la morphologie.

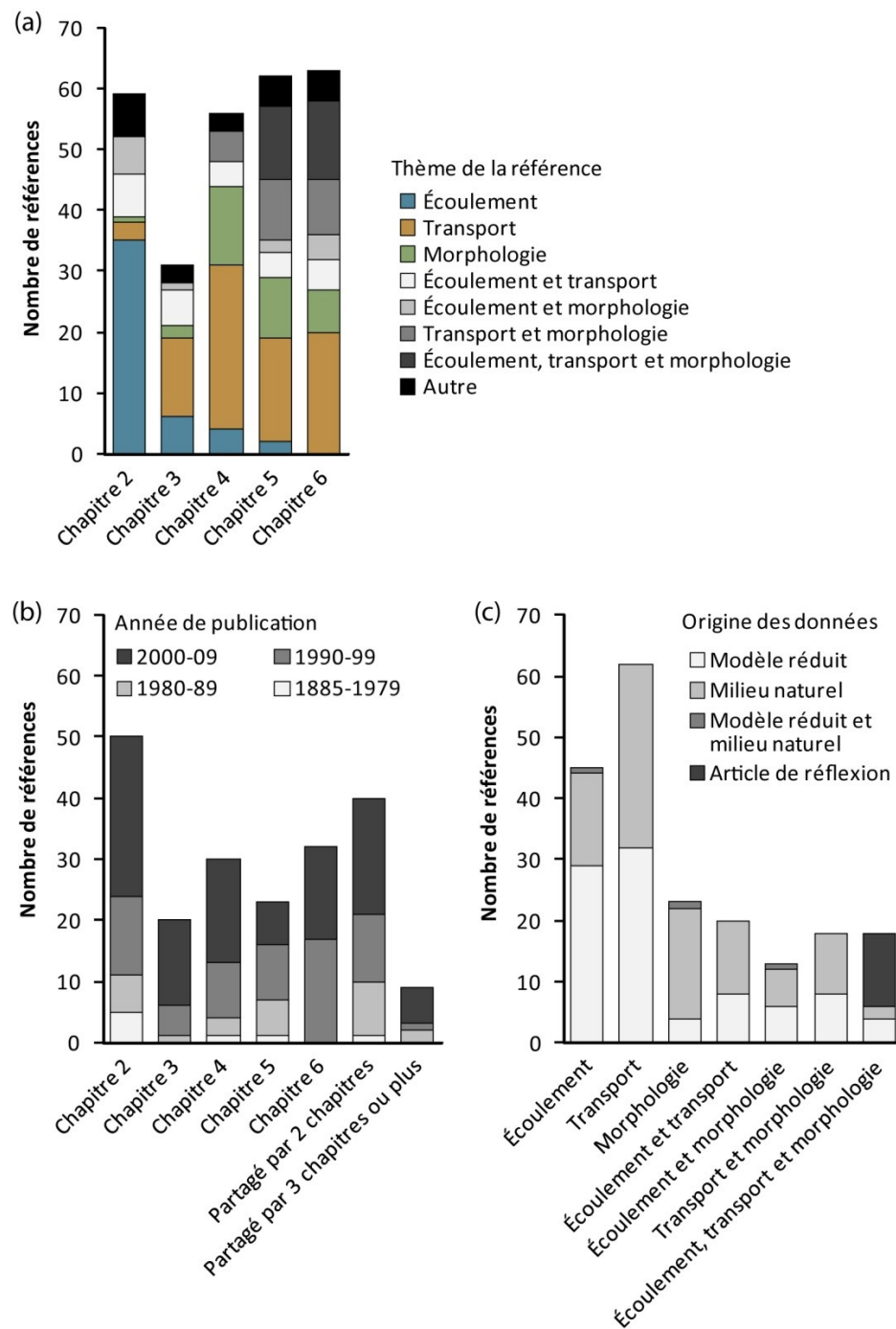


Figure 1.4 Compilation des références citées dans les chapitres de résultats. (a) Nombre de références par chapitre selon le thème traité. (b) Nombre de références uniques à chacun des chapitres et partagées par plusieurs chapitres représentées selon l'année de publication. (c) Nombre de références par thème et selon l'origine des données. Voir le texte pour des explications sur le classement des références.

Finalement, il y a les articles qui traitent de la *trinité fluviale* dans son ensemble. Pour des raisons de simplification, aucune distinction entre les échelles d'études n'a été faite. Par exemple, les articles classés dans le groupe «écoulement» englobent autant les études détaillées de la couche-limite turbulente que l'estimation de la force critique de cisaillement pour une section entière de cours d'eau. Dans le même ordre d'idées, les articles portant sur un développement méthodologique n'ont pas été distingués car ces travaux utilisent généralement des cas choisis afin d'illustrer une application particulière dans l'étude des dynamiques fluviales. Les références qualifiées de «autre» sont majoritairement des livres de base ou encore des articles traitant d'analyses quantitatives ou autre thème ne faisant pas partie du corpus de littérature rattaché à la géomorphologie fluviale. À noter que ces références ne sont pas comptabilisées dans les Figure 1.4a et b.

Pour le deuxième classement, les références ont été distinguées selon l'approche méthodologique dominante, à savoir si les mesures ont été récoltées sur le terrain, en laboratoire dans un modèle réduit ou encore en combinant les deux approches. Une quatrième catégorie représente les articles de réflexion, soient ceux qui utilisent de multiples exemples pour discuter de différents thèmes ou proposer une recension de la recherche dans un champ donné. Comme cette recherche est entièrement basée sur des mesures, très peu de références citées traitent de modèles, qu'ils soient empiriques, théoriques ou numériques. De plus, les articles portant sur les modèles utilisent en général des données pour calibrer ou valider le modèle. Donc, ces articles ont été classés selon l'origine des données utilisées.

La Figure 1.4a illustre la distribution des thèmes basés sur la *trinité fluviale* selon les différents chapitres. Sans surprise, les thèmes des articles évoluent en fonction des thèmes traités dans les chapitres de la thèse. Particulièrement, on voit que la dominance des références traitant d'un seul thème diminue avec la progression des chapitres qui traitent progressivement d'interactions de plus en plus complexes. Toutefois, on observe que la majorité des références traitent d'un seul thème et que les articles traitant d'interactions sont plus rares (Figure 1.4c). Ce constat illustre clairement le besoin d'augmenter les études étudiant spécifiquement les interactions entre les processus fluviaux. La morphologie est plus rarement étudiée en isolation et souvent son étude est couplée soit avec l'investigation de l'écoulement ou du transport de sédiments. Bien que les études centrées sur l'interaction entre deux processus soient moins nombreuses, les études traitant de deux interactions ou

plus le sont encore davantage. De plus, plus de 50 % des références traitant de la dynamique selon une approche globale en considérant simultanément l'écoulement, le transport de sédiments et la morphologie sont en fait des articles de réflexion ou de discussion (Figure 1.4c).

Cette thèse étant basée sur des mesures de terrain, nous avons consacré une attention particulière aux études également basées sur des mesures en milieu naturel afin de comparer les résultats. Malgré ce biais dans la recherche bibliographique, les études citées dans les chapitres proviennent en proportions égales de recherches sur le terrain que de recherches en chenal expérimental. Cet état de la situation illustre bien les tendances de la recherche en géomorphologie fluviale, soit la difficulté d'obtenir des résultats probants sur les processus à partir de mesures réalisées en milieu naturel par rapport au test d'hypothèse réalisé en milieu contrôlé comme dans un chenal expérimental. Donc, une fois encore, cette analyse souligne la pertinence de développer un programme de mesure intensif en milieu naturel.

## 1.5. Considérations méthodologiques

La récolte de données pour cette thèse s'est déroulée entre 2006 et 2009 et le design expérimental et les processus étudiés sont donc fortement influencés par l'héritage réductionniste de la géomorphologie en raison de l'orientation fortement axée sur l'explication des processus par leur mesure. Toutefois la thèse est tout à fait actuelle en ce qui concerne les questions posées car elle met l'accent sur les interactions entre les processus. Particulièrement, les notions d'échelle, d'histoire, de conditions initiales et de changements sont au centre de la recherche. Les mesures intensives en milieu naturel, malgré les inconvénients logistiques et l'absence de contrôle expérimental, permettent d'étudier un système dans son ensemble et elles offrent un fort potentiel pour une meilleure compréhension des rétroactions. En contrepartie, le jeu de données doit couvrir plusieurs situations afin de pouvoir déceler les tendances. L'effort de terrain doit donc être soutenu dans le temps, surtout qu'il est soumis aux aléas météorologiques puisque l'essentiel de l'acquisition de données doit se faire durant des crues suffisamment intenses pour mobiliser les particules grossières du lit du chenal. Dans cette section, seuls les éléments généraux de la méthodologie seront relatés puisque les détails sont confinés dans chacun des chapitres de résultats. L'accent sera mis sur les considérations en jeu lors du choix du site et de l'instrumentation ainsi que des décisions liées au traitement des données brutes.

### 1.5.1. Choix du site

Toute la démarche de la thèse et les conclusions qui en découlent sont basées sur l'échantillonnage de l'écoulement, de la morphologie et du transport de sédiments en charge de fond en milieu naturel. Le choix d'un site de mesure est donc une étape cruciale de la démarche puisque les particularités sédimentaires et morphologiques du chenal teinteront inévitablement les résultats. En raison de la disponibilité des ressources matérielles et des contraintes temporelles, un seul site a été instrumenté pour mesurer le transport de sédiments en charge de fond. Bien que le chapitre 2 comprenne des mesures d'écoulement dans quatre autres rivières et des mesures comparatives en chenal expérimental, seul le site principal d'étude, le ruisseau Béard, sera décrit dans cette section. En effet, les spécificités des autres cours d'eau et le chenal expérimental sont bien décrits dans le chapitre 2. Le ruisseau Béard est réellement la fondation de la thèse puisqu'il se

retrouve dans chacun des cinq chapitres de résultats, et de manière exclusive dans quatre chapitres.

La sélection du ruisseau Béard découle de la visite de plus de 50 sites potentiels dans le sud du Québec durant l'été 2006. Nous avons ratissé les régions suffisamment près de Montréal pour permettre des visites fréquentes et dont les caractéristiques géologiques favorisent les rivières à lit de graviers. Sur le plan géomorphologique, le cours d'eau devaient présenter des indices de mobilité du lit afin d'obtenir un maximum de données de transport de sédiments durant la période de collecte (trois ans) : taille médiane des particules ( $D_{50}$ ) inférieure à 50 mm, pente du lit assez prononcée (0.01 à 0.02) et petit bassin versant possédant un temps de réponse à une précipitation relativement court. Sur le plan de la stratégie d'échantillonnage, le cours d'eau devait être étroit et relativement linéaire afin d'éviter la présence d'écoulements secondaires pouvant compliquer les interactions entre l'écoulement et le transport de sédiments. Finalement, sur le plan logistique, en plus de la proximité de Montréal, l'accès à la berge devait être direct pour faciliter le transport de matériel et des nombreux échantillons de sédiments. Ces critères ont mené au choix du ruisseau Béard, situé près de Bromont, en Estrie Figure 1.5. Le tronçon d'étude est caractérisé par une morphologie de seuil-mouille avec à l'occasion la présence de bancs alternés, un  $D_{50}$  de 40-50 mm, une largeur variant de 4 à 6 mètres et une pente d'environ 1 %. Le transport y est actif environ 5 à 10 fois par année et le niveau plein bord est de l'ordre d'un mètre avec un débit d'environ  $2.5 \text{ m}^3\text{s}^{-1}$ . Le bassin versant mesure 8 kilomètres carrés et les dépôts de surface sont un till glaciaire avec une matrice fine et un contenu en blocs et graviers constituant la principale source de sédiments grossiers pour le cours d'eau (Figure 1.5). Le temps de réponse hydrologique suite à un évènement de pluie oscille entre 2 et 8 heures en fonction de l'intensité et de la durée de la précipitation et des conditions antécédentes d'humidité. D'autres informations sur le site sont fournies dans chacun des chapitres selon l'objectif traité.

### **1.5.2. Stratégie d'échantillonnage**

Deux sections d'une longueur de 20 m chacune situées près de l'exutoire du bassin versant ont fait l'objet d'un suivi intensif. Les deux sections ont été choisies afin d'élargir le jeu de données en exposant des conditions différentes aux même crues vu l'impossibilité logistique d'instrumenter deux cours d'eau différents. Elles sont situées à environ 75 mètres

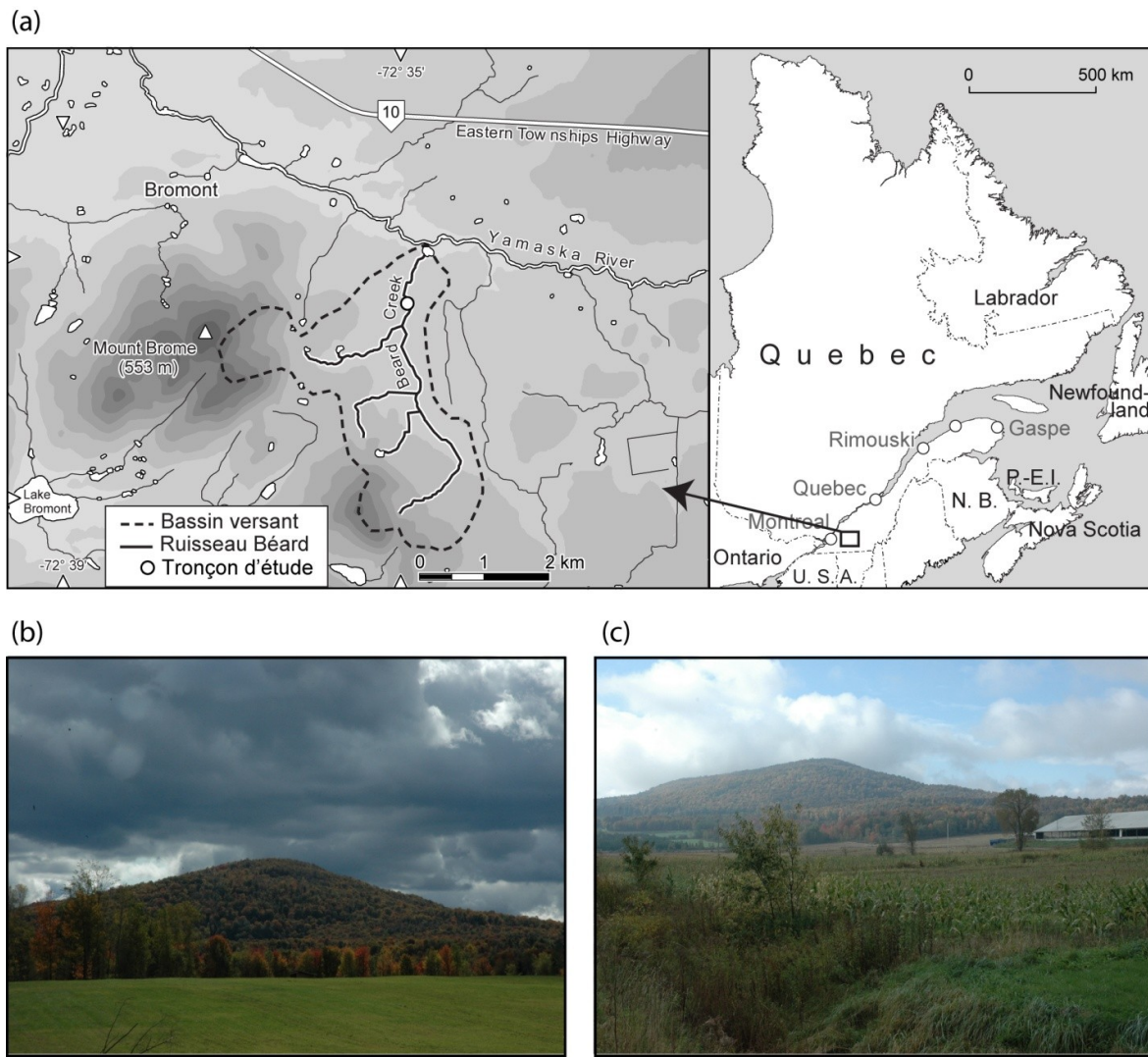


Figure 1.5 (a) Localisation et topographie du bassin versant du ruisseau Béard. (b) Photo du bassin versant du ruisseau Béard prise vers le Sud-ouest. (c) Photo du bassin versant du ruisseau Béard prise vers le Sud.

l'une de l'autre. Cette distance assure une certaine «indépendance» entre les processus morphologiques et sédimentaires des deux sections. De plus, elles ont des morphologies contrastées, ce qui permet d'augmenter le spectre des réponses morphologiques aux crues mobilisatrices des sédiments en charge de fond. La section aval est caractérisée par un banc d'accumulation latéral longeant un thalweg régulier et linéaire avec peu d'éléments de rugosité sur le lit et une taille médiane des particules de 43 mm. La section amont est caractérisée par deux séquences seuil-mouille bien définies sans réservoir de sédiments sous forme de banc d'accumulation. On y observe la présence de plusieurs éléments de rugosité tels que des amas de galets et des alignements latéraux de galets sur les seuils et

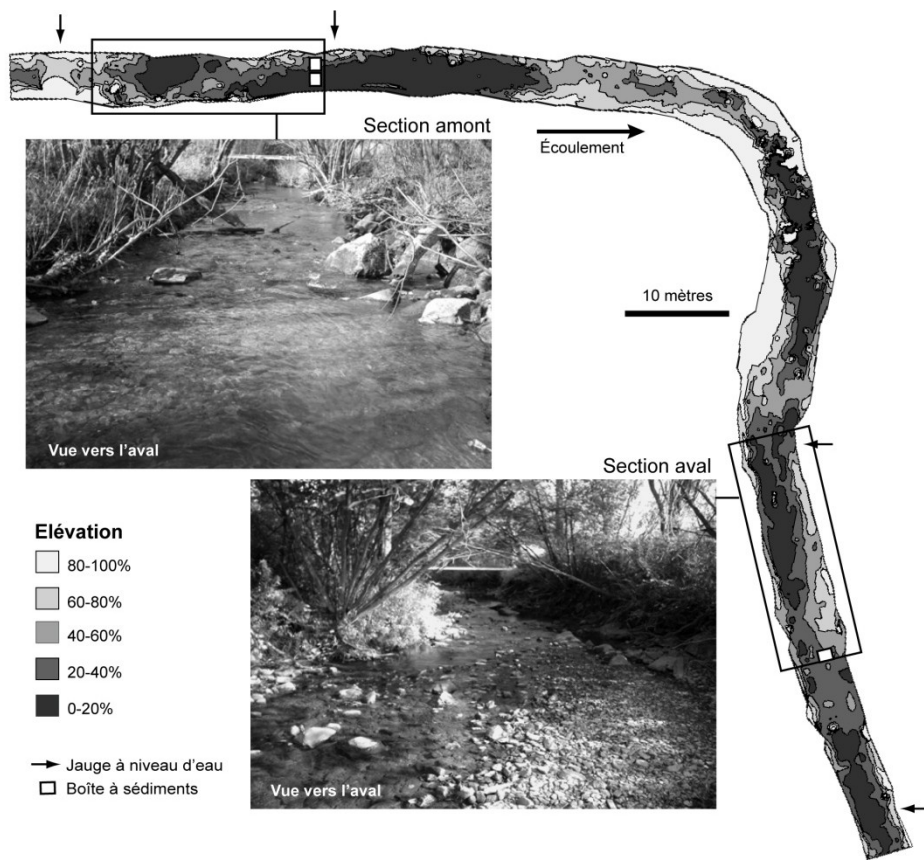


Figure 1.6 Emplacement des instruments automatisés et topographie du tronçon d'étude d'après l'interpolation des élévations résiduelles du lit (sans la pente du tronçon). Les classes d'élévation représentent un pourcentage de la distribution des élévations résiduelles de la section dont l'étendue est de 1.15 m. L'emplacement des sections est identifié par les encadrés le long du tronçon et leur allure générale est visible sur les photos.

une taille médiane des particules de 50 mm. Un schéma du tronçon et la localisation des instruments sont présentées à la Figure 1.6.

Idéalement, afin de pouvoir analyser les processus fluviaux à diverses échelles temporelles, un suivi automatisé de tous les processus à haute fréquence d'échantillonnage est nécessaire. Ce type de suivi est disponible pour la mesure de l'écoulement et du transport en charge de fond. Toutefois, aucune technologie n'est encore disponible pour suivre l'évolution des changements morphologiques au cours d'une crue en milieu naturel. Le plus petit pas d'échantillonnage possible est à l'échelle de la crue. Sur le plan pratique, cette échelle a l'intérêt d'être la plus facilement utilisable pour générer des modèles explicatifs. De plus, peu d'études à long terme ont suivi l'évolution morphologique du chenal à l'échelle de la crue. Souvent, le suivi morphologique est effectué annuellement et

donc les changements présentent l'effet cumulatif de plusieurs évènements de crue (Ashmore et Church, 1998).

Alors que la mesure de l'écoulement et celle de la morphologie sont guidées par des protocoles relativement standards, la mesure du transport en charge de fond peut être faite à partir d'une multitude d'instruments et d'approches. Des développements méthodologiques sont encore en cours comme l'illustre par exemple la conférence internationale *Monitoring bedload and debris flows* qui se tiendra en Octobre 2012 en Italie. Comme la stratégie d'échantillonnage préconise un suivi intensif des processus fluviaux en continu afin de pouvoir déterminer les conditions initiales et l'historique des changements morphologiques et des flux de transport pour chaque évènement de crue, la mesure du transport en charge de fond doit être automatisée. Cette contrainte limite grandement le choix des méthodes. Les boîtes à sédiments de type *Birkbeck* ont été choisies pour leur capacité à mesurer le transport de toutes les tailles de particules permettant ainsi de connaître les caractéristiques des particules transportées et autorisant un échantillonnage temporel de haute fréquence au cours d'une crue. Les boîtes à sédiments sont des échantillonneurs insérés dans le lit qui récoltent les particules en mouvement sur le lit dans une boîte ayant ouverture sur le côté exposé à la surface du cours d'eau. Les boîtes ont l'avantage d'affecter minimalement l'écoulement et de fournir une bonne précision de la mesure du transport en charge de fond (Laronne et al., 2003). Malgré les avantages de ces instruments, ils n'ont été installés que sur un nombre limité de sites en raison de leur coût élevé et de l'entretien intensif qu'ils exigent (Reid et al., 1980; Lewis, 1991; Kuhnle, 1992; Laronne et Reid, 1993; Harris et Richards, 1995; Alvera et Garcia-Ruiz, 2000; Garcia et al., 2000; Sear et al., 2000; Habersack et al., 2001; Cohen et Laronne, 2005; Vericat et Batalla, 2010). Les boîtes à sédiments sont généralement construites sur mesure en fonction des caractéristiques du site où elles sont déployées. La capacité de la boîte doit pouvoir accommoder les flux susceptibles de se produire dans le cours d'eau alors que la largeur de l'ouverture doit au moins être de la largeur du 90<sup>e</sup> percentile de la taille médiane des particules du lit (Bergman et al., 2007).

La particularité des boîtes à sédiments de type *Birkbeck* est qu'elles contiennent un système de mesure du poids permettant le suivi en continu des flux de transport en charge de fond. Les premières boîtes de ce genre ont été équipées d'un coussin de néoprène rempli d'eau « *pressure pillow* » dont les variations de pression sont reliées à l'accumulation des

sédiments dans la boîte (Reid et al., 1980). Pour améliorer la précision du poids mesuré et simplifier la conception de l'instrument, les coussins ont été remplacés par des cellules de charge au début des années 1990 par Lewis (1991). Lorsqu'une pression est appliquée sur la cellule, elle déforme des ponts de résistance ce qui induit un signal électrique proportionnel à la force appliquée. Comme la réponse est linéaire, il suffit de calibrer l'instrument avec des poids étalons. L'utilisation des cellules de charge améliore la mesure en continu de la charge de fond car elle est insensible aux variations du niveau d'eau lorsque ce dernier est inférieur à un ou deux mètres (Sear et al., 2000). Le seuil de détection des cellules de charge oscille entre 10 et 40 grammes en utilisant un système de répartition et de stabilisation du poids (Sear et al., 2000). La fréquence d'échantillonnage peut être très élevée car la réponse de la cellule de charge à une contrainte est immédiate. Seule la cellule de charge doit être calibrée annuellement et l'intérieur de la boîte nettoyé ce qui minimise les opérations d'entretien.

Trois boîtes à sédiments de type *Birkbeck* avec des cellules de charge permettant la mesure en temps réel du transport de sédiments en charge de fond durant une crue ont été installées au ruisseau Béard. Une seule boîte est utilisée dans la section aval, entre le banc latéral et le thalweg, ce qui représente un compromis dans la représentation de la variabilité latérale des taux de transport (Figure 1.6). Deux boîtes ont été installées dans la section amont à un tiers et deux tiers de la largeur de la coupe transversale (Figure 1.6). En amont, les ouvertures des boîtes occupent 6 % de la largeur du chenal alors qu'en aval l'ouverture couvre 2.5 %. Bien que les taux de transport soient reconnus pour être variables spatialement (Gomez, 1991; Powell et al., 1999), le chenal est relativement petit et la coupe transversale relativement trapézoïdale, ce qui favorise l'uniformité spatiale des taux de transports. De plus, l'analyse des taux de transport mesurés par les boîtes qui sont côte à côte dans la section amont montre qu'il existe une bonne corrélation entre les mesures ( $r > 0.5$ ), bien que la magnitude du transport soit différente due à la résistance des berges (Powell et al., 1999). Ainsi, la valeur absolue des taux de transport présentés dans cette thèse n'est probablement pas juste. Toutefois, s'il y a erreur elle n'a aucun impact sur les conclusions puisque les analyses portent sur la variabilité des taux de transport en relation avec différents facteurs causaux et ne sont pas axées sur la prédiction exacte de la charge en sédiments.



Figure 1.7 Photos des diverses composantes des boîtes à sédiments installées au ruisseau Béard. (a) Extérieur de la boîte avec le couvercle. (B) Intérieur de la boîte sans le couvercle et sans le boîtier interne. (c) Appareil de répartition du poids qui s'insère au fond de la boîte à sédiments. (d) La cellule de charge. (e) La cellule de charge dans son compartiment permettant la répartition du poids. (f) La boîte à sédiments de la section aval. Notez que le boîtier interne amovible est accessible lorsque le couvercle est retiré.

Les boîtes à sédiments ont été fabriquées par Martin Lambert et Jean-François Myre de l'atelier du Département de chimie de l'Université de Montréal (Figure 1.7). Elles ont été construites à partir des plans utilisés par Sear et al. (2000). Le plastique a été privilégié comme matériau pour minimiser les contractions et les expansions thermiques afin que les boîtiers soient le plus stables possible pour la durée de l'étude. Les boîtiers internes qui permettent de recueillir les sédiments en mouvement mesurent 30 cm de haut par 38.5 cm de large et 48.5 cm de long pour une capacité de totale de  $0.06 \text{ m}^3$  soit environ 85 kg de matériel sec. La largeur de l'ouverture est de 12 cm, ce qui correspond environ au 95<sup>e</sup> percentile de la distribution des tailles des particules du lit, et sa longueur est de 38 cm, environ 10 fois la taille médiane des particules du lit afin d'assurer que les particules en

saltation ne passent pas au-dessus de la boîte (Laronne et al., 2003). Des cellules de charge submersibles (Interface 2400, 0-110 kg) ont été placées sous les boîtiers internes dans un système de répartition du poids. Le design de l'instrument a permis d'atteindre un seuil minimal de détection d'environ 15 g (Figure 1.7). Le mécanisme interne des cellules de charge est compensé pour la température (-10 à 45°C) assurant ainsi un signal stable peu importe les conditions. Les calibrations en laboratoire (avant l'installation) et sur le terrain (après l'installation) sont toutes excellentes. Les relations entre les poids réels et le signal électrique de la cellule de charge montrent dans tous les cas une variance expliquée supérieure à 95 %, même après plusieurs années d'utilisation. Les boîtes ont été vidées après chaque crue mobilisatrice de la charge de fond et 25 % des sédiments ont été tamisés à des intervalles de un demi  $\Phi$ . Le traitement des séries temporelles mesurées avec les cellules de charge a été fait selon les standards établis (Habersack et al., 2001; Laronne et al., 2003).

Bien que les boîtes à sédiments permettent d'obtenir des informations détaillées sur les flux de sédiments et les caractéristiques des particules transportées, elles ne permettent pas de savoir d'où proviennent ces sédiments. En réponse à cette lacune, un relevé de l'activité du lit a été déployé dans les deux sections. Ce relevé consiste en une grille de marqueurs insérés dans le lit selon une grille référencée sur les berges de 4 par 20 mètres, pour un total de 80 marqueurs par section. Les marqueurs utilisés sont des rondelles de 35 mm de diamètre, une dimension similaire à la taille médiane des particules tel que prescrit par les chercheurs ayant développé la méthode (Konrad et al., 2002). Chaque marqueur est inséré entre les particules du lit parallèlement à l'écoulement. Ainsi, le marqueur est entraîné seulement si les particules l'enserrant sont mobilisées. Un relevé de la présence ou de l'absence des marqueurs a été effectué après chaque crue mobilisatrice de la charge de fond. Plus de détails sur la méthodologie employée et le traitement des données sont disponibles au chapitre 4.

En plus des mesures directes du transport en charge de fond et de l'activité du lit, la morphologie de chaque section a été caractérisée à l'aide d'une station totale robotisée de marque Trimble après chaque événement de crue mobilisant les particules du lit. La méthodologie du relevé, de la technique d'interpolation des données et de l'analyse des erreurs est expliquée en détails au chapitre 4.

Finalement, la mesure continue de l'écoulement a été automatisée au moyen de quatre jauge à niveau d'eau de marque Solinst. La jauge située complètement en aval du tronçon a servi à la construction d'une courbe de tarage afin de pouvoir estimer le débit. La courbe de tarage compte 22 mesures de débit récoltées manuellement à l'aide d'un vélocimètre à hélice pour différentes hauteur d'eau. La hauteur maximale échantillonnée est de 0.7 m, ce qui correspond à un débit de  $2.1 \text{ m}^3\text{s}^{-1}$ . Des données n'ont pu être récoltées à de plus fort débit pour des raisons de sécurité. La relation polynomiale d'ordre 2 qui lie les débits aux hauteurs d'eau est excellente, avec un coefficient de détermination de 98 %. Bien que la forme de la relation entre le débit et la hauteur d'eau est inconnue au-delà de 0.7 m, la relation de la courbe de tarage a été utilisée pour extrapoler les données car la forme de la coupe transversale était régulière. Les trois autres jauge ont été installées stratégiquement le long du tronçon afin de pouvoir estimer la pente de la surface de l'eau pour chacune des sections ainsi que pour l'ensemble du tronçon. La fréquence d'échantillonnage de tous les instruments automatisés est de 1 minute (boîtes à sédiments et jauge à niveau d'eau). Cette fréquence élevée permet de capter la variabilité des événements de très forte magnitude où les taux de changements de l'écoulement sont très rapides en raison de la petite taille du cours d'eau.

### 1.5.3. Jeu de données

Le suivi intensif de l'écoulement, du transport de sédiments en charge de fond et de la morphologie au ruisseau Béard a la particularité de combiner plusieurs méthodes de mesures du transport de sédiments en charge de fond. En effet, aucune des méthodes disponibles ne permet de mesurer à la fois la variabilité temporelle et la variabilité spatiale du processus. À notre connaissance, le jeu de données comptant 21 crues qui ont eu lieu durant le printemps, l'été et l'automne des années 2007 à 2009 est le plus complet jamais publié (Tableau 1.1). Le suivi intensif du ruisseau Béard s'inspire d'une tradition où des efforts ont été déployés pour mesurer tous les aspects de la géomorphologie fluviale; par exemple, la rivière South Esk en Écosse (Bridge et Jarvis, 1982), la confluence des rivières Bayonne et Berthier (Boyer et al., 2006) ou le ruisseau Moras (Macvicar et Roy, 2011), tous les deux situés au Québec. Ces sites représentaient un contexte morphologique particulier, soit un méandre, une confluence et une mouille forcée par un obstacle. Bien que l'écoulement, le transport de sédiments et la morphologie y aient été mesurés pour plusieurs débits, il manquait soit un enregistrement continu d'un des processus soit un synchronisme

entre les différentes mesures. Particulièrement, dans les rivières Bayonne-Berthier et South Esk, le transport de sédiments en charge de fond a été mesuré ponctuellement avec des échantilleurs Helleys-Smith. Au ruisseau Moras, le suivi de particules individuelles à l'aide de transpondeurs passifs a été utilisé pour mesurer le transport en charge fond.

Ce qui distingue notre recherche au ruisseau Béard, c'est la mesure en continu du transport en charge de fond dans une configuration morphologique relativement générique. Ceci permet l'intégration totale des processus. Plusieurs sites de suivi automatisé du transport de sédiments en charge de fond avec des boîtes à sédiments existent (e.g. Rio Cordon, Italie ; Nahal Yatir, Israël ; Ribera Salada, Espagne) mais pour aucun d'entre eux la morphologie et l'activité du lit n'ont été suivis après chaque évènement de crue. La combinaison des données d'écoulement, de transport de sédiments et de morphologie du lit permet de générer directement ou indirectement une multitude de variables ou d'indicateurs couvrant la plupart des facettes connues de la dynamique fluviale. Par exemple, la superposition des relevés d'activité du lit et des relevés morphologiques permet d'identifier les zones du lit où un cycle d'érosion et d'accumulation au cours d'un même évènement de crue a résulté en un changement d'élévation nul, un phénomène répandu dans les rivières à lit de graviers (Ashmore et Church, 1998). Aussi, le suivi intensif des processus pour chaque évènement de crue permet de connaître avec précision les conditions initiales et d'évaluer l'effet de l'historique des crues sur le transport de sédiments et les changements morphologiques.

Les calculs pour estimer les variables et indicateurs sont présentés en détails dans chaque chapitre. Toutefois, une philosophie générale a été adoptée quant au choix des variables. En effet, comme toutes les analyses portent sur des processus complexes, des variables et des indicateurs qui sont les plus simples possible ont été générés. Ainsi, en diminuant le nombre de transformations des données brutes, l'interprétation des résultats est plus directe. De plus, dans plusieurs cas, les variables ont été élaborées en se basant sur une appréciation logique des processus qu'elles devaient représenter puisque peu d'études équivalentes existent sur lesquelles on pourrait calquer la transformation des variables. En contrepartie, un effort substantiel a porté sur l'exploration de techniques d'analyse univariée et multivariée afin de tirer un maximum d'information du jeu de données et aussi pour révéler des interactions complexes et non linéaires. Chaque chapitre exploite des techniques d'analyse de données qui sont rarement utilisées dans le domaine. Pourtant ce

Tableau 1.1 Informations sur les caractéristiques et les données disponibles de chaque évènement de crue échantillonné au ruisseau Béard.

Information				Données disponibles					Évènements analysés			
Numéro de l'évènement	Date	Débit de pointe (m <sup>3</sup> s <sup>-1</sup> )	Nombre d'hydrogramme	Enregistrement du transport <sup>b</sup>	Boîtes pleines <sup>b</sup>	Conditions morphologiques avant / après	Activité du lit	Historique de la crue précédente	Chapitre 3	Chapitre 4	Chapitre 5 & 6 (transport de sédiments)	Chapitre 5 & 6 (morphologie)
1.	07-10-19	1.9	1	2 / 1	2 / 1	X	X					
2.	07-10-23	2.4	1	2 / 1	2 / 1	X	X	X	X	X	X	X
3.	07-10-27	3.8	1	2 / 1	2 / 1	X	X	X	X	X		X
4.	07-11-15	0.8	1	2 / 1	0 / 0	X	X	X		X	X	X
5.	07-11-22	1.2	1	2 / 1	0 / 0	X	X	X		X	X	X
6.	08-04-28	0.9	1	2 / 0	0 / 0	X	X		X	X		
7.	08-05-31	1.8	2 <sup>a</sup>	2 / 0	0 / 0	X	X	X		X	X	X
8.	08-06-04	1.0	1	2 / 0	0 / 0	X	X	X		X	X	X
9.	08-07-20	1.3	1	2 / 1	0 / 0	X	X	X	X	X	X	X
10.	08-07-24	3.1	2 <sup>a</sup>	2 / 1	2 / 1	X	X	X		X		X
11.	08-08-08	6.8	1	2 / 1	2 / 1	X	X	X		X		X
12.	08-10-25	2.3	1	2 / 1	0 / 0	X	X	X	X	X	X	X
13.	08-10-28	1.4	1	2 / 1	0 / 0	X	X	X	X	X	X	X
14.	09-06-15	0.9	1	0 / 1	0 / 0	X	X			X		
15.	09-06-29	1.8	1	2 / 1	1 / 0	X	X	X	X	X	X	X
16.	09-07-03	7.9	1	2 / 1	2 / 1	X	X	X	X	X		X
17.	09-07-26	6.1	1	2 / 1	2 / 1	X	X	X	X	X		X
18.	09-08-10	8.0	1	2 / 1	2 / 1	X	X	X		X		X
19.	09-10-24	2.0	1	2 / 1	1 / 1	X	X	X		X	X	X
20.	09-11-14	1.6	2 <sup>a</sup>	2 / 1	1 / 1	X	X	X		X	X	X
21.	09-11-27	4.7	1	2 / 1	2 / 1	X	X	X	X	X		X

<sup>a</sup> Hydrogrammes de crue aggloméré et analysés comme un seul évènement de crue.

<sup>b</sup>Dans l'ordre, le nombre de boîtes à sédiments amont / aval ; il y a 2 boîtes en amont et 1 boîte en aval.

sont ces analyses «non classiques» qui, dans cette thèse, auront permis d'arriver aux conclusions les plus intéressantes et ayant le plus de potentiel de généralisation.

Bien que le jeu de données soit exhaustif quant aux processus couverts, certains compromis ont dû être faits lors de la prise de mesures ou du traitement des données. La décision de ne pas mesurer le transport de sédiments en hiver a été faite en raison des risques élevés que les instruments soient endommagés par le gel. Cette décision réduit le jeu de données avec des informations complètes sur l'historique de la dernière crue à 18 événements plutôt que 21 événements. En effet, les instruments étant réinstallés au printemps, les conditions du dernier événement de transport sont inconnues pour la première crue de l'année, même si la morphologie a été mesurée avant l'événement. Ce choix de ne pas mesurer l'hiver a toutefois l'avantage de simplifier le nombre de processus à considérer, puisque le couvert de glace est un agent de transport de sédiments supplémentaire lors des crues hivernales et printanières. Ces décisions ont permis de cibler l'étude sur les crues avec transport de sédiments en charge de fond strictement d'origine pluviale sans couvert de glace.

Maintenir un site équipé avec des instruments automatisés sans avoir de données manquantes et assurer une présence après chaque événement de crue pour vider les boîtes à sédiments et recueillir les données morphologiques et d'activité du lit est un défi considérable. Malgré tous les efforts pour minimiser les données manquantes, certains problèmes ont entraîné une chaîne de décisions dans le traitement des données. Pour ce qui est de l'écoulement, les jauge à niveau d'eau utilisées ont un principe de fonctionnement fiable et une batterie interne d'une durée de 10 ans qui n'a pas eu besoin d'être changée. Donc, la mesure du débit et de la pente de la surface de l'écoulement sont en continu, sans aucune mesure manquante ou encore des données aberrantes dues à un mauvais fonctionnement. Dans le cas des relevés morphologiques et d'activité du lit, il est arrivé à trois reprises que le délai entre deux crues soit si court que le temps pour échantillonner a manqué (Tableau 1.1). Dans deux cas sur trois, les crues étaient de faible magnitude et bien que les boîtes n'aient pas été vidées entre les deux événements, elles n'étaient pas pleines. Dans le troisième cas, le premier événement était de forte magnitude et a rempli les boîtes à sédiments avant le deuxième événement. Considérant que pour deux de ces situations les données de transport de sédiments sont complètes, il était préférable de considérer ces doubles événements comme un seul. En effet, il a été jugé que les avantages d'un jeu de

données couvrant le plus d'évènements possibles sont supérieurs aux inconvénients liés à l'agglomération de deux évènements de crue en un seul. Ainsi, le terme évènement de crue ou de transport de sédiments dans la thèse désigne en réalité le nombre de relevés morphologiques et non le nombre d'hydrogrammes de crue distincts. Les mesures recueillies durant les 21 évènements de crue sont présentés au Tableau 1.1.

Les mesures de transport de sédiments ont été interrompues à l'occasion suite à des problèmes de fonctionnement ou par une capacité insuffisante des boîtes à sédiments lors de certaines crues. Les problèmes sont les suivants : 1) En 2008, le signal de la cellule de charge située en aval s'est mis à dériver, engendrant de grandes imprécisions dans l'estimation du taux de transport pour les trois premières crues de l'année. Toutefois, le début et la fin du transport de sédiments étaient toujours visibles dans le signal ce qui rendait possible l'estimation d'un taux moyen de transport en charge de fond pour ces évènements en pesant les sédiments recueillis dans la boîte. 2) La batterie alimentant les cellules de charges dans la section amont s'est déchargée lors de la première crue de l'année 2009, il est donc impossible d'estimer un taux de transport pour cette crue. 3) À plusieurs occasions les boîtes à sédiments ont été remplies avant la fin de l'évènement de crue. Ici, la définition d'une boîte pleine est lorsque les sédiments occupaient plus de 80 % du volume du boîtier interne, le seuil à partir duquel l'efficacité des boîtes à piéger les sédiments diminue drastiquement (Habersack et al., 2001). À quatre occasions, une, deux ou trois boîtes ont été remplies à la toute fin de l'évènement de crue et il a été considéré ici que l'enregistrement du transport de sédiments était complet puisque les boîtes à sédiments ont été remplies à des taux de transport très faibles qui ont un impact marginal sur l'estimation d'un taux moyen de transport de sédiments pour l'ensemble de l'évènement. 4) À huit occasions, les trois boîtes à sédiments étaient pleines bien avant la fin du transport en charge de fond et parfois même avant le pic de crue. Le traitement de ces évènements a varié selon les objectifs de chaque chapitre où ces données sont utilisées.

Le traitement des données manquantes et la sélection des évènements considérés pour fin d'analyse ont varié en fonction des objectifs abordés dans les chapitres qui suivent (Tableau 1.1). Au chapitre 3, les données de l'écoulement et les taux de transport de sédiments sont analysés de manière fine pour des périodes de cinq minutes. Seules les données de la boîte située dans le thalweg de la section amont ont été retenues. En effet, cette boîte à sédiments est la seule située dans le thalweg et cette localisation apparaît

comme étant la plus sensible aux variations de courte échelle de l'écoulement. De plus, le chapitre a été rédigé sous forme d'une lettre dont le but est de mettre de l'avant une idée originale portant sur le rôle de l'accélération sur le transport durant une crue. Ainsi, l'explication de la méthodologie a été simplifiée pour pouvoir mettre l'accent sur des résultats inédits. Les événements sélectionnés pour l'analyse sont ceux dont les signaux des cellules de charge ont le moins besoin de traitement pour dériver des taux instantanés. En effet, à de faibles intensités de transport en charge de fond, les signaux des cellules de charge sont sujets à des oscillations dus à l'arrivée intermittente des sédiments. Les événements où les boîtes se sont remplies en quelques minutes ont aussi été rejettés à cause du faible nombre de périodes de cinq minutes pouvant en être extraites. Finalement, l'événement où le signal n'a pas été enregistré en raison d'une panne de batterie a aussi été rejeté. Au total, dix événements ont été retenus pour les analyses du chapitre 2.

Dans les chapitres 4 à 6, les analyses ont été faites à l'échelle de crue, sans considérer la variabilité temporelle au cours de la crue. Ainsi, une seule valeur est estimée pour l'ensemble de la crue pour chacune des variables sélectionnées. Les boîtes à sédiments ont été installées durant l'été 2007 et la perturbation du lit de la section a pour conséquence que le transport de sédiments lors du premier événement de crue n'est pas considéré comme représentatif. Pour cette raison, les données de la crue du 19 octobre 2007 sont utilisées uniquement pour déterminer les conditions antécédentes de la crue suivante, celle du 23 octobre 2007. Au chapitre 4, les conclusions importantes sont basées essentiellement sur les relevés de la morphologie et de l'activité du lit. Le taux de transport moyen durant la crue est utilisé uniquement pour une comparaison qualitative avec les estimés dérivés des deux relevés spatiaux de la section. Dans cette perspective, les taux de transport manquant dans les séries temporelles ont été estimés en utilisant un modèle de calibration avec le débit pour chacune des boîtes. L'estimation des taux de transport à partir d'une relation avec le débit est reconnue pour être incertaine mais comme les répercussions sur les conclusions étaient minimes, cela a permis d'inclure 20 événements de crue dans l'analyse. Dans les chapitres 5 et 6, la sélection des événements a été faite à deux niveaux. Dans un premier temps, l'analyse de l'historique de la crue précédente éliminait de facto le premier événement de chaque année. Les variables et indicateurs morphologiques ont été estimés pour l'ensemble des 18 événements restants. Par la suite, une deuxième sélection a été faite pour ce qui est des variables liées au transport de sédiments, car pour plusieurs des

événements l'enregistrement était incomplet dû à un des problèmes de mesure du transport de sédiments dans les boîtes tels que décrits plus tôt. Comme l'objectif général de la thèse est d'analyser des mesures de processus et d'éviter les problèmes liés aux imprécisions de l'estimation, seuls les 11 événements avec un enregistrement complet du transport de sédiments en charge de fond ont été retenus pour les analyses concernant ce processus dans les chapitres 5 et 6.

## **CHAPITRE 2. IMBRICATION D'ÉCHELLES : IMPACT DE LA MORPHOLOGIE SUR L'ÉCOULEMENT**

---

### **2.1. Contexte**

À première vue, le chapitre 2 fait figure à part dans la thèse car il est le seul à ne pas traiter directement du transport en charge de fond. Sa présence dans la thèse s'explique par la forte composante conceptuelle liée à l'imbrication des échelles temporelles des processus en rivière. Le but général du chapitre 2 est de définir les fluctuations de l'écoulement pour une gamme d'échelles dans deux articles scientifiques <sup>1-2</sup>. Cet objectif découle d'une réflexion dont le point de départ est la variabilité du transport de sédiments en charge de fond, un thème central de la thèse. Les fluctuations turbulentes de l'écoulement sont probablement la première cause de variabilité du transport de sédiments tel que l'a identifié Leeder (1983). Toutefois, la turbulence de l'écoulement dont les fluctuations sont de l'ordre de la seconde et moins ne permet pas d'expliquer les fluctuations des taux de transport dont les cycles en rivières graveleuses durent souvent plusieurs minutes. Ainsi, le premier article, sous forme de lettre, explore l'organisation temporelle des caractéristiques turbulentes de l'écoulement, et particulièrement des structures turbulentes cohérentes, à des échelles de temps plus longues. Ceci permet de vérifier s'il y a une adéquation entre les échelles des fluctuations de l'écoulement et celles du transport de sédiments en charge de fond.

Sur le plan méthodologique, les mesures récoltées se distinguent par la durée des séries temporelles des vitesses instantanées de l'écoulement qui sont de plusieurs dizaines de minutes, alors que la plupart des études reposent sur des séries qui durent tout au plus une à deux minutes. Ces longues séries temporelles permettent d'apprécier les imbrications des échelles temporelles de fluctuations allant de la turbulence à des échelles plus grandes. Pour y arriver, il a fallu développer une approche analytique pour détecter les fluctuations de vitesse de basse fréquence dont la variance est largement inférieure à la variance des fluctuations de haute fréquence. Suite à l'identification de pulsations de l'écoulement durant plusieurs minutes et dont les caractéristiques sont similaires à celles des structures turbulentes cohérentes dans une rivière à lits de graviers, le deuxième article s'interroge sur

les origines de ces pulsations. Autrement dit, la durée des pulsations est-elle due à une auto-organisation des structures turbulentes cohérentes ou à un contrôle morphologique ? Il vise à comprendre les interactions entre les différentes échelles temporelles et comment celles-ci s'imbriquent. Aussi, il met en lien la turbulence de l'écoulement et la morphologie de grande échelle du lit des rivières, une piste encore jamais explorée.

1- Marquis G.A. et Roy A.G. (2011) Bridging the gap between turbulence and larger scales of flow motions in rivers. *Earth Surface Processes and Landforms*, 36(4), 563-568.

2- Marquis G.A. et Roy A.G. (soumis sur invitation) From coherent flow structures to flow pulsations in gravel-bed rivers: speculation on their origin and controls. Dans *Coherent flow structures at the Earth's surface*, édité par Venditti, J.G., Best J., Church M. et Hardy R.J., John Wiley & Sons.

## 2.2. Bridging the gap between turbulence and larger scales of flow motions in rivers

### 2.2.1. Abstract

Although flow turbulence in rivers is of critical importance to earth scientists, ecologists and engineers, its relations with larger flow scales are not well understood, thus leaving a fundamental gap in our knowledge. From an analysis of long time series of the streamwise and vertical flow velocity fluctuations measured in a gravel-bed river, we show that the signature of the fundamental turbulent flow structures (e.g. ejections and sweeps) is embedded within increasingly larger flow scales in a self-similar manner. The imbrication of turbulent structures into large flow pulsations of flow acceleration and deceleration covers more than two orders of magnitude from a few seconds to nearly ten minutes. This property is explained by the clustering of turbulent events creating an emergent pattern at larger scales. The size of the larger flow pulsations scales with the spacing of the pools and riffles in the river. This implies a mutual adjustment between turbulence generation mechanisms and long pulsations of flow acceleration and deceleration controlled by the bed morphology. These results bridge a gap in our understanding of flows in rivers and offer a new perspective on the interactions between the turbulent flow with larger scales of flow motion that are critical for sediment transport, habitat selection and fish behaviour.

### 2.2.2. Introduction

Our understanding of turbulence in rivers has progressed tremendously in recent years and this advance in knowledge has had a fundamental impact in the earth sciences, engineering and ecology (e.g. Liao et al., 2003; Best, 2005; Liao, 2007; Nikora, 2010). The existence of turbulent coherent flow structures in the boundary layer over smooth and rough surfaces has long been established mostly from pioneer work in flume experiments (e.g. Kline et al., 1967; Grass, 1971; Grass et al., 1991; Nezu and Nakagawa, 1993; Shvidchenko and Pender, 2001). In the turbulent boundary layer, the basic set of structures consists of ejections of slow fluid moving away from the bed toward the surface interspersed with sweeps of fast fluid moving toward the bed. Ejections and sweeps also form the core of the low- and high-speed wedges that are the most important macroturbulent structures in gravel-bed rivers (Kirkbride and Ferguson, 1995; Ferguson et al., 1996; Buffin-Belanger et al., 2000; Roy et al., 2004). These elongated wedges develop

over the entire depth of the flow and their length is two to five times the flow depth ( $Y$ ) (Roy et al., 2004). Recent field and laboratory studies have highlighted the role of the macroturbulent flow structures on fish behavior (Enders et al., 2003; Liao et al., 2003) and on the motion of individual grains as bedload (Paiement-Paradis et al., 2011). These macroturbulent structures have a short duration (in the range of a few seconds) with respect to the scale of the river reach and of the long flow pulsations that have been reported in the literature (Lapointe, 1992; Dinehart, 1999). In most cases, the presence of flow pulsations is associated with the movement of low-relief bedforms such as dunes or bedload sheets. For instance, Dinehart (1999) has reported the presence of large flow pulsations lasting from seconds up to the minutes in a large gravel-bed river where flow stage was high and sediments moving. The length of these pulsations was two to three times greater than the length predicted for macroturbulent structures like boils (Jackson, 1976). To our knowledge, this type of pulsations has not yet been observed at low flow over an armored gravel-bed.

At present, there is gap in our knowledge linking macroturbulent flow structures with flow motion at larger scales. This gap is evident in the power spectrum of the velocity fluctuations over temporal scales ranging from the turbulent to the annual scales published by Nikora (2007). The estimate of the variance associated with hydraulic phenomena at scales just greater than macroturbulence is tagged with a question mark (Figure 2.1). A clear lack of evidence exists in order to establish a continuum of velocity properties across this range of temporal scales. Inasmuch as short lived turbulent events contribute to imprint the properties at larger temporal scales like average flow velocities, it is surprising to note that very few investigations have addressed the relations and interactions between scales of flow motion from the smallest turbulent phenomena to the larger flow signatures. The study of flows in rivers is often conducted as if the scales of motion were disconnected and independent leaving out the critical notion that flows at different scales are embedded to form a continuum. While some interactions at the longer time scales such as daily discharges over several years have been examined (Huang et al., 2009; Hirpa et al., 2010), the current lack of knowledge of the connection of flow properties at shorter time scales is clear. Yet, this link between the scales of fluid motion is not only crucial for the understanding of physical processes but perhaps more importantly for connecting the

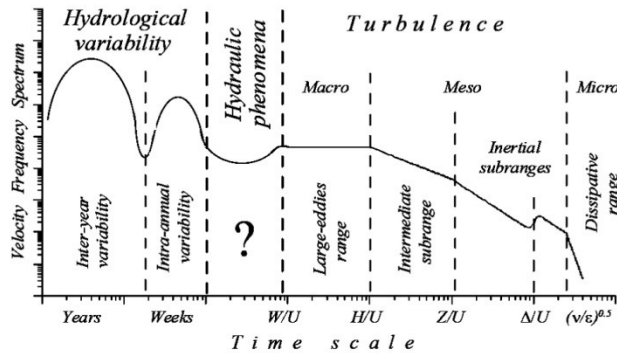


Figure 2.1 Schematized velocity spectra in gravel-bed rivers in the frequency domain, from Nikora (2007).

critical scales in a useful manner for models of river bed dynamics, of habitat selection and of river channel stability (Nikora, 2010).

Even if turbulence is increasingly seen as an important variable in the behavior of organisms, the most meaningful flow variability scales for living organisms are in the range of minutes and hours where our knowledge is thin as stressed in the velocity spectrum of Figure 2.1. The objective of this paper is to address this issue by examining the links and interactions between the turbulent scale of fluid motion and larger scale flow variations in a river system. Using long velocity time series measured in a gravel-bed river, we identified large scale flow pulsations lasting several minutes. To link these pulsations to the turbulence scale, we provide evidence showing that coherent turbulent flow structures within self-similar flow pulsations that are two to three orders of magnitude larger than the turbulent scale. We speculate that these pulsations could scale with the major features of the river bed morphology (i.e. riffle-pool sequence).

### 2.2.3. Methods and analysis

In order to examine the presence of flow structures at a range of temporal scales from the macroturbulence and above, we have collected long, high-frequency time series of the streamwise and vertical velocity components in a gravel-bed river. The measurements were taken at low flow in two shallow pools in straight reaches of the Eaton North River, Québec (Figure 2.2). The width of the wetted section varies between 15 and 20 meters in the studied reaches. The two locations were chosen for their contrasted mean flow velocities and their similar flow depth. In the center of each pool, velocities were measured

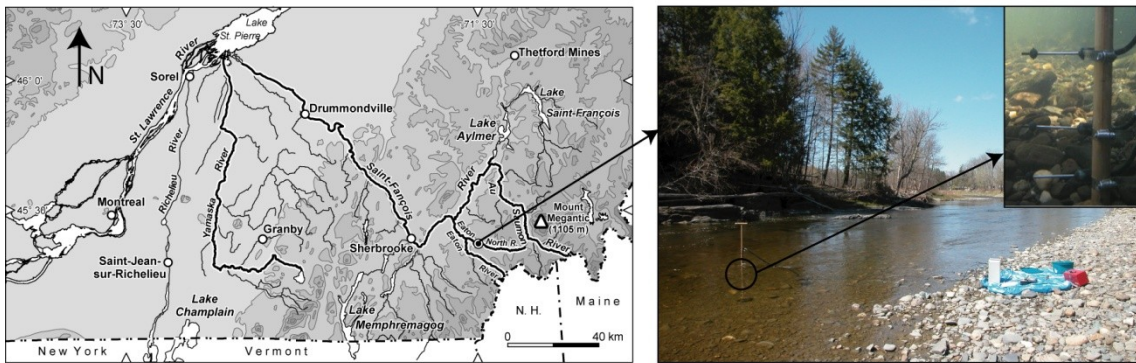


Figure 2.2 Field site location in Southern Québec (Canada) on the left side and a downstream view during the recording in pool B joined with an underwater picture of the ECM's on the right side.

simultaneously on a vertical array of three Marsh-McBirney electromagnetic current meters (ECMs) that were positioned at 0.06, 0.14 and 0.22 m above the river bed (Figure 2.2). The sensors have a diameter of 13 mm and do not modify substantially the flow characteristics. In order to remove the electronic noise in the high frequencies, the signals are passed through a R-C filter with a time constant of 0.05 seconds (halfpower of 3.18 Hz) (Roy et al., 1997). Streamwise ( $u$ ) and vertical ( $v$ ) velocities were sampled simultaneously on all three sensors at a frequency of 20 Hz during 20 minutes. Except for mean flow velocity that is higher in pool B, the hydraulic and grain size characteristics of the sites of measurements are similar (Table 2.1). The velocity records did not exhibit any significant trend and the signals were stationary. In Table 2.1, the mean flow velocity ( $U$ ) and the friction velocity ( $u^*$ ) were estimated using the law of the wall:

$$u = \frac{u^*}{\kappa} \ln \left( \frac{h_i}{h_0} \right) \quad \text{Equation 2.1}$$

where  $u$  is the flow velocity at a given height,  $\kappa$  is the Von Karman constant (0.4),  $h_i$  the height above the bed,  $h_0$  the height where the flow velocity equals zero. The shear stress  $\tau$  was then estimated:

$$\tau = (\rho u^*)^2 \quad \text{Equation 2.2}$$

where  $\rho$  is fluid density ( $1000 \text{ kg/m}^3$ ).

To assess the characteristics of the flow structures over a range of scales, we have used three different analyses. This approach is warranted by the need to investigate different aspects on the flow phenomena but also to confirm if a flow phenomenon is robust

Table 2.1 Sampling location characteristics

Pool	A	B
Flow depth $H$ (m)	0.35	0.35
Mean Velocity <sup>1</sup> $U$ (m/s)	0.32	0.55
Turbulent Intensity <sup>1</sup> (%)	15	14
Friction velocity $u^*$ (m/s)	0.036	0.035
Shear stress $\tau$ (N/m <sup>2</sup> )	1.23	1.23
$D_{50}$ (mm)	35	45
$D_{84}$ (mm)	90	100

<sup>1</sup>Estimated from velocity time series at 14 cm from bed

enough to be detected by different methods. The primary detection of flow structures at a range of temporal scales rests on the cumulative time series of the instantaneous velocity fluctuations around the mean of the streamwise ( $u'$ ) and vertical ( $v'$ ) velocities. For means of easier visualization, the values of the curves are standardized. The interpretation of the cumulative curves focuses on periods where there is an ascending (dominated by positive velocity fluctuations) or a descending (dominated by negative velocity fluctuations) trend. This way of visualizing the data is not a classic analysis in turbulence studies but is helpful to highlight low frequency flow fluctuations that have a small contribution to the total variance of the signal by visually dampening the contribution of the high frequency velocity fluctuations. In a second approach, we have investigated the presence of self-similarity using a Hurst Rescale-Range analysis on both the streamwise and vertical velocity components. We estimated the rescaled range ( $R/S$ ), a measure of variance, for geometric time windows length ( $T$ ) ranging from 2 to  $2^{12}$  lags. The largest window size is selected in order to have replicates of the analysis on the whole length of the time series (Feder, 1988). The presence of a power law scaling relationship between  $R/S$  and  $T$  with an exponent  $HE$ , the Hurst exponent, ranging between 0.5 and 1, implies that the time series is persistent meaning that it is positively autocorrelated and shows coherence and structure. The fractal dimension  $D_f$  of the time series can be estimated as  $D_f = 2 - HE$ . Turbulent flows are known to exhibit self-similarity over a range of scales with a fractal dimension in the range of 1.35-1.70 (Sreenivasan and Meneveau, 1986). Finally, we assessed which type of structures (ejection or sweep) is dominant over three time windows of 1 s, 12 s and 120 s. The quadrant technique is used to detect ejections and sweeps from the joint distribution of the simultaneous streamwise and vertical velocity fluctuations (Lu and Willmarth, 1973).

Ejections are associated with Quadrant 2 (Q2) events ( $u' < 0$  and  $v' > 0$ ) while sweeps are Quadrant 4 (Q4) events ( $u' > 0$  and  $v' < 0$ ).

#### 2.2.4. Results and discussion

Although some oscillations are visible in the twenty minutes velocity records there are no obvious sign of long flow pulsations (Figure 2.3ab). A first hint at the presence of low frequency fluctuations is an observed variation of as much as 15 % in the average flow velocity for each minute of the time series. The cumulative curves of the velocity fluctuations, however, reveal large-scale cycles lasting several minutes (Figure 2.3cd). These cycles are composed of long periods of a generally ascending curve followed by a long descent. Figure 2.3 shows only the time series for one height above the bed but the largest cycles seen in Figure 2.3cd do occur over the entire flow depth. For the raw velocity signals of both sites, the correlation coefficients between the three heights of velocity measurements range from 0.49 to 0.58 for  $u'$  and from 0.25 to 0.32 for  $v'$  and they are significant at  $\alpha = 0.01$ . The lower values for the vertical velocity are expected because of the typical dominance of the higher frequencies in the signals. The correlation coefficients of the cumulative curves between the three heights increase drastically, because the large scale pulsations revealed by the method that dampens the high frequency fluctuations occur over the entire flow depth. For the streamwise velocity cumulative curves, the coefficients vary between 0.62 and 0.76 but they are even much higher for the vertical velocity cumulative curves ranging from 0.74 to 0.86 (significant at  $\alpha = 0.01$ ).

An important feature of the curves is the mirror image created by the opposite behavior of the streamwise and vertical velocity signals (Figure 2.3c-h). The two curves are out of phase. This behavior is typical of turbulent flow structures found in the boundary layer where ejections and sweeps are characterized by negative correlations between the streamwise and vertical velocity components (Clifford and J.R., 1993; Buffin-Belanger et al., 2000; Roy et al., 2004). In the data reported here, the correlation coefficient between  $u$  and  $v$  velocity components is -0.40 at the bed and -0.29 near the surface in pool A and from -0.42 to -0.26 in pool B (significant at  $\alpha = 0.01$ ). The novelty is that similar patterns showing an inverse relationship between the streamwise and vertical velocity components exist at much longer time scales. The correlation coefficients between the cumulative streamwise and vertical velocity components range between -0.40 at the surface and -0.86

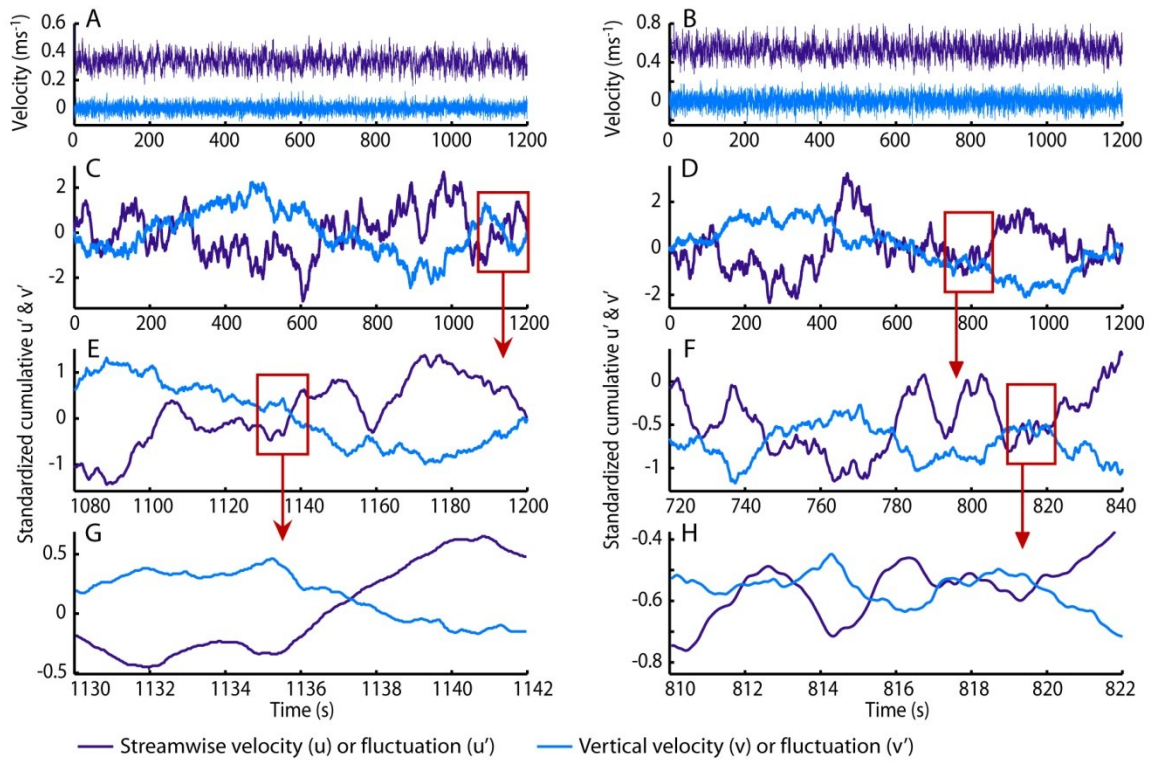


Figure 2.3 (a, b) Velocity time series. (c, d) Cumulative curves of the velocity fluctuations. (e, f, g, h) Zoom of the cumulative curves, location show with the box on the previous curve. All data are presented for ECM located at 0.14 m above the bed for both velocity measurements in pools A (left) and B (right).

near the bed (significant at  $\alpha = 0.01$ ). The similarity of the velocity signatures at different time scales is shown for three time periods that cover two orders of magnitude for both velocity signals. The same mirrored pattern observed at the smallest time scale is present at the longer ones (Figure 2.3c-h). Smaller macroturbulent structures lasting a few seconds are embedded within flow structures with a similar velocity signature but that are much longer (Figure 2.3gh). At the intermediate time scale, smaller individual structures are present within larger oscillations of the curve (Figure 2.3ef). These are in turn seen within the largest structures present over the whole cumulative curve (Figure 2.3cd). The examples in Figure 2.3 were selected where the cumulative velocity curves cross in order to facilitate the visualization of the phenomenon but these embedded turbulent structures occur over the entire length of the signals.

The self-similarity observed using cumulative velocity time series in Figure 2.3 is also verified quantitatively. Turbulent flows are known to exhibit self-similarity over a

range of scales with a fractal dimension in the range of 1.35-1.70 (Sreenivasan and Meneveau, 1986). The velocity time series display self-similarity as the fractal dimensions estimated from the Hurst Rescaled-Range analysis vary from 1.30 to 1.38 for the streamwise velocity and from 1.41 to 1.52 for the vertical velocity. All power law relations have an  $R^2$  equal to or greater than 0.95 and the largest time window used in the analysis was 200 s. The streamwise velocity time series show that the signals are persistent in time but more importantly that the structures exhibit a self-similar behavior at a range of temporal scales down to less than one second, even if those smaller structures are not visible in the cumulative curves of Figure 2.3cd. Self-similarity means that the properties of flows are scale-invariant, which allows one to model the larger scales of the turbulent flow from the knowledge of a single scale.

To further explain and illustrate the cycles visible in Figure 2.3c-h, we have examined the frequency and magnitude of the turbulent flow structures (Quadrant 2 and 4) at different time scales. We determined the dominant characteristics of the signal over three time windows covering two orders of magnitude (1, 12 and 120 s). We estimated which of the ejections (Q2) or sweeps (Q4) were occupying most of the time for each time window (Figure 2.4ab). We also repeated this signal classification but based on the magnitude of the Reynolds shear stress  $-\rho u'v'$  of both types of turbulent events (Figure 2.4cd). These stresses play a critical role in river dynamics as they are associated with both suspended and bedload sediment transport (e.g. Lapointe, 1992; Nino and Garcia, 1996; Schmeeckle et al., 2007; Paiment-Paradis et al., 2011). While this analysis shows alternating periods of dominance of ejections and sweeps which is to be expected, it also highlights the temporal clustering of events of a certain type giving rise to a dominant velocity signature at larger scales. The differences observed between the temporal dominance and the Reynolds shear stress dominance of turbulent structures in Figure 2.4 are mainly observed during periods where the cumulative curves of  $u'$  and  $v'$  are changing from an acceleration trend to a deceleration trend and vice-versa in Figure 2.3cd. The transitional zones do not exhibit a preferred organization in terms of turbulent flow structures. The signatures for the 120 s windows display periods in Figure 2.4 that are in phase with those seen in the cumulative time series of Figure 2.3cd.

It is very interesting to note that the velocity signals coming from two similar environments in the same river, but yet with differences in their local features such has the

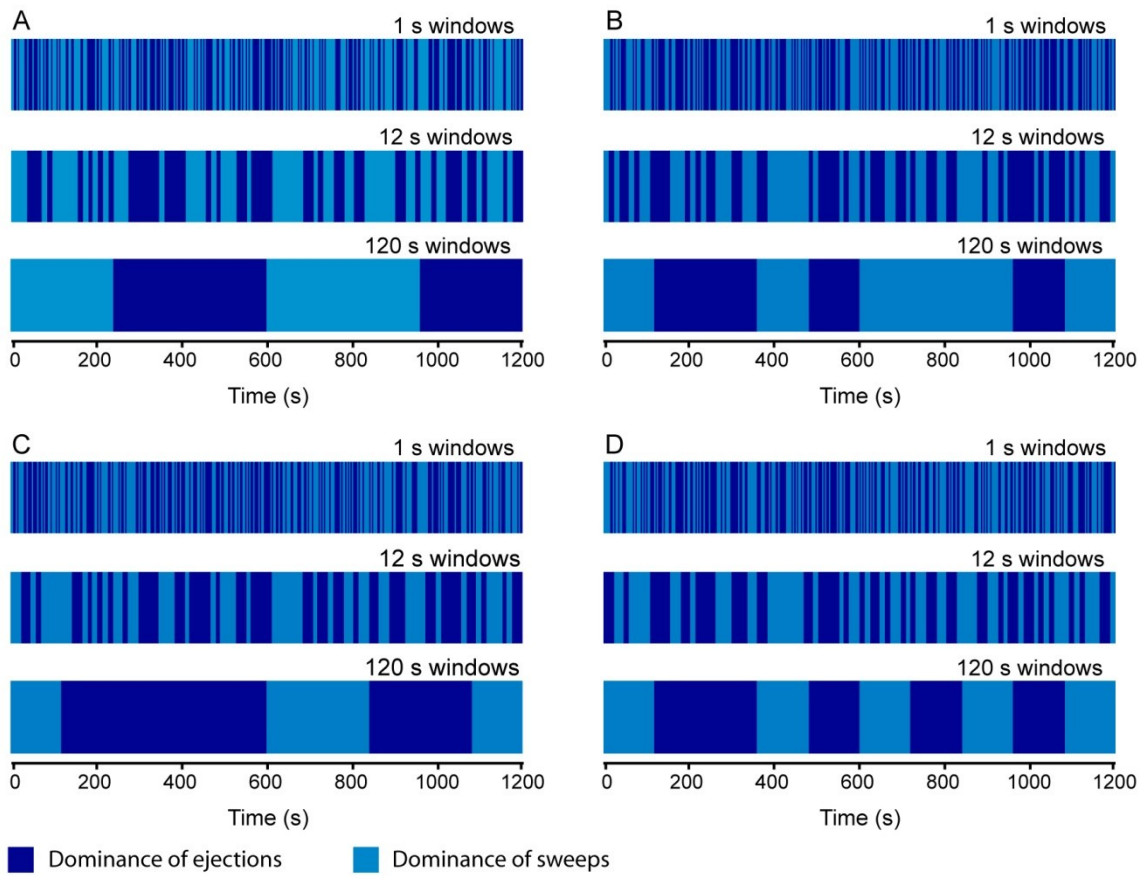


Figure 2.4 Representations of the dominance of ejections and sweeps over time windows of 1, 12 and 120 seconds. (a, b) Dominance by duration of the turbulent structures. (c, d) Dominance by the magnitude of the Reynolds shear stress during the passage of the turbulent events. All data are presented for ECM located at 0.14 m above the bed for both velocity measurements in pools A (left) and B (right).

slope or the bed material arrangement and clast protrusion exhibit very similar patterns at larger time scales. The main difference is that the large scale pulsations are shorter for the velocity time series of pool B where mean flow velocity is higher than in pool A (Table 2.1). The examination of the classified signal in Figure 2.4 from 1 s to 120 s windows also shows that the imbalance between both types of turbulent flow structures is small but yet a reality. This observation leads to the question: do the macroturbulent events lasting a few seconds in a boundary-layer flow cluster in an organised fashion to create the large scale pulsations (bottom-up process) or is there an external factor controlling the duration of pulsations during which the generation of a given type of turbulent flow structure is favored (top-down process)?

Support for a bottom-up process is given by the patterns associated with the groupings of turbulent flow structures of a given type. This suggest that the clustering of the structures is the result of a self-organizing process within the turbulent flow (Bak and Chen, 1991; Paiement-Paradis et al., 2003) perhaps through vortex shedding and wake flapping in the lee of protruding particles (Hardy et al., 2009). According to this interpretation, flow structures at longer time scales emerge from the self-organization of the small-scale turbulent structures with a similar velocity signature. This interpretation is also consistent with the results of the Hurst Rescale-Range analysis that shows the self-similarity of the velocity time series.

There is, however, another view that challenges this conventional bottom-up approach on the generation of large flow pulsations if taken in the perspectives of the top-down process. We have stressed earlier the idea that the large scale flow pulsations in both pools observed in Figure 2.3 and Figure 2.4 are very similar, showing alternate patterns of fluid acceleration and deceleration. The difference lies in the duration of a full cycle to go from an accelerating sweep-dominated pulsation to a decelerating ejection dominated phase. Because the hydraulic characteristics of both pools were similar except for the average flow velocity, the frequency of the flow pulsations may be linked to the regular pattern of the bed morphology, the riffle-pool spacing. In the Eaton-Nord River, the riffle-pool spacing varies between 150 to 200 m, in the anticipated range of five to seven times the bankfull width (30 m). The mean length of the longest time scale cycle is in the order of 600 s and 360 s for velocity signals in pools A and B respectively (see Figure 2.4). Converting these durations to lengths through the average flow velocity at each site (Table 2.1), we obtain similar flow pulsation lengths of 192 m and 198 m corresponding to the upper value of the riffle-pool spacing. This suggests the hypothesis that bed morphology controls the large scale flow motion through a feedback mechanism where large-scale pulsations would interact with the frequency and magnitude of the smaller scale turbulent structures of the flow. We speculate that periods of flow deceleration and acceleration would correspond to periods of fill and spill of pools where the release of water would be intermittent but somewhat periodic.

### 2.2.5. Conclusion

The embeddedness of the turbulent processes within flow pulsations at larger scales challenges the assumption that the flow is stationary even at a low flow stages. Streamwise flow velocities averaged for each minute of the time series used here varied by as much as 15 % of the average velocity for the whole series. These changes in streamwise velocity are concomitant over the whole flow column and periods of acceleration and deceleration are associated with concomitant changes in the vertical velocity component. These findings change how flow directly and indirectly affects other aspects of the physical and biotic fluvial environment. For instance, the temporal clustering of accelerating turbulent flow structures could be of critical importance for driving the initiation and maintenance of sediment transport events as bedload. The number and intensity of sweeps which are thought to be associated with bedload transport (e.g. Drake et al., 1988) are not evenly distributed within the flow. Sustained periods of flow acceleration could be related to the temporal variability in bedload sediment transport reported in several studies (e.g. Reid et al., 1985; Gomez et al., 1989; Nelson et al., 2001). The clustering of turbulent events may also be an important control in fish bioenergetics and feeding patterns (Enders et al., 2003). For instance, the variability of flow pulsations may be much more important for organisms than turbulent fluctuations as they shape their immediate environment more directly. The strong connections between flow pulsations and macroturbulence may be of critical importance in understanding habitat structure, fish behavior and population dynamics in river ecosystems (Biggs et al., 2005).

### Acknowledgements

The authors acknowledge the financial support of the Natural Sciences and Engineering Research Council of Canada and of the Canada Research Chair program.

## 2.3. From turbulent coherent flow structures to flow pulsations in gravel-bed rivers

### 2.3.1. Abstract

This study presents an extensive description of a new type of coherent flow structures (CFS) in gravel-bed river flows. These structures, here called flow pulsations, are present over the entire flow depth ( $H$ ) and they can extend to more than  $100H$  and last for several minutes. The identification of the flow pulsation might have important consequences for our understanding of fluvial processes such as bedload transport. Measurements were made in order to test (i) the ubiquity of these structures in rough flows and (ii) the role of large morphological features such as riffle-pool sequences on the flow pulsations scaling. The study relies on long records of instantaneous velocity and water height fluctuations in natural rivers with distinct pool-riffle morphology and in a laboratory flume with a flat gravel bed. Flow pulsations are present in all measured flows and have similar characteristics compared to other turbulent CFS such as sweeps and ejections. These results are agreement with the hypothesis of a self-organization of the small CFS into larger flow pulsations. We also found that flow pulsations are more regular and have greater amplitude in the presence of large morphological features. The relative submergence of isolated roughness elements and of the riffles combined with the pool spacing control flow pulsation length.

### 2.3.2. Introduction and research context

The study of the generation, transport and dissipation of coherent flow structures (CFS) has led to the identification of multiple scales of flow motions. Turbulent CFS that are longer than a few times the flow depth ( $H$ ) or the boundary layer thickness ( $\delta$ ) have drawn a great deal of attention as a key component of the turbulent boundary layer. These large-scale motions (LSMs) are responsible for most of the turbulent production as exemplified by the work of Liu et al. (2001) who showed that these CFS contain half of the total turbulent kinetic energy and up to three-quarters of the Reynolds shear stress. It is now widely recognised that LSM are a predominant feature of open channel flows (Falco, 1977; Nakagawa and Nezu, 1981; Shvidchenko and Pender, 2001; Roy et al., 2004). They consist of alternating fronts or wedges of high and low-speed fluid occupying the entire depth of the flow. While the low-speed LSMs are mainly associated with slow upward motion

(ejection), high-speed LSMs consist mainly of a rapid downward motion (sweep). The angles of inclination of the wedge fronts generally vary between  $20^\circ$  and  $36^\circ$  in the downstream direction (Nezu and Nakagawa, 1993; Roy et al., 2004). It is generally acknowledged that these LSMs scale mainly with flow depth (Shvidchenko and Pender, 2001; Nikora, 2007). In gravel-bed rivers, LSMs are typically 2 to 6  $H$  in length and about 0.5 to 1  $H$  in width (Roy et al., 2004). A secondary scaling with mean streamwise velocity ( $U$ ) was also identified by Shvidchenko and Pender (2001) in a flume experiment and partly confirmed by Marquis and Roy (2006) from velocity measurements taken in a natural gravel-bed river.

The origin of the LSMs is still under speculation. On the one hand, one hypothesis suggests that LSMs originate from coherently organised packets of hairpin vortices (Zhou et al., 1999). Even though the coalescence mechanism is largely accepted near the wall of the boundary layer, some doubt still exists as to whether other mechanisms might be involved in the turbulent structure generation in the outer layer to explain the presence of such large-scale turbulent motions (Adrian, 2007). An interesting alternative hypothesis is the oscillatory theoretical model for wall-bounded turbulence proposed by Levi (1983). Based on the typical bursting period  $T_B=2\pi H$ , he suggested that the bursting process was stimulated by an outer oscillatory perturbation. In a turbulent regime, travelling waves of length  $2\pi H$  at the surface of the flow excite the generation of ejections and sweeps. Our aim here is not to review all possible formation processes for LSMs but to highlight the fact that plausible explanations with opposite starting point (bottom-up vs top-down) coexist in the literature.

The size of the smallest turbulent CFS is limited by the fluid viscosity but the upper limit for the larger scale turbulent phenomena remains mostly unknown. Most estimates are lower bound mainly because of the instruments used and of the types of analysis one can apply to the data. CFS that are much longer than the LSMs, the very large-scale motions (VLSMs), were first identified within the logarithmic turbulent boundary layer of fully developed turbulent pipe flow. By means of pre-multiplied energy spectra, Kim and Adrian (1999) have identified a low wave mode that can extend up to 12-14 pipe radii in the streamwise direction over the entire logarithmic layer. The estimated wavelengths are a lower bound of the actual wavelengths of VLSMs because they have been inferred from frequency spectra, which suffer from a loss of correlation due to the convection velocity.

According to the speculations of the authors, the VLSMs are not a new coherent flow structure but merely the consequence of coherence in the alignment of the LSMs which themselves are composed of the agglomeration of several hairpin vortices.

The first instantaneous snapshots of the VLSMs were provided experimentally using PIV in the streamwise/spanwise plan (Ganapathisubramani et al., 2003; Tomkins and Adrian, 2003). The logarithmic region of the turbulent boundary layer appears to be characterized by its own streaky structure, notably at a much larger scale than the near-wall streaks (Kline et al., 1967). Long regions of streamwise low momentum were found interspaced with high-speed fluid and were also identified as dominant contributors to the overall Reynolds shear stress (Ganapathisubramani et al., 2003). From an experiment using a hot-wire rake in a wind tunnel, Hutchins and Marusic (2007) identified what they called *superstructures* that have a size consistent with outer scaling, extending over length up to  $20\delta$ . Instantaneous views in the wind tunnel and from one set of field data suggest that the superstructures are meandering substantially along their length. This characteristic can severely curtail the length scales inferred from techniques like the correlation between velocity measurements at two points or pre-multiplied energy spectra. From these experiments, the authors speculated that the inner and outer-scaled turbulent flow structures are probably two different regimes that overlap and intertwine in a complex manner. This situation made them wary of the explanation of the VLSMs as a building up of smaller CFS. In a recent experiment, Dennis and Nickels (2011) made a 3D analysis of PIV measurements in order to further study VLSMs. They found that few structures had a length greater than  $7\delta$ , which contradicts the existence of the VLSMs. But, they also showed that the LSMs can be aligned in the streamwise direction to form long meandering streaks. Their findings raise the question concerning the existence of the alignment of LSMs into the VLSMs (or the superstructures) as being produced either at random or by a specific mechanism.

The answer as to whether or not these superstructures exist is not yet fully resolved unambiguously and if they exist, their origin remains nebulous. We have published results from long records of velocity fluctuations measured in a gravel-bed river describing what we have called *flow pulsations* (Marquis and Roy, 2011). We found that there is a range of imbricated scales of self-similar flow motions over several orders of magnitude with durations varying from the second up to a few minutes. Flow pulsations, the largest scale

detected, can extend to several hundred times the flow depth and are therefore much larger than VLSMs or superstructures. The detection of the flow pulsations was made possible by using cumulative sums of the velocity fluctuation time series which dampens the high frequency signal in order to highlight the low frequency oscillations of the time series. This analysis overcomes the problem of the two-point velocity correlation and of the spectral density analysis to detect low frequency oscillations in the instantaneous velocity time series. Flow pulsations have similar characteristics than those of the low and high-speed LSMs as they occupy the entire flow depth and exhibit a negative correlation between the streamwise and vertical velocity fluctuations. We have speculated about their origin in two ways: the bottom-up and top-down approaches. The bottom-up perspective is easy to argue as there is a range of self-similar imbricated flow structures organized from the smallest to the largest ones. The top-down explanation is more difficult to justify but is appealing because it may provide a stronger physical grounding to the flow pulsations. In our article, we have proposed that the length of the flow pulsations was controlled by the pool spacing in the manner of a *fill and spill* process. Nikora (2007) has outlined the gap in our knowledge that exists between the turbulence scale of flow motion and the much larger scales such as the intra- and inter-annual variability of flow variations. The flow pulsation concept may in part bridge this gap in our understanding of the interactions between scale of flow motions in rivers and hints to possible links between turbulent processes and river morphology.

Independently of the possible origins of the flow pulsations, this type of flow motion offers a new perspective to deepen our understanding of sediment transport variability in rivers. In particular, bedload transport is known to have a pulsating behaviour where the peak and troughs are not related to main flow variables such as discharge or stream power (e.g. Reid et al., 1985; Gomez et al., 1989). Flow pulsations lasting several minutes were reported by Dinehart (1999) during a high flow stage in a gravel-bed river. These pulsations were correlated with the migration of low relief gravel bedforms. Spectral analysis of very long velocity time series (about 20 hours) in a flume with a mobile gravel bed has also shown that the migrating bedforms influence the low frequency variability of the flow (Singh et al., 2010). The authors could detect even the largest bedforms that were 10 m long migrating at rates of 14 and 22 m/h. When considered in the perspective of the possible existence of large scale flow pulsations, these results lead to the question of the

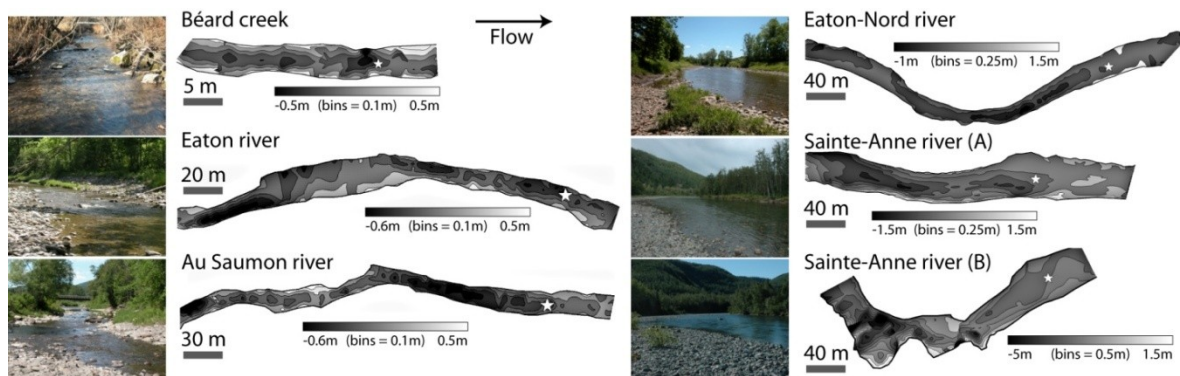


Figure 2.5 Study reaches with the photos taken looking upstream and the interpolated maps of the morphological surveys. The white star represents the location of the time series measurements.

possible complex interactions between the turbulent flow and the migration of bedforms. In this paper, we aim to (i) show that very long ( $\gg 20 H$ ) flow pulsations are a characteristic feature of flows in gravel-bed rivers and (ii) to speculate on the possible origin of the flow pulsations regarding two opposite hypothesis: the self organisation of LSMs into increasingly larger structures up to the flow pulsations and the morphological control by the pool spacing on the flow pulsations length.

### 2.3.3. Methods

#### 2.3.3.1. Data sampling

Data were collected both in the field and in a flume in order to test the hypothesis of a morphological control against a self-organising process of the large scale flow pulsations. We will compare measurements taken in rivers presenting a well developed bed morphology with an environment where the bed was flat and uniform. Five gravel-bed rivers with distinct pool-riffle morphology were chosen along a gradient of flow widths ranging from 3 m to 41 m. (Figure 2.5). Table 2.2 presents the characteristics of the six sampled reaches. Measurements were repeated at the same location for different flow stages for four of the reaches (Table 2.2). For Béard Creek and the Eaton-Nord River, we obtained data at low (LF) and moderately high flows (HF) without bedload transport. For the Au Saumon and Eaton rivers, the measurements were repeated at very low (VLF) and low flows (LF). For all field surveys, instantaneous velocities were measured using three

Table 2.2 Characteristics of the surveyed reaches.

	Béard creek		Eaton river		Au Saumon river		Eaton-Nord river		Sainte-Anne river	
	LF	HF	VLF	LF	VLF	LF	LF	HF	LF(A)	LF(B)
Flow stage state										
Bed slope (%)		0.94		0.29		0.34		0.14	0.17	0.19
$D_{50}$ (mm)		50		52		55		38	65	60
$D_{84}$ (mm)		73		96		103		68	96	85
Pool spacing (m)		12		63		85		188	290	315
Reynolds number ( $\times 10^{-3}$ )	13.7	106	76	100	68	70	92	372	275	539
Mean flow depth $Y$ (m)	0.16	0.28	0.24	0.31	0.21	0.26	0.47	0.70	0.88	1.24
Riffle flow depth $Y_R$ (m)	0.10	0.20	0.09	0.14	0.05	0.06	0.21	0.35	0.39	0.75
Pool flow depth $Y_P$ (m)	0.21	0.33	0.19	0.27	0.20	0.25	0.43	0.64	0.64	1.67
Flow width $W$ (m)	2.79	4.15	7.20	8.78	8.90	10.29	20.28	24.60	36.51	41.45

Marsh-McBirney 523 electromagnetic current meters (ECMs) positioned at  $0.25H$ ,  $0.50H$  and  $0.75H$  above the bed and mounted on a vertical wading rod. The ECMs sensing probes have a diameter of 1.3 cm and a 0.05 s time constant of the R/C filter. The sampling frequency was 20 Hz. The ECMs are easy to deploy as a vertical array to obtain simultaneous measurements of the streamwise ( $u$ ) and vertical ( $v$ ) velocity components at different heights in the flow. To verify that the sampling was conducted under a constant flow depth, an ultrasonic sensor model DCU-7110 from Scientific Technologies Inc was deployed over the ECMs array to sample the flow depth ( $h$ ) at a frequency of 10 Hz. The instruments were mounted on an aluminum frame of 1.5 by 1.5 meters to allow stable long term measurements. The frame was located in the thalweg at the downstream end of a pool where the river bed allowed for a locally uniform flow with no drastic bed elevation variations or protruding obstacles upstream of the instruments (Figure 2.5). Time series were sampled for a duration that was as long as possible given the river scale, the stability of the flow stage and the practical constraints such as the time available once the instrumental set-up was positioned. The duration of the time series and the principal flow characteristics are presented in Table 2.3. The field sampling was completed by a pebble count of 300 particles and by a total station survey covering two riffle-pool units upstream of the measurement location except for the two reaches of the Sainte-Anne River (Figure 2.5). For these reaches, only the first riffle-pool unit was surveyed due to time considerations. The second riffle-pool unit was only measured using a tape. All the morphological dimensions given in Table 2.2 were extracted from the interpolation of the

Table 2.3 Field time series characteristics (shown for  $0.5H$  except when mentioned).

	Béard creek		Eaton river		Au Saumon river		Eaton-Nord river		Sainte-Anne river	
<i>Raw time series</i>										
Flow stage state	LF	HF	VLF	LF	VLF	LF	LF	HF	LF(A)	LF(B)
Time series duration (min)	132	60	90	88	56	90	143	105	385	150
Flow depth $H$ (cm)	20	30	22	30	25	30	30	50	57	57
RMS $h$ (cm)	0.08	0.35	0.10	0.30	0.18	0.05	0.07	0.20	0.26	0.15
Mean flow velocity $U$ (cm)	6.9	35.3	34.6	33.2	27.4	23.6	30.7	74.4	48.2	94.5
RMS $u$ (cm)	1.6	5.4	2.7	7.5	5.3	2.0	4.1	10.1	7.1	9.9
RMS $v$ (cm)	1.1	4.0	2.7	4.8	4.0	1.7	2.7	7.8	4.0	6.2
Correlation $u$ and $v$	-0.31	-0.29	-0.19	-0.30	-0.21	-0.31	-0.39	-0.33	-0.41	-0.29
Correlation $u$ and $h / 0.75H$	-0.05	-0.05	-0.02	-0.10	-0.06	-0.06	-0.04	-0.03	-0.02	-0.05
Correlation $v$ and $h / 0.75H$	0.05	0.13	0.03	0.03	0.03	0.05	0.07	0.08	0.08	0.18
Correlation $u / 0.25 - 0.5H$	0.34	0.22	0.36	0.53	0.34	0.28	0.42	0.37	0.46	0.51
Correlation $v / 0.25 - 0.5H$	0.12	0.37	0.15	0.23	0.19	0.17	0.32	0.10	0.24	0.18
<i>Cumulative time series</i>										
Correlation $u$ and $v / 0.5H$	-0.62	-0.49	-0.42	-0.52	-0.56	-0.69	-0.79	-0.81	-0.26	-0.62
Correlation $u$ and $h / 0.75H$	-0.38	-0.73	-0.45	-0.48	-0.27	-0.71	-0.81	-0.51	-0.57	-0.35
Correlation $v$ and $h / 0.75H$	0.67	0.71	0.51	0.49	0.72	0.57	0.25	0.42	0.62	0.68
Correlation $u / 0.25-0.5H$	0.91	0.73	0.67	0.86	0.54	0.91	0.90	0.76	0.66	0.51
Correlation $u / 0.5 - 0.75H$	0.59	0.76	0.51	0.56	0.55	0.81	0.94	0.55	0.87	0.61
Correlation $v / 0.25 - 0.5H$	0.24	0.48	0.68	0.46	0.24	0.56	0.41	0.47	0.16	0.62
Correlation $v / 0.5 - 0.75H$	0.76	0.51	0.81	0.59	0.60	0.13	0.22	0.45	0.47	0.56

total station surveys presented in Figure 2.5. Note that to distinguish the flow depth of the velocity measurements exact location  $H$ , we use  $Y$  to identify the average section flow depth,  $Y_R$  and  $Y_P$  for the riffle and pool flow depths.

The laboratory measurements were conducted in a flume that was 10 m long, 0.3 m wide and 0.5 m deep. The flume bed was covered with a 15 cm thick sediment layer of well sorted gravel with a  $D_5 = 4$  mm,  $D_{50} = 10$  mm and  $D_{95} = 16$  mm. Special care was taken to ensure that the gravel thickness was uniform across the flume. Velocity time series were collected in the test section at 5.9 m downstream from the flume inlet using a Vectrino acoustic Doppler velocimeter from Nortek. The instrument was always located at  $0.5H$  above the bed. Twelve 30 minutes velocity time series were sampled at 20 Hz at three flow depths (0.08, 0.12 and 0.16 m) and four average flow velocities (approximately 0.08, 0.20,

Table 2.4 Flume time series characteristics.

Run	A1	A2	A3	B1	B2	B3	C1	C2	C3	D1	D2	D3
Flume slope (%)	0.2	0.2	0.2	0.2	0.2	0.2	0.5	0.5	0.5	0.5	0.5	0.5
Reynolds number ( $\times 10^{-3}$ )	6.7	10	13	15	24	33	33	52	68	50	79	91
$H$ (cm)	8	12	16	8	12	16	8	12	16	8	12	16
RMS $h$ (cm)	0.05	0.02	0.01	0.03	0.05	0.03	0.27	0.24	0.18	0.29	0.35	0.27
Mean flow velocity $U$ (cm)	8.4	8.4	8.1	18.9	20.3	20.8	40.9	42.5	42.3	61.9	65.6	57.2
RMS $u$ (cm)	1.8	1.8	1.3	4.4	3.5	2.7	7.4	6.6	5.1	10.9	9.5	7.2
RMS $v$ (cm)	0.8	0.7	0.5	1.7	1.4	1.1	3.1	2.6	2.2	4.0	3.7	3.1
Correlation $u$ and $v$	-0.51	-0.45	-0.44	-0.41	-0.51	-0.41	-0.62	-0.61	-0.52	-0.68	-0.61	-0.57
Correlation $u$ and $h$	-0.06	-0.10	-0.06	-0.04	-0.06	-0.09	-0.04	-0.04	-0.05	-0.05	-0.05	-0.04
Correlation $v$ and $h$	0.06	0.13	0.05	0.05	0.06	0.09	0.05	0.05	0.05	0.04	0.05	0.04
<i>Cumulative time series</i>												
Correlation $u$ and $v$	-0.86	-0.38	-0.89	-0.92	-0.93	-0.78	-0.79	-0.89	-0.67	-0.63	-0.88	-0.76
Correlation $u$ and $h$	-0.49	-0.46	-0.40	-0.41	-0.56	-0.42	-0.65	-0.44	-0.65	-0.33	-0.52	-0.43
Correlation $v$ and $h$	0.60	0.77	0.36	0.48	0.60	0.70	0.39	0.44	0.29	0.34	0.60	0.39

0.40 and 0.60 ms<sup>-1</sup>). Flow velocities were sampled simultaneously with the measurement of the water surface fluctuations at 10 Hz using the same ultrasonic sensor described previously. The main flow characteristics are presented in Table 2.4. The choice of the combination of flow velocities and flow depths was made in order to avoid any correlation between the two factors. In order to be consistent with the ECMs time series, only the streamwise and vertical velocity components will be considered in this paper.

### 2.3.3.2. Data analysis

Before proceeding to further analysis, the ECMs signals were visually inspected to identify discontinuities and anomalous spikes, most often associated with leaves or other debris hitting the probes. Following data inspection, raw signals were defiltered to remove the effect of the analog R/C filter in the ECM measurements according to the recommendations from Roy et al. (1997). Data spikes were removed using the procedure of Goring and Nikora (2002), and high-frequency electronic noise above the Nyquist frequency was filtered using a third-order Butterworth filter. The raw Vectrino signals were of high quality with correlation values always above 70 % and signal to noise ratios in the order of 30-40. The ultrasonic sensor time series are kept relatively raw, except for the data spikes larger than three times the standard deviation that were replaced by interpolating the

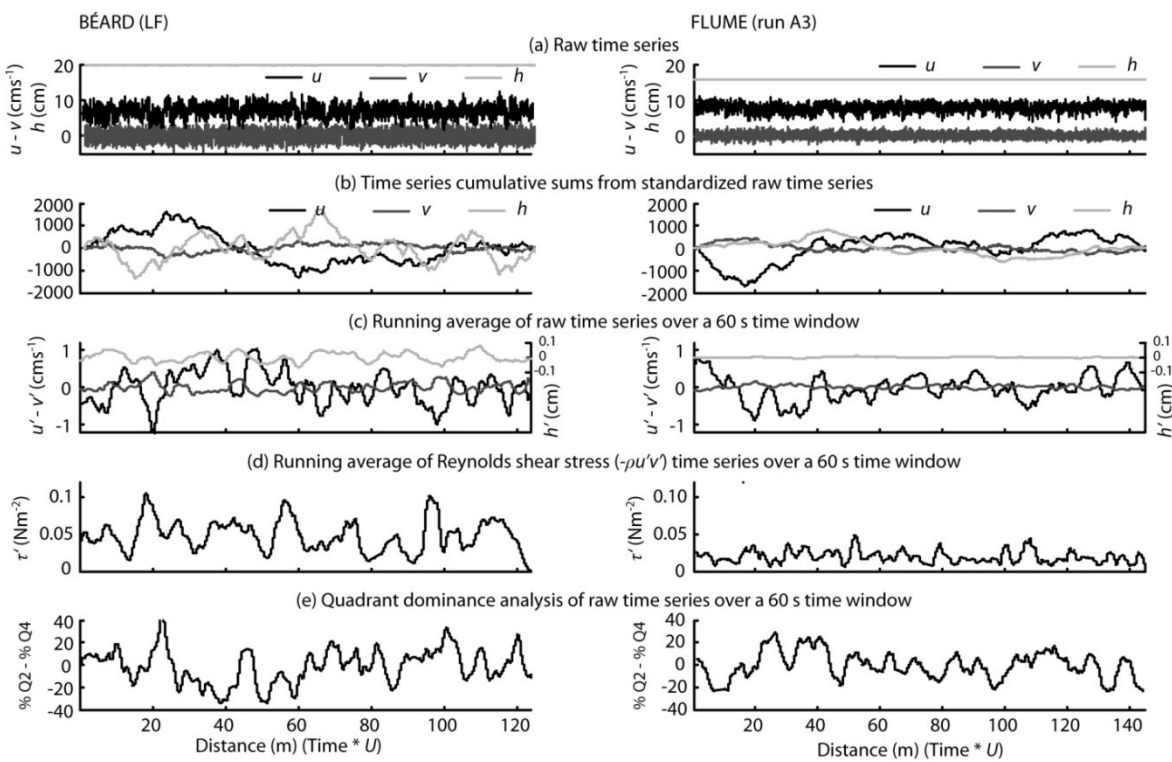


Figure 2.6 Raw time series (a) and transformed times series (b to e) for the low flow stage measurements at Béard Creek and the run A3 in the flume. The examples were chosen for their similar flow depth and average velocity.

nearest data points. Finally, the stationarity of all time series was validated by testing if the slope of the linear regression between the velocity measurements and time was equal to 0. The time series were shortened as needed in order to obtain a zero slope ( $p < 0.01$ ).

The detection of the flow pulsations cannot be done by traditional means of two point correlations or spectral analysis as the velocity signals suffer from a loss in correlation over long time scales (Kim and Adrian, 1999) and possibly because the very large-scale turbulent flow structures may tend to meander (Hutchins and Marusic, 2007). Therefore, we will use several non traditional approaches to detect the presence of flow pulsations within the velocity signal. Figure 2.6a shows an example of 30 minutes of the time series measured at  $0.5H$  for low stage conditions in Béard Creek. There are no obvious low frequency oscillations in the raw streamwise or vertical velocity component of the flow as the high frequency variations display large amplitude. It is also possible to observe that the flow depth remains steady without major variations. But, when transforming the time series by cumulating the sums of the fluctuations of the streamwise ( $u'$ ) and vertical ( $v'$ ) velocity components and of the water depth fluctuations ( $h'$ ), it is possible to observe low

frequency oscillations as the high frequency fluctuations are damped as shown by Marquis and Roy (2011). There are periods when the positive fluctuations are more frequent or stronger than the negative fluctuations (or vice-versa) which results in a positive (or negative) trend of the cumulative sum of the time series fluctuations (Figure 2.6b).

Another way to dampen the high frequency fluctuations is to use running average on the time series of  $u'$ ,  $v'$  and  $h'$ . We used a moving window of 60 s to obtain the series in Figure 2.6c. The choice of the length of the window, even though arbitrary, is based on the fact that the window should be smaller than the smallest pulsation length in the data set with respect to our hypothesis concerning the potential control of the pool spacing on the pulsation length. By dividing the pool spacing of the river (Table 2.2) by mean flow velocity (Table 2.3), the expected pulsation durations are all longer than 60 seconds except for the high flow conditions at Beard creek where the expected duration is 34 seconds. We tested the effect of using a moving time window of 30 seconds compared to 60 seconds on the estimation of the pulsation duration and the effect on the resulting time series was very slight. We decided to use the 60 seconds time window for all the data sets because it is generally recognised that a sample of one minute is the minimum record length to obtain stable parameters to characterize river mean and turbulent flow properties (Buffin-Belanger and Roy, 2005).

The running average time series of  $u'$  were used to calculate the length of the flow pulsations as it is for this component that the oscillations are strongest (Figure 2.6) and also because previous studies on VLSMs and superstructures described in the introduction primarily used the streamwise component of the flow. The detection of the low and high-speed pulsations rested on the application of the *U-level* detection scheme as modified by (Luchik and Tiederman, 1987):

$$|u'| = k \text{RMS}u \quad \text{Equation 2.3}$$

The scheme was applied to the running average time series of  $u'$ , with the  $\text{RMS}u$  estimated as the root mean square of the raw velocity time series. When using a threshold ( $k$ ) equal to zero in the detection scheme identifies high-speed structures when the running average time series is higher than the mean and low-speed structures when the averaged time series is lower than the mean. The duration of a pulsation was considered to be a complete cycle composed of successive *low* and *high-speed* pulsations (Marquis and Roy, 2011). For each

time series, we averaged all durations of the detected flow pulsations at all three heights to obtain a single value for each set of measurements. The average duration was multiplied by the mean flow velocity to obtain a ‘typical’ pulsation length. To appreciate the variability in pulsation lengths for the same time series, we also estimated the 25<sup>th</sup> and 75<sup>th</sup> percentiles of the distribution.

To illustrate the effect of the flow pulsations on the general characteristics of the flow and possibly on river processes such as sediment transport, we also calculated the running average time series with a moving time window of 60 seconds of the Reynolds shear stress ( $\tau$ ):

$$\tau = -\rho u' v' \quad \text{Equation 2.4}$$

where  $\rho$  is the water density of 1000 kgm<sup>-3</sup> (Figure 2.6d). Finally, we also estimated over moving time windows of 60 seconds the duration imbalance between the two dominant turbulent flow structures, the ejection and sweeps by using the quadrant detection technique (Lu and Willmarth, 1973). Ejections (quadrant 2, Q2) correspond to the situation where we have simultaneously  $u' < 0$  and  $v' > 0$  while sweeps (quadrant 4, Q4) correspond to the situation where  $u' > 0$  and  $v' < 0$ . Over a given 60 s window, we detected the structures and subtracted the percentage of time occupied by sweeps and the percentage of time occupied by ejections. This procedure allows us to obtain a time series of the coherent turbulent flow structure dominance over time (Figure 2.6e). In this paper, we focused only on the sweeps and ejections as these structures are known to be responsible for most of the momentum exchange between the inner and outer regions of the flow in the turbulent boundary layer (Kline et al., 1967).

### 2.3.4. Results

#### 2.3.4.1. Main flow characteristics

The velocity time series measured in the field are comparable to other steady uniform fully developed turbulent flows in gravel-bed rivers (e.g. Kirkbride and Ferguson, 1995; Buffin-Belanger et al., 2000; Roy et al., 2004). In Table 2.3, the raw time series characteristics are shown mainly for the sensor located at 0.5H in the flow. The other two sensors at heights of 0.25 and 0.75H display very similar characteristics. In general, the correlation values between the  $u$  and  $v$  components are negative while there is a positive

correlation between velocity components measured at different heights above the bed for both the  $u$  and  $v$ . This indicates the presence of high- and low-speed LFM s occupying the entire flow depth and the dominance of ejections and sweeps in the turbulent flow. As for the correlations between the water height fluctuations and the two velocity components, the correlation values are weak even though the signs of the correlation coefficients may be what one would expect: an inverse relation between  $u$  and  $h$  and a positive relation between  $v$  and  $h$ . This means that when there is a low-speed turbulent flow structure, the water surface tends to bulge, as there is a dominant vertical velocity toward the surface and when there is a high-speed flow structure, water height tends to decrease corresponding to a dominant vertical velocity oriented toward the bed. The characteristics of the time series measured in the flume cover a similar range of mean flow velocities as in the field except that the vertical turbulent intensities do not exceed 10 % and the correlations between  $u$  and  $v$  are stronger probably because of the smoother bed surface and of the absence of bed morphology (Table 2.4).

### 2.3.4.2. Flow pulsation characteristics

Figure 2.6 presents two examples, the first from the data measured at Béard creek at low flow conditions and the second, the results from a run in the flume with similar mean flow velocity and a slightly shallower flow than the field example. Both time series are 30 minutes long. The horizontal axes of the plots in Figure 2.6 represent distances estimated using the Taylor frozen turbulence hypothesis instead of time to give an idea of the length scales considered here. From the typical instantaneous velocity time series shown in Figure 2.6a, low frequency oscillations are revealed in the streamwise and vertical velocity and in the water height signals from both the cumulative sum of the fluctuations and the moving average analyses (Figure 2.6bc). These low frequency oscillations are meters long, can last several seconds up to a few minutes and they correspond to flow pulsations that are detected in both velocity components. These pulsations have a direct consequence on the variability of the Reynolds shear stress that also exhibits well defined and quite regular low frequency cycles in synchronicity with the velocity oscillations (Figure 2.6d). The low frequency pulsations in the streamwise and vertical components also result in marked fluctuations of the balance between time proportions occupied by ejections and sweeps (Figure 2.6e). The two examples shown in Figure 2.6 are typical of what can be observed for all field and flume velocity and water height time series.

When examining the correlations estimated for the field data set between the two flow components and between the measurements at different heights above the bed for the cumulative sums time series, the same characteristics as those observed from the analyses of the raw velocity time series are revealed but in a stronger fashion (Table 2.3). The high correlation values between the  $u$  and  $v$  components show that the structure of the flow pulsations is self-similar to the structure of the LSMs. The pairwise correlation coefficients between the streamwise velocity components measured at different flow depths range between 0.51 and 0.94. This confirms that the flow pulsations occupy the entire flow depth in shallow gravel-bed rivers. In addition, the correlations between the cumulative fluctuations time series of  $u$  and  $h$  are strongly negative while those of  $v$  and  $h$  are strongly positive. This suggests that strong interactions between the flow and the water surface oscillations may play a role in the generation of multiple scale coherent flow structures. Similar strong relations between  $u$ ,  $v$  and  $h$  are observed for the cumulative time series measured in the flume experiments, confirming the presence of low frequency oscillations embedded in the signals in an environment without large-scale morphological features (Table 2.4).

An examination of the amplitudes of the running average time series of  $u$ ,  $v$  and  $h$  confirms that the coherent organisation of the flow is strongest in the streamwise direction. Through a comparison of all time series obtained for each types of analysis reported in Figure 2.6b-e, it is possible to observe that generally, the amplitude of the low frequency oscillations is more important for Béard creek time series compared to the flume time series, even though the two data sets exhibit similar turbulent flow conditions. Extending this comparison to the whole data set, the amplitude of the flow pulsations for the streamwise and vertical components is slightly greater in the field data than in the flume measurements (Figure 2.7a). There is, however, a marked difference for the water surface and the Reynolds shear stress with average field pulsation amplitudes about twice as large as those revealed in the flume data. This tendency is also observed with an even stronger difference between the field and flume flows when comparing the standard deviation of the cumulative sums time series (Figure 2.7b). The difference is also detected in the ejection/sweep imbalance minima and maxima (Figure 2.7c). For means of comparison, we have generated twelve normally distributed random time series of  $u$ ,  $v$  and  $h$  having the same duration and characteristics as the twelve flume runs. Applying the same procedures

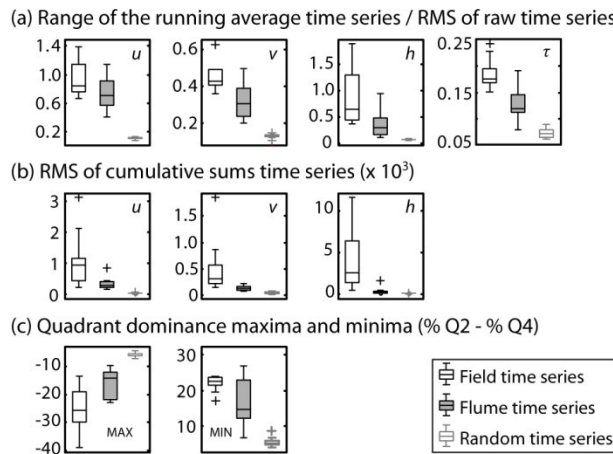


Figure 2.7 Comparisons of the flow pulsation amplitudes for different analyses between the field time series, the flume time series and random time series (generated based of the characteristics of the flume time series).

and analyses to assess the amplitude of the resulting signals clearly shows that the flow pulsations detected in the field and in the flume are not artefacts of our analyses. The amplitude of the random time series is much smaller than the amplitude of the flume time series and the difference is even greater for the field data (Figure 2.7).

### 2.3.4.3. Flow pulsations length

Flow pulsations length varies from 5 to 100 m for the flume data set and from 10 to 300 m for the field data sets. Figure 2.8 and Figure 2.9 present the relations between pulsation length and the main flow and morphological variables. Figure 2.8a shows the relation between the mean pulsation length and the mean flow velocity for all three flow depths of the flume experiments. The relation is very strong ( $R^2 = 0.87$ ) but the variability in pulsation lengths is high. Also, we can observe that there is no specific pattern that would reveal a scaling with flow depth. Figure 2.8b shows flow pulsation length against mean flow velocity for the field data. The slope of the relation is steeper than for the flume data. This is mainly due to the Sainte-Anne river B data which pull the slope of the relation upward and enhance its strength. There is, however, a striking difference between the flow pulsations identified from the field data when compared to the flume measurements: their length is much less variable. Figure 2.9a presents the scaling between flow pulsation length and pool spacing. As there are 30 % of the points that do not fall near the 1:1 line, we also present the scalings with other morphological variables. Pulsation length does scale with

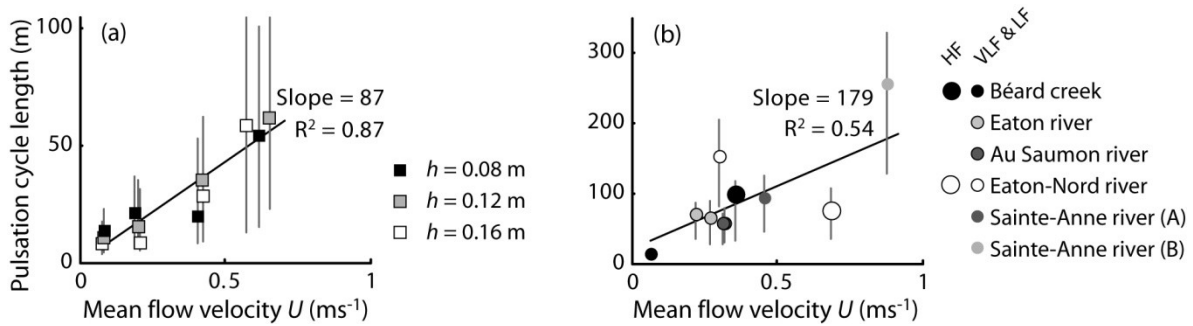


Figure 2.8 Relations between the pulsation cycle length and the mean flow velocity for (a) the flume data set and (b) the field data set. The grey vertical lines represent the range of values between the percentiles 25 and 75 of the pulsation lengths.

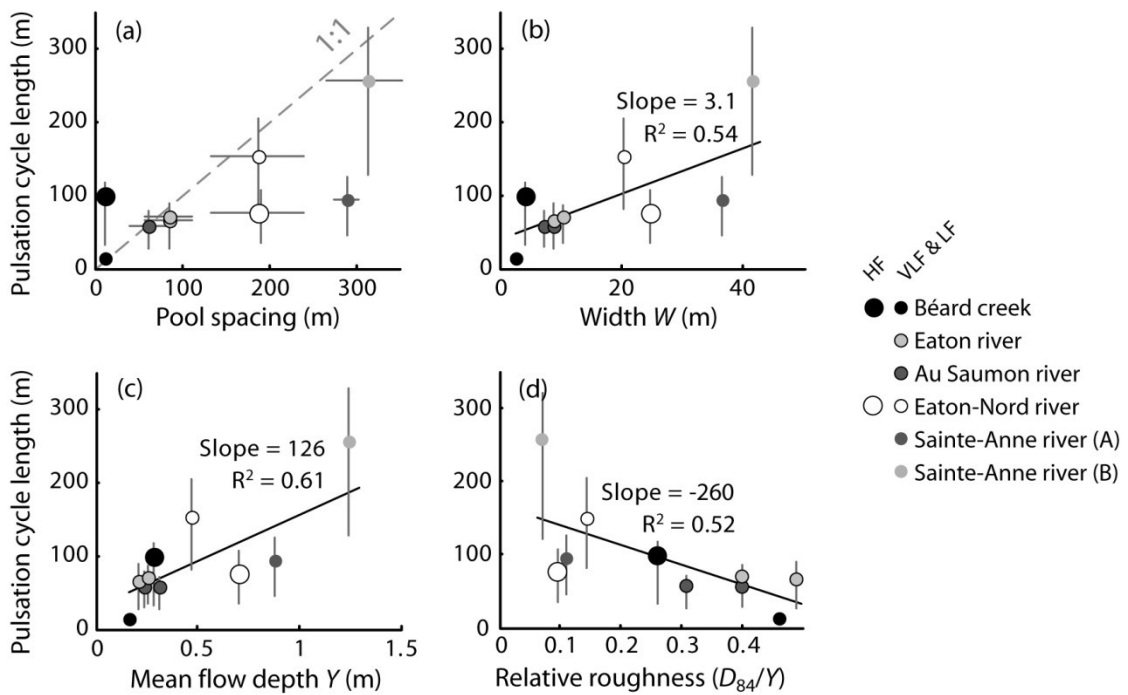


Figure 2.9 Relations between the pulsation cycle lengths measured in the field and (a) the pool spacing, (b) the channel flow width, (c) the mean flow depth of the reach and (d) the relative roughness of the reach. The grey vertical lines represent the range of values between the percentiles 25 and 75 of the pulsation lengths. The horizontal grey lines in (a) represent the range of pool spacing upstream of the measurement point.

the channel width occupied by the flow and flow depth but the relations display some scatter (Figure 2.9bc). Figure 2.9d shows that as the relative submergence of isolated roughness elements ( $D_{84}/H$ ) increases, flow pulsation length decreases. The scalings presented in Figure 2.8 and Figure 2.9 do not allow for a simple confirmation of the

morphological hypothesis suggesting the pool spacing would control pulsation length but the results can provide a basis for speculation on the mechanisms that could explain the origin of the pulsations.

### 2.3.5. Discussion

In this paper, we have identified low frequency oscillations, that we have called flow pulsations, in the streamwise and vertical instantaneous velocity signals and in the flow depth fluctuations. The flow pulsations identified here are larger than any reported in the literature for flows over a static bed as their length is around one hundred times the flow depth. The only low frequency oscillations of similar scales were reported for a flow over mobile bedforms in a river by Dinehart (1999) and in a flume by Singh et al.(2010). Our first objective was to show that such long cycle flow pulsations are characteristic features of shallow flows over rough river beds. Our measurements of long velocity time series both in the field and in a flume present low frequency oscillations (i.e. flow pulsations) embedded in the signal. We used non traditional analyses to reveal these oscillations because two points correlation and spectral analysis are not appropriate to identify low frequencies in time series due to convection velocity (Kim and Adrian, 1999). Overall, the high correlation coefficients observed for the cumulative velocity and water height time series when compared to the raw time series suggest that the low frequency oscillations have a greater coherency than the higher frequency oscillations of the flow (Table 2.3 and Table 2.4). This seems to be an intrinsic characteristic of steady turbulent flows in shallow open-channel flows with a rough bed. The comparison between the flume and field flow pulsation amplitudes with those of randomly generated time series confirms that the detection of flow pulsations is not an artefact of the analyses (Figure 2.7).

Our second and principal objective is to speculate on the possible origin of the flow pulsations regarding two opposite hypotheses: self-organisation of turbulent LFM's into larger flow pulsations and the morphological control on the pulsation lengths. One of the main schools of thought in the study of turbulence seeks to break the complex, multiscaled, random fields of turbulent motion down into more elementary organized motions (Adrian, 2007). Many have argued that individual turbulent CFS were the building blocks that form larger coherent structures such as VLSMs or superstructures with lengths up to  $20\delta$  (Hutchins and Marusic, 2007). In this book, Adrian put a question mark on the maximal

extent of the build-up of small structures into larger ones. The pulsations described in this paper could very well be a bottom up process as they are self-similar to the typical LSMs. Firstly, the flow pulsations are present in the flume data set even in the absence of large scale morphological features or isolated roughness elements on the gravel bed. Secondly, the flow pulsations have self similar characteristics to the LSMs as they occupy the entire flow depth and exhibit a negative correlation between the streamwise and vertical velocity component (Table 2.3 and Table 2.4). They are also scaling with mean flow velocity like for the LSMs (Shvidchenko and Pender, 2001) (Figure 2.8). Thirdly, the scaling of the flow pulsations with various morphological features is not straightforward, as we would expect if there was a single morphological control on the formation of flow pulsations (Figure 2.9). But, one cannot tell if the build-up of large flow motions from small turbulent structures is a coherent process or an alignment by chance (Dennis and Nickels, 2011).

The fact that the flow pulsations observed in the flume have a weak amplitude, more irregular lengths and do not scale with flow depth (which is the only outer scaling that changes) when compared to the flow pulsations identified in the field data suggests that there might be an external control in action. The hypothesis of a pool-spacing control on the pulsation length as proposed by Marquis and Roy (2011) implies that for a given river, pulsation length would remain constant for different flow stages. In Figure 2.9a, even if most of the data points (7 out of 10) are close the 1:1 line, there are three outliers that prevent us to confirm unambiguously the pool-spacing control on pulsation lengths. We have explored other morphological variables and the best fit was with the relative submergence of isolated roughness elements. Even though these elements are known to only have a local effect on the flow (Lamarre and Roy, 2005; Lacey and Roy, 2007; Legleiter et al., 2007), it is plausible to assume that when local roughness elements protrude relatively high in the flow, there is less chance that long flow structures form and travel downstream. In other words, they limit the maximal extent of the flow pulsations. But isolated roughness elements also increase the turbulence intensity of the flow (e.g. Buffin-Belanger and Roy, 1998) so they may be responsible for the larger amplitude of the pulsations observed in the field data. These results lead us to consider also the relative submergence of the riffles defined as  $(Y_R - Y_P)/Y_P$ . Redrawing Figure 2.9a, the relation between pulsation length and pool spacing, with the data points that are proportional in size to the riffle relative submergence reveals that the three outliers (in shaded grey in Figure

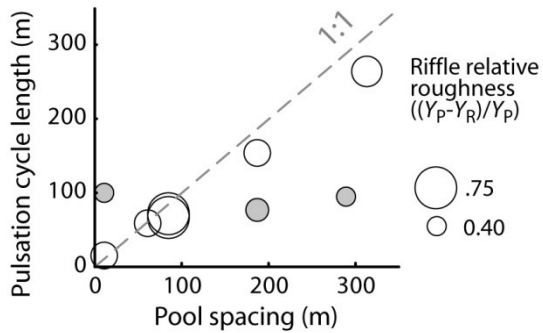


Figure 2.10 Relation between the pulsation cycle lengths measured in the field and the pool spacing. The size of the data points is proportional to the riffle relative roughness. The outliers are identified by grey circles instead of white.

2.10) have the smallest relative riffle roughness (around 0.4). Two of these points correspond to high flow stages measured at Béard creek and the Eaton-Nord river. The third point is the low flow stage set of measurements at Sainte-Anne river B. This site is an elongated pool without marked flow expansion at the entrance or flow contraction at the exit (Figure 2.5). All measurements taken at very low and low flow stages have pulsations length scaling with pool spacing. The riffle relative roughness would act as a control of the flow pulsation cycle length perhaps by a fill and spill process associated with the flow contraction over the riffle. This control would also be confirmed by the presence of low frequency oscillations in water surface height fluctuations that correlate with the streamwise and vertical velocity pulsations (Table 2.3 and Table 2.4). Our measurements of the water surface fluctuations also support Levi's hypothesis (1983) concerning the outer control of coherent flow structures generation by travelling surface waves. The constriction of the flow imposed when riffle submergence is high might have an effect on the flow surface which in turn affects the velocity fields. However, nothing in our data set prevents us to argue the contrary to the effect that the morphology influences the velocity field which in turn influences the water surface.

### 2.3.6. Implications and conclusions

According to our results, flow pulsations seem to find their origin in a mixture of bottom-up and top-down processes. We propose that flow pulsations tend to exist by themselves in a turbulent flow above a rough bed but that there is a positive feedback mechanism through the relative submergence of isolated roughness elements and of riffles

as it is combined with pool spacing that reinforces their structure (i.e. the amplitude) and that modulates their length. In spite of the interest of the discussion on the origin of the flow pulsations, the simple fact that such pulsations exist and are ubiquitous in shallow flows over gravel beds is a major issue for the understanding of fluvial processes in general and for the understanding of bedload transport in particular. During a flood, bedload often occurs in a pulsating manner (Reid et al., 1985). These pulses are often associated with bedload sheets travelling downstream (Whiting et al., 1988) but their formation procession is not yet fully understood (Recking et al., 2009). The measurements of flow while gravel bedforms were travelling downstream have led to the hypothesis that the travelling bedforms were inducing low frequency oscillations in the velocity signals (Dinehart, 1999; Singh et al., 2010). Here, we have shown that flow pulsations exist without travelling bedforms and even without bedforms at all. It is highly likely that flow pulsations interact with bedload transport to create pulses of grains travelling downstream. Furthermore, flow pulsations have a strong impact on variables that contribute to individual grain entrainment. The Reynolds shear stress and the quadrant dominance through time are also exhibiting low frequency oscillations with large departures from the mean values (Figure 2.6de). Therefore, the implications of a better understanding of the flow pulsation scalings that we have explored in this paper could allow us to predict their scale and maybe relate them to the scale of bedload pulses.

## Acknowledgements

The authors would like to thank Rachel Thériault and Claude Gibeault for their help in the field. We would like to thank Steve Rice for granting the access to their equipment and facilities. We also acknowledge the financial support of National Science and Engineering Council (NSERC) and the Canadian Foundation for Innovation (CFI).

## 2.4. Paragraphe de liaison, chapitres 2-3

Dans le chapitre 2, l'existence de pulsations de l'écoulement durant plusieurs minutes a été démontrée. La détection des pulsations pour différents niveaux d'eau dans les cinq cours d'eau étudiés et dans un chenal expérimental suggère que la présence de ces structures est universelle dans les écoulements en rivières à lit de graviers. Bien que les mesures aient été récoltées en l'absence de transport de sédiments en charge de fond, la taille et la durée des pulsations a le potentiel de correspondre aux échelles de fluctuations caractéristiques du transport de sédiments en charge fond lors d'une crue. Malgré des efforts soutenus et répétés durant le temps qu'a duré cette recherche doctorale, il n'a pas été possible de vérifier cette hypothèse en mesurant simultanément le transport en charge de fond et des séries temporelles de vitesse à haute résolution temporelle en milieu naturel pour des raisons essentiellement logistiques. Toutefois, cette hypothèse a permis de générer une réflexion sur l'utilisation des données d'écoulement disponibles sous la forme de mesures de hauteur d'eau prises à différents endroits le long d'un tronçon d'une rivière graveleuse. En effet, la principale conséquence des pulsations de l'écoulement est la mise en lumière que l'écoulement n'est pas constant, même si les mesures ont été récoltées pour des écoulements apparemment stables.

La reconnaissance de l'importance des taux de changement de l'écoulement a des implications majeures sur la compréhension des dynamiques fluviales. En effet, la plupart des concepts de base utilisés dans l'étude du transport de sédiments en charge de fond sont issus d'équilibre de forces où les conditions sont considérées comme étant constantes. Cette simplification de la réalité très utile dans plusieurs situations est probablement erronée lorsque les taux de changement sont rapides, empêchant l'ajustement progressif du système aux nouvelles conditions imposées. Si on reporte cette reconnaissance de la variabilité continue de l'écoulement à ce qui se passe en période de crue, il devient rapidement évident que la montée et la récession des hydrogrammes de crue imposent des gradients d'accélération et de décélération majeurs et très variables d'une crue à l'autre. Donc, le chapitre 3 évalue les conséquences de la variabilité temporelle de l'ordre de la minute de l'accélération temporelle et spatiale sur les taux de transport de sédiments au cours de plusieurs crues au ruisseau Béard. Sa rédaction sous forme de lettre<sup>1</sup> a pour but de

transmettre le message important à la communauté scientifique de manière directe et synthétique.

1-Marquis G.A. et Roy A.G. Fluid acceleration and deceleration during flood hydrographs as drivers of bedload sediment transport. Manuscrit préparé pour la revue *Nature Geoscience*.

## **CHAPITRE 3. GRADIENTS DE CHANGEMENT : IMPACT DE L'ACCÉLÉRATION SUR LE TRANSPORT DE SÉDIMENTS**

---

### **3.1. Fluid acceleration and deceleration during flood hydrographs as drivers of bedload sediment transport**

#### **3.1.1. Abstract**

The extreme variability in bedload sediment transport observed in rivers even for very similar flow discharges poses a significant scientific challenge. The explanation of this variability has focused on the role of sediment characteristics and supply while the effects of rapidly varying flow conditions during a flood have not been examined. Using data sampled in a small gravel-bed river, we show that flow unsteadiness and non-uniformity as revealed by acceleration or deceleration gradients at short time scales during a flood event play a critical role in the explanation of bedload fluxes. The combined effect of the spatial and temporal accelerations explains as much of the bedload variability as stream discharge itself. This result opens a new avenue for understanding sediment transport in rivers and for developing predictive formulae. The variability in flow accelerations and its effects on bedload are associated with the shape of the hydrograph which is very sensitive to local and global environmental changes.

#### **3.1.2. Context**

The prediction and modelling of the movement of particles as bedload in rivers are still eluding scientists even though bedload transport is crucial in shaping the river bed and in ensuring a diversity of fluvial habitats (Diplas et al., 2008; Church, 2010; Jerolmack, 2011). The prediction of bedload transport rates is not only crucial for our understanding of the evolution of rivers but also for the implementation of adequate designs and of human infrastructures. Simply put, the problem of predicting when a particle on the river bed will move as bedload is a matter of determining when the forces of the flow will exceed the resistance of the particle to move. As simple as this may seem, bedload transport rates in a natural river can vary by one or two orders of magnitude for a given flow strength (Reid et al., 1985; Buffington and Montgomery, 1997), especially when the flow strength is near the threshold of particle motion (Jerolmack, 2011). Despite many attempts in developing

'geomorphic transport laws' in the past century (Dietrich et al., 2003), there is no satisfactory specific law to predict bedload transport, even though some useful approximations have been proposed (Church, 2010).

Much attention has been devoted to understand the causes of the spatial and temporal variability and of the intermittency of bedload processes in natural streams. Several factors linked with the sediment characteristics have been identified to be important such as the grain size distribution (Ferguson et al., 1989; Wilcock et al., 2001; Curran and Wilcock, 2005), the collective behaviour of the individual grains (Frey and Church, 2009), the sediment sources and supply (Dietrich et al., 1989; Gaeuman et al., 2005), the vertical sorting of the sediments (Parker and Sutherland, 1990; Wilcock and Detemple, 2005) or the changing bed particles packing (Marquis and Roy, 2012). The identification of so many factors renders the ultimate goal of improving bedload transport predictions far more complex to achieve.

To this date, very little attention has been given to the variability of the flow characteristics during a flood as a possible way to refine bedload predictions. The exception to this rule is the notable differences in sediment transport rates associated with the rising and falling limbs of the hydrograph (Kuhnle, 1992; Hassan and Church, 2001; Hsu et al., 2011). This phenomenon is mainly explained by the sediment characteristics such as the breaking of the armor layer at the beginning of the flood leading to higher bedload rates on the falling limb (Reid et al., 1985; Hassan and Church, 2001). However, most bedload transport formulae and experiments simplify the bedload transport problem using uniform and steady flow. But, a flood in a natural stream is unsteady by nature (Cao et al., 2010) and potentially non-uniform depending on the bed morphology. Temporal flow unsteadiness and spatial non-uniformity create acceleration gradients that influence drastically the general turbulent flow characteristics and the distribution of the shear stress forces (Song and Graf, 1996; Macvicar and Roy, 2007; Yang and Chow, 2008). The role of flow acceleration begins to be recognised as a key factor in the initiation of sediment transport (Drake and Calantoni, 2001; Puleo et al., 2003; Calantoni and Puleo, 2006), in the migration of sandbars in coastal environments (Hoefel and Elgar, 2003) and more recently in the motion of individual particles as bedload under turbulent flow acceleration in rivers (Venditti et al., 2010; Paiement-Paradis et al., 2011). Even though these observations were

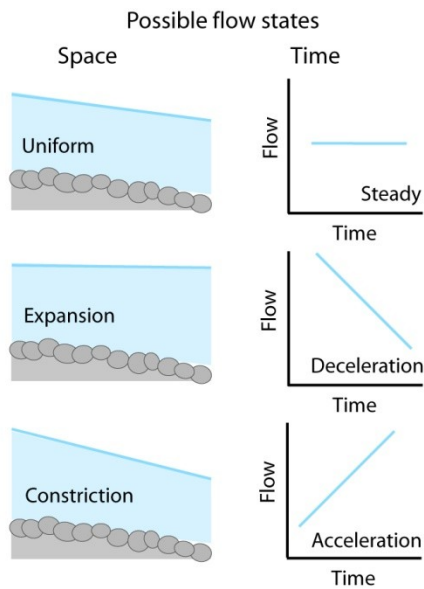


Figure 3.1 Possible flow conditions during a flood even. In space, the configuration of the river bed combined with the slope of the water surface determines if the flow is locally uniform (the bed and water surface slope are parallel), in expansion and decelerating (the bed slope is steeper than the water surface slope) or in constriction and accelerating (the water surface slope is steeper than the bed slope). In time, the rate of increase or decrease in flow depth during the rising and falling limb determined if the flow is steady, in acceleration or deceleration. Note that the spatial and temporal flow conditions can be combined with each other.

conducted at the grain scale, flow acceleration may play a critical role in the variability of bedload fluxes at a range of scales, a hypothesis that has not been yet tested.

### 3.1.3. Research question and hypothesis

This approach emphasises the fact that rates of fluctuations of the flow properties at short time scales during a flood may be related to the variability of bedload sediment transport. For instance, flow steadiness and uniformity conditions given by the temporal and spatial rates of change in flow depth may fluctuate greatly during a flood (Figure 3.1). This suggests that hydrographs with similar overall flow strength may have highly different behaviors that could be revealed by a fine scale analysis of the flow depth and of the water surface fluctuations. The question is how much of the variability in bedload transport rates is associated with the small scale fluctuations within a flood?

Here, we show that flow acceleration both in space and time explains a substantial portion of the variability in bedload transport rates in a natural gravel-bed river. Intense

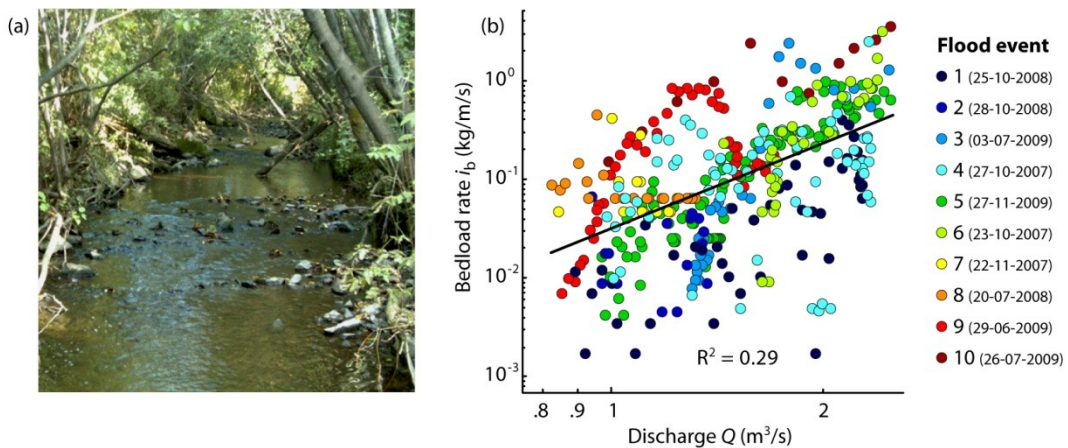


Figure 3.2 (a) Upstream view of the study section at Béard creek (Montérégie, Québec, Canada). (b) Unit bedload flux rate computed for periods of five minutes against average discharge during the same period estimated using a flow stage rating curve. For the remaining analyses in the paper, we used the standardized bedload rate residuals of the regression presented here. The color coding designates individual floods ranked in an ascendant order of the value median of the bedload rate residuals.

flow accelerations are known to create strong horizontal pressure gradients that act on the sediment and therefore lead to an increase in sediment fluxes (Drake and Calantoni, 2001). The varying pressure exerted on the bed surface changes the distribution of forces around individual grains (Smart and Habersack, 2007). Spatial acceleration or deceleration is defined as a gradient of flow depth in the downstream direction that is related to a flow constriction or a flow expansion (Figure 3.1). Temporal acceleration is the change of flow discharge as measured by flow depth where the rising limb of a flood hydrograph is mainly characterized by flow acceleration and the falling limb by flow deceleration (Figure 3.1). The role of acceleration on bedload motion is expected to be complex as there might be different combinations of the possible spatial and temporal states during a flood event in addition to differences in magnitude of the changes in acceleration.

### 3.1.4. Data sampling and transformations

To test the hypothesis, we measured bedload transport rates and the spatial and temporal flow acceleration in a small gravel-bed river (Figure 3.2a). Béard creek is 5 m wide with a bed slope of 0.01, a median size of the bed particles of 50 mm and a bankfull discharge reaching  $2.5 \text{ m}^3\text{s}^{-1}$ . Unit bedload rates ( $i_b$ ) were measured using a Birkbeck sampler with a load cell allowing for the real time measurements of the weight of the

particles falling into the sampler slot. Temporal flow acceleration was obtained using a flow stage gage installed on the bank alongside the bedload sampler. Flow depth was measured every minute allowing us to estimate the temporal change in the average flow depth through time ( $\Delta Y$ ) at intervals of 5 minutes. The spatial acceleration of the flow was estimated from the difference between the water surface slope ( $S_w$ ) and the bed slope ( $S$ ) immediately upstream of the bedload sampler. The bed slope was measured using a total station before each flood event and is assumed to remain constant during the flood. This assumption seems reasonable given the morphological stability of the river bed (Marquis and Roy, 2012). The water surface slope was estimated using the height difference between two flow stage measuring stations, the first being located on the bank of the cross-section where the bedload sampler was installed and the second 20 m upstream. For more information on the field site apparatus and data sampling, see Marquis and Roy (2012).

Because we are interested in the variability of bedload transport at conditions when we observe intermittent transport that occurs below full transport conditions, only data collected at flow stages below the bankfull discharge were used in this analysis. The data are obtained from 10 different flood events separated by at least 5 days over a period of three years for a total of 385 individual data points representing individual periods of five minutes. Floods 3 and 10 exceeded the bankfull discharge and therefore only the bedload data on the rising limb of the hydrograph are used, corresponding to the period before the sediment sampler was full. During floods 4 and 6 bedload samplers were full before the end of the event. However, it occurred during the falling limb and the peak discharge was below the bankfull discharge. The six remaining flood events have a complete record of bedload transport rates and discharge during the hydrograph. Bedload transport rates computed for periods of 5 minutes are presented as a function of discharge ( $Q$ ) in Figure 3.2b. There is a significant relation ( $p < 0.01$ ) between the two variables and it explains 29 % of the variance in transport rates. It is noticeable that bedload transport rates are scattered over two to three orders of magnitude for a given discharge value, a result that is comparable to observations reported in many previous studies on gravel-bed streams (Reid et al., 1985; Reid and Laronne, 1995). The regression residuals ( $\hat{t}_b$ ) represent the portion of the bedload rates that is not explained by the flow magnitude, which is 71 %. From this point, the analyses will focus on these residuals in order to test the effect of variations in flow acceleration (deceleration) on bedload.

### 3.1.5. Results and discussion

Figure 3.3a presents the distribution of the residuals in bedload rates for each flood, standardized by their root mean square error (RMS  $\hat{t}_b$ ). The scatter is wide for any given flood event but not as large as the possible range of values of the whole data set. Some of the events are well above the average expected bedload rate and others well below. Flood events are ordered according to the magnitude of the median residual value in bedload transport rates. This representation highlights clearly that a large portion of the bedload transport variability is not due solely to flow strength (Figure 3.3d). This hints at the role of specific governing flow conditions that may vary from one flood event to the other even if they have similar overall magnitude. Figure 3.3b and Figure 3.3c show the distribution of the temporal and spatial acceleration values for each flood event. The range of values for the temporal acceleration is large for a given flood event but it also varies greatly among the events. As for the spatial acceleration, the conditions remained relatively uniform during each flood event. This may reflect the fact that a unique value of bed slope estimated before a flood event begins is used in the analysis. Given that the river bed may adjust during a bedload event, there may be more variability in spatial acceleration during the flood than what is reported here. We consider, however, that the initial bed slope may still provide a good estimate of the situation because we expect most of the variability to come from the water surface slope fluctuations rather than the bed slope changes. Spatial acceleration values vary from flood to flood, ranging from moderate flow expansion (negative values) to very strong flow constriction with most of the data corresponding to moderate flow constriction.

A multiple regression between both acceleration variables and bedload transport rates residuals explains only 11 % of the variance, or 8 % of the bedload rates. Even though the determination coefficient is low, the regression model is significant ( $p < 0.01$ ). Both variables vary positively with bedload but the temporal acceleration has a stronger effect than the spatial acceleration. From this analysis, it would be natural to conclude that flow unsteadiness and non-uniformity influence bedload response only marginally. From a conceptual point of view, however, it is possible that bedload responds non-linearly to flow acceleration and that it has to adjust to the rapidly changing conditions. There might be a threshold that must be reached before any change is observable in the signal as it has been shown for the effects of pressure fluctuations on individual grains at the turbulent scale

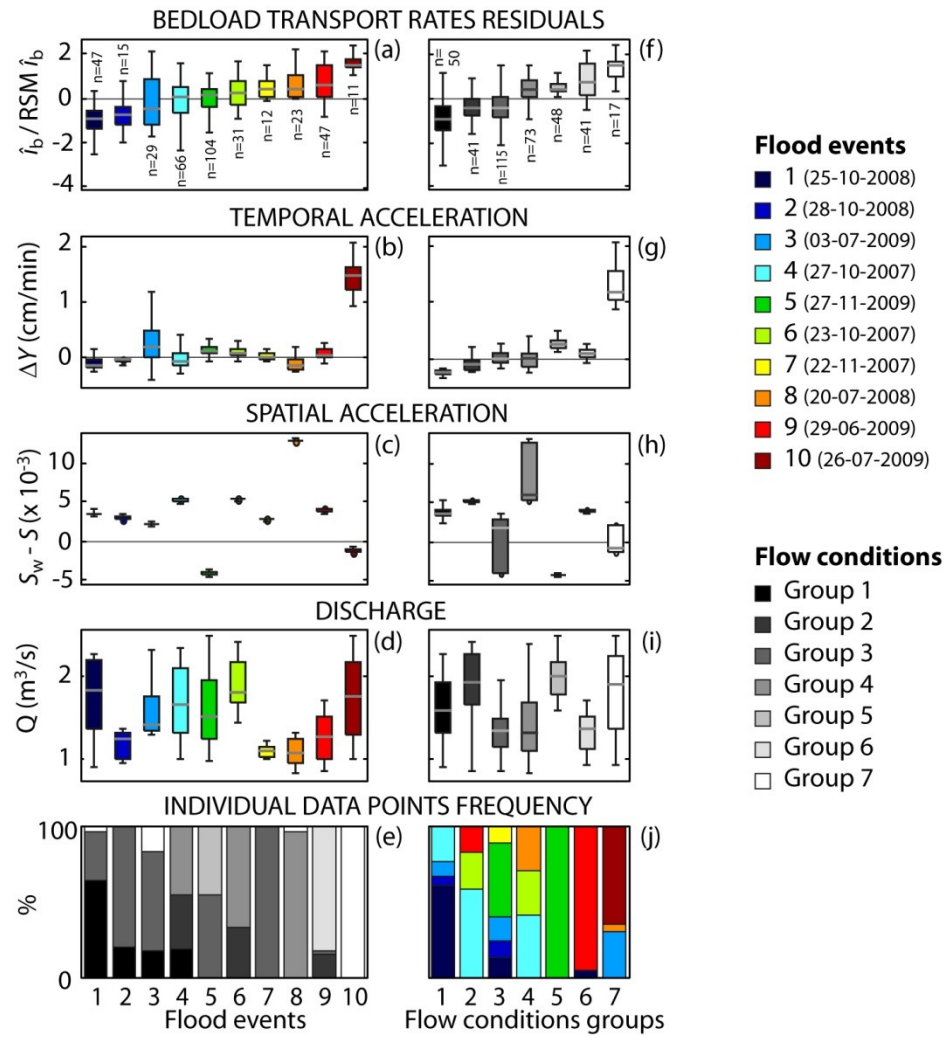


Figure 3.3 (abcd) The distributions of the variables used in the analysis for each flood event. (fghi) The distributions of the variables by flow condition groups defined through a regression tree model analysis. (e) Individual data points membership to flow condition groups for each flood event, the group colors are the same as in Figure 3.3g-i. (j) Individual data points membership to flood events for each flow condition group, the flood colors are the same as in Figure 3.2b and Figure 3.3a-d. In (a) and (f), the number of individual data points for a flood or a flow condition group is indicated.

(Diplas et al., 2008). Also, the joint effect of the spatial and temporal acceleration may not be additive and one variable may be prominent over the other during a flood.

To explore the non-linear response of bedload to flow acceleration, a regression tree analysis was performed on the data set (Breiman et al., 1993). The use of regression trees is suitable when the form of the relationship between the variables is unknown and potentially non-linear. The algorithm of the regression tree analyses considers the predictor variables,

in this case spatial and temporal accelerations, one at a time to build a nested sequence of individual groups that are as homogenous as possible in terms of bedload response. At each level or node, a recursive search finds the predictor that splits the groups into the most two dissimilar subsets. Because of their hierarchical nature, classification trees may reveal two different sets of conditions that lead to the same response. This could be very important for the interpretation of fluvial processes. Regression trees also have the advantage of detecting thresholds separating distinct behaviours. In this analysis, the final tree was pruned using a 10-fold cross-validation to obtain the smallest tree that is within one standard error of the minimum cost tree (Breiman et al., 1993). When applying the decision rules of the final tree to the data, the model split the data set into seven groups and explained 40 % of the variance of the bedload transport rates residuals. It also explains 28 % of the variance of the raw bedload rates which is as much as the variance explained by discharge. Given the important variability observed in bedload sediment transport rates, these results are highly meaningful.

Figure 3.3f presents the distribution of the individual residuals of bedload transport rates once classified according to the regression tree model. Analysing the flow conditions by group in Figure 3.3g, Figure 3.3h and Figure 3.3i, we can draw several important observations that confirm that flow unsteadiness and non-uniformity both play an important role in the variability of bedload transport rates:

1. Temporal acceleration has an important effect on bedload transport rates when the gradient is very high or very low. Strong deceleration diminishes the bedload transport and strong acceleration increases the bedload transport independently of the spatial acceleration flow state (Flow condition groups 1, 2, 5 and 7). It appears that there is a positive relationship between temporal acceleration and bedload transport rates mainly for extreme values.
2. When the temporal acceleration/deceleration is mild, the spatial state of the flow determines if the bedload rates are above or below the average rate for a given flow magnitude. Flow condition groups 3 and 4 have similar distributions of temporal acceleration values and they occur under similar overall flow strength but group 4 is characterized by a stronger flow constriction, which seemingly increases the bedload transport rates compared to those of group 3.

3. When the two acceleration variables act in the same direction, this results in an increase in bedload transport rate for a given flow strength. For example, group 6, characterized by moderate spatial and temporal flow acceleration values under low discharge, is the group with the second highest mean bedload rates residuals.

These results support the hypothesis that spatial acceleration plays a role in the variability of bedload rates but only when the flow is quasi-steady or when temporal acceleration reinforce the effect of the spatial acceleration. Otherwise, temporal acceleration dominates the explanation of the bedload rates variability.

Figure 3.3e shows the membership of the individual data points to the flow conditions identified through the regression tree analysis for each flood. Most floods are characterized by multiple flow conditions, confirming that the spatial and temporal accelerations play a role at a shorter time scale than solely the rising/falling limb opposition. Figure 3.3j shows the membership of the individual data points to the floods for each flow condition. Specific flow conditions are repeated in several floods, confirming that flow conditions are not characteristic of a single flood event. This suggests that spatial and temporal accelerations represent a causal factor in bedload variability and that our results do not represent flood specific processes associated with sediment characteristics such as sediment supply or bed particle packing.

### **3.1.6. Perspectives**

The overall significance of these results is that hydrographs characterized by a relatively similar signature as revealed by peak discharge or other flow strength measures may differ substantially in their behavior at a finer scale thus explaining a substantial part of the variability in bedload transport rates. In our study, flood events differed in terms of their overall strength as well as in the spatial and temporal rates of change in flow depth. This highlights the fact that the flood hydrograph regime at all scales is a major factor in predicting bedload transport rates variability. This research introduces a new avenue for the study of bedload transport variability and it has major implications in the context of environmental changes where the type of flood events may change substantially. Local and global environmental changes modify not only the magnitude of floods but also the shapes of the storm hydrograph thus affecting the acceleration gradients and therefore bedload

sediment transport. This study shows that it will be critical to consider these effects in order to predict sediment mobility and transfer in gravel-bed rivers.

### **Acknowledgments**

The authors would like to thank Mr. and Ms. Cloutier for allowing access to their land. Martin Lambert and Jean-François Myre were of great support for the design and construction of the bedload samplers. We are also grateful to Christine Bergeron-Verville, Vincent Cardin-Tremblay, Laurence Chaput-Desrochers, Sylvio Demers, Claude Gibeault, Hélène Lamarre, Olivier Lalonde, Kevin Partington, Mathilde Péloquin-Guay, Mathieu Roy, Katherine Sicotte, Rachel Thériault, Julie Therrien and Michèle Tremblay for their help in the field and in the lab. This research was supported by the Natural Sciences and Engineering Council and the Canadian Foundation for Innovation.

### 3.2. Paragraphe de liaison, chapitres 3-4

Les résultats des chapitres 2 et 3 ont traité de la variabilité temporelle de l'écoulement de l'ordre de la minute afin de mieux cerner la variabilité de transport de sédiments au cours d'une crue. Ils soulignent l'importance des taux de changement à une échelle de temps relativement courte et ont mis l'accent sur des sources expliquant la variabilité temporelle du transport de sédiments en charge de fond. Or, ce phénomène est reconnu pour être également variable dans l'espace. Toutefois, il n'existe aucune technique de mesure qui permette de suivre simultanément les aspects temporels et spatiaux du transport en charge de fond. De ce problème essentiellement technique découle l'étude segmentée des différentes facettes du processus et donc probablement une sous-estimation des facteurs en jeu et de leurs interactions dans l'explication de la variabilité spatio-temporelle du transport de sédiments en charge de fond. Afin de mieux appréhender la complexité du phénomène, plusieurs méthodes de suivi simultanées ont été mises en place au ruisseau Béard. Le chapitre 4 illustre l'avantage indéniable d'utiliser plusieurs méthodes pour cerner un même processus puisque cette multiplication de l'information a ici permis de découvrir une nouvelle dynamique des rivières à lit de graviers, soit la dilatation et la contraction des particules du lit au ruisseau Béard. Ces processus de réorganisation *in situ* des particules structurantes du lit lors d'une crue illustrent l'importance de la variabilité temporelle de l'organisation des particules du lit des rivières. Ces résultats ont des implications majeures pour la compréhension des interactions et des rétroactions entre la structure du lit et la variabilité du transport de sédiments et des changements morphologiques. L'article<sup>1</sup> a reçu un appui enthousiaste et unanime des lecteurs critiques et a été sélectionné par les éditeurs du *Journal of Geophysical Research-Earth Surface* pour faire l'objet d'un *Research Spotlight* dans l'hebdomadaire *Eos* de l'*American Geophysical Union* qui rejoint des milliers de scientifiques de par le monde.

<sup>1</sup>-Marquis, G. A., and A. G. Roy (2012) Using multiple bedload measurements: Towards the identification of bed dilation and contraction in gravel-bed rivers, *Journal of Geophysical Research*, 117: F01014, doi: 10.1029/2011JF002120.



## **CHAPITRE 4. COMBINAISON DE MÉTHODES : VERS L'IDENTIFICATION D'UNE NOUVELLE DYNAMIQUE MORPHOLOGIQUE**

---

### **4.1. Using multiple bedload measurements: towards the identification of bed dilation and contraction in gravel-bed rivers**

#### **4.1.1. Abstract**

This study examines bedload transport processes in a small gravel-bed river (Béard Creek, Qc) using three complementary methods: bed elevation changes between successive floods, bed activity surveys using tags inserted into the bed, and bedload transport rates from bedload samplers. The analysis of 20 flood events capable of mobilizing bed material led to the identification of divergent results among the methods. In particular, bed elevation changes were not consistent with the bed activity surveys. In many cases, bed elevation changes were significant (1 to 2 times the  $D_{50}$ ) even if the bed surface had not been activated during the flood, leading to the identification of processes of bed dilation and contraction that occurred over 10 % to 40 % of the bed surface. These dynamics of the river bed prevent accurate derivation of bedload transport rates from topographic changes, especially for low magnitude floods. This paper discusses the mechanisms that could explain the dilation and contraction of particles within the bed and their implications in fluvial dynamics. Bed contraction seems to be the result of the winnowing of the fine sediments under very low gravel transport. Bed dilation seems to occur on patches of the bed at the threshold of motion where various processes such as fine sediment infiltration lead to the maintenance of a larger sediment framework volume. Both processes are also influenced by flood history and the initial local bed state and in turn may have a significant impact on sediment transport and morphological changes in gravel-bed rivers.

#### **4.1.2. Introduction**

In gravel-bed streams, bedload transport has been described as occurring in at least two distinct phases (e.g. Ashworth and Ferguson, 1989; Warburton, 1992). In phase I, transport rates are low. As the critical flow for motion is slightly exceeded, the transport is

partial or size selective and thus only the smaller grains are entrained over the bed surface. In phase II, coarser grain fractions are mobilized, disrupting partially the initial bed surface and exposing underlying grains, thus increasing greatly the bedload rates compared to transport phase I. In some cases, a Phase III may appear where all sizes of particles are mobile and the bed surface is completely disrupted. Partial transport (Phase I and II) is more frequent than full mobility (Phase III) but the transport rate can be highly variable in time and space due to the fact that the entrainment threshold is only slightly exceeded (Wilcock and Mcardell, 1993). Our understanding of bedload transport at low rates has been approached mainly by examining how the near-bed flow field interacts with sediment particles (e.g. Schmeeckle et al., 2007). Recently, Frey and Church (2009) have suggested that the interactions between the particles themselves, as studied from a granular physics perspective, might be as strong a driver as the flow magnitude in controlling bedload transport and the consequent characteristics of morphological features such as the armor layer of the bed.

To further complicate the issue of understanding the mechanisms driving sediment transport and the response of the river bed, our current knowledge on how material moves as bedload is based on a plethora of sampling methods. The accurate measurement of bedload transport is one of the greatest obstacles to understanding the process (Church, 2006a). The ideal measurements would have to be simultaneous and continuous both in time and space because bedload transport is known to be highly intermittent and spatially variable. Unfortunately, most methods cover only one aspect of the bedload space-time continuum. As bedload generally occurs over short periods of time, a compromise must be struck between an extensive spatial survey with short record of local measurements and long records sampled at a few locations. Depending on the objectives of the study, one must choose the most appropriate method to document and record bedload transport rates and processes. The available methods can mainly be divided into the direct and indirect approaches to bedload transport estimates. Direct methods estimate an actual bedload transport rate by means of samplers such as the Helleys-Smith, which measures at one point in the river for a short period of time, or sediment pit traps/samplers that can operate continuously and integrate sediment transport over longer periods. The accuracy of measurements depends upon the design of the samplers and upon the sampling parameters (frequency, duration and location on the river bed). The temporal resolution and accuracy

of the bedload measurements can be very high as in the case of Birkbeck bedload samplers implemented with a weighing instrument such as a pressure pillow (e.g. Reid et al., 1980) or load cells (e.g. Lewis, 1991).

Indirect methods are numerous but often require laborious calibration procedures; in many cases they provide a low precision estimate of bedload transport rates. For example, many types of sensors have been used to measure a specific characteristic of the bedload like acoustic sensors (e.g. Thorne et al., 1989) or impact sensors (e.g. Reid et al., 2007). Another example is the estimation of bedload fluxes via the travelled distances of tracer particles (e.g. Wilcock, 1997). The easiest and most popular indirect method is the estimation of bedload yields from the difference in bed elevation between two successive topographical surveys of a river reach (Carson and Griffiths, 1989; Lane et al., 1995; Ashmore and Church, 1998). The reliability of this method depends largely on the appropriate knowledge of the deformation style of a specific channel morphological type (Church, 2006a). If the deformation style is unknown, the estimate of bedload is based on a calculated volume of erosion and deposition from cross sections (e.g. Griffiths, 1979) or more simply and more accurately from digital elevation models (Lane et al., 1995; Fuller et al., 2003). In coarse channels where full mobility is rarely achieved, the bed morphology is often only slightly deformed if at all. Therefore, the coarse sediment budget derived from morphological surveys will be a lower-bound estimate as scour and fill may compensate for one another (Lindsay and Ashmore, 2002).

In this study, we used three simultaneous, complementary methods to estimate bedload sediment transport rates and morphological changes in a small gravel-bed river and to assess the strengths and weaknesses of the methods themselves. The analysis of the data revealed an unexpected outcome: areas of the bed that were not mobilized by bedload sediment transport according to a bed activity survey often showed a significant change in bed elevation (1 to 2 times the  $D_{50}$ ), sometimes the bed being higher, sometimes lower than the bed elevation before the flood. These two morphological responses of the bed correspond to a *dilation* or a *contraction* of the bed. Here, we define dilation and contraction as an *in situ* reorganization of the bed framework particles that leads to a significant change of the space occupied by these particles. Dilation is the reorganization of the larger particles into a looser packing and contraction corresponds to a tighter packing than what was observed before the flood event. Dilation of the gravel framework was

observed by Allan and Frostick (1999) in a flume experiment just before the initial motion of bed particles but they did not report that the gravel framework remained dilated after the episode of sediment transport. To our knowledge, dilation and contraction of the gravel framework as a result of a flood with partial transport has never been reported before. The variability in the bed volume might be of crucial importance to understand the large variability in bedload transport rates under conditions of partial transport, as dilation and contraction of the framework change the availability of the particles to move as bedload.

Therefore, such changes in the volume of the bed will be the focus of this study and will be explored in four different parts of the paper by: (1) demonstrating that the occurrence of these processes is not an artifact of the data precision and analysis; (2) describing the effect of dilation and contraction on the interpretation of morphological changes derived from topographical surveys; (3) exploring the physical processes that can explain this type of bed behavior; and (4) illustrating how these processes play a role in the morphological response of gravel-bed rivers to bedload. In parallel to the description of contraction and dilation processes, we will also show that areas of the bed that experienced compensated scour and fill are extensive. The identification of these dynamics in gravel-bed rivers also allows us to stress the importance of using multiple methods to measure bedload processes, as their combination sheds new light on the current assumptions underlying the use of the morphological method to estimate bedload transport rates in gravel-bed rivers.

#### **4.1.3. Field site & data collection**

The study was conducted at Béard Creek, a small gravel-bed river located in Southern Québec, Canada (Figure 4.1a). Upstream from the study site, the 8 km<sup>2</sup> watershed is mainly covered by mixed forest, pasture areas and cultivated fields. Surficial deposits are mostly inherited from the last glacial period and the area is mainly covered by a sandy-silty matrix till containing a large amount of coarse material. The banks of the stream are cut into the glacial till and are a moderate source of gravel to the stream. The overall morphology and the average elevation of the stream bed remained relatively stable over the five years of measurement. Average bankfull channel width, depth and discharge at the study site are 6 m, 0.7 m and 2.5 m<sup>3</sup> s<sup>-1</sup> respectively and the average channel slope is 1 %. The material composing the surface of the bed has a  $D_{50}$  varying from 40 to 65 mm and is

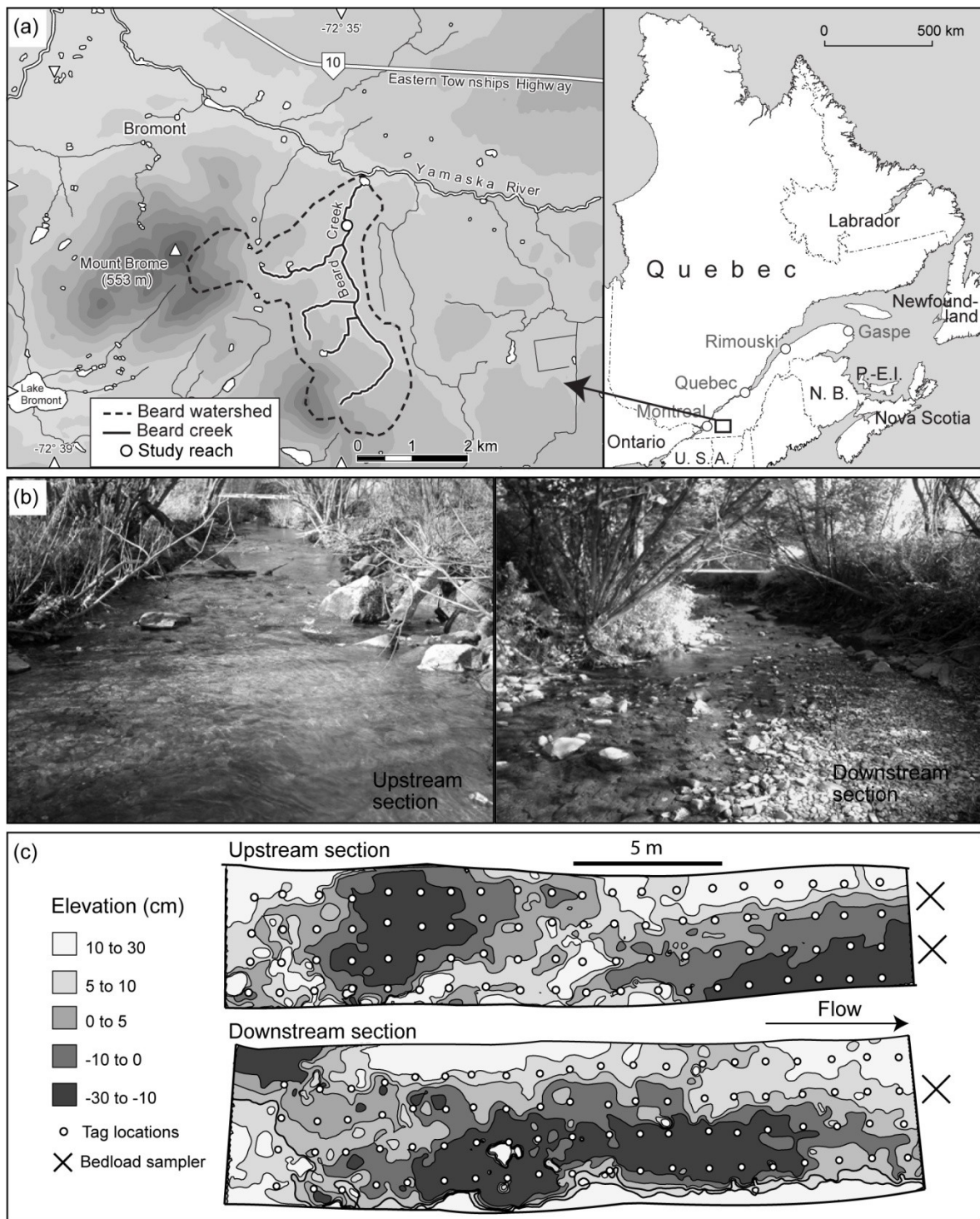


Figure 4.1 (a) Location of Béard Creek and the study reach in the Eastern Townships, Québec, Canada. (b) Downstream views of both study sections. (c) Contour maps (generated from DEMs) of the initial topographic elevation of both study sections.

moderately sorted. The armor ratio is about 2 and the subsurface material is matrix supported. Pool-riffle sequences with small occasional lateral bars are the main features of the bed morphology. Bedload transport does not seem to proceed through the migration of bedforms but rather in the form of broad bedload sheets, as suggested by the stability of the morphological features during the study period.

Two measurement sections 75 m apart were equipped with bedload samplers measuring real time bedload with submersible load cells (Interface 2400, 0-110 kg) (Figure 4.1bc). The load cell signals are compensated for temperature (-10 to 45 °C), and have a static error band of 0.1 % of total capacity. Their minimum detection range is approximately 15 g in field conditions. The samplers have a capacity of 0.06 m<sup>3</sup> or 85 kg of dry material when full. The slots of the samplers are 0.12 m wide, which corresponds to  $D_{95}$  of the bed surface gravel, and the length of the slot is 0.4 m, about 10 times the  $D_{50}$  of the bed material. The bedload samplers were constructed according to the design proposed by Sear et al. (2000) with some modifications. The dimensions of the slot were based on different considerations outlined by Laronne et al. (2003). The upstream section has two bedload samplers positioned at 1/3 and 2/3 of the cross section (Figure 4.1c). The downstream section is equipped with only one sampler located at the edge between a small lateral bar and the thalweg (Figure 4.1c). Two water stage gauges installed upstream and downstream of the sections allowed for the estimation of water surface slope and discharge through a stage-discharge rating curve. We did not correct the relation for discharges above bankfull as it did not occur often enough and because the cross-section used for stage-discharge rating curve has a trapezoidal shape.

After each flood mobilizing bedload, the sediment contained in each sampler was weighed and 25 % was subsampled for sieving. Also, a topographical survey with a density of 4-7 points/m<sup>2</sup> was performed using a robotic total station on the 20 meters upstream of the two cross sections where the bedload samplers were installed (Figure 4.1c). The sampling strategy was systematic for regular surfaces and focused on breaks in slope of specific morphological features, as recommended by Lane et al. (1994). In the two sections where bed morphology was repeatedly mapped, a bed activity survey was performed using a dense grid of bed tags (Figure 4.1c). This allowed us to map the active bed areas which are defined as any location of the channel where the bed surface particles are different after a flood with bedload transport, without a distinction between scour or deposition processes.

Bed tags were steel washers installed with a short (5 cm) plastic flag making the tags easily visible under water. Using a reference system on the banks of the sections, the tags were inserted vertically between two particles in a position that is flush with the bed surface and parallel to the flow direction (see case 1A in Figure 4.2 for an illustration). The diameter of the washers, 35 mm, was slightly smaller than the  $D_{50}$ . After a flood, the state of each tag was surveyed based on the principle that if the bed was active, the tags were either buried or scoured as the particles retaining it were mobilized. The bed state was said to be inactive when the tag was at its initial location in the same vertical position. After each survey of the bed tags, the grid was reinitialized where necessary by reinserting new tags into the bed.

Even though the survey does not differentiate between erosion and deposition, it gives a reliable estimate of the proportion of the bed surface that was mobilized during the flood. It is possible that the tags could be removed from the bed due to clast vibration or collisions with overpassing particles. We believe, however, that this must occur only during very large floods on areas that were probably mobilized later during the flood. As the bed tags were inserted flush with the bed surface, this scenario is not likely to occur during low magnitude floods where small gravel is not likely to collide with enough force to displace the tag. Therefore, this type of error should be rare and should not influence the results. According to Konrad et al. (2002), the method is reliable if the size of the steel washers does not exceed that of the surrounding particles and if the bed surface is relatively imbricated with few unconstrained particles.

The data set consists of 20 rain-triggered flood events with bedload measured over a period of three years (Table 4.1). We will use the expression ‘bedload event’ to refer to any of these 20 floods. The data cover a large spectrum of bedload transport conditions ranging from very low transport to a fully mobilized bed during different hydrologic responses from very long and sustained to very flashy hydrographs. All surveyed events are successive during the summer and fall seasons (no data were measured during winter and snow melt) and most events have a single peak in the hydrograph. Nevertheless, three events (6, 9 and 19) have two distinct discharge peaks with some time separation during which there was no bedload, but it was logistically impossible to survey the stream and retrieve the sediments in the samplers in the time interval between the two peaks. The data from the two peaks were merged and analyzed as a single event. Three other flood events (2, 10 and 18) also

Table 4.1 Principal characteristics of the surveyed bedload events listed in chronological order. Basic information about flow (peak discharge and average stream power), bedload transport (duration, quantity and size) and morphological changes (active bed surface from the bed tag surveys, volumes of erosion and deposition from the DEMs of difference) are presented for each surveyed section of Béard creek.

Flood event	Date	Peak discharge (m <sup>3</sup> s <sup>-1</sup> )	$\omega_{\text{mean}}$ (kg m <sup>-1</sup> s <sup>-1</sup> )	Bedload duration (h)	$D_{50}$ bedload (mm)*	$D_{95}$ bedload (mm)*	Total load (x 10 <sup>3</sup> kg)*	Active area (%)*	Deposition (m <sup>3</sup> )*	Scour (m <sup>3</sup> )*	Samplers full**
1.	07-10-23	2.4	3.8	5.3	8/9	47/45	10/14	69/74	0.58/1.14	1.44/1.18	2/1
2.	07-10-27	3.8	3.8	16.5	8/8	46/41	38/92	89/95	1.59/3.49	1.16/0.66	1/1
3.	07-11-15	0.8	1.5	3.3	6/6	13/42	0.08/0.08	34/28	1.09/0.44	0.80/3.64	0/0
4.	07-11-22	1.2	2.2	4.4	6/6	21/40	0.14/0.15	39/33	0.60/1.10	1.76/1.07	0/0
5.	08-04-28	0.9	1.3	11.9	4/5	24/29	0.25/9.5	34/30	1.04/1.06	0.73/0.85	0/0
6.	08-05-31	1.8	1.4	29.8	9/7	74/40	1.1/35	69/55	0.65/1.07	0.94/0.74	0/0
7.	08-06-04	1.0	1.6	4.1	5/4	16/29	0.31/5.1	15/14	1.95/0.77	0.42/0.71	0/0
8.	08-07-20	1.3	1.8	3.2	6/5	15/16	0.74/0.66	58/54	0.39/0.69	1.96/1.00	0/0
9.	08-07-24	3.1	2.9	11.2	7/5	35/20	25/47	70/73	0.70/1.06	0.70/0.78	2/1
10.	08-08-08	6.8	6.0	2.7	8/6	59/28	18/89	100/96	1.00/0.97	3.16/1.32	2/1
11.	08-10-25	2.3	3.1	4.3	13/9	47/43	0.70/1.8	59/49	1.29/0.85	0.34/0.63	0/0
12.	08-10-28	1.4	2.2	3.9	5/7	14/37	0.11/0.37	34/20	0.43/0.34	0.67/1.54	0/0
13.	09-06-15	0.9	1.4	3.2	6/3	17/12	1.6/0.05	24/18	0.68/0.60	0.33/1.67	0/0
14.	09-06-29	1.8	2.2	9.8	6/6	22/60	11/1.1	40/46	0.31/1.40	1.03/0.62	1/0
15.	09-07-03	7.9	6.4	5.6	19/9	72/54	149/175	91/83	1.49/0.70	1.24/1.83	2/1
16.	09-07-26	6.1	5.5	4.3	8/11	53/72	137/84	84/98	0.37/1.30	1.66/1.00	2/1
17.	09-08-10	8.0	5.6	4.5	11/7	60/42	304/116	79/84	0.66/1.11	0.76/1.13	2/1
18.	09-10-24	2.0	3.0	6.4	6/4	43/16	9.3/1.4	81/64	0.82/1.18	0.48/0.61	1/1
19.	09-11-14	1.6	1.7	32.3	5/4	17/12	8.7/0.53	45/28	0.58/0.62	0.40/1.00	1/0
20.	09-11-27	4.7	5.0	18.3	4/6	29/33	171/349	93/94	1.22/1.46	1.37/1.69	2/1

had a double peak hydrograph but without a return to a low flow stage and are therefore also considered as single events. Battery and/or malfunctions preventing the continuous recording of bedload rates occurred at the downstream section during flood 5 and at the upstream section during flood 13.

#### 4.1.4. Analyses

The analyses relied on three different methods to estimate bedload transport and bed activity: (1) the bedload samplers, (2) the morphological surveys and (3) the bed activity surveys. Bedload transport rates and total sediment yields estimated from the samplers are used as the basis for a comparison with the volume and area changes of the bed derived from the two spatial surveys. For the events where the samplers were full before the end of the flood and for other floods where technical problems with the load cell signal recording occurred, some extrapolation was needed to obtain an estimate of bedload rates. There were seven events where the three bedload samplers were full before the end of the flood, of which five exceeded the bankfull flow. Otherwise, on four occasions one or two samplers were full before the end of the event, leaving nine flood events for which the bedload was captured for its full duration at all samplers (Table 4.1). The load cell measurements were used to construct time series to estimate real-time bedload transport using the same methods described in Sear et al. (2000) for both the *in situ* calibration and for the signal treatment. For the events for which the bedload record was incomplete, we estimated bedload values using a rating curve between discharge and bedload constructed using averaged data over 15 min periods. For the flashiest floods, the periods were reduced to 2 minutes as discharge was changing very rapidly. For the whole data set, this analysis included 345, 440 and 708 periods for each sampler covering bedload rates from 0 up to a peak of  $15 \text{ kg m}^{-1} \text{ s}^{-1}$ . The explained variance of each power law model is 66 % for the sampler located downstream and 59 % and 64 % for the samplers in the upstream section. We consider that these models are strong enough to extrapolate the missing data in order to obtain mean bedload rates and the total yield for a flood. Even though the extrapolation for the largest floods can be an order of magnitude off, we believe that these errors have a negligible impact on the conclusions of this study and we prefer to keep the data set as large as possible.

The quality of the referencing system of the raw data points of the morphological survey is good according to the errors estimated from four reference points located on large boulders ( $D > 1 \text{ m}$ ) on the margin of the channel. The maximum elevation error never exceeded 4 mm but was generally in the range of 1 mm. The precision on the easting/northing location was less than 10 mm and generally around 3-5 mm. Even though the Triangulated Irregular Network (TIN) interpolation method is widely used for

morphological surface investigation and is often preferred to other techniques (e.g. Fuller and Hutchinson, 2007; Heritage et al., 2009), we decided to use the Natural Neighbor interpolation method to construct the bed Digital Elevation Models (DEMs) from the raw data points. Although similar to the TIN method in principle, the errors between a subsample of data points not used in the interpolation and the DEMs were smaller using the Natural Neighbor interpolation provided in the Vertical Mapper interpolation software. This interpolation method is suitable for elevation data points that are scattered in space and it considers the data points to be accurate values, which is a valid assumption for the total station data measured over short distances. A network of natural neighbor regions (Voronoi diagram) is built using the original data. The grid cell value is determined by averaging the point values associated with surrounding natural neighbor regions and weighted according to the area that is encompassed by a temporary natural neighbor region generated around the grid cell. The parameters were held constant for each interpolated map, the grid size being 0.05 m, allowing the algorithm to smooth the bed surface but preserve exact values for local maxima and minima. These DEMs of the sections were used to detect and evaluate the morphological changes following a flood by subtracting successive DEMs that result in DEMs of Difference (DoDs). The method used to quantify uncertainty in the DEMs is explained in section 4.1.5.1.

The data from the bed tag surveys are informative when matched with the DoDs. This combination of methods allowed us to identify the new bed dynamics of bed dilation and contraction. The bed elevation differences are used to classify bed responses into stable elevation, elevation decrease or increase. The bed tag surveys produce a binary variable of the bed response at a location, as either active or inactive. When combining the surveys, six bed responses can be differentiated (Figure 4.2). Apart from the bed responses that can be identified from the morphological surveys alone (scour (case 3B), deposition (case 2B), and stability (case 1A)); three other bed reactions to a flood can be identified: locations where scour compensated fill, leading to a null elevation change (case 1B); dilation when the bed surface is inactive and the bed elevation is higher than before the flood (case 2A); and contraction when the bed surface is inactive and the bed elevation is lower than before the flood (case 3A).

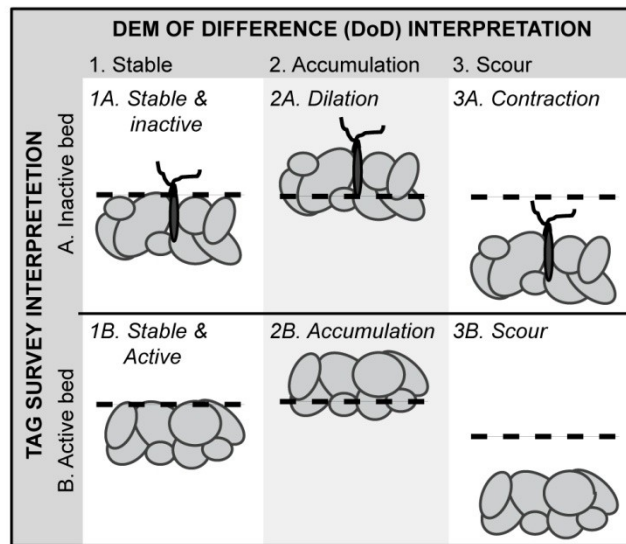


Figure 4.2 Case scenarios of morphological changes following a bedload event when combining information from the DoDs and the bed tag surveys. Diagrams are in the cross-sectional plane of the stream bed. Case 1A: Bed elevation did not change and the bed was inactive, thus the bed was similar to the initial state. Case 1B: Bed elevation did not change but the bed was active, suggesting that scour compensated fill during the event. Case 2A & 3A: The grains did not move during the event but the bed elevation changed. Case 2B & 3B: The bed was active and the bed elevation changed.

In this paper, we used the average unit stream power of the effective runoff during a bedload event to relate bedload data to the flow, as it is a common variable used in bedload studies and predictive bedload formulas (e.g. Martin, 2003). Also, the unit stream power dimensions relate directly to those of the bedload transport rates when the computation is done using these variables :

$$\omega = \rho Q S_w / W \quad \text{Equation 4.1}$$

where  $\rho$  is water density ( $1000 \text{ kgm}^{-3}$ ),  $Q$ , stream discharge,  $S_w$ , the water surface slope calculated with the most distant stream gauges thus obtaining the same value for both sections and  $W$  is the average width of the sections.

#### 4.1.5. Results

##### 4.1.5.1. Data inspection and validation

The detection of bed dilation and contraction is dependent on the uncertainty of the DEMs and the accuracy of the bed tag surveys. The uncertainties in DEMs must be

considered in order to distinguish between a morphological change and inherent noise. This is of critical importance in this study because the method used to identify morphological changes will influence the classification of the morphological scenarios presented in Figure 4.2. Lane et al. (1994) and Lane (1998) stated that the quality of a DEM depends on the accuracy and precision of the individual data points and on the density and spatial distribution of the points with respect to the features of the sampled surface. In this study, topographical surveys were always done by the same operator using the same total station. As a result, the density of points and the sampling strategy remained constant throughout the study, and the quality of the DEMs can therefore be assumed constant. The most common way to manage uncertainties is to use a minimum level of detection that discards any elevation change that does not exceed a given threshold (e.g. Fuller et al., 2003). This procedure assumes that the errors are spatially uniform even though there might be spatial differences due to the local slope, the local bed roughness or the location of the surveyed areas (wet versus dry river beds) (Lane et al., 2003; Wheaton et al., 2010). The use of a spatially uniform error in DEMs leads to the underestimation of erosion and deposition volumes in DoDs (Milan et al., 2011). Advanced procedures accounting for spatial differences in uncertainties allow for the detection of more subtle changes than those identified using a minimum level of detection threshold. For example, this could be the case of shallow deposits over a smooth bar surface (Wheaton et al., 2010). Nevertheless, we have chosen to use a spatially uniform minimum level of detection threshold because we wanted to remove uncertainties in a severe way, in order to not overestimate the dilation and contraction processes. Consequently, the areas of dilation and contraction presented here are lower bound estimates. For the same reason, stable or active areas with no elevation change will be slightly overestimated and the scour and deposition areas underestimated. Also, we believe that it is reasonable to assume that the errors in the DEMs are spatially uniform because the surveyed areas are small and located in the main channel where there are no extreme variations in roughness and local slope.

The minimum level of detection threshold was estimated by repeating five topographical surveys of one bed morphology state in the upstream section and then by comparing the resultant DEMs of these five surveys as in Brasington and Smart (2003). The surveys were independent as the total station was mounted and removed each time. The upstream section was selected for this exercise because its bed is rougher than that of

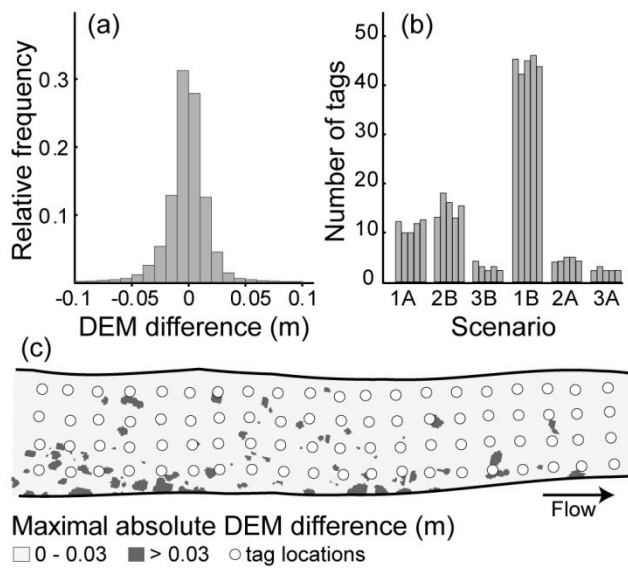


Figure 4.3 Error estimation among five repeated morphological surveys of the upstream section using a total station. (a) Distribution of the DEM elevation differences of all possible pairs of the five repeated surveys. (b) Classification of the bed tag survey between the six different case scenarios using the DoDs between the five successive surveys and the survey following the flood of 24 October 2009. (c) Binary representation of the spatial distribution of the maximal absolute error between the five repeated surveys (95 % of errors are in the range 0 to 0.03m).

the downstream section and it is therefore subject to larger errors in the topographical survey. The distribution of the differences between all possible pairs of DEMs is symmetric and narrow, 75 % of the differences being in the range -0.015 m to 0.015 m and 95 % in the range -0.03 m to 0.03 m (Figure 4.3a). The mapping of the absolute maximum error for each grid cell of the section DEMs shows that errors larger than 0.03 m are mostly associated with local roughness elements (Figure 4.3c) and are generally located on the right bank of the section (Figure 4.1b). Consequently, we concluded that an elevation change between two consecutive bed surveys is significant when the difference between two grid cells is larger than 0.03 m, a value very similar to the  $D_{50}$  of the section. For successive DEMs differences ranging from -0.03 m to 0.03 m, the bed elevation is considered to have remained the same. We did not correct all the remaining elevation change values as the  $\pm 0.03$  m error distribution is assumed to be random, meaning that if a change of 0.04 m was detected, we did not apply any correction as there was no way of knowing if the error was positive or negative.

To further validate the choice of the minimal level of detection threshold, we produced five DoDs by subtracting the DEM of the survey carried out after the following flood that occurred on 24 October 2009. This flood resulted in the activation of about 80 % of the bed surface with a peak discharge of  $2 \text{ m}^3 \text{ s}^{-1}$  and a maximum stream power of  $3.7 \text{ kg m}^{-1} \text{ s}^{-1}$  (Table 4.1). The comparison of five independent morphological budgets shows that our uncertainty procedure results in stable estimates. The largest difference in the estimated active areas is  $1.95 \text{ m}^2$ , or 2.5 % of the surveyed section. The erosion volumes range between 0.45 to  $0.57 \text{ m}^3$  with an average estimate of  $0.48 \pm 0.05 \text{ m}^3$ . The range is slightly greater for the deposition volumes, from 0.73 to 0.92, with an average estimate of  $0.82 \pm 0.09 \text{ m}^3$ . The range of values is very small compared to the average volume changes between successive floods as shown in Table 4.1. For the 24 October 2009 flood, the error represents about 10 % of the estimated volumes, which is far less than the maximum absolute error of 50 % if accounting uniformly for the minimum level of detection of 0.03 m. When applying the  $\pm 0.03 \text{ m}$  error on the scour and accumulation volume calculations from all 20 DoDs, the maximum relative error is constant at around 50 % without a distinction between small or large volumetric changes. This could be due to the relatively shallow active layer of Béard Creek leading to the mobilization of particles over larger areas with increasing flow magnitude rather than over a substantial depth of the bed.

The way we accounted for DEM uncertainties seems reliable for estimating significant morphological changes. The next step is to verify if the DoDs errors influence the classification into the six morphological scenarios presented in Figure 4.2 derived from the combination of the topographical survey and the bed activity survey. To classify each tag location, we had to account also for the errors associated with the potential mismatch between the location of the bed tags and the interpolation cells. Thus, we defined a buffer zone of 0.25 m radius around each bed tag and retained the median difference within the enclosed area, thus eliminating the effect of the isolated error values in the DEMs. Depending on the tag absence or presence and on whether the elevation of the bed has decreased ( $< -0.03 \text{ m}$ ), increased ( $> 0.03 \text{ m}$ ) or stayed the same (i.e.  $\pm 0.03 \text{ m}$ ), we classified the morphological response of each bed tag location for each DoD calculated between each of the five repeated DEMs and the DEM of the bed after the following flood (24 October 2009). Even though there are differences between each replication, the counts for particular morphological scenarios usually vary by one or two tags with a maximum of

four in the case of 2B (accumulation) (Figure 4.3b). Therefore, we believe the classification into the morphological scenarios seems relatively robust even though there are uncertainties in the DEMs. Also, the differences between the classifications of the five repeated surveys do not affect the interpretation of the morphological responses of the section after the flood. For example, about 20 % of the bed surface was scoured and filled during the flood while 60 % showed a null elevation change and around 20 % of the bed surface was not mobilized, with one third of this surface appearing to have dilated. The very low percentage of bed contraction might be a true reflection of the processes but it might also result from an error in the DEMs or in the bed tag survey itself. Errors in the bed tag survey may occur when the area around the tag has changed while the bed has remained in place at the precise location of the tag. We assumed that this kind of error might occur over very limited portions of the bed surface. As it is impossible to identify when it occurs, we considered it as a part of the random error inherent to field data sets. From the comparisons of five repeated morphological surveys to estimate DEMs uncertainties and of the effect of these differences on the identification of the morphological responses of the bed after a flood, it appears reasonable to conclude that the detection of the dilation and contraction states of the bed is not an artifact of the sampling procedure or of the analysis of the data.

The last step in the validation of the bed tag method is to examine its sensitivity to reflect bedload processes. Figure 4.4 shows the relations between bedload response and flow intensity for all three bedload estimates used in this study. The average bedload transport rate exhibits a power relationship with the average unit stream power as expected from the results of many other studies (e.g. Reid and Laronne, 1995) (Figure 4.4a). The total active bed area estimated from the bed tag surveys also shows a strong positive relation to stream power (Figure 4.4b). Even though the bed tags picked only local effects of the bed activity, the grid of  $1 \text{ m}^2$  appears to be dense enough to detect the overall response of the reach to flood intensity. The scatter observed for a given stream power is quite large especially at low values, but no more than for bedload rates estimated from the bedload samplers (Figure 4.4a). Figure 4.4c shows a very weak relation where only 14 % of the variance is explained between the total bed volume changes (addition of the absolute values of the total scour and the total deposition derived from the DoDs) and stream power. This result is not surprising but we would have expected a stronger dependence at least for the above bankfull events. Nevertheless, it clearly illustrates that the bed tag survey does

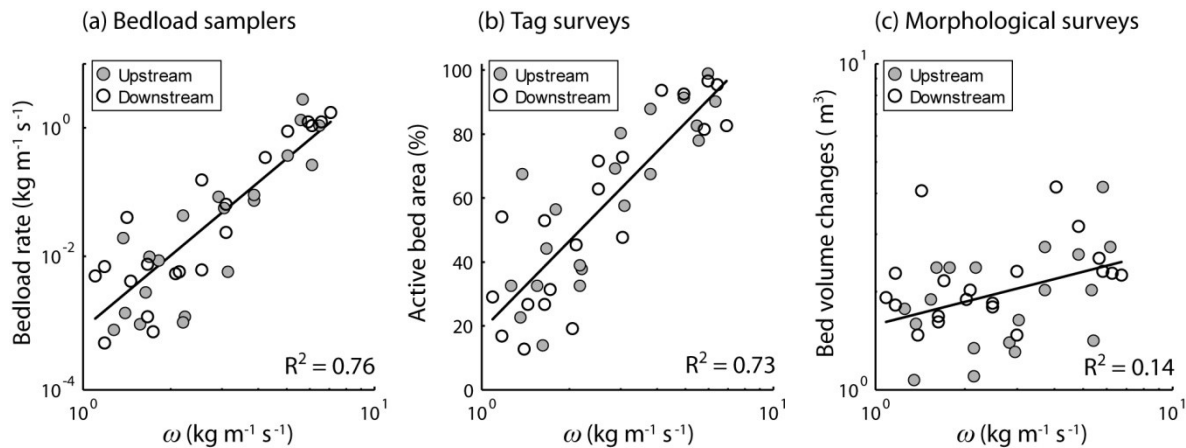


Figure 4.4 Bedload estimates from three different sampling methods for the upstream and downstream sections of Béard Creek. Each dot represents one flood event. Unit stream power ( $\omega$ ) is averaged over the period when the bedload transport was active. Bedload rate is calculated as submerged material.

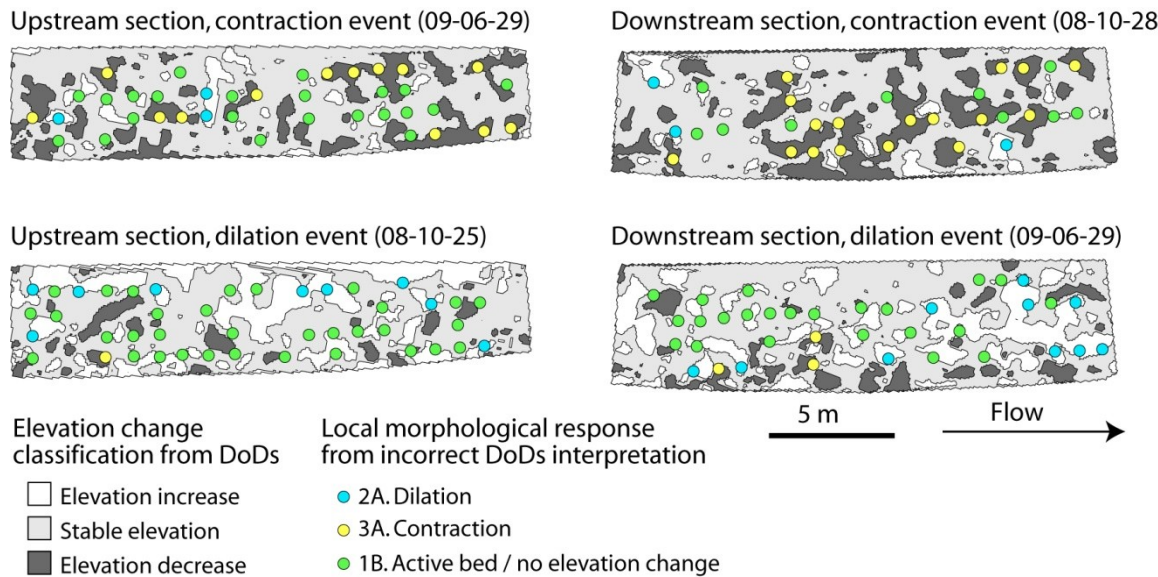


Figure 4.5 Examples of the classification of the DoDs into increased, decreased or stable elevation using the minimal level of detection  $\pm 0.03$  m. The color dots are the locations of three morphological scenarios that cannot be identified when using only the DoDs derived from the morphological surveys. Examples were chosen to illustrate the typical spatial distribution of large dilated or contracted bed areas for each section.

not yield redundant results with respect to the topographical surveys, but that it contributes useful complementary information.

#### **4.1.5.2. Morphological response of the bed to a bedload event**

Figure 4.5 shows examples of the morphological response of the bed for both sections. The three scenarios that cannot be detected from DoDs (dilation, contraction and active areas without elevation change) are represented as color dots superimposed on the DoDs contour maps. Floods that produced relatively large areas of bed dilation and contraction were chosen for both sections. The locations where bed dilation or contraction occurred tend to cluster on relatively smooth areas of the bed, mainly on the bar in the downstream section and in the pools in the upstream section. The absolute bed elevation changes associated with the bed dilation and contraction was between 0.03 and 0.10 m, the average being around 0.05 m, which corresponds roughly to the  $D_{50}$  of Béard creek. Also, we can observe in Figure 4.5 that large areas of the bed that were apparently not mobilized by the flood were in fact active areas where scour compensated fill.

The distribution of the morphological responses is shown in Figure 4.6 for each bedload event for both study sections. The dilation and contraction scenarios do not occur systematically and the covered areas vary greatly among the floods indicating that there are no systematic biases due to the sampling or interpolation of the data. The use of the methods reveals a complex behavior of the bed in its response to sediment transport events with several cases where bed dilation and contraction occur. This type of response is, however, observed on fairly small areas of the bed after a flood (0-20 % for most surveys with two exceptions at about 40 %). The occurrence of different morphological responses reveals patterns of interest for a better understanding of fluvial processes in gravel-bed rivers. Many observations can be drawn from Figure 4.6, the most important ones are:

1. There is an almost constant interpretation error of about 50 % of the DoDs due to active areas with a stable elevation and to dilation /contraction of the bed.
2. The apparent compensation of scour and fill is by far the most important process explaining these incorrect DoDs interpretations (40 % on average), but the importance of this process fluctuates from flood to flood.
3. Bed dilation and contraction over areas larger than 5-10 % of the sections occur during small floods, when only a small proportion of the bed surface is mobilized.

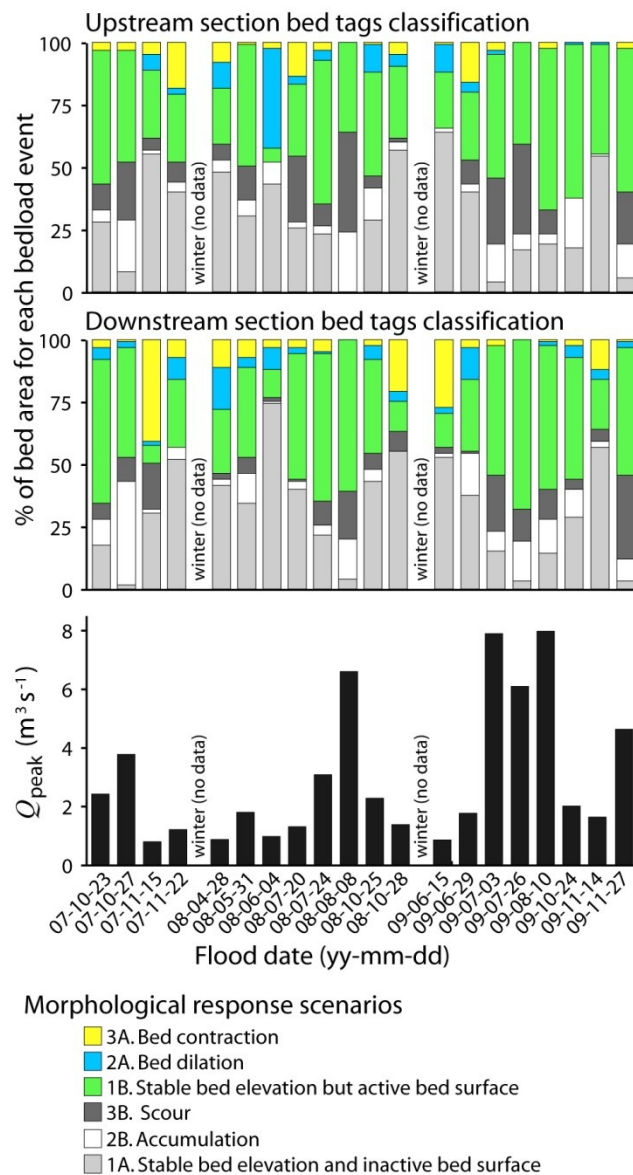


Figure 4.6 Proportion of each of the six case scenarios of morphological changes after each of the 20 bedload events in the data set. Data are presented in percentage of the section area in chronological order. All flood events are successive except for the winter period for which no data are available. The peak discharge is also represented to put the morphological response into context.

4. Proportions of the bed that are dilated or contracted are rarely equal to one another during a flood, one type of morphological response being dominant over the other.
5. Bed dilation or contraction can occur over large areas in one study section while the other section may exhibit a different behavior with at times the opposite response being dominant.

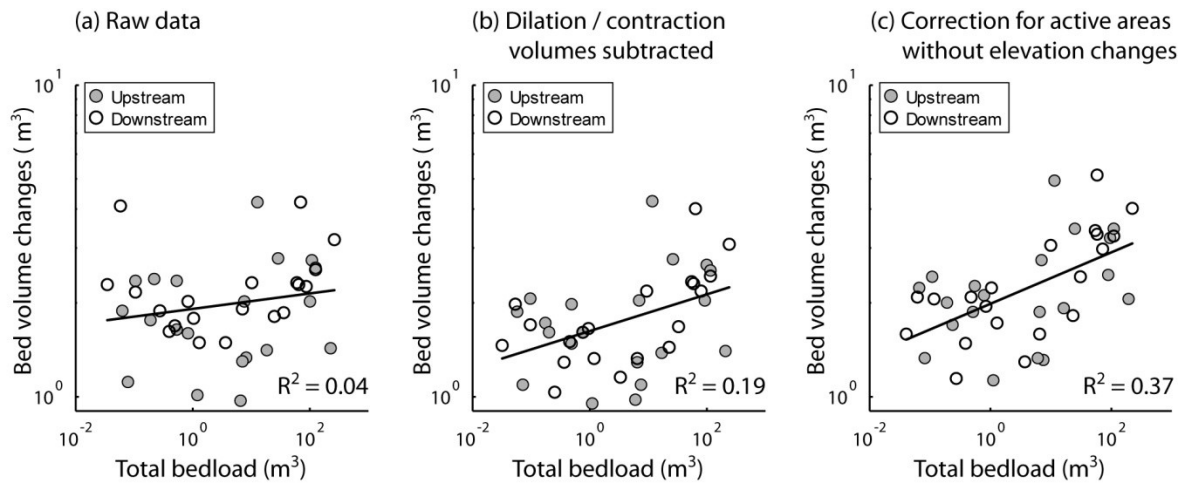


Figure 4.7 Bed volume changes in relation to total bedload yield for each bedload event for both sections. Bed volume changes corresponded to the addition of the absolute erosion and accumulation estimated from the DoDs. (a) Raw bed volume changes estimated using only the DoDs. (b) Bed volume changes after the subtraction of the dilation and contraction areas elevation changes as these areas did not experience local bedload transport. (c) Bed volume changes corrected for dilation and contraction volumes and to which an estimated volume for the active areas without elevation change is added. The total bedload rate is estimated for the width of the section and for the period when bedload was active during the flood.

#### 4.1.5.3. Dilation and contraction effect on topographical data

As a result of the weak response of the bed morphology to flow intensity (Figure 4.4c), it is not surprising to find that bed volume change is not significantly ( $p < 0.01$ ) related to total bedload yield (Figure 4.7a). In Figure 4.6, about 50 % of the morphological response of the bed is misinterpreted when using the DoDs alone. Therefore, we introduced a correction of bed volume changes by excluding areas where the bed elevation changed but the tags indicated that the bed surface particles were not mobilized. This correction led to an improved relation and induced a positive slope between bed volume changes and the total bedload with an explained variance of 19 % (Figure 4.7b). The relation is still weak probably because bed dilation and contraction dynamics do not account for the largest errors in the topographical surveys. The largest error is the underestimation of the sediment movements in areas that have experienced bed activity and perhaps a cycle of scour and fill during the flood, leading to a null elevation change. These areas can occupy as much as 60 % of the bed surface in a section for a given flood event (Figure 4.6). Even without a

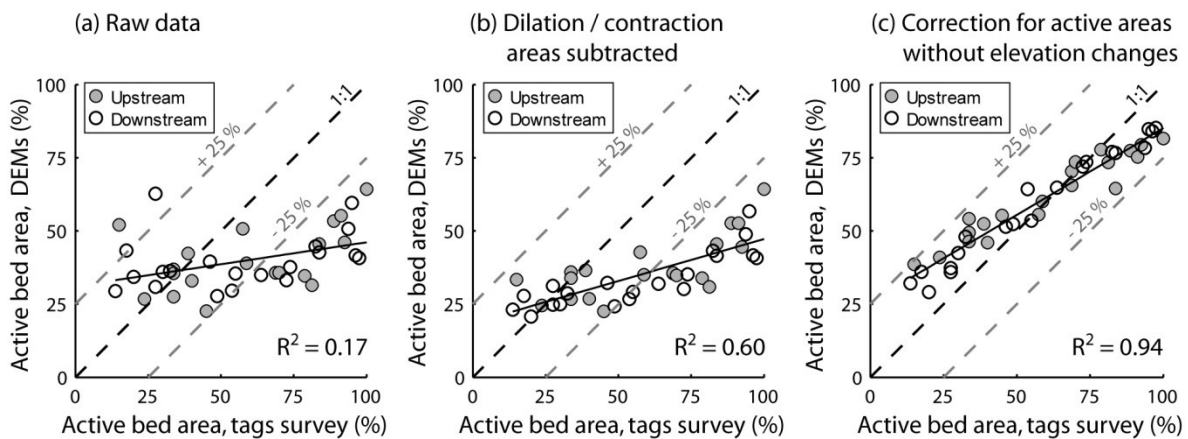


Figure 4.8 Comparisons of the active bed areas estimated using the morphological and bed tag surveys for each bedload event for both sections. In principle, the areas should be identical and the dots all on the 1:1 line. (a) Raw data. (b) The dilation and contraction areas are subtracted from the active areas estimated from the DoDs. (c) The dilation, contraction and active areas without elevation change are subtracted from the active areas estimated from the DoDs.

precise knowledge of the depth of the active layer in these areas, we opted to correct bed volume changes by multiplying the active areas without elevation change by the average of the absolute values of bed elevation changes during the flood. These estimated volumes are considered to be the minimal morphological response of the bed. The relation with total bedload is improved with an explained variance of 37 % (Figure 4.7c). The relation between bed volume changes and unit stream power also improves from 14 % of explained variance when using DoDs data only (Figure 4.4c) to 40 % of explained variance when correcting for dilation/contraction areas and to 52 % when adding the active areas without bed elevation changes (not shown). When correcting the data of the DoDs with the information obtained from the bed tag surveys, the interpretation of the morphological response switches from being not statistically significant to a somewhat positive and significant relation with bedload transport intensity.

As bed volume changes estimated only from the DoDs are not related to stream power or bedload transport rates, the active areas of the bed are consequently underestimated when compared to the active areas estimated from the bed tag surveys (Figure 4.8a). The active areas estimated from the DoDs are almost constant at about 35-40 % for both sections and all floods. In the absence of the knowledge gained from the bed tags, we would conclude that bed morphology is not responsive to flood magnitude.

But, when correcting for dilation and contraction areas, the active areas observed for small floods become adequately estimated (Figure 4.8b). Furthermore, when correcting for the active areas without elevation change, the active areas derived from the DoDs and those from the bed tag surveys become very strongly related with a slope that is slightly less than unity (Figure 4.8c). The estimated areas are not exactly the same because the DoDs are continuous over the bed surface while the bed tag surveys are discrete. Nevertheless, results of Figure 4.7 and Figure 4.8 tend to confirm the reliability of the bed tag surveys and show that important information is missed when relying only on morphological surveys.

#### **4.1.5.4. Conditions leading to dilation and contraction**

The conditions leading to dilation and contraction are probably a mixture of hydraulic conditions, bedload transport processes, grain-grain interactions and local morphological history. We inspected our data set for relations with many hydraulic parameters such as flow intensity, hydrograph flashiness or falling limb duration but none were really relevant apart from the flow magnitude, as bed dilation and contraction occur mainly during small floods. The causes for the absence of a clear relation might be : 1) the critical hydraulic factors are local, such as flow downwelling and upwelling near the dilation and contraction areas, and therefore the section average hydraulic variables are irrelevant; 2) the data set is too small to detect relations involving hydraulic parameters; 3) the hydraulic effect is minor with respect to the bedload processes, the grain-grain interactions and the local morphological history; and 4) hydraulic conditions at low flows might also influence the bed packing density and add noise to the data. In effect, the surveys were usually conducted a few days after a bedload event and what is considered to be an initial setting for the following event might have changed because of an extensive low flow period.

By using the three estimates as indicators of bedload processes and grain-grain interactions and by extension of local hydraulic conditions, statistically significant relations emerged probably because the measurements reflect the more local conditions occurring in each section during the flood. For example, if bedload transport rates are low for a given flow magnitude, it probably indicates that there is a low sediment supply and/or a tight packing of the bed particles just upstream of the bedload samplers. Here, we present two

Table 4.2 Standardized coefficients for each explanatory variable and the total coefficient of determination ( $R^2$ ) of the multiple regression models for the contraction and dilation areas for floods where the bed active area was less than 60 %.

	Contraction area	Dilation area
Transported sand	0.60**	-0.42
Transported gravel	-0.71**	0.44
Active bed area	0.04	-1.17*
Total bed volume change	0.43	1.20*
$R^2$	0.45	0.33

\*\* significant at  $p < 0.01$ , \* significant at  $p < 0.05$

simple multivariate regression models to explain the variability in the proportions of the bed affected by dilation and contraction. The explanatory variables of the models are derived from the surrogate methods used in this study to measure bedload. These variables are: 1) the transport rate of sand, 2) the transport rate of gravel, 3) the proportion of active bed surface, and 4) the total volumetric change of the bed corrected for bed dilation and contraction. In order to remove the scale effect of the flood magnitude, all four variables were divided by the total volume of effective runoff. The effective runoff is the runoff under which bedload transport was active, which can be determined from the load cell signals. The distributions of the variables were all strongly right skewed and were therefore normalized through a logarithmic transformation. To obtain linear relations between the explanatory variables and the response variables, the same transformation was applied to the proportions of bed dilation and contraction. For the purpose of comparison between the regression coefficients, explanatory and response variables were standardized.

Bedload events with more than 60 % of active bed areas were removed from the analysis because the remaining stable area was judged to be too small to be representative of the dilation-contraction dynamics under investigation. Therefore, the regressions were performed with 22 individual cases covering 11 floods for both sections: six when the dilation area was greater than 10 %, six when the contraction area was more than 10 %, once when the contraction and dilation areas were both larger than 10 %, leaving 9 events when none of the two processes were judged to be important (Figure 4.6). Given the reduced number of variables in the model, 45 % of the variance of contraction areas and 33 % the variance of dilation areas are explained, both models being significant at  $p < 0.05$ . Table 4.2 presents the standardized coefficients of the multiple regressions for contraction and dilation. Interestingly, the significant regression coefficients are different for the two

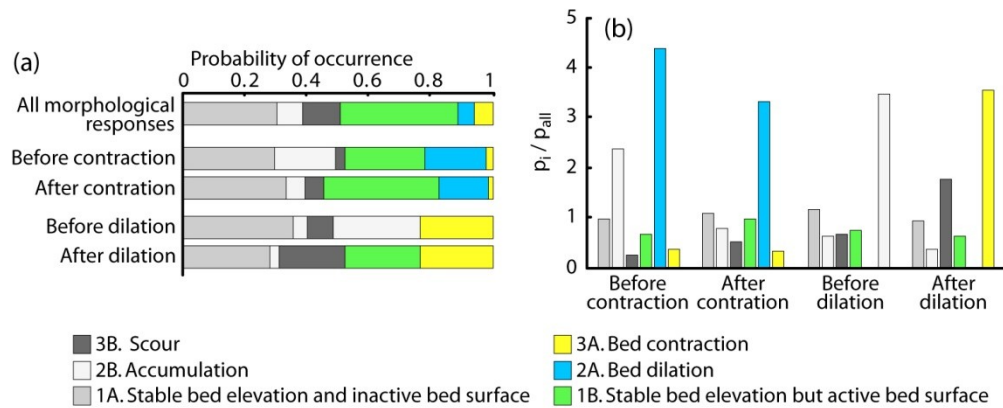


Figure 4.9 Morphological response sequences for local bed dilation and contraction (i.e. locations of the bed tags). For every occurrence of bed dilation and contraction in both study sections, previous and following local bed states are compiled. (a) Probability of observing a specific morphological state before contraction, after contraction, before dilation and after dilation at a particular location of the bed. The probability of occurrence of all morphological responses for the whole data set is shown for comparison. (b) To appreciate the differences between the general probability of occurrence of one morphological scenario ( $p_{\text{all}}$ ) and the probability of occurrence before or after a specific morphological scenario ( $p_i$ ), we show the ratio  $p_i / p_{\text{all}}$ . If the ratio is greater than one, this means that this succession of morphological responses is more likely to occur.

processes. Areas where contraction occurred increase with the proportion of sand found in the bedload samplers indicating low gravel mobility, while dilation areas are associated with a small active area and relatively larger bed total volumetric changes. Even though the regression coefficients for the transported sand and gravel are not statistically significant for the dilation model, it is still interesting to observe that their signs are opposite to those of the contraction regression model. This suggests that, there is less transported sand found in the bedload samplers when dilation occurs on large surfaces of the bed.

The local morphological history is also a contributing factor to explain bed dilation and contraction. For example, a freshly dilated area is more likely to experience scour as the particles are loosely packed. Over the whole data set, there were 119 occurrences of bed dilation and 164 occurrences of bed contraction. These numbers are not large enough to see if bed dilation and contraction occurs in preferential zones of the bed. We can calculate, however, the probability of each of the six morphological responses before and after local bed dilation and bed contraction occurrences (Figure 4.9a). By dividing these probabilities by the absolute probability of occurrences of each morphological scenario obtained for the

whole data set, it is possible to detect if a specific response is more likely to occur or not (Figure 4.9b). There is a clear trend of an oscillating process between contraction and dilation for a specific location of the bed. There are also other notable interactions. For example, dilation is likely to occur over a stable area and is not likely to occur on freshly active areas where the particle packing is probably relatively loose. Also, dilated areas have as much as twice the chances of being scoured during the next flood compared to any other area of the bed. Whereas contraction of the bed occurs often after sediment deposition and once the bed is tightly packed, there is a slightly greater chance that the location remains stable during the next flood. These results highlight the key role of the morphological history on the bed volume changes, independently of hydraulic factors and bedload processes.

#### 4.1.5.5. Effects of dilation and contraction on fluvial processes

The previous section hints at the potential causes leading to the dilation and contraction of the river bed but can these bed responses have an effect on bedload and morphological processes? From intuition, we would expect that after a bed contraction the bed particles are more difficult to entrain as they are more tightly packed. Therefore, the next bedload event will be characterized by lower than expected gravel bedload transport rate, active areas and erosion volumes. The opposite would be expected for flood following bed dilation as the bed sediments are looser. Also, bed contraction would increase the critical threshold for entrainment while it would be the opposite for bed dilation. Using the water slope  $S_w$  and depth  $Y$  at the moment when bedload is initiated, we estimated the dimensionless critical entrainment threshold for each flood using these equations:

$$\theta_{ci} = \rho g Y S_w \quad \text{Equation 4.2}$$

$$\theta_{ci}^* = \theta_{ci} / g(\rho_s - \rho) D_{50} \quad \text{Equation 4.3}$$

where  $\rho_s$  is the bedload material density ( $2670 \text{ kg m}^{-3}$ ) and  $D_{50}$  is the median particle b axes for each section (50 mm upstream and 43 mm downstream).

Figure 4.10 illustrates the effect of bed contraction/dilation on the next bedload event characteristics. The signal is noisy because the dilated and contracted areas only cover a fraction of the entire bed surface but we can observe the expected trends for small floods ( $\omega < 3-4 \text{ kg m}^{-1} \text{ s}^{-1}$ ) experiencing partial transport (Figure 4.10). The relation seems

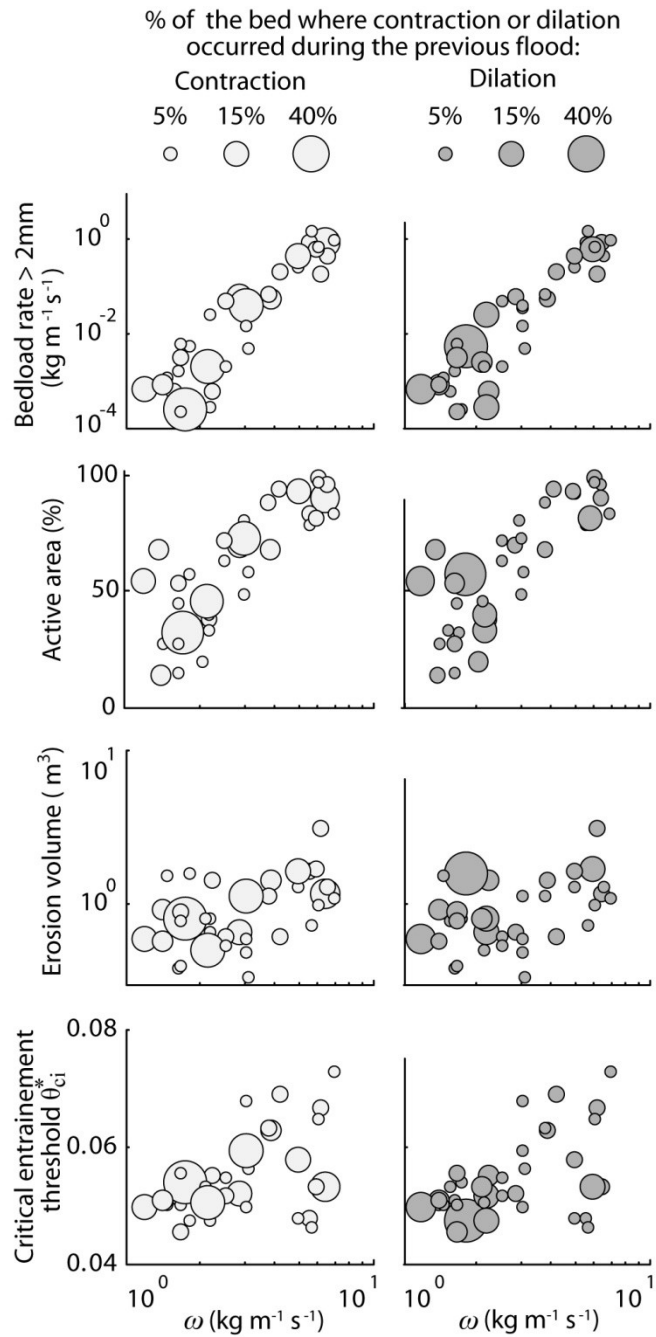


Figure 4.10 Bedload and morphological variables that are likely to be affected by the occurrence of bed areas where contraction or dilation occurred during the previous flood, thus changing the initial conditions of the bed. Erosion volumes are corrected for dilation and contraction areas. Each dot represents one flood event and its size is proportional to the contracted or dilated areas of the previous flood. Unit stream power ( $\omega$ ) is averaged over the period when the bedload transport was active.

to be stronger in the case of bed dilation. For example, the flood following the largest bed dilation affecting about 40 % of the bed surface is characterized by a higher bedload rate when compared to other floods of similar magnitude. This high bedload rate is associated with a large active area, large erosion volumes and one of the lowest initial entrainment thresholds. Particle motion appear to be globally facilitated by a looser packing of the bed. On the other hand, the effect on bedload of the flood following the largest bed contraction of about 40 % of the surface is not as clear. Indeed, even though a large proportion of the bed was more imbricated, the active area and erosion volume was not lower on average than during other floods of similar magnitude. Nevertheless, the entrainment threshold was in the range of the highest values and the bedload transport very low.

#### **4.1.6. Discussion**

The results of this study highlight the fact that some morphological processes are not detected by using solely DoDs but are revealed through a combination of multiple methods to estimate bedload transport leading to a better understanding of river dynamics. The results also point towards the identification of new processes in gravel-bed rivers: the contraction and dilation of the bed. These processes suggest that the particles creating the bed structure experience an *in situ* reorganization leading to a change of volume, hence to an observable change in bed elevation of one to two  $D_{50}$ . The results raise the crucial question: how can the bed change its volume during a flood? We do not have direct evidence of the processes involved, but after careful consideration of the possible driving factors, we hypothesize that bed dilation and contraction are primarily due to grain-grain interactions that are in turn controlled by hydraulic and bedload processes in the context of a local morphological history. In this discussion, we consider a series of processes and mechanisms that might contribute to *in situ* reorganization of the bed.

##### **4.1.6.1. Possible causes of dilation and contraction**

There are many studies in fluvial geomorphology on bed particle organization and sorting leading to bed armoring, bedform development, or downstream fining. It is generally accepted that the armor layer packing and imbrication can vary both in space and time due to various factors such as the sediment supply (e.g. Hassan and Reid, 1990), the presence of microforms (e.g. Reid et al., 1985) or the shape of the hydrograph (e.g. Hassan et al., 2006). Here, we argue that similar factors, and probably others, are acting on the

packing density of the bed at depths greater than the surface layer. The traditional approach to understand the sources of bedload transport variability and the subsequent sediment organization consists in studying the variations of the fluid forces. But, the grain-grain interactions are probably also a crucial driving factor as many analogies exist between dry granular flows and bedload transport (Jerolmack, 2011). More recently, fluvial geomorphologists have reintroduced explicitly granular physics concepts in the understanding of bedload and the formation of armor layer in a gravel-bed (Frey and Church, 2009; Frey and Church, 2011). In that context, properties of quasi-static granular flows allowing changes in gravel framework packing density (the volume occupied by a given number of particles) may serve as a conceptual basis to our empirical observations of bed dilation and contraction. In a mixture of two grain sizes where one size compose the framework and the small size the matrix, the packing density of the framework will change as a function of three main causes: 1) the size ratio between the matrix and the framework grains; 2) the volume ratio between the matrix and the framework and 3) the vibration of the framework (Mitarai and Nori, 2006). We will discuss only the latter two causes as the size ratio between the matrix and the framework is probably not varying enough to significantly affect the bed packing density at Béard Creek.

The volume ratio between the matrix and the framework will determine how the cohesionless grains behave from a framework supported structure to a matrix supported structure. It appears, however, that the situation can be very complex. In a study with a binary mixture of spheres, Yu and Standish (1988; 1991) have shown that the particles forming the framework are usually the largest size fraction with some disturbances of the framework due to the infiltration of the smaller size fraction. Small grains will disturb the skeleton of the framework when they are too large to continue to percolate through the pores, forming a new structure of both small and coarse grains and therefore contributing to the pore dilation and to an overall increased volume occupied by the largest size fraction. One would expect that these disturbances are more frequent when increasing the complexity of the mixture by adding different grain sizes, irregular shapes and densities.

In rivers, the volume ratio between the framework and matrix particles can change depending on the fine sediment supply. It is well established that fine grains (clay, silt and sand) can move inside a static gravel framework by gravity and interstitial hydrodynamics (e.g. Packman and Brooks, 1995; Packman et al., 2000; Packman and Mackay, 2003).

Exchanges between the free surface flow and the interstitial flow are mainly driven by the variation of the local slope and bedforms, thus creating zones of downwelling and upwelling where fines are pushed into the bed or expulsed from it (Packman and Brooks, 2001). The infiltrated material is both fed from the suspended load and the smaller fraction of the bedload (Frostick et al., 1984). The rate of supply, the grain sizes, the size and shape of the pores and the local morphology of the channel are among the many physical factors controlling the infiltration of fine particles (that can be of small gravel sizes) into alluvial frameworks (Frostick et al., 1984). In a flume experiment, Gibson et al. (2009) observed rapidly filling zones of the bed just prior to or following the arrival of a bedload front. This process, combined with the natural heterogeneity of a gravel bed and the hyporheic exchanges associated mainly with the presence of bedforms, is an interesting hypothesis to explain the local increase or decrease of the proportion of fine particles within the bed. These results point to the role of pore-filling particles as a vast reservoir of possible modifying agents of the bed structure.

In a granular mixture, vibrations can either increase or decrease the packing density of the framework as exemplified by the study of Nowak et al. (1998). When freshly poured sediments mixture is subjected to vibration, the density will slowly increase toward a steady state. There are, however, large density fluctuations about that average value depending on the vibration intensity and on the depth within the substrate. In general, density fluctuations increase in magnitude while their frequency decreases with depth into the mixture. For an unknown reason, some experiments have also led to a significant shift of the average density in some layers of the mixture. These changes are possibly due to the random reorganization of the bridges or force networks among the particles during the vibration. All the particles composing the framework of the mixture are contributing to its stability, but the grains forming the bridges support most of it (Mehta et al., 2009). During vibration, if the bridges are broken, the reorganization of the material will lead to a change in its packing density that is not proportional to the force applied on the structure (Jaeger et al., 1996).

The vibration of the sediment mixture leading to changes in packing density is probably more difficult to translate in terms of fluvial processes. During a flood, unsteady flow, high turbulence intensity, downward and upward hyporheic flows and bedload traveling on non-mobilized surfaces can generate vibrations through the gravel bed. In a

mixed sand and gravel bed, Allan and Frostick (1999) have observed just prior to gravel entrainment a significant lift and dilation of the gravel framework followed by a rapid infiltration of the sand through the pores. They evaluated the bed volume to increase by as much as 50 % of the initial volume of the first three grain layers. In a similar experiment, Middleton et al. (2000) have measured upward vertical displacements of the framework gravel ( $D_{50} = 5.8$  mm) of about 4 mm. Brasington et al. (2000) hypothesized that the dilation process might create a downward pressure in the flow thus leading to the rapid infiltration of sand into the gravel framework. The vibration of grains prior to entrainment has also been observed in the field in fine sediment patches (Garcia et al., 2007). These observations are related to the work of Reynolds (1885) showing that a granular material must expand in order to flow or deform at all. Bagnold (1954) later suggested that the phenomenon could be explained as the result of a dispersive grain pressure acting normal to the bed.

#### **4.1.6.2. Dilation and contraction of the bed at Béard Creek**

Acknowledging that vibration is seemingly playing a role in bed dilation and contraction, the behavior of the fine matrix sediment may be the key to understanding changes in bed framework volume. Fine matrix material in gravel-bed rivers is important in controlling river-bed properties such as hydraulic conductivity (Frostick et al., 1984) and bedload intensity (Wilcock et al., 2001). The grain size distribution of the matrix is highly variable both in space and time depending on the degree of surface armoring, the sediment supply and on the flood history but it is not correlated with the framework character (Frostick et al., 1984). The fact that the occurrence and combination of bed dilation and contraction can be different between the two studied sections hints at the role of local hydraulic and sedimentological factors associated with the contrasting morphologies of the sections (Figure 4.1bc). For instance, the armor ratio of the stream varies from 1.6 in the riffle to 2.2 on the bar. The sand content is between 10 and 30 %, meaning that the bed is still clast-supported while the pores are filled with sand (Wilcock and Kenworthy, 2002). Also, the bedload transport rate, the total area of active bed and the intensity of the morphological changes during a flood are often different between the two sections (Figure 4.4). Furthermore, local conditions may change from flood to flood, also hinting at the variability in morphological responses after apparently similar floods due to different local morphological trajectories (Figure 4.9).

Examining again the explanatory regression models presented in Table 4.2, contraction seems to be associated with very low bedload mobility and with the presence of proportionally more sand in the bedload samplers compared to other floods. This suggests that there was more sand removed from the bed than added. Removal of sand that may have been part of the bed structure allows for a reorganization of the framework grains into a tighter packing structure. We may also hypothesize a vibration process that has favored the increase in particle packing density. Contraction relates well to the mechanisms associated with particle imbrication and the development of static armors except that it occurs at greater depths within the bed.

Dilation of the bed is more difficult to comprehend in terms of fluvial processes, even if it could be explained by granular physics via the inclusion of small grains into the framework, the vibration of the particle pack and the reorganization of the force chains. From the regression models shown in Table 4.2, the very small active areas associated with dilation of the bed suggest that the flow conditions only exceed slightly the critical threshold for entrainment. The process could also be akin to the one observed by Allan and Frostick (1999), Middleton et al. (2000) and Brasington et al. (2000). It seems that the dilated areas were on the brink of motion just before the flood recession and their density remains loose while allowing sand to infiltrate the bed and disturb the framework structure. This possible scenario is confirmed by the low quantities of sand in the bedload sediment samplers. It is also possible that hyporheic exchanges are exacerbated by the deeper scour and/or greater deposition in the active areas that changes the flow path inside the bed during a flood. Bed dilation seems to be associated with very specific hydraulic, morphological and sedimentological conditions, perhaps explaining why lesser proportions of the bed experience dilation than contraction.

#### **4.1.6.3. Perspectives**

In gravel-bed streams with an armored layer, the resultant imprint of bedload processes on the morphology can be relatively small (Wong and Parker, 2006). The presence of extensive areas (average of 40 %) where scour and fill compensate each other raises questions about the morphological stability at Béard Creek. The location of the areas might control local hydraulics that would favor the maintenance of the macroforms from flood to flood. We have shown that, in addition to compensated scour and fill, the

occurrence of bed dilation and contraction challenges the use of successive morphological surveys to obtain estimates of bedload transport. This suggests that DoDs need to be interpreted with care for gravel-bed rivers where bedload processes are mainly in the form of bedload sheets like in Béard Creek. However, it is possible that the studied stream is a unique setting, and that bed dilation and contraction occurs only over marginal areas of bed in other streams. But, there are equal chances that such processes occur over larger areas of bed. For that reason, bed dilation and contraction should be measured in other streams. The bed tag surveys have allowed us to identify errors of process interpretation based on the DoDs. But, the applicability of this technique in large rivers may be problematic and new methods need to be developed. Further studies of bed dilation and contraction should focus of the measurement of inbed processes such as vibration and fine sediment content both in the field and in controlled laboratory experiments.

Bed dilation and bed contraction occurred on areas covering from 0 to 40 % of the bed surface with an average of 15-20 % when the processes were present. The average height of bed elevation change ranged between 5 and 6 cm but it could reach 10 cm in places. These changes in the gravel framework volume seem to have an influence large enough to affect bedload processes and bed morphology response of Béard Creek for the next flood. The notion that the packing density of the particles can change over time also holds for freshly deposited sediments. This could explain why floods following a large bedload transport event sometimes have larger or smaller than expected bedload transport rates. The variability of the gravel framework packing density might therefore be of greater importance than suspected in explaining bedload variability in gravel-bed rivers. This calls for future research from the basic description of the spatial and temporal variability of these bed dynamics, through the identification of the driving mechanisms and to the possible implementation into bedload and morphodynamics equations and models.

#### **4.1.7. Conclusions**

In this paper, we have used three methods to estimate bedload activity of a small gravel-bed river, Béard Creek. Matching two of these methods (changes in bed topography between successive floods and bed activity surveys) has led to the identification of divergent results: elevation changes are not always consistent with the presence or absence of bed activity. Two of these states correspond to a dilation or contraction of the bed

occurring over partial areas of the surveyed sections as a result of floods where particles were moving as bedload. These bed dynamics are critical to explain discrepancies between various types of bedload measurements. It is clear that the morphological method is affected by the intensity of the dilation-contraction phenomena as it is by the scour and fill process. This study also emphasized the benefits of using multiple methods to measure bedload in order to capture the full range of bed responses to floods that move the sediments as bedload.

Dilation and contraction are a type of bed response that has not been observed or reported before in the literature. From the multiple and simultaneous measurements of flow, bedload and bed morphology before, during and after 20 flood events, we have shown that the occurrence of these processes is not an artifact or a bias of the data precision and analysis. The dilation-contraction dynamics result from the complex interactions between flow intensity, flood history, sediment supply and the initial conditions of the gravel bed prior to the mobilizing flood. We have highlighted the importance of considering grain-grain interactions as a key factor to understand the observed changes of the gravel bed framework volume by invoking processes associated with dry granular flows. We have also shown the importance of the local morphological trajectory in determining the next response of the bed to a flood. This can also be a source of noise that prevents the identification of clear relations between bedload transport and flow hydraulics. Admittedly speculative, the mechanisms involved in the dilation or contraction of the bed after a flood and their potential effect on the initial conditions of the next flood provide a range of hypotheses that require future work. These results widen our perspective in our understanding bedload variability in gravel-bed rivers.

## Acknowledgements

The authors would like to thank Mr. and Ms. Cloutier for allowing access to their land. Martin Lambert and Jean-François Myre were of great support for the design and construction of the bedload samplers. We are also grateful to Christine Bergeron-Verville, Vincent Cardin-Tremblay, Laurence Chaput-Desrochers, Sylvio Demers, Claude Gibeault, Hélène Lamarre, Olivier Lalonde, Kevin Partington, Mathilde Péloquin-Guay, Mathieu Roy, Katherine Sicotte, Rachel Thériault, Julie Therrien and Michèle Tremblay for their help in the field and in the lab. This research was supported by the Natural Sciences and

Engineering Council and the Canadian Foundation for Innovation. The authors also thank three anonymous reviewers and the associate editor for their careful reading and useful comments on the initial manuscript.

## 4.2. Paragraphe de liaison, chapitres 4-5-6

Le chapitre 4 a permis de mieux définir l'interaction entre le transport de sédiments et la morphologie du lit qui se manifeste par une réorganisation de la structure du lit. Cette dynamique de contraction et de dilation explique en partie la grande variabilité des processus fluviaux en particulier ceux qui sont responsables de l'évolution morphologique du lit. Une autre conclusion majeure des résultats présentés dans le chapitre est que les changements morphologiques tels qu'estimés par la différence de volume de sédiments avant et après une crue ne sont pas corrélés aux flux de transport de sédiments. En effet, le passage de crues de magnitude similaire peut mener à des réponses contrastées du transport de sédiments et de la morphologie. Au contraire, deux crues de magnitude différentes peuvent mener à une réponse similaire du cours d'eau, particulièrement sur le plan morphologique. Ces constats remettent en question le lien direct entre le transport de sédiments en charge de fond et les changements morphologiques. Dans cette optique, le chapitre 5 développe cette idée en examinant les interactions entre de multiples aspects du transport en charge de fond et de la réponse morphologique à l'échelle de la crue au ruisseau Béard. Cette étude détaillée permet de s'interroger sur la façon d'opérationnaliser le transfert d'échelle entre les processus de relativement petite échelle du transport en charge de fond et les processus émergents de grande échelle sur le plan morphologique. Il ressort de l'étude une séparation entre les processus morphologiques et les processus de transport à l'échelle de la crue et ce, malgré quelques interactions complexes qui font intervenir les variables représentant la rugosité du lit.

Dans la foulée du chapitre 5, différentes sources potentielles de la variabilité de la réponse morphologique et du transport de sédiments au ruisseau Béard sont examinées au chapitre 6. En effet, bien que certains aspects de l'écoulement autre que sa magnitude peuvent expliquer la variabilité du transport de sédiments comme le suggèrent les résultats présentés aux chapitres 2 et 3, il existe de nombreux autres facteurs qui influencent la direction de changement d'un cours d'eau. Les facteurs ciblés dans cette étude, mis à part la magnitude de l'écoulement, sont la forme de l'hydrogramme de crue, les conditions morphologiques initiales (topographie et structure du lit), l'historique des étiages et celle des changements morphologiques. L'identification des interactions, effets et rétroactions exige l'utilisation d'une approche systémique qui considère simultanément l'ensemble des

processus. Dans les chapitres 5 et 6 qui seront soumis en tant qu'articles compagnons<sup>1-2</sup> le nombre élevé de variables et la volonté de considérer les dynamiques fluviales dans son ensemble ont exigé de renouveler l'approche analytique (e.g. techniques multivariées) afin de considérer explicitement la complexité des interactions qui se produisent à différentes échelles. Le fil conducteur des résultats se retrouve dans la mise en lumière progressive de l'importance du rôle de la structure du lit pour connecter les processus de transport de sédiments en charge de fond et les changements morphologiques. Aussi, l'utilisation d'une approche analytique renouvelée permet d'identifier les interactions non-linéaires et les rétractions multiples.

1-Marquis G.A. et Roy A.G. Morphodynamics of gravel-bed rivers. A- Morphology and bedload transport responses. Manuscrit préparé pour la revue *Journal of Geophysical Research – Earth Surface*.

2-Marquis G.A. et Roy A.G. Morphodynamics of gravel-bed rivers. B- The effects of flow, flood history and initial conditions. Manuscrit préparé pour la revue *Journal of Geophysical Research – Earth Surface*.



## **CHAPITRE 5. TRANSFERTS D'ÉCHELLE : DU TRANSPORT DE SÉDIMENTS À LA RÉPONSE MORPHOLOGIQUE**

---

### **5.1. Morphodynamics of gravel-bed rivers. A- Morphology and bedload transport responses**

#### **5.1.1. Abstract**

Using an exhaustive field data set collected over three years in a small gravel-bed river, we investigate the response of bed morphology to the intensity of bedload sediment transport using data analysis techniques that are well suited to detect non-linear relationships. Our result show that bedload processes relate in a complex fashion to changes in the river bed structure but not to changes in bed topography. The decoupling between bed topography and bedload transport is due to an offset of the temporal scales of response. The resultant topographical change after a flood seems to result from the last moments of the bedload transport and not from the total bedload fluxes during the flood. This hypothesis is based on the strong negative relationship between changes in bed slope and in bed elevation that suggests that bedload transport predominantly proceed by the migration of bedload sheets at Béard Creek. These results offer a broad perspective on the realization that the bed structure might be a better indicator of the morphological response of the bed than changes in bed topography in this case. A companion paper investigates the causal factors that may explain bedload transport and morphological responses to a flood, with a special emphasis on the effects of flow history and of initial conditions.

#### **5.1.2. Introduction**

##### **5.1.2.1. General context**

The core of the research in fluvial geomorphology is centered on the understanding of the channel morphology evolution through space and time. Since the middle of the twentieth century, research has focused on the processes by which the form of a channel is transformed (Church, 2010). The fundamental process is the flux of sediment moving as bedload, which is driven by the flux of water. Most of our knowledge on processes driving river morphology can fit in the famous fluvial ‘*trinity*’ first published by Leeder (1983) and

later revisited by Best (1993). The erosional and depositional processes of a river depend upon the interactions between turbulent flow, sediment transport and bedforms. Rivers work as a continuous feedback system. This conceptualization of fluvial processes was mainly based on bedforms on a sandy bed like ripples and dunes. In parallel, studies of gravel-bed rivers have identified the role of imbricated structures such as pebble cluster and transverse ribs on the incipient motion of bed material and its potential effect on bedload transport rates (Brayshaw et al., 1983; Clifford et al., 1992). The geometric properties of these gravel structures have also a significant influence on flow properties like resistance, vortex shedding and energy dissipation (Lawless and Robert, 2001b; a; Lacey and Roy, 2007; Hardy et al., 2009). For instance, the bedforms phase diagram has been extended to gravel sizes (Best, 1996). Even though the trinity was mainly developed for sand bedforms, it is globally applicable to all fluvial forms, including gravel bedforms (Robert, 2003).

According to the '*trinity*', bedforms result from sediment transport and often represent the bulk of sediment transport itself. Near-bed turbulent flow fields control local rates of sediment transport. These near-bed flow fields are in turn affected by bed topography. Finally, changes in bed elevation along and across streams are modified by sediment fluxes (Leeder, 1983; Best, 1993). Leeder (1983) has stated that the fluvial '*trinity*' must be apprehended as a whole and has warned against the danger of investigating one portion in isolation. Nevertheless, few studies have addressed the study of fluvial processes in a holistic manner, examining the interactions between all three end members of the '*trinity*' at once. This is especially true of field studies where experimental control is limited and measurements are costly both in terms of money and time. In these companion papers, we will revisit the fluvial '*trinity*' using an extensive field data set collected in a small gravel-bed river.

Bed morphology, flow and bedload transport were measured during 21 floods capable of moving particles as bedload in two sections of a gravel-bed river, Béard creek. Special attention will focus on the floods for which we have a complete record of the previous flood where bedload was mobilized. This approach will allow us to investigate not only the interactions between bedload transport, flow and bed morphology response for individual flood events, but also to explore retroactions and feedbacks to previous flow conditions and initial bed morphology. The general aim of the papers is to move forward our understanding of the complexity of gravel-bed rivers morphodynamics by exploiting a

unique field data set. Variability of river morphodynamics is often assumed to be natural and ‘stochastic’ and thus, difficult to explain. This paper proposes to explain part of this variability using (1) an exhaustive data set covering the critical aspects of the fluvial system that allow to envision explicit interactions among processes and (2) nontraditional (i.e. in fluvial morphology) analytical approaches that take into account the lack of experimental control that are particularly suitable for measurements in a natural river, and that are better suited for the detection of non-linear relations as well as threshold base responses.

Underlying the exhaustive data set is the problem of the variables selection among multiple possibilities. From the collected data, it was possible to derive dozens of variables but we decided to focus on a restricted number of them in order to represent as much as possible the various aspects of the river dynamics. It would have been possible to choose other variables but in the end this would not have led to greatly different conclusions in our understanding of the complexity of fluvial dynamics. Furthermore, as there are no comparable data sets, it was impossible in the case of some variables to base our estimation method on those used in previous studies. Our choices were based on an informed knowledge and on sound assumptions while keeping the estimates as simple as possible in order to avoid further complications in the interpretation of the results.

Reporting on this research will be done from two separated but closely linked perspectives as presented in two companion papers. The first paper will address the issue of the stream response to a flood, specifically, how bedload processes during a flood affect bed morphological changes. We will show that the morphological response that results from a flood is relatively independent of the bedload transport that occurred during the flood. This result questions the validity of using the difference between successive morphological surveys as a proxy for the measurement of bedload fluxes. Using a range of data analysis techniques, we will show that bedload transport and morphology do interact under specific conditions undetectable using traditional linear analysis. In the second paper, we will link the stream response to causal factors such as the flow, the initial conditions and the history of morphological changes due to previous floods. We will show that initial bed conditions are as important as the flow to understand the stream response to a flood. We will illustrate the advantage of using nontraditional analytical methods through examples where a given response of the stream to a flood can result from different sets of causal factors. Finally, we will conclude the companion papers by analyzing simultaneously

multiple aspects of the stream bed response to a flood according to multiple possible causes. This will illustrate the potential of improving our understanding of fluvial processes by using a holistic approach compared to a simplified analysis of the fluvial processes that rests mainly on pairwise relations between variables.

### **5.1.2.2. Bedload transport and morphology interactions in gravel-bed rivers**

Depending on the delivery of coarse material to the stream and on the properties that determine the transport capacity of the stream, the bed will be characterized by typical morphological features (Montgomery and Buffington, 1997). Bedload transport rates do not respond solely to the flow as complexity arises from interactions between the grains and the bed structure. In that context, bedload processes should in part reflect morphological features and vice-versa. This assumption has led, for example, to the use of successive morphological surveys to infer bedload processes (Griffiths, 1979; Carson and Griffiths, 1989; Lane et al., 1995; Martin and Church, 1995; Ham and Church, 2000; Lindsay and Ashmore, 2002; Fuller et al., 2003; Heritage et al., 2009). In environments with large sediment supplies such as braided rivers, conditions that favor aggradation or erosion have been identified in relation to bedload transport rates and surface grain size (e.g. Ashworth and Ferguson, 1986; Hoey and Sutherland, 1991). The large deviations of the bedload transport rates from the relationship with discharge can usually be tied to morphological changes associated with channel incision, bank erosion or channel infilling mainly controlled by the upstream sediment supply (Goff and Ashmore, 1994). During periods of high rates of morphological change, there appear to be phases of deposition and scour which occur independently of discharges variations (Goff and Ashmore, 1994). Even though the qualitative relations between bedload and morphology are well identified, the links between bedload transport rates and bed morphology are difficult to define quantitatively because of the dependence on the previous history of channel morphological development (Hoey and Sutherland, 1991). Also, not all progracial braided rivers have obvious process-form relationships (Nicholas and Smith, 1998).

In many gravel-bed rivers, sediment supply is insufficient to meet the transport capacities of the stream which usually leads to a riffle-pool or bar-pool morphologies when the reach has a medium to low slope. These morphological features tend to be fairly stable because the full range of sediment sizes is rarely mobilized during a flood (Montgomery

and Buffington, 1997). When sediment supply is lower than the transport capacity, surface coarsening occurs through the vertical sorting of the grains, a layer of coarse particle resting on a matrix of finer ones (Dietrich et al., 1989). This armored layer is one or two coarse grain thick, and the ratio of the median grain size to the subsurface material typically ranges between 2 and 4 (Church, 2006a). Various processes have been proposed to explain the formation of the armor layer but as yet there is no consensus. Whether the stream armor is formed by the winnowing of the surface layer (e.g. Proffitt and Sutherland, 1983) or during equal mobility transport where large particles offer shelter to finer ones (e.g. Parker et al., 1982a; Parker and Klingeman, 1982) or by the interactions of different sediment sizes that lead to the granular phenomenon of vertical sorting (Frey and Church, 2009), sediment transport is directly linked to bed armoring. Even though the armor layer strength can evolve during a flood or between floods, the overall size distributions of particles at the bed surface show little variation (Wilcock et al., 2001). However, variations in grain packing and imbrication change the critical flow threshold at which the bed surface is disrupted. The increased bed resistance due to particle imbrication enhances the stability of the stream, further limits sediment supply, and interacts with other bedforms in limiting their height and amplitude (Wilcock and Southard, 1989), thus complicating the interactions between bedload and morphology.

Regardless of the balance between sediment supply and transport capacity, variations in sediment transport rates in gravel-bed rivers have been described as sediment waves and pulses (Reid et al., 1985; Whiting et al., 1988; Gomez et al., 1989; Dinehart, 1992; Nicholas et al., 1995). The periodic sediment waves should result in cycles of aggradation and degradation of the river bed (Nicholas et al., 1995). According to Hoey (1992), sediment pulses exist at multiple scales and are due to different fluvial processes. For example, there is an important distinction between the processes responsible for generating meso and macroforms. Mesoforms (at the scale of flow depth) such as pebble clusters and gravel ribs are due to variations in the fluid dynamic regime of the boundary layer. At the scale of the channel width, the macroforms such as gravel sheets, riffles and unit bars are in phase with the geomorphic regime and are transient features associated with bedload transport. These various pulses or sediment waves can be endogenous to the in-channel bedload processes or exogenous by sediments ingressions external to the river channel (Nicholas et al., 1995).

At the scale of the flood and the river reach, bedload sheets are probably the type of macroforms that has been the most often identified to explain the variability of bedload transport and subsequent channel morphology changes (e.g. Kuhnle and Southard, 1988; Whiting et al., 1988; Ashmore, 1991; Bennett and Bridge, 1995b; Recking et al., 2009). These highly mobile low-relief bedforms are a few grain diameter thick and several centimeters or meters long (Whiting et al., 1988). In a recent flume experiment, the migration of periodic bedload sheets was associated with cycles of aggradation and degradation with fluctuations of the mean and local bed slope, of the bed state (fining and paving) and of the associated bedload rates (Recking et al., 2009). Different spatial and temporal scales of bedload pulses may coexist and the time series of bedload transport rates and sediment storage (i.e. bed morphology) may exhibit stochastic fluctuations (Hoey, 1992). A travelling wave is susceptible to interact with the local morphology, rather than obliterating it (Wathen and Hoey, 1998). This means that the initial sediments of the wave are exchanged with bedforms during their downstream routing. The rate of exchange will depend on the stability of the bedforms. If sediments are deposited in stable locations, erosion in adjacent areas is likely to occur whether or not the sediments enter an unstable location; it may trigger a widespread instability resulting in an increase of sediments travelling with the wave. Therefore, the occurrence, dimensions and dynamics of bedload sheets are primarily controlled by local sediment supply (Dietrich et al., 1989; Nelson et al., 2009). Nevertheless, if a stream is at dynamic equilibrium, bedload time series should exhibit variations at the characteristic scales of the processes associated with sediment waves occurring in the stream (Hoey, 1992).

These studies point towards the fact that there is an intimate relation between bedload transport and river bed morphology. On a conceptual basis, there is a general consensus that the flow will drive bedload transport and that in turn the morphology adjust to the fluxes of bedload material. Nevertheless, a better knowledge of the gravel bed composition and morphology should contribute to an improved understanding of sediment transport processes (Carling and Reader, 1982). In the context of supply limited streams where the main sediment sources are the river bed and banks, bedload transport will also be modulated by the organization of bed particles which is mainly associated with the particles packing density and the presence of micro and macroforms. From this chain of interactions and retroactions, one would expect that bedload sediment transport would relate in some

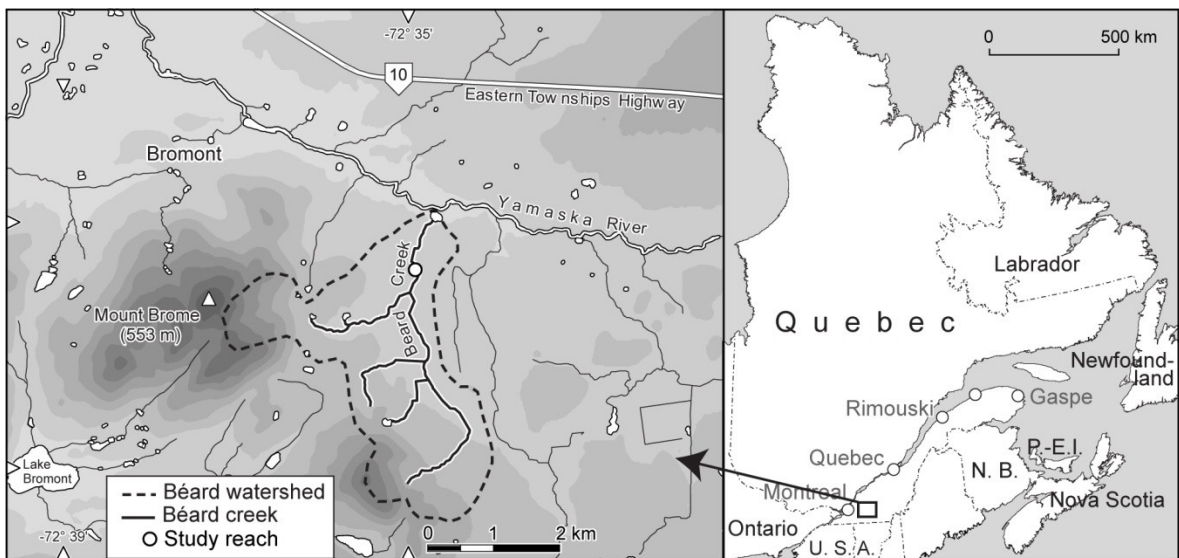


Figure 5.1 Field site location.

ways to some measures of bed topography. However, few studies have directly linked these processes due to the difficulty of acquiring the relevant data (Singh et al., 2010). In this paper, we will show that these complex interactions might result in no apparent quantitative relation between bedload transport and bed morphology and will speculate for possible explanations of that result.

### 5.1.3. Methods

#### 5.1.3.1. Field site and data collection

The data were sampled at Béard Creek, a small gravel-bed river with a riffle-pool morphology located in the Eastern Townships, Quebec, Canada (Figure 5.1). The average bankfull width is 6 m, bankfull depth is 0.7 m and the bankfull discharge ( $Q_{bf}$ ) is  $2.5 \text{ m}^3 \text{s}^{-1}$ . Bed slope ( $S$ ) is around 1 %. The watershed is covered with forests, pastures and some cultivated fields over a glacial till which is the main reservoir of sand and coarse particles for the stream. Because most of the bank tops are vegetated with bushes and trees and that the channel is decoupled from the valley slopes, the main supplies of coarse material are the bed and banks of the stream. Two measurement sections 75 m apart were chosen near the outlet of the watershed for their contrasted morphologies (Figure 5.2). In the upstream section, there are two sequences of riffle-pool and the median particle size ( $D_{50}$ ) is 50 mm estimated from a surface pebble count of 400 particles (Figure 5.3). The downstream

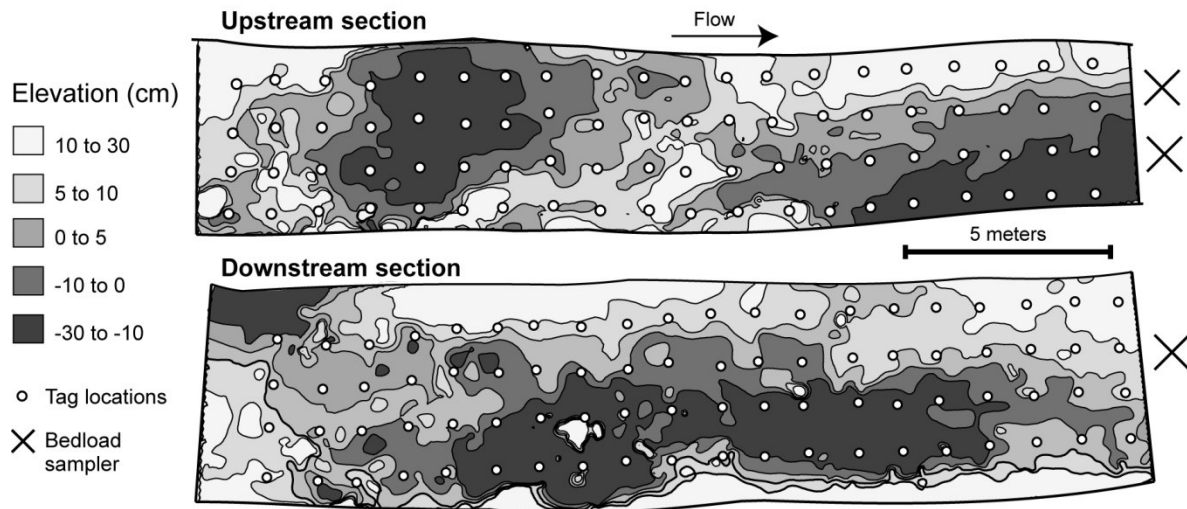


Figure 5.2 Detrended initial morphology of the surveyed sections and instruments location.

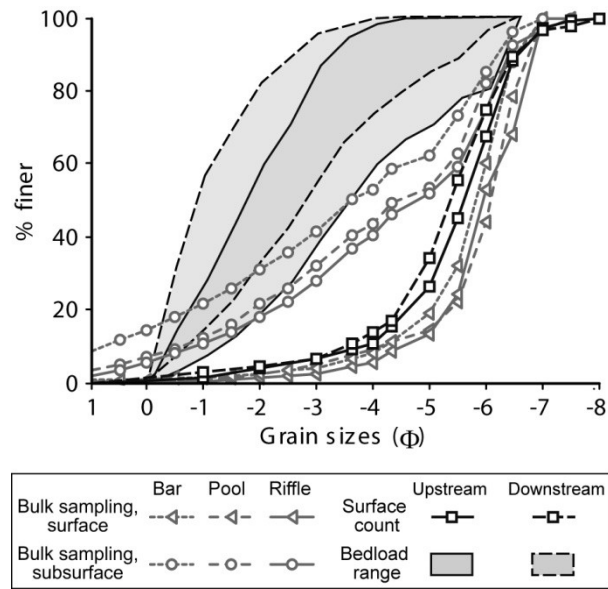


Figure 5.3 Cumulative particle size distributions. The bedload curve is for average distribution events below bankfull discharge  $Q_{bf}$ . Surface pebble counts are based on 400 particles measured at each section. Bulk sampling is based on the sieving of about 40 kg samples.

section is characterized by a lateral bar and a straight thalweg with a lower  $D_{50}$  of 43 mm estimated from the measurement of 400 particles (Figure 5.3). The supply-limited condition of the stream is clear from Figure 5.3 where the size distributions of the surface and subsurface sediments in three different morphological units are shown. Taking the sand

portion into account, the armor ratio is 4.5 on the sampled bar, 3.2 in the pool and 2.8 on the riffle. When considering only the gravel size material, the armor ratios are 2.2, 2.0 and 1.7 in the bar, pool and riffle respectively. The flow is measured using two gauging stations located 100 m apart upstream and downstream of the sections allowing the estimation of the water surface slope ( $S_w$ ) used to compute the averaged bed shear stress for the whole reach. Discharge ( $Q$ ) is estimated through a stage-discharge rating curve established at the downstream section.

Bedload was measured in each section with Birkbeck bedload pit samplers constructed according to the design proposed by Sear et al. (2000) with some modifications. The upstream section has two bedload samplers positioned at 1/3 and 2/3 of the cross section (Figure 5.2). The downstream section is equipped with only one sampler located at the edge between a small lateral bar and the thalweg (Figure 5.2). The slots of the samplers are 0.12 m wide, which corresponds to  $D_{95}$  of the bed surface gravel and the length of the slot is 0.4 m, about 10 times the  $D_{50}$  of the bed material. These dimensions were based on different considerations outlined by Laronne et al. (2003). The capacity of each sampler is 85 kg of dry sediments or a volume of 0.06 m<sup>3</sup>. Each sampler has a submersible load cell (Interface 2400, 0-110 kg) that measures bedload in real time. The load cell signals are compensated for temperature (-10 to 45 °C) and have a static error band of 0.1 % of total capacity. Their minimal detection range is approximately 15 g in field conditions. After each bedload event, the samplers were emptied and 25 % of the sediments were sieved at half-phi intervals.

The morphology of the stream was surveyed after each bedload event 20 meters upstream of the bedload samplers using a total station (Figure 5.2). The point density of the survey was of 4-7 pts/m<sup>2</sup> and the sampling strategy was mostly systematic but with a higher density of points at breaks of slope in order to correctly represent isolated obstacles or changes between morphological units. The planar precision of each survey was around 3-5 mm and the error in elevation ranged between 1-4 mm. Digital elevation models (DEMs) were derived from the topographical surveys using the nearest neighbour interpolation algorithm in the Vertical Mapper software. Further details on the interpolation choice can be found in Marquis and Roy (2012). The difference between successive DEMs allows us to identify zones of bed stability but also zones subject to scour or deposition.

Bed activity was estimated using a 1 m<sup>2</sup> grid of 80 bed tags as shown in Figure 5.2. The tags were steel washers of 35 mm in diameter which is slightly smaller than the  $D_{50}$ , as recommended by Konrad et al. (2002) who introduced this method. Each tag is inserted vertically in the bed and is aligned parallel to the flow to assure that the tag would not be entrained by itself but only if the surrounding particles are mobilised. A short plastic flag was attached to each tag to facilitate its visual detection on the stream bed. After each flood, locations where bed tags were not found in place (either entrained or buried) were classified as active. After the survey, the missing bed tags were replaced so the grid was complete before each flood. The reliability of the survey is discussed in Konrad et al. (2002) and Marquis and Roy (2012). The bed activity survey allows us to detect more accurately the active areas of the bed than the differential DEMs because there are areas where scour and fill both occur during a flood and result in no elevation change.

### 5.1.3.2. Data set

The data in this paper were collected over three years during the spring, summer and fall of 2007, 2008 and 2009. A total of 21 rain-triggered events generating a wide range of peak discharges ( $Q_{pk}$ ) up to three times the bankfull discharge ( $Q_{bf}$ ) with measurements of the initial conditions and the resulting bedload transport and morphological changes are used in this paper (Figure 5.4). The data of the first flood of each year are used only to establish the initial conditions and history for the second flood of each year, leaving 18 flood events to analyse. From these events, seven were above bankfull discharge with large bed mobility and high bedload transport rates causing a filling of the bedload sampler before the end of the flood, sometimes before the flood peak. Therefore, these events were removed from the analysis each time bedload transport related variables were calculated. This choice was necessary to ensure that the analysis of the links between measured processes was conducted without any estimation or extrapolation of variables. From our data set, we estimate that bankfull discharge is approximately the threshold between partial transport and full mobility. In effect, floods above bankfull discharge all have bed surface mobility greater than 80 %. This threshold is in line with observations from other studies (e.g. Ryan et al., 2005).

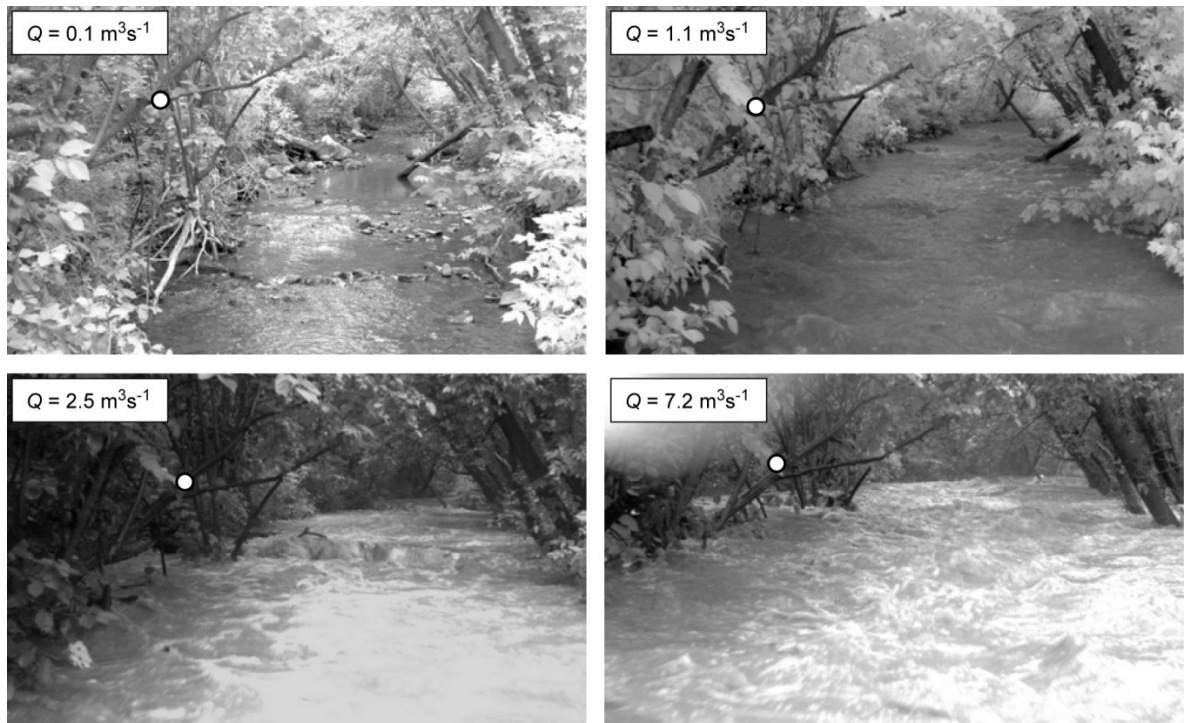


Figure 5.4 Pictures looking upstream for various discharges at the upstream section. The white dot serves as a reference point from picture to picture. Note that the bankfull discharge is  $2.5 \text{ m}^3 \text{s}^{-1}$ .

Also, three events presented in this paper are in reality two distinct events but the short delay between the two flood peaks prevented us to obtain the relevant data for each individual event. These events are the second and fifth in 2008 and the seventh in 2009. Two of these sequences were composed of small events as the bedload samplers were not full. The other sequence is a very small event in terms of bedload transport rate followed by a very intense bedload event that probably obliterated the signature of the previous event. Weighing the pros and cons of removing or not the agglomerated events from the data set led us to conclude that it was more important to have as many data points as possible and that the loss of precision was compensated by the gain in knowledge that can arise from a larger data set. The data set is therefore composed of 36 individual data points (18 events for two sections) for the morphological processes and 22 individual data points (11 events below the bankfull discharge for two sections) for the bedload processes.

Table 5.1 Bedload and morphology response variables.

	n	Mean	Std. dev.	Min	Max	Skewness	$\lambda$
Dimensionless bedload rate $i_b^*$	22	$2.0 \times 10^{-4}$	$3.0 \times 10^{-4}$	$7.3 \times 10^{-6}$	$1.0 \times 10^{-3}$	1.74	-0.14
Dimensionless median bedload size $D_{50}^*$	22	0.14	0.05	0.08	0.26	1.16	-0.80
Bed activity area $MOB$ (%)	22	46	19	14	81	0.05	
Dimensionless entrainment threshold $\theta_{ci}^*$	36	0.06	0.01	0.05	0.08	1.41	-3.17
Slope change $\Delta S$ (%)	36	0.04	0.19	-0.36	0.63	0.87	
Dimensionless macroform roughness change $\Delta \tau_f''$	36	0.05	0.61	-1.44	1.86	0.20	
Dimensionless microform roughness change $\Delta \tau_g'$	36	0.01	0.08	-0.20	0.19	-0.08	
Dimensionless bed elevation change $\Delta E$	36	-0.04	0.29	-0.76	0.62	-0.09	

### 5.1.3.3. Bedload and morphology variables

From our data set, we can derive many different variables to describe bedload transport and the bed morphological response. But, for means of simplicity, we have opted for a subset of variables that seem to be distinct and meaningful in terms of understanding the various components of fluvial dynamics (Table 5.1). The choice of the variables and of further transformations applied to remove the dimensions were made to ensure that all variables are derived from independent measurements and do not depend on each other in the calculations in order to avoid redundant information and spurious correlation. Eight key variables were retained for the analysis in order to capture bedload and morphology. Bedload transport is usually characterized by its quantity and intensity and by the sizes of the mobilized particles. Therefore, the variables associated with bedload processes are the bedload flux, the caliber of the transported sediment and the proportion of the bed surface that was active where there was either scouring and/or filling of the bed. The morphological response can also be defined in terms of resulting topography and bed particle organization. The variables associated with morphological response are the mean elevation change, the bed slope, the critical threshold for motion, and two types of bedforms indicators, the macroform roughness (i.e. at the scale of riffle-pool morphology) and the microform roughness (i.e. at the scale of large grains, pebble clusters and transverse ribs). We considered that the critical threshold for entrainment is a morphological indicator because it reflects temporal changes in bed structure and therefore influences the driving forces acting on the bed (Turowski et al., 2011).

The unit bedload flux rate  $i_b$  was calculated using the total submerged weight of sediments in the samplers and the period over which the load cell time series show active transport divided by the sampler slot width. It was then multiplied by the ratio of particles larger than 1 mm because smaller particles are considered to have travelled mostly in suspension in the water column. For the upstream section, we used the mean of the two samplers and for the downstream section, we used the values from only one sampler. We considered the variability in bedload across the river channel to be minimal as the two sections are relatively narrow and straight and the morphology is simple. The dimensionless transport rates were obtained using the median size  $D_{50}$  of the surface particles of each section:

$$i_b^* = i_b / \rho_s [g D_{50}^3 (\rho_s - \rho) / \rho]^{0.5} \quad \text{Equation 5.1}$$

where  $g$  is the gravity acceleration ( $9.8 \text{ ms}^{-2}$ ),  $\rho$  is the water mass density and  $\rho_s$  ( $1000 \text{ kgm}^{-3}$ ) is the sediment mass density ( $2700 \text{ kgm}^{-3}$ ). We have chosen  $D_{50}$  as the indicator of the caliber of the transported particles as other sizes such as  $D_{84}$  or  $D_{99}$  vary linearly with the  $D_{50}$  in our data set (Figure 5.3).  $D_{50}$  of the transported material was estimated only for the gravel fraction ( $D > 2 \text{ mm}$ ). When particles larger than 1 mm were included in the calculations, the variability among floods was greatly damped. We suggest that this is mostly due to the large reservoir of sand in the banks that resulted in larger proportions of sand in the bedload samplers during small flood events than that of the gravel. The dimensionless median size of the transported particles  $D_{50}^*$  was calculated using the  $D_{50}$  of the bed surface. The mobilised or active bed area (*MOB*) was directly estimated by dividing the number of missing bed tags by the total number of tags in the section (80 by section).

Using the average water slope ( $S_w$ ) over the two sections, the flow depth ( $Y$ ) and the bed surface  $D_{50}$  of each section at the moment when bedload was initiated, we estimated the dimensionless critical entrainment threshold ( $\theta_{ci}^*$ ) using:

$$\theta_{ci} = \rho g Y S_w \quad \text{Equation 5.2}$$

$$\theta_{ci}^* = \theta_{ci} / g(\rho_s - \rho) D_{50} \quad \text{Equation 5.3}$$

The four other morphological variables are estimated from the section DEMs. The elevation ( $E$ ) is simply averaged over the whole DEM. In order to estimate the microform roughness ( $\tau_g'$ ), we divided the surveyed area into 80 subareas centered on the bed tags location and calculated the standard deviations of the elevation values in each subarea. The

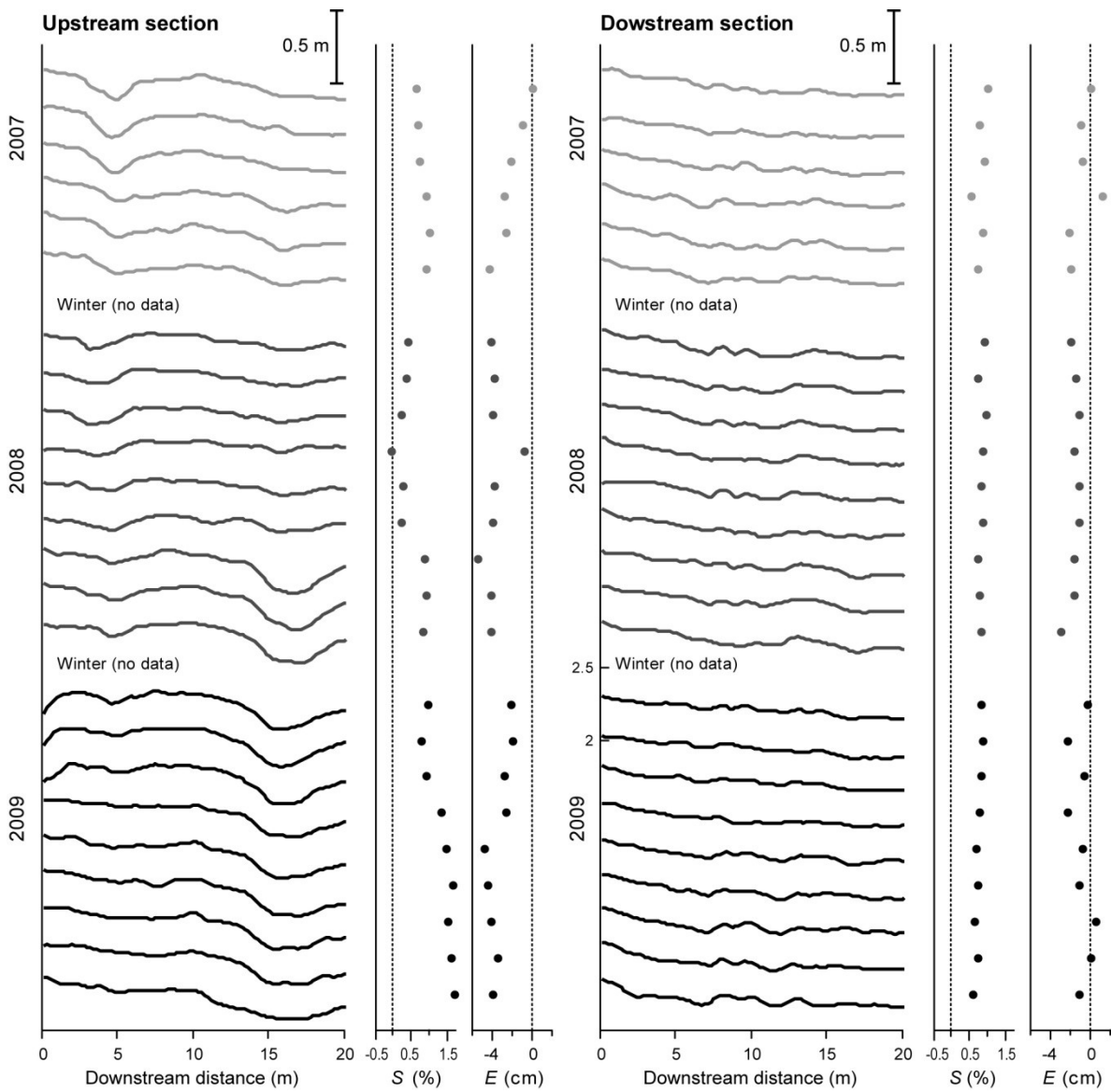


Figure 5.5 Thalweg profile, slope  $S$  and elevation  $E$  evolution through time. The profiles were surveyed between each flood mobilising particles as bedload, no data was collected during winter. See text for explanation on the estimation of the data.

80 elevation standard deviations were then averaged to obtain a value for the whole section that represents  $\tau_g'$ . This estimate may not be accurate but because the total station surveys were mostly done by the same operator with a constant point density, it is a fair indicator of the grain roughness. The macroform roughness ( $\tau_f''$ ) and the bed slope ( $S$ ) were estimated using smoothed thalweg profiles. Three longitudinal transects for each section and each event were extracted from the DEMs, one located in the thalweg and two 0.5 m on either

side of the thalweg (Figure 5.5). Averaging these three transects accounts for the thalweg migration over the duration of the measurement period. The bed slope was estimated directly by fitting a simple linear regression through the averaged thalweg profiles. The macroform roughness was simply estimated using the range of elevations for each thalweg profile. This simple indicator accounts for the global changes in riffle-pool roughness. We did not use these morphological indicators directly in the analysis. We chose to use differences ( $\Delta$ ) between successive events instead of absolute values of the boundary conditions because we are interested in the direction of change of the morphological variables in relations to bedload processes. For example, instead of analysing the absolute elevation of the river bed, we analysed the change in elevation due to a flood. A similar procedure was applied for the slope, the micro and macroform roughness. The length dimension of the changes in elevation, micro and macroform roughness was removed by dividing the values by the corresponding section  $D_{50}$ .

#### 5.1.3.4. Data analysis

To explore the relations between the bedload transport and the morphological responses, we used four types of quantitative analyses. Firstly, we compared the data in a dichotomous fashion: upstream *vs* downstream section and partial *vs* full transport. The comparisons relied on a two-way analysis of variance test. In the analyses of the global response of the two sections in this paper and the companion paper, we assumed that the causes of the bedload and morphology responses are based on general principles and are not site specific. Therefore, the responses should not be statistically different between the sections. The comparison between flood events with partial transport and those with full transport is more difficult to perform because we do not have complete records of bedload fluxes, bed surface mobility and grain sizes under full mobility conditions. However, we have a complete record of the morphological response. Therefore, by comparing the two types of flood event, we gain information on the similarity of the morphological response related to the intensity of bedload transport. Because processes involved in partial transport conditions or full mobility are different, they should produce different morphological responses (Warburton, 1992). In our data set, the general threshold between partial transport conditions and full mobility is around the bankfull discharge ( $2.5 \text{ m}^3\text{s}^{-1}$ ). In addition to the ANOVA test, we also used a Chi-Square variance test in order to find if

variables have a greater range of responses between the two sections and between floods below and above bankfull discharge.

Secondly, we used simple linear correlations to estimate Pearson  $r$  for each possible pair of the eight response variables. This procedure is repeated for each section and for both sections taken as a single data set. The purpose of this analysis is to detect at which level of response the two sections are similar or dissimilar.

Thirdly, considering that we often wish to understand either the direction of change (i.e. aggradation vs degradation) or the magnitude of the processes (i.e. low or high bedload rate compared to the mean), we divided the data set into groups to see if this simplification can reveal more interactions between the different characteristics of the bedload and morphological responses to floods. For each variable, using the normalised and standardised values, we divided the groups based on the  $z$  scores -0.5 and 0.5. These limits split the data set into more or less even groups. For the bedload flux, the median transported particle size, the bed mobility area and the threshold for motion, the data are grouped as lower, equal or higher than the mean. For four variables that are indicators of morphological change, the changes of slope, macroform roughness, microform roughness and bed elevation, the groups correspond to a decrease, stability or an increase of the attribute. We performed multiple ANOVA tests on all the response variables according to each of the eight groupings in order to see if at least one group was statistically different from the other. Even though ANOVA is a linear method, this group analysis allows us to account for small number of individual data points but also to detect possible non linear variations between two variables. For example, if only the ‘high’ group is different from the two groups, it will be detected by the ANOVA and not by the Pearson’s  $r$ . Also, these groups will be used further in the companion paper to examine their links with possible causal factors.

Lastly, we used principal component analysis (PCA) in order to analyse the data set as a whole. This will demonstrate the advantages of a holistic view over a pairwise analysis of the variables for understanding river dynamics. PCA is a tool that allows the visualization of observations of possibly correlated variables in a reduced space by an orthogonal transformation. The transformation is defined in a way that first principal component (PC) has the maximum variance extracted from the observations. The following principal components with decreasing variance are all orthogonal, meaning that they are not

correlated. The number of principal components is equal or lower than the number of variables in the analysis. The more the variables are correlated, the more variance will be contained in the first principal components. The PCA was performed using the CANOCO software. In the selection of the number of principal components we used the generally accepted rule that a principal component is worth analysing when its variance exceeds the average variance by variable which is 12.5 % for our data set (100 % / 8 variables) (Legendre and Legendre, 1998). The results of the data transformation are shown using biplots which are the projections of the individual data points and of the variables as arrows. Biplots are useful to interpret the correlation between the variables, which is proportional to the angle between the arrows in the reduced space. More than representing the organisation of the data set in the orthogonal space, it is also possible to extract from the PCA outputs the distribution of the variance of each variable between the principal components. In a similar fashion, it provides the distribution of the variance of each individual data point between the principal components. This information is useful to detect groups of variables/data points with similar behavior.

All quantitative analyses were done on normally distributed variables. A Lilliefors test was performed on all variables to test the goodness-of-fit to a normal distribution (Table 5.1). This test is akin to the Kolmogorov-Smirnov test for normality but can be used when the fully specified null distribution of the variables is unknown and the parameters of this distribution must be estimated (Lilliefors, 1967). The variables that failed the normality test ( $p < 0.1$ ) were normalized using the Box-Cox transformation which is a family of power transformations searching for the exponent  $\lambda$  (Table 5.1) that maximises the Log-Likelihood Function:

$$data(\lambda) = (data^\lambda - 1)/\lambda \quad \text{Equation 5.4}$$

All variables were subsequently standardized to facilitate comparisons between  $z$  scores ranges. All statistical tests in the paper (ANOVA and Pearson  $r$ ) will be considered significant if the estimated probability of rejecting the null hypothesis is below 10 %. We choose this non severe threshold because the tests are executed on a relatively small number of points representing measurements that are expected to show large variability.

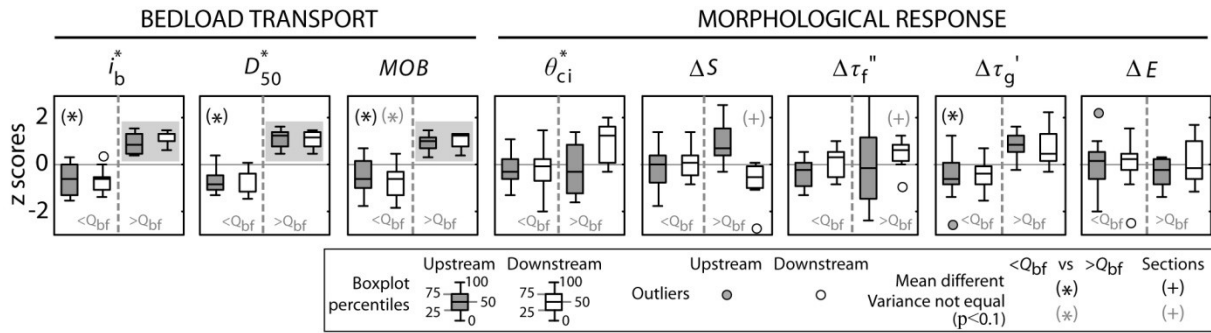


Figure 5.6 Distributions of bedload and morphology response for both sections and separated for floods below and above bankfull discharge. Boxplots over a shaded gray area indicate data that are not used in further analyses because of their inaccuracy due to estimation or incomplete flood record. We show that data only for general information.

### 5.1.4. Results

Figure 5.5 presents the chronological sequence of the thalweg profiles for both sections. The downstream section is remarkably stable throughout the three years and the upstream section is more dynamic showing cycles of aggradation and erosion due mainly to the filling and scouring of one of the two pools found in the section. The difference between the maximum and minimum average bed elevation during the survey period is about 5 cm for both sections. The upstream and downstream sections have degraded on average by 4 and 1 cm respectively from the first to the last morphological survey. Bed slope has ranged between near 0 up to 1.6 % in the upstream section and from 0.7 up to 1.1 in the downstream section. These morphological changes over the three year period were produced by a wide range of flow conditions (Figure 5.4) and associated with a broad spectrum of bedload activity.

In Figure 5.6, we present the split of the flood events in two groups below and above bankfull discharge ( $2.5 \text{ m}^3 \text{s}^{-1}$ ). The bedload rate, transported particle size and bed surface activity for flood above bankfull discharge are not used in our analysis but are shown for general appreciation of process intensity in a qualitative fashion. For these high magnitude floods, bedload rates are estimated through a rating curve (Marquis and Roy, 2012) and the bedload caliber is represented as  $D_{84}$  instead of  $D_{50}$  as the bedload samplers were full before the peak discharge and the  $D_{50}$  would underestimate the size of the transported particles. Figure 5.6 and the ANOVA and variance tests comparing sections and magnitude of floods show that:

1. There is no difference between the mean values for all bedload and morphological response variables between the two sections ( $p < 0.1$ ).
2. Only for floods above the bankfull discharge is there a significant difference ( $p < 0.1$ ) between the mean slope changes between the sections. Bed slope tends to increase in the upstream section and there is a tendency to degradation in the downstream section.
3. The variance of the bed slope change and macroform roughness change are different between the sections, the variability of the downstream section being significantly lower ( $p < 0.1$ ) as was already seen in Figure 5.5.
4. The increase in the bedload response intensity is not matched by a concomitant morphological response, except for the microform roughness changes between flood events below and above the bankfull discharge ( $p < 0.1$ ).

Globally, the differences between the response of the two sections are small even though they have contrasted morphologies and local sediment supplies, the upstream section exhibiting autogenic riffle-pool sequences and the downstream section having a straight thalweg and a small lateral bar serving as a local reservoir of sediments. When estimating the correlation coefficients separately between pairs of variables for each section, some differences arise between the sections (Figure 5.7). In the upstream section, the macroform roughness increases concomitantly with the active bed surface and the size of transported particles. In the downstream section, there is a trend to aggradation as the mobilised bed area increases. Nevertheless, the differences between the sections are small and from this point, analyses will be conducted on the whole data set without distinction between the sections. Indeed, the contrast between the section responses is small compared to the sharp difference between the bedload transport and morphological responses to discharge. As bedload processes become more intense for floods above bankfull discharge, the morphological response remains in the same order of magnitude as for floods below bankfull discharge (Figure 5.6). This offset between bedload and morphological responses is clearly visible from the pairwise correlation coefficients between all variables in Figure 5.7. There is no significant correlation between bedload transport variables and the five morphological response variables when considering both sections as a unique data set.

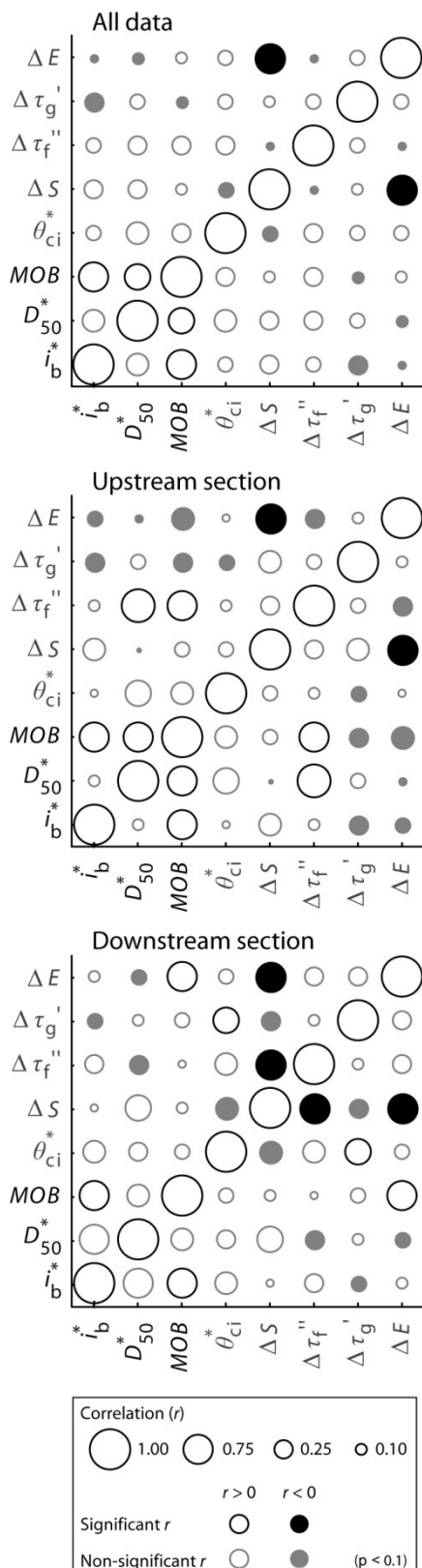


Figure 5.7 Correlation matrices (Pearson's  $r$ ) of bedload (black names) and morphological response (grey names) variables for both sections and for each section separately. Note that only floods below bankfull discharge are used for  $i_b^*$ ,  $D_{50}^*$  and **MOB**.

When examining the relations among the bedload variables, there is a clear correlation between the active bed surface and the bedload flux (Figure 5.7). The size of the transported particles is significantly correlated to the active bed surface but not to the bedload transport rate in the upstream section and is correlated to neither in the downstream section. In the case of the morphological variables, most of the significant correlations are negative (Figure 5.7). For example, in both sections, aggradation occurs simultaneously with a slope decrease and degradation is accompanied by a steeper slope. This is to be expected. In the downstream section, the steepening of the slope occurs also with a decrease of the macroform roughness. Also, a high initial threshold for entrainment favours an increase of the microforms roughness. There is consistency in the response of the variables describing bedload transport and also among the variables describing the morphological response. However, the morphological response is not clearly tied to bedload response in general and to bedload fluxes in particular, as one would expect.

Figure 5.8 shows the distribution of the values of all variables grouped according to the magnitude of each variable. The interactions among variables show a more complex picture than what we have first described from the correlation matrix. Five significant differences among the groups ( $p < 0.1$ ) were detected (in dark shaded gray in Figure 5.8). Among these, the variables that were significantly correlated in Figure 5.7 show the same behavior with the group treatment, except the correlation between transported particle size and bed surface mobility. However, some other significant differences that were not detectable from the linear correlations are detected. These differences are often due to the fact that a single group deviates from the other two, suggesting that a threshold needs to be exceeded in order for a change to occur. For example, only when the bed activity area is higher than the average value do we see that the macroform roughness change is always positive. Macroform roughness can increase with lower bed mobility conditions, but can also remain stable or decrease, thus showing a complex and non linear behavior. The macroform roughness stability occurs under high bedload flux while the greatest changes are seen mostly during lower bedload flux.

Figure 5.9 presents two projections of the variables and the individual data using the first four principal components in the orthogonal space of the PCA. These four principal components respectively explain variances of 27 %, 23 %, 15 % and 13 %, for a total of 78 %. Note that the individual flood events of a given section do not cluster in any of the

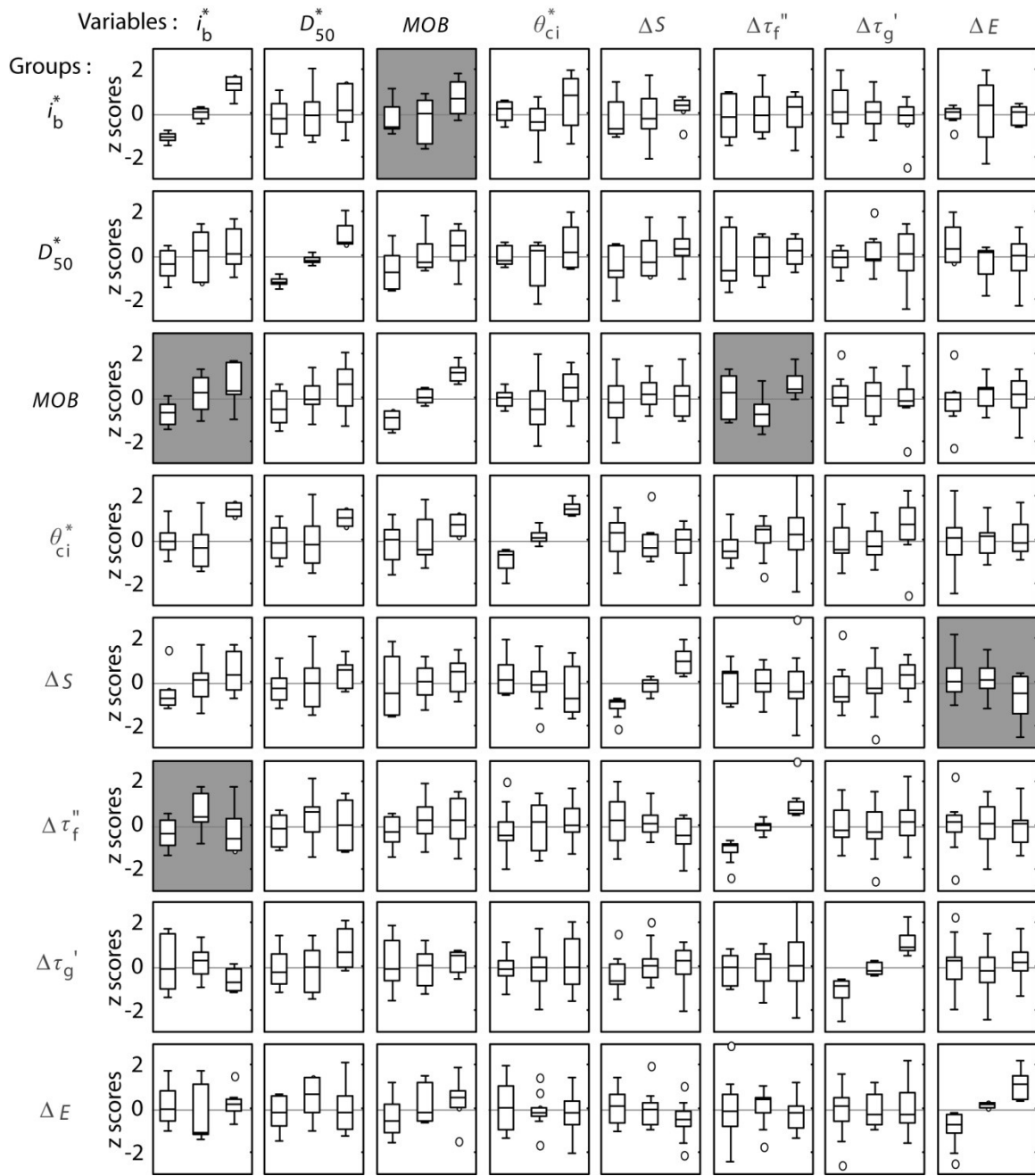


Figure 5.8 Distributions of all variables for groups of low, medium and high values or decrease, stable and increase values of each variable. Group limits were zscores values -0.5 and 0.5 of the normalized (if needed) and standardized distributions of each variable. Each row of subplots represents the grouping of the data points according to the distribution of one variable. Each column of subplots shows the distribution of the variables according to a specific grouping. The subplots in shaded gray highlight that at least one group is different according to an ANOVA test ( $p < 0.1$ ). Note that only floods below bankfull discharge are used for  $i_b^*$ ,  $D_{50}^*$  and MOB ( $n = 22$ ). For the other variables, all floods with sediment transport are used ( $n=36$ ). Bedload variable names are in black and morphological variable names in grey. See Figure 5.6 for boxplot legend.

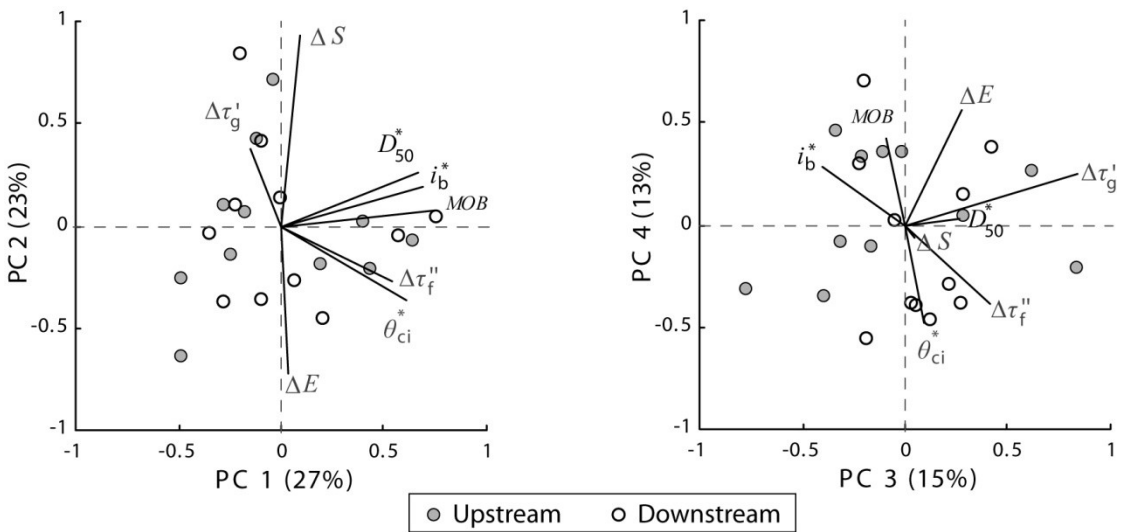


Figure 5.9 Principal component analysis of all bedload (names in black) and morphological response (names in grey) variables for flood events (dots) below bankfull discharge. The first four PCAs represent 78% of the variance of the whole data set and their individual variance exceeds 12.5%, the value of the variance if all axes were equal. All variables were standardized so that the variance was equal to 1 for each variable. Biplots of principal components (PC) 1 to 4 are drawn to see how the variables (arrows) correlate in the orthogonal space of the PCA, as the projection used preserves the correlation between the variables.

biplots. These results confirm that even though both sections have different characteristics, their responses do not exhibit trends associated with site specific conditions. The interactions between the variables is very complex, as it was apprehended from the foregoing analyses. The covariations that were detected in the correlation matrix are still present mainly in the projection of the first and second principal components. However, the projection using the third and fourth principal components reveals interactions between variables that have not been detected by previous analyses. For example, there is a positive correlation between the size of the transported particles and the microform roughness change. Considering all the variables together instead of the individual pairs also reveals new relations as shown by the positive correlation between the threshold for motion and the change in macroform roughness. The two projections also highlight opposite effects. For example, in the projection of the first and second principal components where the threshold for entrainment is positively correlated with bed mobility but negatively correlated in the projection of the third and fourth principal components. Both situations may be relevant for the understanding of fluvial processes.

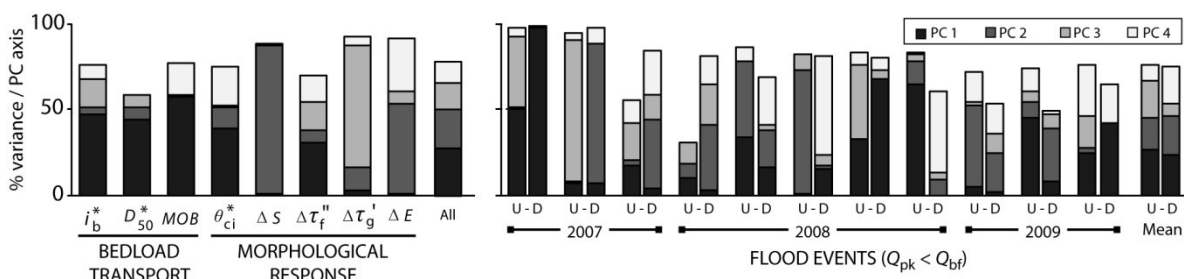


Figure 5.10 Fraction of variance for the first four PCs for each variable and all variables together (left) and for each individual flood event and average for each section (right). As in Figure 10, only flood events below bankfull discharge are used.

The distribution of the variance of each variable per principal component is presented in Figure 5.10. A grouping of variables arises depending on which axis most of their variance is captured. The variance of the bedload rate, particle size, bed mobility and the initial threshold for motion captured by the first principal component is around 50 %, marginal proportions are found on the other axes. The variance of the slope and the bed elevation changes is mainly on the second principal component, illustrating the independence of these variables with respect to the other bedload and morphological variables. All the other variables have a marginal variance on the second principal component. The microform roughness change is the only variable with most of its variance on the third principal component. In the case of the macroform roughness change, its variance is mostly split between the first, third and fourth components, showing a relatively complex response. This variable and the transported particle size have the lowest variance captured on the first four principal components, highlighting very complex responses. Their variance is split on the entire eight axes more or less evenly. Figure 5.10 also shows how the variance of each individual data points is split among the first four principal components. The main result is that all possible scenarios are found. Both sections can show a similar or a very different pattern for a given flood. Also, the variance of some flood events is evenly split on the first four axes while the variance of other events is found predominantly in a single principal component. Finally, the variance of some other events is almost entirely in the first components as others have most of it on the last components. All these observations suggest the complexity of fluvial processes and that almost every flood is unique in terms of bedload and morphological response. But overall, the PCA have shown that the interactions between bedload and morphological responses exist but at a complex level of interactions and feedbacks among the variables.

### 5.1.5. Discussion

Fluvial dynamics have been approached through ‘system sciences’ which seek to provide an explanation by integrating the effects of many elements and processes (Church, 2010). Even though the driving factors are physically based, their juxtaposition at a given place and time, their various temporal and spatial scales, the influence of prior history and the existence of thresholds leading to abrupt changes (Church, 2010) are susceptible to produce a response that is apparently ‘stochastic’ (Chen and Stone, 2008) or dominated by deterministic uncertainty (chaos) (Gomez and Phillips, 1999). The style and magnitude of channel response depend on the superposition of multiple external and internal factors with contrasted variability and a range of frequency distributions (Buffington, 2012). It is generally accepted that bedload transport and morphological changes should be related as these processes occur simultaneously in response to flow. In the introduction, we have reviewed studies that have investigated the complex interactions between sediment transport as bedload and bed morphology. We have concluded that there is no general scheme that allows forecasting the morphological response to a specific magnitude of bedload transport. Geomorphic transport laws are still not capable of predicting quantitatively the morphological changes of the river bed (Dietrich et al., 2003).

In this paper, we have presented a unique data set collected during an intensive flood based field survey of the bedload transport and morphological processes in two sections of a gravel-bed river, Béard Creek. Sediment transport is known to exhibit an apparent noisy behavior that prevents the prediction of behavior of fluvial systems even under steady forcing (Jerolmack, 2011). However, it is possible to understand the complex processes involved in bedload transport and in bed morphology responses to a flood event by using simultaneous measurements of the different processes. The main objective of this paper is to understand the interactions between bedload transport and morphological changes at the scale of the flood event. The data set used here is exhaustive by the standards in fluvial geomorphology, where bedload events are infrequent and difficult to monitor in the field. This rarity of events impinges strongly on our ability to detect significant correlations among the variables. Our analytical scheme was selected to deal with the low number of replicates. We used multiple approaches, pairwise correlations, group analyses and multivariate analyses, in order to explore all possible levels of interactions. The group analysis (Figure 5.8) and the principal component analysis (Figure 5.9) allowed us to detect

correlations among variables that were not detectable using pairwise linear correlations. Our analyses have shown that there is no linear correlation between any aspect of the bedload transport (fluxes, particle sizes, bed area mobilized) and the resulting morphological changes after a flood (initial threshold for motion, elevation, slope, micro and macroform roughness). Therefore, there is no direct or simple relations that can be used to predict the stream bed response based on sediment transport during a flood event or vice-versa. This has important implications for the use of successive morphological surveys as an indicator of bedload processes but also for the understanding of fluvial processes.

We will highlight briefly the advantages of using nontraditional analytical methods for the geomorphology discipline, as it will be more important in the companion paper. As a general appreciation, using these analyses has provided a more refine interpretation of the complex interactions between the processes. For example, in one biplot projection (PC1 and PC2), the initial threshold for motion is positively correlated to bedload processes but negatively in another biplot projection (PC3 and PC4) (Figure 5.9). If a high initial threshold for entrainment is an indicator of a bed surface tight packing, when the armor layer is broken, there is a release of subsurface sediments thus increasing bedload transport. On the other hand, if the flood was not strong enough to break the armor, thus will lead to low bedload transport. It is also anticipated that we observe high bedload transport when the initial threshold for motion is low because sediments are readily available for motion during the flood. In both cases, a high initial threshold for motion leads to an increase in macroform roughness, whether the bedload transport is low or high (Figure 5.8 and Figure 5.9). When the initial threshold for motion is low it is also possible that larger bed surfaces experience balanced quantities of scour and fill leading to limited morphological change. As a result, both the group analysis and the PCA could be used to identify new hypotheses to be tested in controlled laboratory experiments, thus illustrating how the field can inform experimental work.

The use of non-traditional data analysis techniques (Figure 5.8, Figure 5.9 and Figure 5.10) has also revealed complex relationships between morphological and bedload transport variables. The initial threshold for motion, the micro- and macroform roughness are all related in one way or another to the bedload transport processes thus is reasonable as these morphological variables are indicators of the bed structure which is an important factor controlling bedload transport. The topographical variables, slope and elevation

changes, interact strongly together but are not related to any of the bedload processes or bed structure indicators. In gravel-bed streams with an armored layer, the resultant imprint of bedload processes on the topography can be relatively small (Wong and Parker, 2006). This is partly due to a cycle of scour and fill during a flood event, often leading to no change in elevation (Lindsay and Ashmore, 2002). At Béard Creek, this situation occurs over 40 % of the bed surface on average (Marquis and Roy, 2012). Even though the magnitude of the correlation is damped by compensating scour and fill, this should not prevent the detection of a relationship between bedload transport and elevation and slope changes where it exists.

What can the absence of correlation between sediment transport and bed topography reveal about fluvial morphodynamics? The negative correlation between slope and elevation change strongly suggests that bedload transport at Béard Creek is driven by bedload sheet migration. This idea is reinforced by the fact that the active layer is apparently shallow, as shown by the strong correlation between bedload fluxes and bed surface mobility present in all analyses. In a study of ten streams similar to our field site in terms of particle sizes and slope, Devries (2002) found that the active layer depth rarely exceeded  $D_{90}$  and concluded that bedload transport rates in these streams increase primarily with the mobile fraction of the bed surface and grain velocity rather than with the layer thickness. At Béard creek, the river bed response is relatively insensitive to bedload magnitude whether there is partial transport or full transport (i.e. when the entire surface is disrupted) (Figure 5.6). Finally, the median size of transported particles is weakly correlated to the bedload fluxes and bed surface mobility. This is in agreement with the signature associated with the migration of bedload sheets. The occurrence, dimensions and dynamics of bedload sheets are primarily controlled by local sediment supply (Dietrich et al., 1989; Nelson et al., 2009). Bedload sheets result from the interactions between the coarse and fine fractions of the sediments during bedload transport (Dietrich et al., 1989) leading to the formation of periodic patches with contrasting particle sizes (Whiting et al., 1988) as a result of various longitudinal and vertical sediment sorting (Recking et al., 2009). The bed surface grain layer acts as a filter for particle exchange between the subsurface layer and the bedload (Wilcock and Southard, 1989). Therefore, depending on the scale and period of bedload sheets during a flood, the median particle size found in the bedload sampler may vary for a given bedload transport rate.

The results of this study also relate to the flume experiment conducted by Recking et al. (2009) where the passage of bedload sheets coincides with slope variations and cycles of aggradation and scour. Bedload sheets were initiated when the local slope attained a maximum at the end of an aggradation cycle. At this point, an abrupt increase of gravel mobility produced local erosion and transport of finer material. Depending on the phase in the bedload sheet cycle (formation – travel – dismantlement), bedload fluxes measured at the flume outlet varied greatly. Bed slope was measured simultaneously with the migration of the sheets, allowing the authors to relate directly bed topography changes to the bedload transport processes. If we scale up what was measured and observed by Recking et al. (2009), it is reasonable to hypothesize that the resulting elevation and slope changes are due to the immobilization of a bedload sheet when the flow capacity decreases below the motion threshold. Therefore, the observed changes in slope and elevation are mainly due to the last moments of bedload transport and are not the result of the entire bedload volume during the flood. The stream bed topography at the end of the flood does not change according to the total flood bedload transport and there is an offset of temporal scales between bedload transport and stream bed changes. This is supported by the fact that when bed elevation and bedload transport are measured simultaneously, the statistical characteristics of their short term fluctuations are similar (Singh et al., 2009).

Bedload sheets and associated bedload transport pulsations were observed in several field experiments (Whiting et al., 1988; Kuhnle, 1989; Dinehart, 1992; Kuhnle, 1992) but to our knowledge this is the first time a morphological signature has been measured for a sequence of floods. These concomitant measurements have allowed us to highlight the decoupling of measured bedload rates and topographical changes resulting from the passage of the flood. When compared to braided rivers where morphological changes are dynamic and can be related to successive sediment pulses (Hoey and Sutherland, 1991; Goff and Ashmore, 1994), supply-limited streams have a more complex behavior. The range of bedload sheet scales will imprint differently the morphology and further complicate the interpretation of the morphological response to bedload processes. In that perspective, there is a need to measure simultaneously bedload transport and topographical changes during floods in the field in order to understand the characteristic scales of bedload sheets.

### 5.1.6. Conclusion

In this paper we have analyzed in detail interactions between channel changes and bedload transport in response to individual floods. The main conclusion is that bedload intensity during a flood has little bearing on the resultant bed morphology after the flood. The apparent decoupling of bedload processes and the resultant stream bed morphology has been mainly shown through the use of nontraditional data analysis techniques that are better suited for the study of non-linear interactions. Group and multivariate analyses have allowed the interpretation of the interactions to be refined. Indicators of the river bed structures (initial threshold for motion, micro- and macroform roughness) do interact with the bedload processes (fluxes, transported particles size and bed surface activity) but in a complex non-linear manner. The topographical indicators, the changes of bed slope and elevation, are not related to any bedload or bed structure variables. The strong negative correlation between the bed slope and elevation changes strongly suggests that the migration of bedload sheets is the dominant mode of bedload transport at Béard Creek. We hypothesized that the resultant morphology after a flood is mainly the legacy of a single bedload sheet that was travelling through the section while the flood receded. Therefore, it is impossible to relate the average bedload flux of a flood to topographical changes because the processes are not operating on the same time and spatial scales. Bedload sheets can also play a role in the other complex non-linear and, in some cases, weak interactions between bedload transport processes and bed structure indicators. Even though we have collected measurements in a single stream, these results may have general implications for gravel-bed streams with a limited sediment supply coming from the banks and the bed and sharing similar morphological characteristics (i.e. a mild slope, an armor layer and the presence of large-scale morphological features such as pools, riffles and bars). In the second companion paper we will investigate the causal factors underpinning the links between the initial conditions of the bed before the flood, the flow and the stream bed response after a flood. This will provide a complementary view on fluvial processes that emphasizes the role of the historical legacy on river dynamics.

### Acknowledgements

The authors would like to thank Mr. and Ms. Cloutier for allowing access to their land. Martin Lambert and Jean-François Myre were of great support for the design and

construction of the bedload samplers. We are also grateful to Christine Bergeron-Verville, Vincent Cardin-Tremblay, Laurence Chaput-Desrochers, Sylvio Demers, Claude Gibeault, Hélène Lamarre, Olivier Lalonde, Kevin Partington, Mathilde Péloquin-Guay, Mathieu Roy, Katherine Sicotte, Rachel Thériault, Julie Therrien and Michèle Tremblay for their help in the field and in the lab. This research was supported by the Natural Sciences and Engineering Council and the Canadian Foundation for Innovation.

## **CHAPITRE 6. APPROCHE SYSTÉMIQUE : LA RÉPONSE D'UN COURS D'EAU À UN ÉVÈNEMENT DE CRUE**

---

### **6.1. Morphodynamics of gravel-bed rivers. B-The effects of flow, flood history and initial conditions**

#### **6.1.1. Abstract**

In this paper, we examine the factors that can explain the variability of the bedload transport processes and morphological responses of a stream after a flood event as it was reported in the first companion paper. Based on an extensive data set from a small gravel-bed stream (Béard Creek) collected over a three year study we present the interactions and feedbacks related to flow magnitude, flood history (both the low flow history and the bed mobility history) and the initial conditions of the bed (both the initial topography and bed structures). The variables and indicators were analyzed using several techniques including multivariate approaches in order to compare the results with the linear pairwise regression that is widely used in process-form studies. Multivariate analyses are more powerful and detect more interactions than linear regression as they are better designed to handle predictor interactions in the absence of experimental control. We show that the temporal variability of the bed structure and roughness is a key factor in understanding the effect of bedload transport on the morphological evolution of the stream. This highlights the prominent role played by flood history and of initial conditions of the bed sediments organisation to understand the variability of bedload sediment transport and river morphodynamics.

#### **6.1.2. Introduction**

##### **6.1.2.1. General context**

The relation between bedload transport and the morphological response of rivers has been an ongoing research topic in fluvial geomorphology for at least a century (Buffington and Montgomery, 1997). The factors involved in bedload motion have proven numerous and their interactions, complex, preventing researchers from developing a complete general theoretical framework. The fluvial '*trinity*' is a useful conceptual idea to which helps

comprehend fluvial dynamics, even though it has its limitations (Leeder, 1983; Best, 1993). The understanding of how, why and when coarse particles are mobilized in streams in relation to the flow and of the interactions between bedload transport and bed morphology remains a fundamental research objective in the study of gravel-bed rivers. In the companion paper (chapter 5), we have shown that bedload events do not necessarily induce morphological changes that are proportional to their magnitude. Bedload transport and morphological response interact in a complex manner. For instance, indicators of the bed structure such as the micro- and macroform roughness interact in a non-linear fashion with bedload transport processes. On the other hand, topographical changes in bed slope and elevations seem independent of bedload transport processes at the scale of the flood. Indeed, there may be a misfit of scales as the resulting bed topography after a flood is probably not a legacy of the bedload transport during the entire flood but only of the last moments when bedload sheets cease movement. This second paper investigates the potential factors that may further explain bedload transport variability (fluxes, mobilized bed surface and transported particle size) but also the morphological changes linked with bed topography (elevation and slope) and the bed structure (initial threshold for motion, micro- and macroform roughness). These factors are the flow magnitude, the flood hydrograph shape, the morphological initial conditions (bed structure and topography) and the flood history (low-flow history and bed mobility history). The investigation of the role of these factors will rely on the same field data set used in the companion paper.

#### **6.1.2.2. Factors of bedload transport and morphological variability**

Under a fairly constant runoff regime and a stable sediment supply and in the absence of major tectonic influences or of other changes in base level, the direction of change in the morphology should be driven by bedload transport processes. The rate of bedload and associated transported grain sizes in gravel-bed streams typically occur in three distinct phases depending on the magnitude of the force of the flow (e.g. Ashworth and Ferguson, 1989; Warburton, 1992). In phase I and II, transport rates are low as the critical flow for motion is only slightly exceeded, the transport is partial or size selective and thus only the smaller grains are entrained. In phase III, coarser grain fractions are mobilized disrupting the initial bed surface and exposing underlying grains, thus increasing greatly bedload transport rates compared to those in phases I and II. In this third phase, transport may be characterized by equimobility, where larger particles have the same probability of

movement as finer grains and on rare occasions full mobility may be achieved. The threshold where phase III transport occurs is not clearly defined and it may vary from stream to stream but it is likely to occur at flows close to or exceeding the bankfull discharge (e.g. Parker et al., 1982b). The mobilization of each grain size fraction occurs over a range of flow strengths but the coarser fractions are transported at rates that are several orders of magnitude less than those of finer fractions (Wilcock and Mcardell, 1993; 1997). Consequently, the size distribution of the bedload is often reported as being finer than that of the surface bed material (e.g. Ashworth et al., 1992; Lisle, 1995; Wathen et al., 1995). As flow strength increases, the bedload grain size distribution should converge toward that of the surface bed material (Wilcock, 1992).

Bedload transport in gravel-bed rivers is highly variable both in time and space (e.g. Gomez, 1991). It is also driven by geomorphic thresholds that occur at multiple temporal and spatial scales (Church, 2002). Many studies have focused on relations between sediment transport rate and hydraulic variables such as discharge or stream power but some studies have reported that transport rates in gravel-bed rivers are not only a function of flow strength but are modulated by the sediment availability (e.g. Hoey, 1992; Nicholas et al., 1995; Cui et al., 2003). For example, in a study of the morphodynamics of a gravel-bed river Lane et al. (1996) have found that erosion increased with discharge but only in the absence of sediment supply. Therefore, bedload transport rates for a specific reach are dependent on the balance between the stream capacity to transport material and the availability of new material to the channel. Once the coarse material is delivered from hillslopes or banks to the stream, particles are entrained as bedload if the critical shear stress is exceeded and are deposited once the shear stress drops below the mobilization threshold. The material will rest on the bed until the critical shear stress is exceeded again. Thus, depending on the delivery of coarse material and on the characteristics of the stream that determine its transport capacity, characteristic morphological features develop on the bed (Montgomery and Buffington, 1997). These features will be maintained or modified according to the patterns of bedload transport. In many gravel-bed rivers, the sediment supply is insufficient to meet the transport capacity of the stream. This situation usually leads to a riffle-pool or bar-pool morphology when the reach has a moderate to low slope. These morphological features tend to be fairly stable as the whole range of particle sizes is rarely mobilized during a flood. The low sediment supply also leads to the formation of an

armor layer (Dietrich et al., 1989). This coarser surface layer complicates the interactions between bedload transport and bed morphology by protecting the underlying finer sediments from entrainment. The armor layer also interacts with micro and macroform roughness elements that strengthen the bed structure and thus decreases bedload transport rates (Robert, 1990). For example, the evolution through time or space of the microform roughness elements such as pebble clusters modifies bedload rates by dissipating large portions of the total flow shear stress (Hassan and Church, 2000).

In addition to the inherent complexity of linking the physical forces of the flow with the mobility of particles in the context of a specific sediment supply, several other factors that influence the structure of the bed may explain the natural variability of bedload. For example, the shape and duration of the hydrograph affect bedload transport rates, the size of the transported sediment and the structure of the bed (e.g. Powell et al., 2001; Sear, 2003; Hassan et al., 2006). Hassan et al. (2006) found that a long lasting symmetrical hydrograph like those associated with a snowmelt period produces greater armoring ratios and a stronger vertical sorting of sediments than asymmetrical hydrographs typical of flash floods. Long hydrograph falling limb winnows the bed armor layer which tends to decrease the size of the particles moving as bedload. Also, a long duration of the flood enhances the possibility of connecting upstream sediment sources and thus of increasing the bedload rates locally (Hassan and Church, 2001). The sequence and timing of bed mobilization events is also important in determining the local sediment supply and the bed structure. For example, long periods of inactivity strengthen the bed surface to the point that bedload transport requires a very high shear stress and is mostly occurring on the falling limb of the hydrograph (Reid et al., 1985). The high shear stress necessary to move the particles due to a prolonged low flow period is not observed in a stream with high fine sediment stores (Sear, 2003). On the other hand, a few researchers have observed the buildup of readily available fine sediments during low flows thus increasing bedload transport rates of the subsequent flood (e.g. Moog and Whiting, 1998; Monteith and Pender, 2005; Haynes and Pender, 2007).

The shear stress history applied to the bed, in terms of magnitude and duration, is also important for the bed stability. In a flume experiment, Monteith and Pender (2005) found that a long flow duration with a low shear stress increases bed stability and decreases the total bedload rate that is subsequently entrained. In contrast, a period with shear stress

near the entrainment threshold decreases bed stability. The increase of bedload entrainment after a high magnitude flood was also observed on gravel bars in the field (Konrad et al., 2002). In general, increasing the duration of a high shear stress flow will cause the particles to rearrange in a tighter and thus more stable river bed (Haynes and Pender, 2007). This phenomenon was also observed for a sand bed flume experiment (Paphitis and Collins, 2005). This adverse effect of the antecedent flow conditions illustrates the complexity of the processes involved in bedload transport and in the consequent morphological response of the bed. The combined effects of the flood hydrograph shape and of the antecedent flow conditions also influence the quantity and spatial distribution of the fine sediments on the river bed (Frostick et al., 1984). The presence of sand size particles during bedload tends to increase the rates of gravel transport (Wilcock et al., 2001).

These interactions between flow strength, sediment supply, flood hydrograph and antecedent flow conditions influence both bedload transport and the size of mobilized particles, the bed structure and composition and ultimately the bed morphology. Carling and Reader (1982) have argued that a better knowledge of the gravel bed composition and morphology should eventually contribute to an improved understanding of sediment transport. Even though this statement is reasonable, it is difficult to substantiate because of the complexity of the relations that are often non linear and threshold driven and also because it is often not possible to discriminate the effects of the various factors and to quantify their respective role. Bed adjustments to floods have been widely investigated but studies rarely lead to similar conclusions depending on the stream characteristics and on the temporal and spatial scales (Buffington, 2012). Even when similar scales of analysis are considered, results from different studies do not converge. For example, Haschenburger (2006) found that in most locations there is an imbalance in scour and fill that leads to adjustments in bed elevations, and that these imbalances increase with flow. But not all areas of the bed experienced deformation during all competent flows (Wilcock and Mcardell, 1997). The flow and sediment transport may not produce a clear morphological response due to local factors that strengthen the bed (e.g. Church et al., 1998) or to a very thin active layer (e.g. Devries, 2002). Such divergent bed morphology responses compared to the bedload transport magnitude have been reported in the companion paper (chapter 5) and the possible causal factors will now be investigated.

### 6.1.2.3. Objectives

Studies covering all aspects of the fluvial ‘*trinity*’ are rare because of the complexity of measuring simultaneously multiple aspects of river dynamics (Powell et al., 2001). In this context, this paper will explore the interactions and feedback between bedload, morphology and the flow from a holistic point of view. It will consider interactions associated with the initial morphological conditions at the onset of a flood (bed structure and topography), the flow magnitude, the hydrograph shape and the history of the bed mobility and low flow period. Inspecting the feedbacks between all processes will deepen our understanding of the interactions between bedload transport and bed morphology. The literature shows the complexity of these interactions, their non linear behavior and sometimes their threshold driven nature, especially in a natural context. Therefore, an underlying objective of this paper is to bring forward the usefulness of using alternative quantitative analyses that are more powerful in the absence of experimental control to study non-linear behaviors. These alternative approaches contrast with linear regression models that are widely used in the search of causal relations between variables in fluvial geomorphology.

## 6.1.3. Methods

### 6.1.3.1. Field site and data collection

In this section, we summarize key information on the field site and data collection. More details can be found in the companion article (chapter 5). The data set was collected at Béard Creek (Quebec, Canada), a gravel-bed river with a riffle-pool morphology with occasional lateral bars (Figure 6.1). Bankfull width, depth and discharge are respectively 6 m, 0.7 m and  $2.5 \text{ m}^3\text{s}^{-1}$ . The longitudinal profile evolution of the thalweg during the study period (three years) varies locally but is fairly stable on the whole as the slope is stable and the bed elevations vary by a few millimetres per year (Figure 6.1). Two sections of 20 m long were intensively surveyed between October 2007 and December 2009. The upstream section is characterized by two riffle-pool sequences without lateral storage associated with sediments in bars and the  $D_{50}$  of the bed surface is 50 mm. The downstream section is a straight reach with a lateral bar and the  $D_{50}$  of the bed surface is 43 mm. The armor ratio of the gravel size particles is around 2.2 on bars, 2.0 in pools and 1.7 in riffles. Each section is

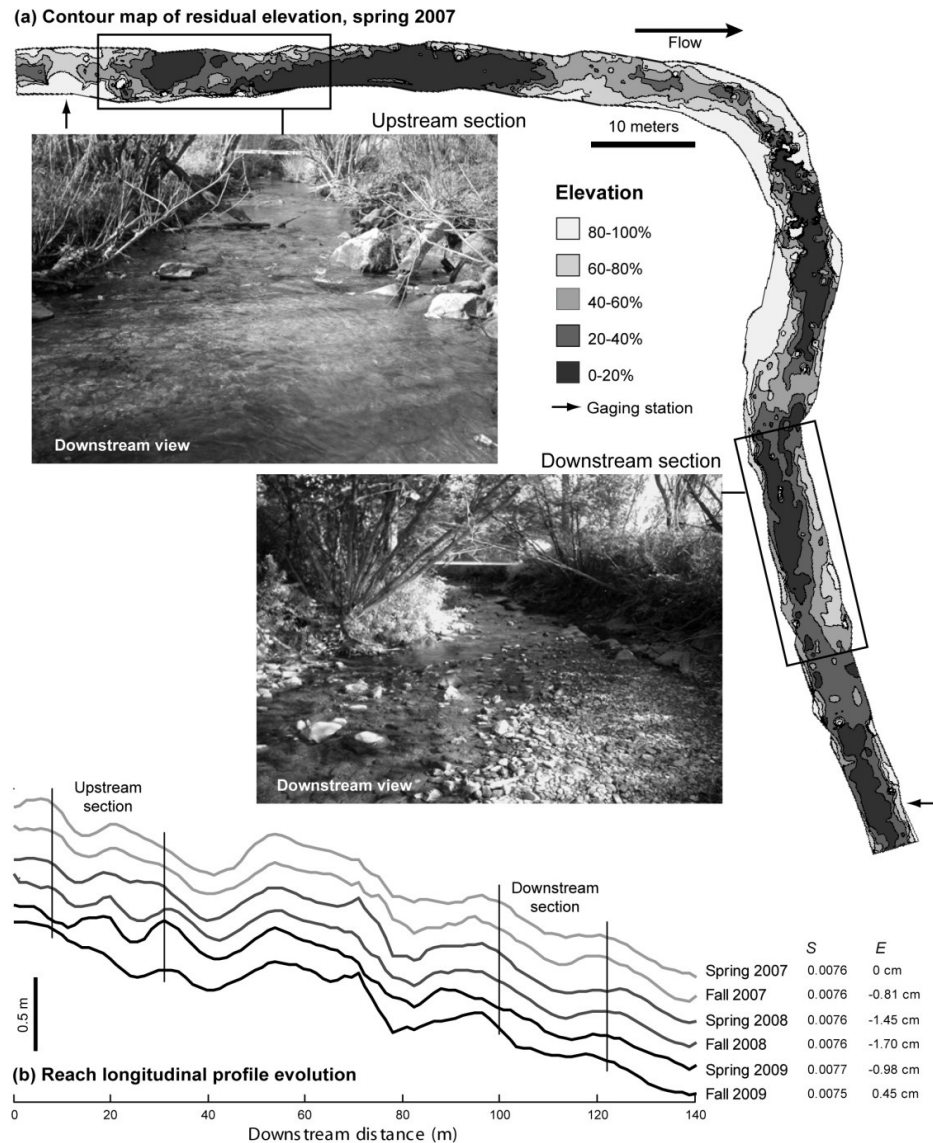


Figure 6.1 (a) Field site morphology and study sections picture (interpolated detrended elevations range is 1.15 m). (b) Longitudinal profile evolution during the study period.

equipped with Birkbeck bedload pit samplers (two upstream and one downstream) implemented with load cells in order to measure real time bedload in the stream. After every bedload event, the bedload samplers were emptied and 25 % of the sediments were sieved at half phi intervals. The morphology was surveyed using a total station in order to obtain successive digital elevation models (DEMs) of the river bed and to quantify the morphological evolution. The area of the bed that was mobilised was estimated through a grid of 80 bed tags per section following the method described by Konrad et al. (2002). After a flood, if the tags were not found, the bed area of approximately one square meter

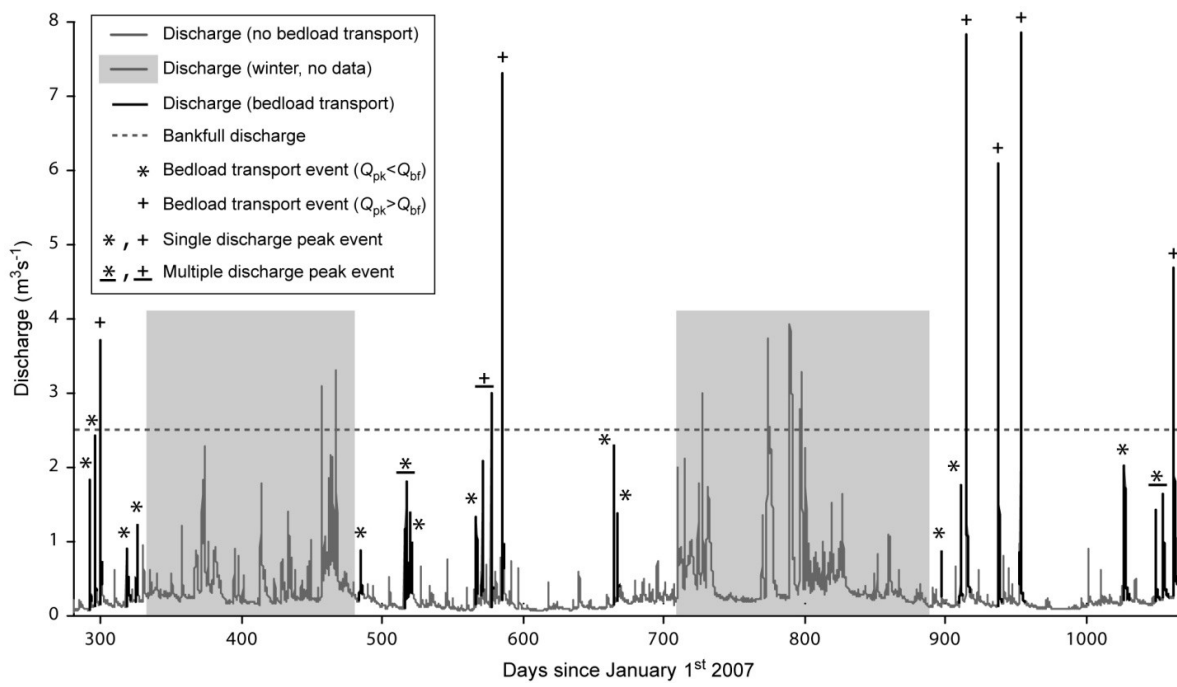


Figure 6.2 Discharge time series during the study period and identification of bedload transport events.

around the tag was recorded as active. This method has proven to be valuable especially in conjunction of the successive morphological surveys to detect the areas where scour compensates fill, which are on average 40 % of the mobilised areas at Béard Creek (Marquis and Roy, 2012). The water level was recorded at two gauging stations in order to estimate the water surface slope and discharge (Figure 6.1).

The data set consists of 21 rain triggered bedload events over three years with a peak discharge reaching  $8 \text{ m}^3 \text{s}^{-1}$  (Figure 6.2). In this paper, like in its companion, the first flood of each year is not analysed because the initial conditions are unknown as no bedload and morphological data were surveyed during the winter. This leaves 18 bedload events to analyse. Three of these events were in effect multiple events as the time interval separating the flood peaks was too short to survey the bed and to retrieve the sediment samplers (Figure 6.2). The events when the peak discharge ( $Q_{pk}$ ) exceeded the bankfull discharge are not considered for the analysis of bedload processes (fluxes and particle sizes) because the bedload samplers were full before the end of the flood, sometimes before the event peak. In the same fashion, the bed surface activity is not analysed for floods above bankfull discharge because all values are similar at around 90 %. These decisions were taken

because our goal was to analyse measured rather than estimated data. The sequence of flood events is interesting by its range of magnitude, duration and timing (Figure 6.2).

### 6.1.3.2. Bedload, morphological and explanatory variables pre-processing

In the companion paper, we explained in details the choice and estimation of three bedload transport (rate, size of mobilized particles and proportion of the bed surface mobilized) and five morphological response variables that indicate the changes resulting from the flood (bed elevation and slope changes, micro and macroform roughness and initial threshold for motion). Their distribution characteristics are shown in Table 5.1. The variables used to explain these response variables are listed in Table 6.1 and were chosen in order to cover as much as possible factors that can influence bedload transport and morphological response of the stream in the context of our measurements. We also kept these estimates as raw as possible with few transformations in order to interpret the results as straightforward as possible. For example, for the indicator of flow magnitude, we chose the dimensionless peak discharge ( $Q_{pk}/Q_{bf}$ ) instead of more complex estimates such as the section shear stress that requires an energy slope estimate. The indicator of the hydrograph shape is the proportion of the runoff on the falling limb ( $Rn_{falling}$ ) which allows for a simple estimate of the flashiness of the flood. The history of the preceding low flow period is simply the number of days since the last time the bed was mobilised (*PF-Days*). This variable partly reflects the packing of the bed particles as long low flow periods can strengthen the armor layer as observed by Reid et al. (1985). But the duration between two flood events can also be an indicator of the availability of sand within the bed. During long periods of low flows, we observed that sand tended to accumulate in patches between clasts on the river bed. Therefore, when a flood occurs after a long period of low flows, the sand is rapidly entrained while the gravel particles forming the bed surface may not be moved.

The initial morphological condition indicators are the thalweg slope ( $S$ ), the macroform roughness ( $\tau_f''$ ) and the microform roughness ( $\tau_g'$ ). The latter two variables are divided by the section  $D_{50}$  to remove the length dimension. These variables are the topographical and bed structure parameters most susceptible to influence the bedload and morphological responses. A detailed explanation of their computation from the DEMs is given in the companion article (chapter 5). The last two explanatory variables are indicators

Table 6.1 Flow magnitude, hydrograph shape, morphological initial conditions and antecedent flow history explanatory variables.

	n	Mean	Std. dev.	Min	Max	Skewness	$\lambda$
Dimensionless peak discharge $Q_{pk}/Q_{bf}$	36	1.30	0.96	0.33	3.19	0.96	-3.47
Proportion of runoff on the falling limb $Rn_{falling}(\%)$	36	80	13	51	93	-0.95	-0.48
Days since previous flood PF-Days	36	17	23	0	76	1.57	0.13
Initial slope $S(\%)$	36	0.81	0.36	-0.06	1.61	0.23	
Dimensionless Initial macroform roughness $\tau_f''$	36	2.97	0.90	1.62	4.74	0.55	
Dimensionless Initial microform roughness $\tau_g'$	36	0.80	0.18	0.51	1.17	0.19	
Dimensionless previous flood bed elevation change PF- $\Delta E$	36	-0.03	0.29	-0.76	0.62	-0.21	
Previous flood active bed area PF-MOB (%)	36	60	26	14	100	-0.19	

of the last bedload events in order to account for the bed mobility history. Previous flood bed elevation change (PF- $\Delta E$ ) was estimated from the DEMs (see companion article). A dimensionless value was obtained by dividing by the section  $D_{50}$ . The previous flood bed mobility area (PF-MOB) was estimated from the bed tags survey as a simple percentage. Note that the section  $D_{50}$  was used to standardize the calculations of the micro and macroform roughness, bed elevation change, bedload transport rate, bedload  $D_{50}$  and initial threshold for motion to allow for the simultaneous analysis of the data from the two sections as bed material size differed slightly.

#### 6.1.3.3. Quantitative analyses

Because of the physical processes involved in sediment transport, least square linear (or pseudo linear) regression is often used to investigate relationships, for example between the flow magnitude and bedload transport rate using data measured in the field. However, it is difficult to detect interactions and effects of other variables without using a more complex analytical approach. Here, we will compare the results of four different quantitative analyses. Linear regressions were performed between all pairs of response and explanatory variables to detect trends and associations between the variables. Also, multiple regression analysis was performed for each of the bedload and morphological response variables in order to identify the interactions among the explanatory variables. In multiple regression analysis, the regression coefficients (slope) represent the unique contribution of the predictor variables when using standardized values. Using variance

partitioning, it is possible to assess the relative importance of each predictor by estimating the proportion of variance explained by each predictor from a series of partial regressions (Legendre and Legendre, 1998). If interactions between the predictors are strong, the unique contributions per variable will be low while the overall coefficient of determination of the multiple regression may be high. In this case, it is not possible to interpret the importance of each variable but it still gives insight into the complex interactions between the variables.

We used two other analyses: the linear discriminant analysis and the classification tree modelling. These techniques are probably better suited for our purpose given the nature of the data set. These techniques are designed to analyse groups so we split each response variable into groups of low, intermediate and high values in order to analyse the direction of change of stream response but not necessarily its magnitude. For the bedload rate, the size of the transported particles, the percentage of bed surface that was mobile and the initial threshold for motion, we used the -0.5 and 0.5  $z$  scores to create the low-medium-high value groups. The same  $z$  scores were also used to create the decrease-stable-increase groups of the slope, microform roughness, macroform roughness and bed elevation changes. See the companion paper for more information on the grouping and on the distribution of the values of the response variables in the groups.

Discriminant analysis is a multivariate regression technique which maximises the distance between known groups of objects in a reduced space consisting of a number of functions ( $n$  groups-1) that combine the variables. It assumes that relations between the variables and the groups are linear so we used the normalized and standardized values of the variables in the analysis. Each function maximises the distinction between the maximum number of groups. The objects can be represented in the reduced space using the functions as axes and the correlations of the variables to the functions can be represented as vectors. It is also possible to evaluate which variables have more weight depending of their coefficient magnitude in the classification of the events. An *a posteriori* classification is performed using the discriminant functions as decisional criteria to classify the objects, a value akin to the coefficient of determination in regression analysis.

The classification tree is a non parametric method that can detect both linear and non linear relations (even threshold-like relations) between groups and variables. They are used to predict group membership of objects from their measurements on one or more

predictor variables. The main difference between a classification tree approach and linear discriminant analysis is its hierarchical nature and its ability to detect triggering thresholds. There is no need to normalize or standardize the values for this analysis. At each level or node, a recursive search finds the predictor that splits the groups into the two most dissimilar subsets. A classification tree was built for each response variable and an *a posteriori* classification ratio to evaluate the validity of the tree can be calculated using the sequence of decision rules. The number of events was too small to use an extensive cross-validation procedure leaving out a subgroup of the data set to validate the structure of the tree but we limited the algorithm by stopping at a splitting of node with two objects. Classification trees are very flexible and the objects belonging to the same group can be split on two different terminal nodes. In terms of fluvial processes, this means that a classification tree can reveal two different sets of conditions that lead to the same result.

Finally, in order to seek meaningful general factors for the stream response as a whole, we ran a k-means clustering to simplify the data set into characteristic groups. This iterative partitioning minimizes the sum, over all clusters, of the within-cluster variance compared to the between cluster variance. Four clusters were created with the eight response variables when only considering the flood events with a peak discharge lower than the bankfull discharge. This analysis is in line with the principal component analysis of the stream response that was described in the companion paper where we have shown that flood event response was split varidly between the eight response variables. It is therefore sensible to find which ones are more alike and if a general pattern of factors has led to these results. The characteristics of the four groups are quite distinct. In effect, an analysis of variance has revealed that for all variables except the change of bed elevation, there is at least one different group mean ( $p < 0.1$ ). Using the k-means cluster method, we performed a discriminant analysis and a classification tree analysis in an attempt to find general processes occurring in fluvial dynamics.

To validate the results of both the discriminant analyses and the classification trees, we used the leave-one-out cross-validation procedure. This procedure is better suited for the relatively small size of the data set used here. It involves using a single observation from the original sample as the validation data, and the remaining observations as the training data. This is repeated such that each observation in the sample is used once as the validation data. A classification ratio can then be estimated for the whole data set. For the

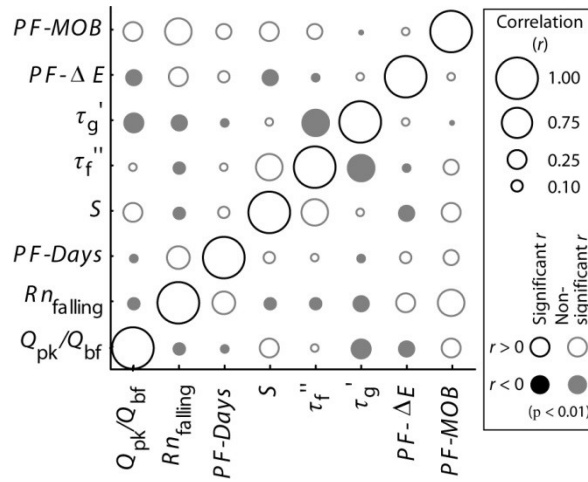


Figure 6.3 Correlation matrix (Pearson's  $r$ ) of explanatory variables.

regression analysis, F-tests were performed and the relationships are considered significant when  $p < 0.1$ . We choose a less severe criterion as the data set is relatively small and therefore a relationship must be relatively strong to be found significant.

As most statistical analyses require variables with normal distributions, we performed a Lilliefors test for normality. When the null hypothesis that the sample values were not from a normal distribution was rejected ( $p < 0.1$ ), we performed a Box-Cox transformation that searches for the exponent  $\lambda$  that, once applied to the data, approximates the most a normal distribution :

$$data(\lambda) = (data^\lambda - 1)/\lambda \quad \text{Equation 6.1}$$

The values of the exponents are in Table 5.1 and Table 6.1 for the variables that were not normally distributed. All variables were subsequently standardized for an easier comparison in figures and also for the requirements of most of the quantitative analyses. Another prerequisite of many quantitative analyses is the independence of the explanatory variables. Figure 6.3 shows that there is no significant correlation ( $p < 0.01$ ) between any of the variables. The use of a severe probability threshold in that case is justified by the need to use independent factors/variables in a multiple regression. This independence between all chosen variables confirms their validity as indicators of different factors that can influence the bedload sediment transport and the morphological response independently.

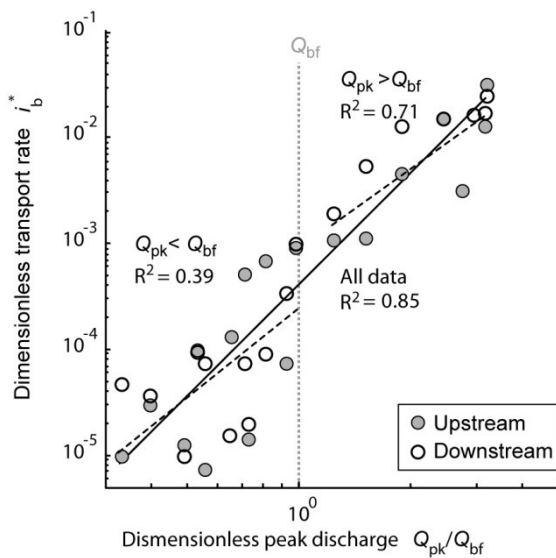


Figure 6.4 Average dimensionless bedload transport rate as a function of the dimensionless flood peak discharge. Note that  $i_b^*$  for floods above bankfull is partly estimated; see Marquis and Roy (2012) for further details.

## 6.1.4. Results

### 6.1.4.1. Data set description

The relation between the average bedload transport rate and peak discharge during the flood is shown in Figure 6.4. As expected, the relation between the variables takes the form of a power function with a scatter covering about one order of magnitude. This type of scatter is sometimes considered to be stochastic (Chen and Stone, 2008) but the goal of this paper is to explore the other possible factors that could explain the variability of bedload transport and the concomitant morphological response for a given discharge. Figure 6.5 illustrates the distribution of all variables for each section and floods above and below bankfull discharge. The data are separated in this way for a visual appraisal of the effect of discharge given that the bankfull stage is approximately the threshold between partial transport and full mobility. Using two-way ANOVA, we identified significant differences between the sections and/or between discharge magnitudes ( $p < 0.1$ ). We also tested for the equality of variance to see if the variability of the variables differed even though they can have the same mean ( $p < 0.1$ ). Note that bedload fluxes, the proportion of the bed surface being mobilized and transported particle sizes are shown for floods above bankfull discharge for information only and will not be further analysed as the bedload

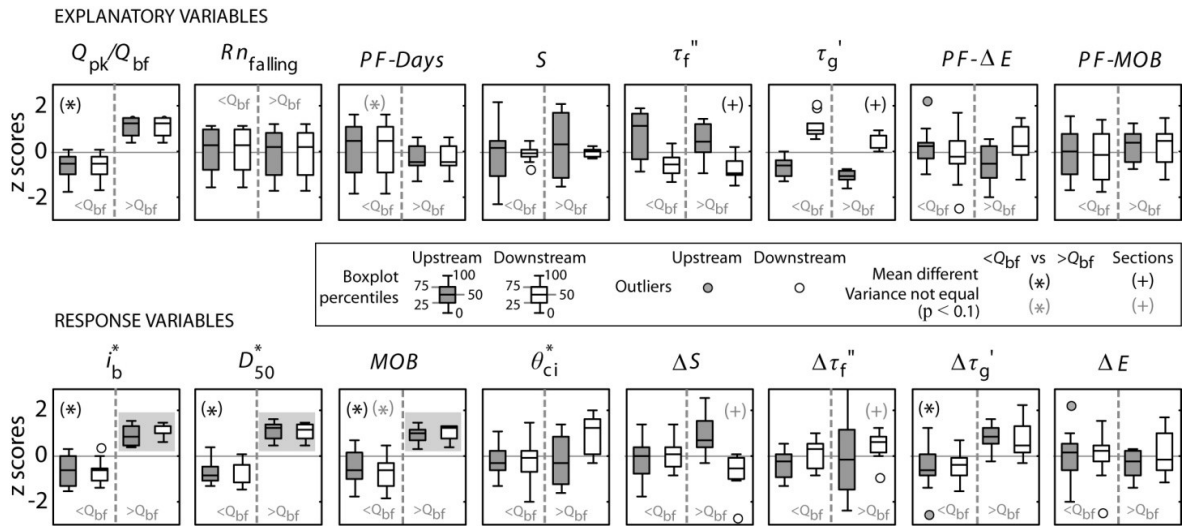


Figure 6.5 Distributions of flow, flood history, initial conditions, bedload and morphology responses for both sections and separated for floods below and above the bankfull discharge. Note that  $i_b^*$ ,  $D_{50}^*$ ,  $MOB$  of floods above bankfull (boxplots over shaded gray area) will not be further analysed as the recorded data were incomplete.

sampling record is incomplete. The downstream section has a low macroform roughness but a high microform roughness compared with the upstream section. Also, the upstream section has a wider range of initial bed slopes compared with the downstream section that has a very stable bed slope during the study period.

Even though the initial conditions are different, the bedload and morphological responses show little variation between the two sections as described in the companion paper. The sensitivity to flood magnitude is marked for the bedload response and is more subtle for the morphological response. The variance of the slope and macroform roughness changes is greater for the upstream section for large floods. The microform roughness tends to increase for large flood events but bed elevation changes are in the same range than the values for both flood magnitudes. Overall, there is no great difference between the two sections in terms of bedload transport and morphological response. This suggests that the data from both sections can be analysed as a single data set.

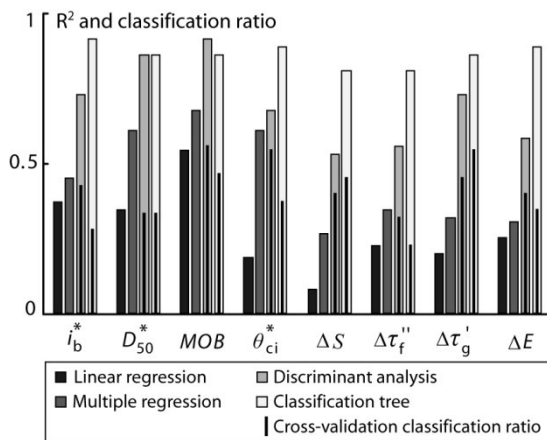


Figure 6.6 Explained variance or classification ratio for each of the four quantitative analyses applied to each response variable. Note that for the linear regression, the  $r^2$  of the variable explaining the highest proportion of variance was chosen.

#### 6.1.4.2. Comparisons of the results among the different analytical schemes

Figure 6.6 compares the performance of the linear and multiple regressions (Figure 6.7), of the discriminant analyses (Figure 6.8) and of the classification trees (Figure 6.9). The lowest explained variance for all response variables comes from the linear regression analysis. The explained variance increases when taking into account all explanatory variables in the multiple regressions. The *a posteriori* classification of the discriminant analysis is above 50 % for all variables, and above 75 % for the bedload response variables. The *a posteriori* classification from the tree models is equal or better than that of the discriminant analysis for all variables, with values ranging between 80 and 90 % of well classified objects. The cross-validation classification ratios are not as high but are most of the time in the same order of magnitude or higher than the explained variance by the multiple regressions. The proportion of the bed that was mobilised by the flood, the initial threshold for entrainment and the microform roughness changes show the highest proportion of explained variance with cross-validation ratios above 50 %. In general, the bedload response variables are better explained by all four types of analysis than the morphological response variables. This demonstrates that including all variables and using more flexible quantitative analyses provide a stronger statistical explanation of the variability of the stream response to a flood. But, are these analyses improving our understanding of river morphodynamics?

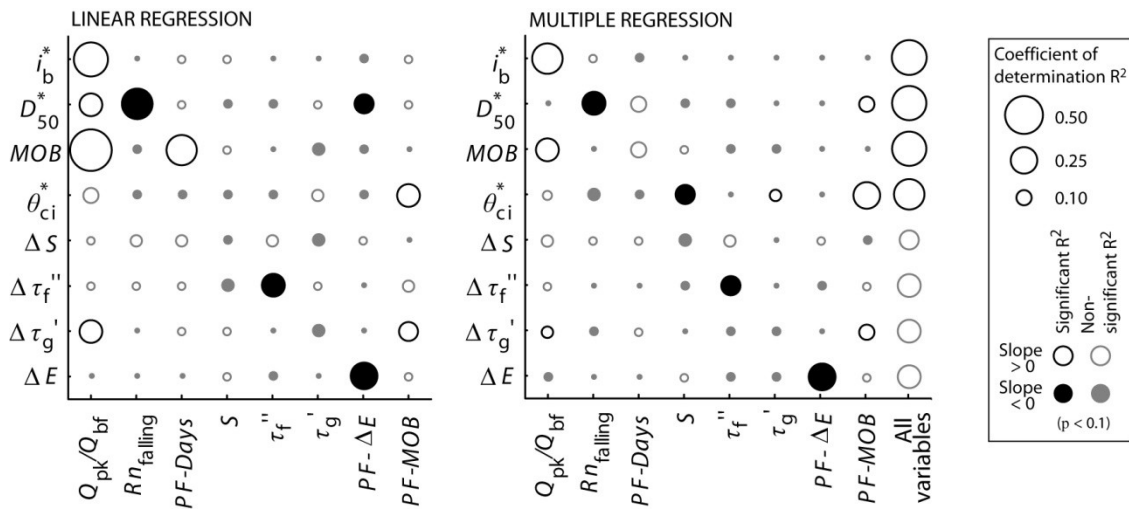


Figure 6.7 Proportion of variance explained for the linear and multiple regressions between all explanatory variables and all response variables. Variance partitioning of the unique contribution per explanatory variable and total variance explained by the multiple regression for each response variables. Note that only floods below the bankfull discharge are used for  $i_b^*$ ,  $D_{50}^*$  and MOB.

We will now examine the results obtained in a comparative mode to highlight what can be learned from each type of quantitative analysis and also to appraise whether there is some convergence among the different results. Table 6.2 presents the signs of the statistically significant relations between the response and explanatory variables. For linear and multiple regressions, the coefficients were tested using a F-test ( $p < 0.1$ ). In the discriminant analysis, we retained only the variables with standardized coefficients larger than 0.5 and for the classification trees, the variables that were used to build the splitting rules. From Table 6.2, we can draw some observations concerning the merits of each method and their potential for understanding river dynamics:

- (1) Linear regressions and multiple regressions are the techniques that detect the fewest statistically significant relationships amongst the variables (Figure 6.7). Multiple regression has the advantage over linear regression of taking into account interactions between the predictors in its calculations. A relationship detected using linear regression might not be as strong in the multiple regression which consider other factors. For example, bed mobility is positively related to the number of days since the last bedload event using pairwise linear regression. But, taking into account all the other explanatory variables in the

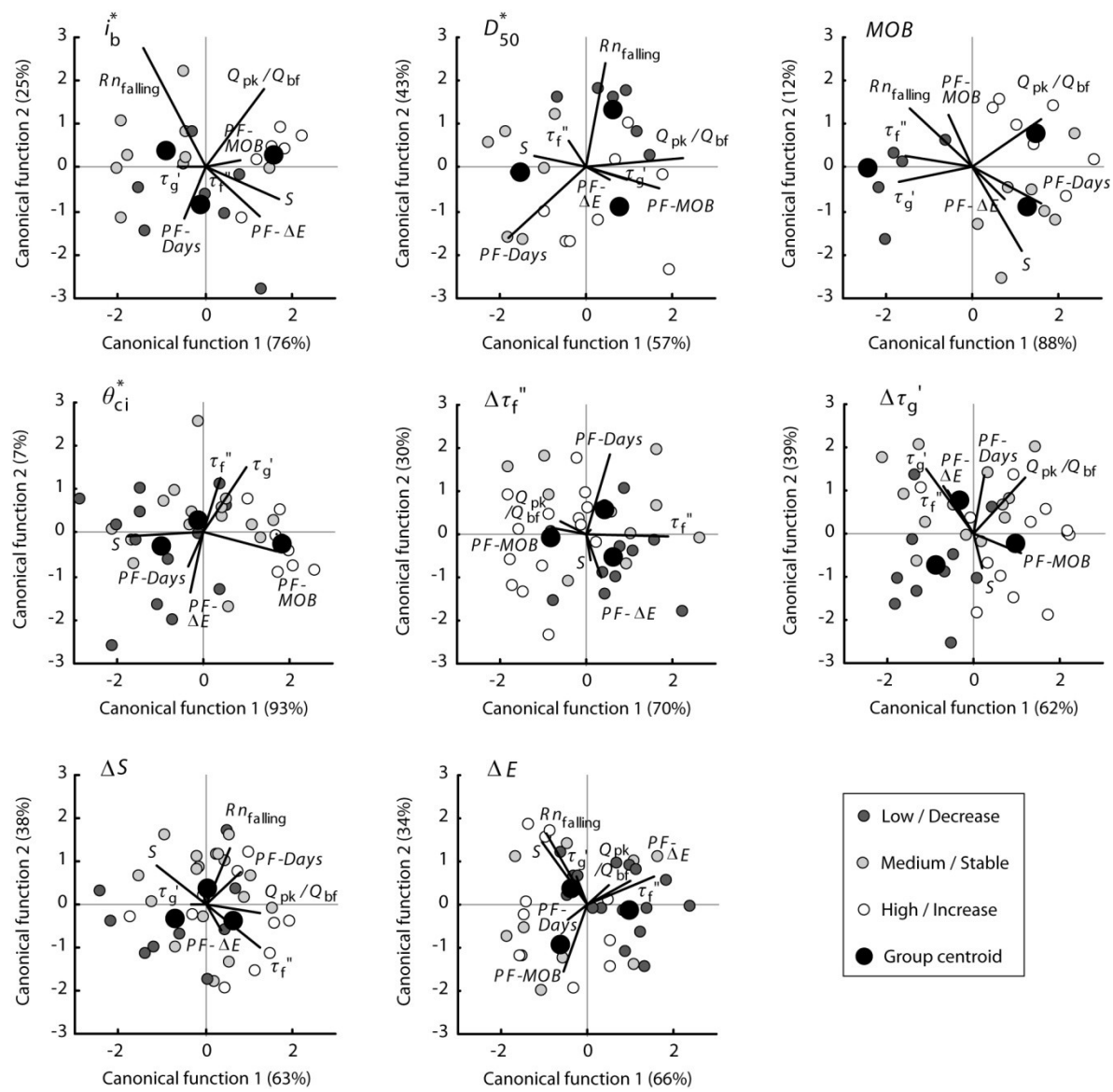


Figure 6.8 Discriminant analysis of the groups of low, medium and high values or decrease, stable and increase values of each response variable. Group limits were zscores values -0.5 and 0.5 of the normalized (if needed) and standardized distributions of each variable. Note that only floods below the bankfull discharge are used for  $i_b^*$ ,  $D_{50}^*$  and  $MOB$ . Note that when the coefficients of a variable were near zero, the variable is not represented.

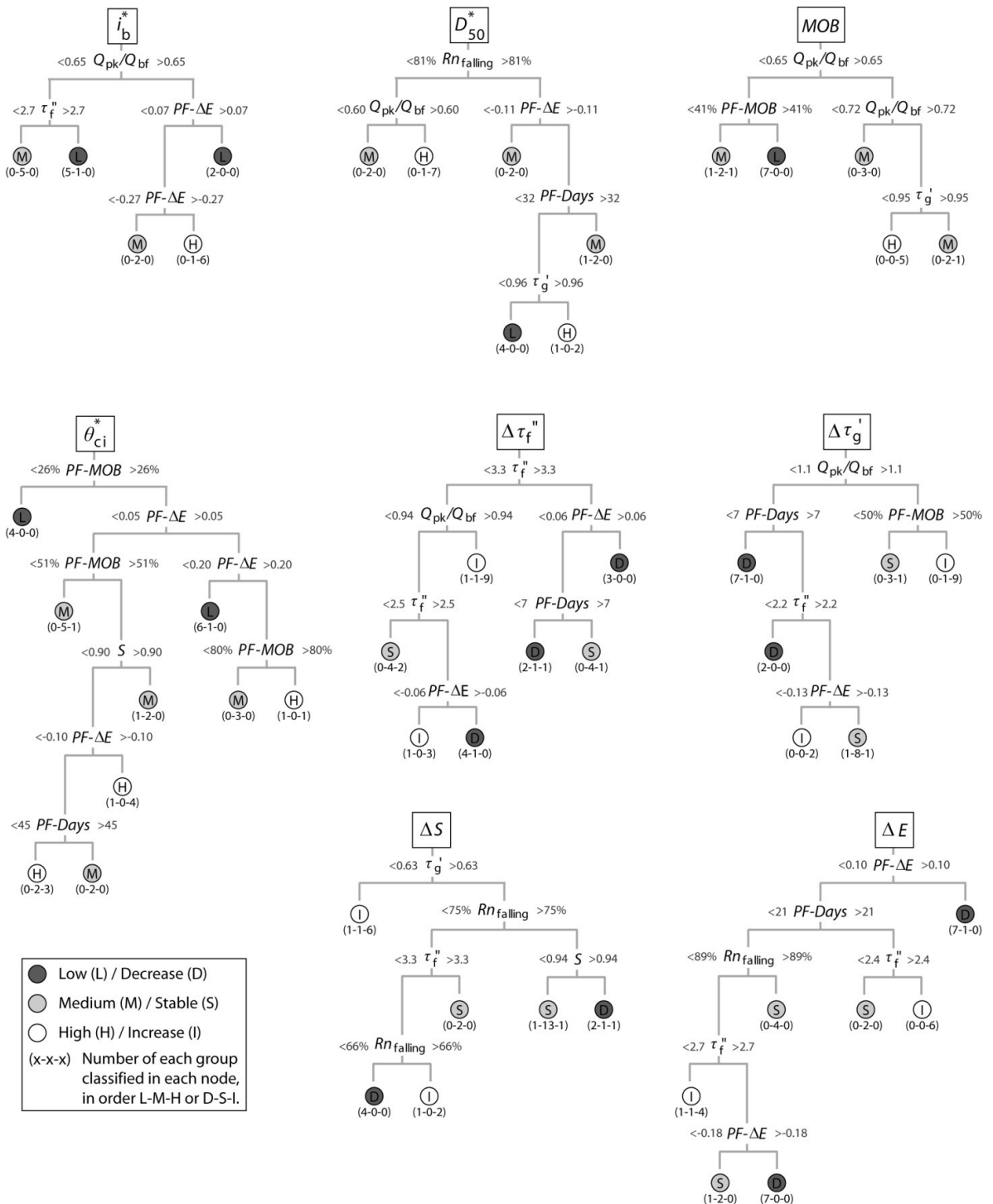


Figure 6.9 Classification trees of the groups of low, medium and high values or decrease, stable and increase values of each response variable. Group limits were zscores values -0.5 and 0.5 of the normalized (if needed) and standardized distributions of each variable. Note that only floods below the bankfull discharge are used for  $i_b^*$ ,  $D_{50}^*$  and  $MOB$ .

Table 6.2 Relationships between explanatory variables and stream response variables detected by the four quantitative analysis (LR: linear regression, MR: Multiple regression, DA: discriminant analysis, CT: classification tree).

	$Q_{pk}/Q_{bf}$				$Rn_{falling}$				PF-Days				$S$	$\tau_f''$			$\tau_g'$			PF- $\Delta E$			PF-MOB				
	LR	MR	DA	CT	LR	MR	DA	CT	LR	MR	DA	CT	LR	MR	DA	CT	LR	MR	DA	CT	LR	MR	DA	CT			
$i_b^*$	+	+	+	+					-		±					-					±	±					
$D_{50}^*$	+		±	+	-	-	-	-	±	±			+					+	-		±		+	+			
MOB	+	+	+	+			±		+			±				-			-	-				±	-		
$\theta_{ci}^*$									-		-	-	-		+		+	+			-	-	+	+	+	+	
$\Delta S$		+				+	+							+	±			-									
$\Delta \tau_f''$			+						+	+					-	-	-										
$\Delta \tau_g'$	+		+	+					+	+			±	+		-					-		+	+	+	+	
$\Delta E$						+	±		±		+			-	±											±	

multiple regressions, this relation is not statistically significant anymore. The consideration of all predictors together also detects more interactions. For example, multiple regression models reveal a positive relation between the bedload median size and the previous flood bed mobility. Compared to pairwise linear regression, it also detects that the initial threshold for motion is positively related to the microform roughness and negatively related with the initial slope.

(2) Some relationships are detected by all four analyses (Table 6.2). Some are well known deterministic relationships such as the link between peak discharge and bedload transport or the proportion of the active bed surface. Some other relationships have been mainly documented in flume experiments until now and, to our knowledge, have never been observed quantitatively in the field. These relationships are: the decrease of the transported  $D_{50}$  as the rising limb duration increases; the higher initial threshold for motion when the bed was previously mobilised over large areas; the decrease of the macroform roughness when the initial macroform roughness is high and vice-versa; the negative relationship between the previous flood change in bed elevation and the actual change in bed elevation resulting of a flood. Finally, another strong effect is the increase of the microform roughness when the bed was mobilized over large areas during previous floods.

(3) Some relationships are detected by three analytical schemes and not systematically by the same ones, which illustrates the sensitivity of some analyses (Table 6.2). It is important to note that many relationships are shown only by the discriminant

analysis and the classification tree, hinting at their advantage to detect potential factors in river dynamics over the more traditional regression analyses. The discriminant analysis is often the only approach to detect a relationship probably because of the arbitrary threshold we choose to designate a relation as significant. In effect, there is no available test to determine whether or not a variable is statistically significant to discriminate the groups and therefore the results strongly depend on personal interpretation of the variables with a weak contribution to the discriminant functions.

(4) Both the discriminant and the classification tree analyses detect non-linear relationships. For example, the size of mobilized particles can be low or high when the delay between two bedload events is short and tends to reach average values when the number of days since the last bedload event is large (Figure 6.8). From the classification tree, we see that when only a few days separate two bedload events, the size of the bedload material is related to the initial microform roughness (Figure 6.9).

(5) Even though the performance of the discriminant analysis and the classification tree is similar in detecting relationships, the classification trees appear to be more informative as a result of the hierarchical nature of the decision rules as it allows us to appreciate the relative importance of predictors. For example, the results highlight the primary control of flow magnitude on bedload, the area of the bed that is mobilized and the change in microform roughness as the dimensionless peak discharge is the predictor used for the first split of the data set (Figure 6.9). For the size of transported particles, the peak discharge plays a role but it is less important than the proportion of runoff on the falling limb of the flood. The situation is similar for the macroform roughness changes as the peak discharge will control its response only under a low initial macroform roughness.

(6) The successive splitting in smaller groups of the classification trees shows that two sets of conditions may produce the same result. For example, the bedload transport is small under low peak discharge and when macroform roughness is high but also when the peak discharge is high but associated with a stable bed as shown by a small bed elevation change from the previous flood (Figure 6.9). Furthermore, a variable may come into play only under certain conditions. For example, macroform roughness will influence bedload transport rate only when the peak discharge of the flood is low.

### 6.1.4.3. A global analysis

The analysis of the processes involved in every aspect of the stream response to a flood is an important step in understanding fluvial dynamics. As multiple factors interact together, it is also relevant to seek specific combinations of factors that would result in a general type of bedload transport and morphological response. We explored this idea by running a cluster analysis on the eight response variables to form four distinct groups. The explanatory and response variable distributions according to these groups are shown in Figure 6.10. The clustering is primarily based on the intensity of the bedload transport and secondarily on the morphological processes. An *a posteriori* analysis of variance shows that for all variables, except the bed elevation changes, there is at least one group that is different from the others. Therefore, all response variables characterize at least one response group and the clustering, although simplifying the data set, still reflects the complexity of the stream response to a flood. From the distributions of the explanatory variables, there is at least one distinct group for the dimensionless peak discharge, the number of days since the last flood event and previous flood bed elevation change according to an analysis of variance ( $p < 0.01$ ). For the other variables, the within cluster variance is large illustrating further the fact that multiple conditions can lead to the same response.

The discriminant analysis on the stream response groups does separate the groups adequately, with an *a posteriori* classification ratio of 86 % and a cross-validation classification ratio of 58 % (Figure 6.11). The first canonical function discriminate between groups 1 and 3 and groups 2 and 4 based mainly on previous flood bed elevation change, the initial form roughness and the peak discharge. The second canonical function discriminates between groups 1 and 4 and groups 2 and 3 based mainly on the number of days since the last flood, the slope and the previous bed elevation change. This analysis is instructive but not as useful as the classification tree. The tree model is based on the previous bed elevation change, the peak discharge, the number of days since the last flood and the previous bed mobility, which were the predictors with the highest effects in single response variable analysis (Figure 6.11). Interestingly, group clusters 1 and 2 are composed of stream responses that can be produced by two different combinations of explanatory variables. Even though the breakdown is uneven, it may represent what happens in the

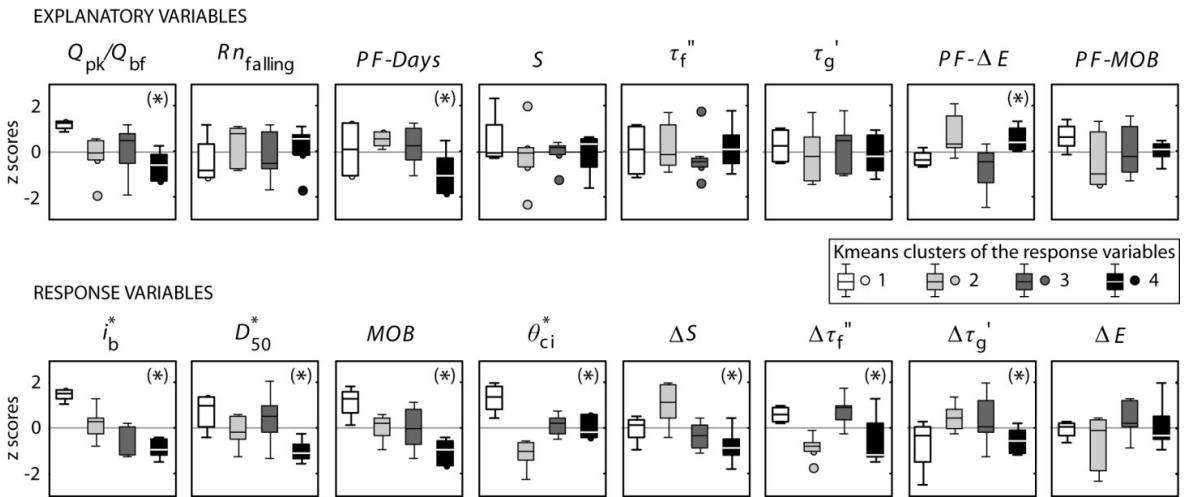


Figure 6.10 Kmeans cluster analysis performed on the response variables and quantitative analysis of the explanatory variables in relation to the groups. Note that only floods below the bankfull discharge are used for the cluster analysis. The symbol (\*) denotes that at least one group mean is significantly different according to an analysis of variance ( $p < 0.1$ ). See Figure 6.5 for boxplot legend.

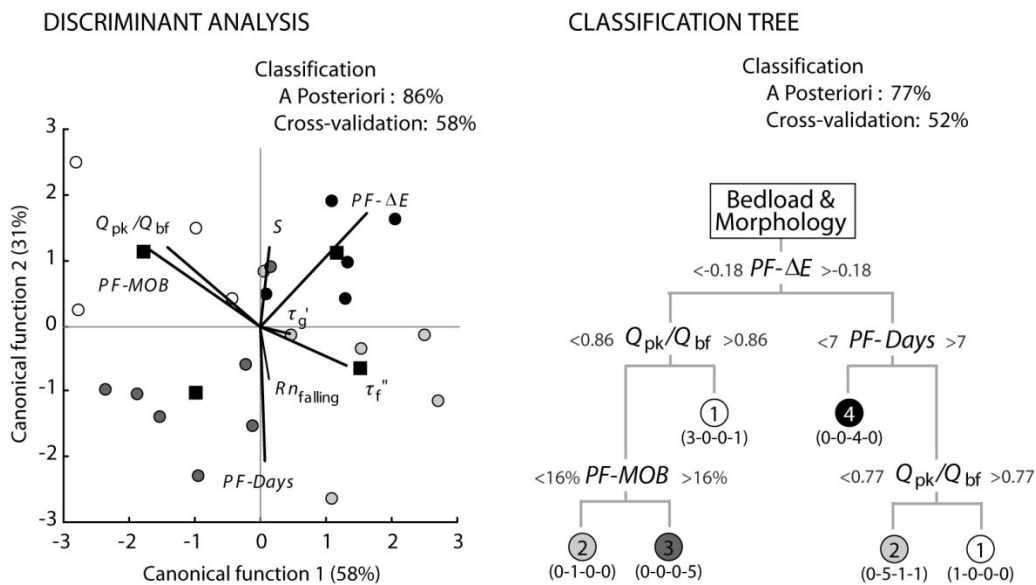


Figure 6.11 Discriminant analysis and classification tree analysis of the four groups based on Kmeans cluster analysis. Note that only floods below the bankfull discharge are used for the cluster analysis. The color coding of the groups is the same as in Figure 6.10.

fluvial dynamics of a small gravel-bed river and these flood events should not be taken as outliers. Generally, clusters 1 and 2 have the highest bedload but have contrasted morphological responses. Cluster 1 is characterized by a high initial threshold for motion, and an increase of the macroform roughness while cluster 2 is characterized by low initial threshold for particle motions and an increase of the slope accompanied by a smoothing of the macroforms and a marked bed scour. On the other hand, it also seems that the same conditions can lead to different results as shown by the misclassified flood events in the classification tree (Figure 6.11). This level of misclassification can be due to measurement errors, or to the fact that the data set is relatively small. It may also reflect that some important factor has not been included in the analysis as suggested by a score of 77 % of the *a posteriori* classification and 52 % for the leave-one-out validation. The combination of the results from the discriminant analysis and the classification tree modeling points towards the critical role of the antecedent flow history in addition to the magnitude of the flow as a driver of bedload motion and bed morphology changes.

### **6.1.5. Discussion**

In this paper and its companion, we have presented a unique field data set covering flow, bedload transport and morphological processes as well as providing knowledge of the initial conditions and previous flood activity for 18 individual flood events in two sections of a small gravel-bed river, Béard Creek. Rare are field based studies surveying simultaneously interactions and/or feedbacks between the flow, the bed morphology and the bedload transport in gravel-bed rivers. To our knowledge, such an approach goes back to the study by Ashworth and Ferguson (1986). Similar studies as for example those of Bennett and Bridge (1995a; b) and Hoey and Sutherland (1991) have been conducted using physical models. In the introduction, we have reviewed case studies that have identified sources of bedload transport variability. There is still some discussion in the scientific community on how to handle bedload transport variability and complexity using a holistic approach that could lead to better prediction of sediment loads and river channel evolution (Phillips, 2003; Murray et al., 2009; Church, 2010; Jerolmack, 2011). One of the proposed approaches is to recognize explicitly the non-linear dynamics and complexity that are ubiquitous in geomorphic processes (Murray et al., 2009; Church, 2010). In this paper, we proposed expanding the analytical approach as a way of handling bedload transport and morphological changes using a case study to illustrate our point of view.

We have shown here how multivariate data analysis can contribute significantly to the understanding of complex fluvial morphodynamic in a single river. We used multivariate techniques (multiple regression, discriminant and classification tree analyses) that have a greater analytical power to detect the presence of interactions compared to pairwise linear regression. We also have illustrated that simplifying the variables by splitting the values into low-medium-high groups allowed us to detect non-linear and complex interactions using the discriminant and classification tree analyses. Depending on the initial conditions, a variable may force the stream response in opposite directions. For example, a high macroform roughness leads to a decrease of bedload flux, which could be explained by the fact that the roughness of the bed dissipates flow energy. In this situation, there is still a chance to observe erosion in the section, even though bedload transport is low. Even if there is consistency among the results from discriminant analysis and the classification tree modeling, the latter technique is better suited for the extensive data set used here because it provides a systematic way of detecting thresholds. This approach decreases the chances of missing important information embedded in data sets with many variables. Also, the hierarchical nature of the classification trees allows us to weight the relative importance of the predictors in explaining a response. Finally, this approach allows one type of response to be explained by two different sets of factors, which represent better the complexity of fluvial systems.

We did the analyses using a total of 16 variables representing all aspects of the fluvial dynamics. Even though some variables may be missing, adding more could lead to some confusion. In an attempt to step back from the results of the foregoing detailed analysis, we agglomerated the stream responses into four groups in order to seek more general patterns. This aims at a global understanding of how similar conditions can lead to different responses and different conditions that can lead to similar responses (Figure 6.10 and Figure 6.11). The classification tree model of these groups uses the four key variables that were dominantly influencing the responses observed in the detailed analyses: flow magnitude, low flow history and history of the bed mobility measured through the bed elevation change and the mobilised bed area since the last flood. This type of empirical model can be useful in the prediction of the stream response based on relatively easy to monitor variables as it provides a reliable and easier way of understanding the river system.

Even though our data set is large for a study based on the effects of floods on bedload and bed morphology in rivers, it remains relatively small when it comes to a detailed quantitative analysis. The size of the data set impinges on the identification of statistically significant interactions among the variables because a specific set of conditions may occur only a very limited number of times. In addition, the fact that the measurements were collected in the field in the absence of experimental controls also affects the potential for detecting meaningful relations. It is clear that a larger data set would improve the power and robustness of the statistical analyses and it would also facilitate stronger validation procedures. Also, the fact that we had to set spatial limits to the detailed measurements of the bed mobility and morphology certainly introduced noise into the data set. We measured the river bed changes 20 meters upstream of the bedload samplers. This distance was set based on the local morphology and on the time needed to conduct the surveys. However, the changes detected might not totally represent the trends over a longer section of the stream. This may partly explain why morphological variables have a lower explained variance for all analytical schemes when compared to the bedload processes.

From the relationships identified in Table 6.2, we have created a summary diagram in order to give an overview of the processes observed in Béard Creek during our study (Figure 6.12). Even though many of the variables are simple indicators derived from three main sources of measurements (stage or discharge, morphological surveys and bedload samplers), we believe that the data used in this analysis captured the essence of the complex fluvial dynamics except for a direct appraisal of the effect of morphological changes on the flow as this was not possible to measure during a flood. All relations detected by at least three analytical approaches are represented by the thickest arrows and are considered as interactions that are always present. All relations that were detected by two analytical techniques are represented as thin arrows and may occur under certain conditions or above certain thresholds only. Interactions that can produce a positive or a negative result on the response variables were tagged as non-linear and the arrows are in dashed lines. Figure 6.12 presents the interactions and feedbacks between the flow, the flood history and the hydrograph shape as external forcings and the response of the bedload transport, the bed structure (e.g. roughness) and topography. Given the number of interactions, one can easily understand why the stream response to a flood is not straightforward. The main interactions are:

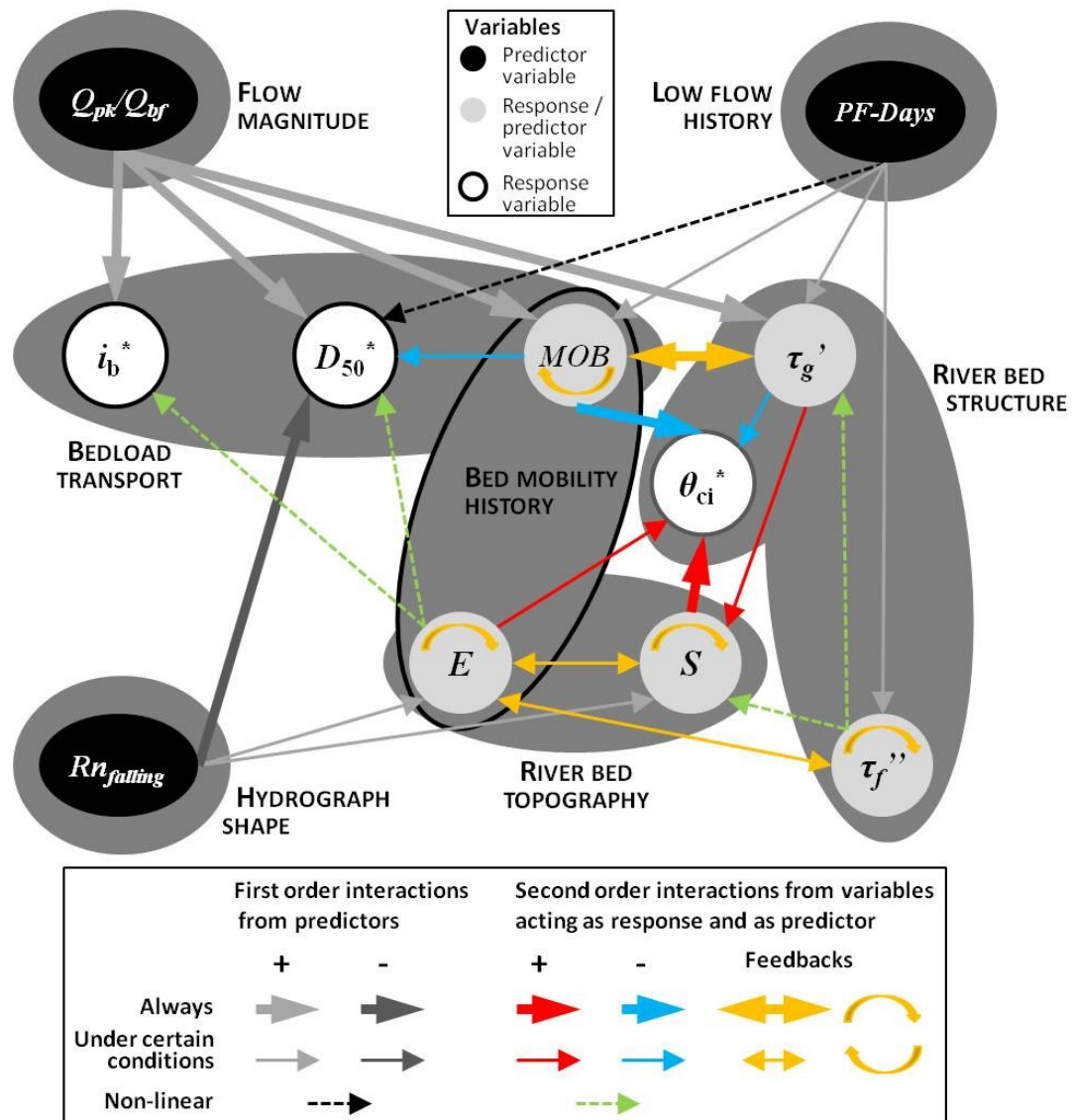


Figure 6.12 Interactions among the variables measured in this study. The interactions represented are shown in for Table 3. Note that the five variables that are both predictor and response variables were represented as a single element for simplification. To interpret correctly the figure, an arrow departing from a variable indicates a predictor while an arrow directed toward a variable is a response. For example, the initial slope controls the initial threshold for motion but the change of slope after a flood is influenced by the initial microform roughness.

(1) Bedload processes are strongly driven by the flow but other factors are also important in modulating this response. The bedload rate, bed activity and size of the transported particles are influenced by different sets of variables which explains the diversity of the bedload process response. Bedload transport is non-linearly influenced by the changes in bed elevations associated with the previous flood only under certain conditions. The bed activity is controlled by the initial microform roughness and by feedback with the area of the bed that was mobilized by the previous flood illustrating the role of flood history. The size of the transported particles is strongly influenced by the hydrograph shape but is slightly affected by the low flow history and by previous bed mobility history. The fact that this variable responded to a number of different controls is probably the main reason why the size of the transported particles was not correlated with the two other bedload process variables (chapter 5).

(2) Topographical changes are driven by weak interactions with the hydrograph shape and the initial micro and macroform roughness. The main drivers of bed slope and elevation changes are the initial slope and bed elevation changes associated with the previous flood through strong feedbacks. This is in agreement with the strong negative correlation between the two response variables and it further confirms their decoupling from the rest of the morphological and bedload responses to a flood (Chapter 5). It also suggests a strong self-organization of the largest morphological features (Kocurek et al., 2010) as the magnitude of their changes is mainly related to their own evolution rather than to the magnitude of the flood.

(3) Bed structure changes are connected to the bedload processes through the proportion of bed area that is mobilised during a flood. Microform roughness changes are strongly influenced by the flow magnitude as these structures are built progressively and they may be destroyed from one flood to the next. Microforms play a major role in the feedback interactions between bedload transport and morphological changes (e.g. Hassan and Reid, 1990; Church et al., 1998; Hassan and Church, 2000; Strom et al., 2004). On the other hand, macroform roughness evolution is mainly controlled by feedbacks from initial morphological state. The initial threshold for motion is the variable that is influenced by the greatest number of bed structure and topography (strongly by the slope) variables as well as by the bed mobility history. This suggests that the variable is a good indicator of the initial

state of bed, both in terms of grain packing and probably available sediment sizes on the bed surface.

(4) Overall, the morphological response, both the topography and bed structure, is characterized by far more interactions than the bedload processes. The morphological variables are as much response variables as they are control variables creating a complex web of feedbacks. Most of these interactions occur only under certain conditions, a situation that may explain that identical responses are generated by different sets of factors. This stresses the importance of the local factors in predicting the direction of evolution of the river bed and the role of the historical trajectory, represented here as the history of bed mobility, in understanding fluvial dynamics of gravel-bed rivers.

Figure 6.12 provides valuable information to help understand the direction of change of the stream bed and the bedload transport processes occurring during a flood. The set of relations in the diagram could also serve to generate new hypotheses in order to inform the design of controlled flume experiments or intensive field studies. From this general portrait of fluvial dynamics, we can stress three major points that should be considered when designing future field and flume experiments to understand fluvial dynamics:

(1) The important effect of the ‘morphological trajectory and history’ to predict future changes. It has been shown previously that sediment transport behaviour displays a strong dependence on the recent history of the stream, especially after high magnitude events (Gintz et al., 1996; Lenzi et al., 2004; Turowski et al., 2009). But, as demonstrated from our results, low and moderate magnitude flood events also play a role in the stream evolution. Changes can only be understood through an understanding of the sequence of configurational events that have marked the evolution of the system (Lane et al., 1996; Lane and Richards, 1997; Roy and Lane, 2003). In fact, we have showed the prominence of this concept for variables such as bed elevation changes and macroform roughness both of which exhibit autogenic behaviour that is marginally influenced by the flow magnitude.

(2) The importance of the organization of the bed structure in the bedload and topographical response of the stream to a flood. The temporal variability of the bed structure is rarely acknowledged in field studies. This point is congruent with recent research suggesting that the sediments have their own dynamics that may in part be

independent from the flow as in dry granular flows (Frey and Church, 2011; Jerolmack, 2011; Marquis and Roy, 2012). Also the bed structure can be greatly influenced by micro and macro invertebrates (e.g. Johnson et al., 2011). The initial threshold for motion is a good indicator of bed structure as it relates to different scales of bed roughness to the stream slope. It was shown in laboratory experiments that the threshold for motion is strongly affected by the relative arrangement of the grains on the bed (Kirchner et al., 1990; Buffington et al., 1992). Furthermore, critical values may change considerably within a transport event and the classical view of a single critical threshold value during a flood has to be reconsidered (Turowski et al., 2011). There is a need to develop measures or indicators of the bed structure that could easily be used in the field.

(3) Changes in bed morphology are difficult to understand from the effects of smaller scale processes such as those involved in bedload transport. Bed morphology is an emergent property of river systems. Nevertheless, bed morphology consists of many aspects represented here by several variables and some of them, such as the microform roughness, are better related to the bedload processes. These variables can therefore serve as an intermediate level in order to upscale small scale transport processes to large-scale morphological changes as was hypothesized in a gravel-bed topography model based on sediment transport (Naden, 1987).

### **6.1.6. Conclusion**

The objective of this paper was to investigate bedload and morphological responses as they relate to flow, initial conditions and flood history. The understanding of the stream response using an analytical framework where one variable is taken at a time is useful to deepen our understanding of river dynamics but it often provides a limited view of the river system. In an attempt to approach in a quantitative manner the complexity of gravel-bed river dynamics, we have used various multivariate techniques that allow the detection of non-linear relationships and of thresholds. Using an extensive, yet relatively small data set as a case study, we have shown that more relevant information and knowledge can be found using an analytical approach adapted to a data set collected in the field without experimental control. For instance, we have shown that the initial topographical and bed structure conditions, the previous bed mobility history, the low flow history are at least as important as the flow magnitude in explaining the stream response. Also, we have

highlighted the concept that two different sets of factors can produce the same response due to the presence of thresholds and interactions of factors at multiple spatial and temporal scales. Finally, we have found that the sediment grains organization on the bed is crucial to our understanding of the dynamics of gravel-bed rivers and might be the missing link to relate small-scale bedload processes to large-scale morphological processes. Examining river morphodynamics from a holistic point of view has the potential to lead to a better understanding of the temporal evolution of the organization of the particles on the river bed and eventually to a more quantitative, rather than conceptual, understanding of bedload transport and morphological changes.

### Acknowledgements

The authors would like to thank Mr. and Ms. Cloutier for allowing access to their land. Martin Lambert and Jean-François Myre were of great support for the design and construction of the bedload samplers. We are also grateful to Christine Bergeron-Verville, Vincent Cardin-Tremblay, Laurence Chaput-Desrochers, Sylvio Demers, Claude Gibeault, Hélène Lamarre, Olivier Lalonde, Kevin Partington, Mathilde Péloquin-Guay, Mathieu Roy, Katherine Sicotte, Rachel Thériault, Julie Therrien and Michèle Tremblay for their help in the field and in the lab. This research was supported by the Natural Sciences and Engineering Council and the Canadian Foundation for Innovation.



## CHAPITRE 7. CONCLUSION GÉNÉRALE

---

Le fil conducteur de la thèse est l'avancement conceptuel de la recherche sur les rivières à lit de graviers en ayant recours à un corpus méthodologique et analytique renouvelé. Cette approche a permis de mettre l'accent sur les interactions complexes entre les différentes dimensions de l'écoulement, du transport de sédiments en charge de fond et des formes du lit. Cette orientation a été choisie afin de générer de nouvelles avenues de recherche pour résoudre en partie l'impasse actuelle où le but ultime de prédire l'évolution des formes n'est pas encore résolu après des décennies de travaux. Dans une certaine mesure, avant la reconnaissance par plusieurs chercheurs des limites de l'approche réductionniste, la compréhension des formes apparaissait probablement plus clairement que suite à la multiplication des études illustrant la variabilité « extrême » des processus fluviaux. Dans cette optique, la thèse ne rejette pas l'approche réductionniste du fait que plusieurs de ses prémisses fondamentales sont issues des relations classiques entre formes et processus, mais elle propose plutôt de considérer ces relations simultanément afin de mieux comprendre la complexité de la réponse d'un cours d'eau à un évènement de crue.

### 7.1. Principales découvertes et avancées conceptuelles

Tout au long des chapitres de cette thèse, il y a une croissance de la complexité conceptuelle ce qui se manifeste par l'ampleur des interactions étudiées. L'originalité de la thèse réside dans une utilisation non conventionnelle de méthodes de mesures et d'analyses, ainsi que dans l'interrogation de jeux de données sous un nouveau jour et ce, à différentes échelles temporelles et spatiales qui sont représentatives des processus actifs dans les systèmes fluviaux. Cette approche qui sous-tend la thèse a permis de générer à la fois des découvertes spécifiques originales et des avancées conceptuelles en utilisant des données mesurées sur le terrain pour illustrer chacun des angles considérés. Les découvertes spécifiques de la thèse sont en lien direct avec les objectifs de départ. Elles découlent directement du fait d'avoir repensé les méthodes de mesure et d'analyse de données, somme toute relativement classiques en elles-mêmes, et d'avoir mis l'accent sur les interactions entre les processus. Dans chacun des chapitres, nous avons établi :

**Chapitre 2 :** Qu'il existe une gamme d'échelles de structures turbulentes cohérentes auto-similaires de la seconde jusqu'à la minute. Les plus grandes structures, nommées pulsations, ont été identifiées pour la première fois et les analyses sur leur origine suggèrent un équilibre entre une auto-organisation de l'écoulement et un contrôle morphologique de leur taille et leur intensité. Ce sont les zones de contraction de l'écoulement comme les seuils le long du profil longitudinal de la rivière qui pourraient expliquer la dynamique des pulsations.

**Chapitre 3 :** Que les gradients d'accélération temporels et spatiaux jouent un rôle majeur sur la variabilité des flux de transport de sédiments en charge de fond durant une crue. Les accélérations et décélérations marquées de l'écoulement augmentent et diminuent de manière brusque les taux de transport pour une même valeur de débit. L'intensité des taux de changements des caractéristiques de l'écoulement fluctue de deux à cinq fois au cours d'un même évènement de crue, ce qui complique la réponse du transport de sédiments en charge de fond.

**Chapitre 4 :** Que l'utilisation simultanée de plusieurs méthodes de suivi du transport en charge de fond et de la morphologie a mené à l'identification d'une nouvelle dynamique des rivières à lit de graviers, soit la contraction et la dilatation du lit. Les changements dans le volume occupé par les particules du lit sont causés par des interactions complexes entre l'écoulement, le transport des sédiments fins et l'histoire de la morphologie locale. Bien que survenant sur des portions limitées du chenal, la dilatation et la contraction du lit ont aussi des répercussions sur la mise en transport des particules et les changements morphologiques qui surviendront lors de la prochaine crue.

**Chapitre 5 :** Que la réponse morphologique, particulièrement la topographie, est insensible à la magnitude du débit ce qui a pour conséquence qu'elle est relativement indépendante du transport de sédiments en charge de fond. Cette déconnexion entre les changements morphologiques et le transport de sédiments remet en question l'utilisation des relevés différentiels de la topographie pour l'estimation des taux de transport en charge de fond. Jusqu'à maintenant, on assumait que la méthode morphologique ne faisait que sous-estimer les flux de transport. Ici, l'utilisation de cette technique simple est assurément remise en cause pour les rivières à lit de graviers avec des sources sédimentaires limitées.

**Chapitre 6 :** Que l'historique de l'étiage et de la mobilité du lit de même que les conditions initiales de la structure et de la topographie du lit sont aussi importantes que la magnitude de l'écoulement dans la compréhension de la réponse du transport de sédiments et de la réponse morphologique d'un cours d'eau à une crue. Particulièrement, les interactions et rétroactions complexes entre tous ces facteurs permettent de mettre en évidence le rôle clé de la structure du lit pour faire le lien entre la réponse du transport de sédiments et la réponse de la morphologie.

D'une certaine manière, les avancées conceptuelles peuvent paraître difficiles à cerner puisqu'elles sont sous-entendues à travers plusieurs découvertes spécifiques issues de l'analyse de données. Dans cette optique, le bilan de la contribution conceptuelle de cette thèse se base sur trois des six axes de développement identifiés par Church (2010) afin de résoudre le problème de la compréhension des formes du paysage. Dans chacun des chapitres, les approches utilisées représentent des pistes de solutions nouvelles ou l'illustration unique d'un concept à partir des données :

(1) L'absence de loi satisfaisante de prédiction du transfert du matériel dans le paysage exige une démultiplication des approches pour mieux cerner le phénomène. Ici, c'est par une approche essentiellement empirique qui n'est en rien révolutionnaire que nous avons réussi à identifier de manière certaine au moins deux facteurs de variabilité du transport de sédiments aux chapitres 3 et 4. Au chapitre 3, la combinaison de différentes méthodes de mesures relativement classiques a permis de cerner un phénomène de dilatation et de contraction du lit des rivières graveleuses qui n'aurait pu être détecté directement par aucune des méthodes utilisées séparément. Au chapitre 4, l'analyse des données de manière non-conventionnelle et la remise en question de la prémissse selon laquelle le transport de sédiments est ajusté aux conditions d'écoulement ont mené à l'identification du rôle majeur de l'accélération/décélération de l'écoulement durant une crue sur les taux de transport. Il faut aussi souligner que la réflexion sur l'absence d'équilibre causée par des gradients d'accélération a mené à l'utilisation des arbres de régression, une technique d'analyse qui permet de détecter l'effet non-linéaire de l'accélération sur les taux de transport.

(2) Il faut réconcilier l'information géomorphologique et la représentation des processus à différentes échelles. Ce problème fait essentiellement référence au transfert d'échelle et à l'imbrication des échelles. Au chapitre 2, nous avons montré comment

l’imbrication de structures turbulentes de petites échelles dans des structures de plus en plus grandes (pulsations) rend possible l’établissement d’un lien entre la turbulence de l’écoulement et les formes de grande échelle du lit d’une rivière, deux phénomènes à prime abord déconnectés. Bien que notre interprétation demeure spéculative, nous avons montré comment un processus auto-organisé, la turbulence, peut aussi être modulé par un contrôle externe, la morphologie, et ce à des échelles encore jamais considérées. Au chapitre 5, la question des transferts d’échelles a été traitée dans le contexte du transport des sédiments. En effet, nous avons spéculé qu’une différence d’échelles peut expliquer la réponse contrastée du transport de sédiments par rapport à la réponse topographique et morphologique du lit. Au chapitre 6, nous avons aussi montré que les échelles auxquelles les processus fluviaux se déroulent pourraient être connectées par l’intermédiaire de la structure du lit (rugosité).

**(3)** On se doit de trouver de nouvelles approches afin d’inclure les dynamiques complexes des systèmes, tel que la non-linéarité, l’auto-organisation, l’autosimilarité, les propriétés émergentes et les comportements autogènes afin d’améliorer notre compréhension et notre capacité de prédiction. La recherche d’approches nouvelles fait partie de tous les chapitres de la thèse. Au chapitre 2, le développement d’une nouvelle approche analytique des séries temporelles de vitesses instantanées de l’écoulement a rendu visibles des structures cohérentes auto-similaires pour une gamme d’échelles temporelles. Aux chapitres 3 et 6, l’utilisation d’arbres de régression a permis d’identifier des relations non-linéaires des dynamiques fluviales mais surtout d’illustrer comment des combinaisons de facteurs peuvent mener au même résultat. Au chapitre 5, l’analyse multivariée des différents aspects de la réponse d’un cours d’eau à une crue a mené à la conclusion que le changement topographique du lit est une propriété émergente qui n’est pas liée à la magnitude du transport de sédiments. Au chapitre 6, nous avons aussi illustré le comportement autogène des changements topographiques en mettant en évidence qu’un des principaux facteurs déterminant ces changements est leur état précédent. Aussi, la présence de nombreuses boucles de rétroaction a été révélée grâce aux analyses multivariées soulignant explicitement l’auto-organisation qui régit un système fluvial.

## 7.2. Modification de la trinité fluviale en une tétralogie fluviale

Ces découvertes et avancées illustrent la pertinence de centrer les études sur les interactions des processus fluviaux et aussi d'étudier le système fluvial dans son ensemble, comme le recommandait Leeder (1983) et bien des années plus tard Raven et al. (2010). Au fur et à mesure de la progression de la thèse et de la prise en compte de plus en plus de processus fluviaux dans chaque chapitre, et particulièrement à partir du chapitre 3, il devient évident que la structure du lit joue un rôle majeur dans la dynamique fluviale. Les particules du lit ont une dynamique granulaire propre indépendante des forces de l'écoulement tel que rappelé aux géomorphologues fluviaux par Frey et Church (2009; 2011). Ce sont probablement ces dynamiques granulaires stimulées par le transport de sédiments fins et l'écoulement interstiel qui mène au processus de contraction et de dilatation du lit décrit au chapitre 4. Aussi, les indicateurs de l'organisation des particules du lit tels que la micro- et la macro-rugosité et le seuil initial d'entraînement des particules jouent un rôle prépondérant dans la réponse du cours d'eau à une crue et sont l'intermédiaire qui permet de relier le transport de sédiments et les changements topographiques dus à une crue.

La structure du lit est intégrée implicitement dans le terme ‘formes du lit’ de la *trinité fluviale*. Il convient ici de rappeler que le cadre conceptuel de la *trinité fluviale* a d'abord été proposé pour les milieux sablonneux (Leeder, 1983; Best, 1993). Dans les lits composés de sable, l'organisation des grains peut varier mais beaucoup moins en comparaison de l'organisation des lits de graviers. Ceci s'explique par les tailles des particules qui sont bien triées et de forme relativement sphérique des grains de sable. En milieu graveleux, les tailles et formes variées des particules favorisent le tri vertical et longitudinal des grains et leur organisation en des formes caractéristiques à différentes échelles. Dans cette optique, il devient essentiel d'intégrer explicitement la structure du lit dans la *trinité fluviale* en distinguant les formes du lit entre la structure et la topographie du lit (Figure 7.1). D'après les résultats présentés dans cette thèse, la structure du lit représente l'organisation plus ou moins serrée des particules de la surface telle que détectée par la mesure du seuil critique d'entraînement et la rugosité du lit. La topographie représente les changements de pente et d'élévation globale du lit.

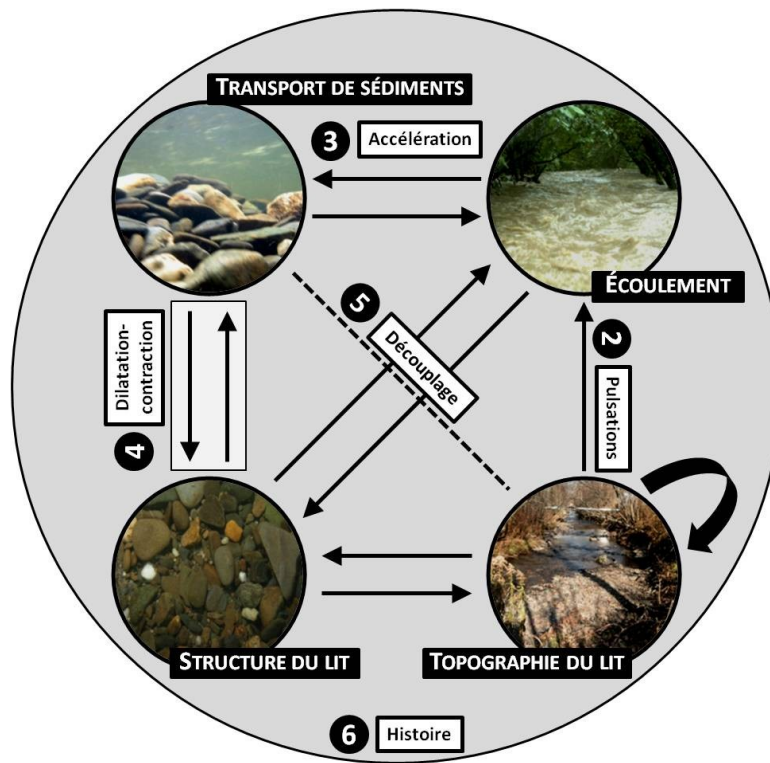


Figure 7.1 *Trinité fluviale* modifiée en *tétralogie fluviale* suite à l'intégration conceptuelle des résultats de la thèse. Pour faire le lien avec la Figure 1.3, les numéros des chapitres et les principales découvertes et avancées sont placés selon les interactions étudiées.

Ce nouveau cadre conceptuel représenté à la Figure 7.1 devient maintenant une *tétralogie fluviale*. Il permet de mieux représenter et comprendre le découplage entre les changements topographiques et le transport de sédiments en charge de fond puisque ces deux processus interagissent par l'intermédiaire de la structure du lit. Le caractère émergent des formes du lit de grande échelle et le fait qu'elles soient plus que la somme du mouvement individuel des particules du lit y sont aussi mieux représentés. Une flèche de rétroaction permet de souligner le caractère autogène de la topographie observée au ruisseau Béard. Cette séparation des caractéristiques de la morphologie du lit en est en fait une d'échelle, la structure du lit étant à plus petite échelle spatiale que la topographie. Ces échelles sont autant spatiales que temporelles, et la variabilité importante de la structure du lit explique probablement aussi son interaction plus marquée avec le transport de sédiments. Ce cadre conceptuel découle de l'intégration de tous les résultats de la thèse dont les principaux se retrouvent dans leurs chapitres respectifs. Il a le potentiel d'être généralisable à toutes les rivières à lit de graviers dont les sédiments sont mal triés et qui

sont donc caractérisées par des structures du lit à une gamme d'échelles. Il est particulièrement applicable aux cours d'eau dont le chenal est relativement stable, sans tendance marquée vers la dégradation ou l'aggradation. Toutefois, il serait intéressant de voir comment interagissent le transport en charge de fond et la topographie du lit dans un chenal en déséquilibre pour vérifier si les processus sont autant découplés. Dans ce contexte, les conditions topographiques initiales jouent probablement un rôle moins important dans la détermination des changements subséquents de la topographie, ce qui simplifie le nombre d'interactions et probablement la réponse générale du cours d'eau.

### 7.3. Recherche future

Bien que l'objectif ultime de la géomorphologie fluviale soit la prédiction de l'évolution des formes du lit, les conclusions de cette thèse ne contribuent pas directement à l'élaboration de modèles prédictifs fiables. Les conclusions illustrent plutôt comment répondre autrement à des questions classiques et permettent d'apprécier le problème (ou les problèmes...) sous un nouveau jour. Les découvertes et avancées qui sont développées ici ont toutefois un fort potentiel de généralisation conceptuelle. Le fait que les résultats soient essentiellement basés sur un seul site ne constitue pas un problème majeur puisque les conclusions de la thèse visent autant à proposer de nouvelles approches pour l'étude de la dynamique fluviale qu'à présenter des résultats probants sur les processus fluviaux. L'absence de réPLICATION à partir d'observations à d'autres sites que le seul ruisseau Béard est compensé par un nombre élevé d'événements de crue mesurés par rapport aux standards que l'on observe dans ce genre d'étude en géomorphologie fluviale. Le suivi serré d'un nombre élevé d'événements durant une période d'observation relativement courte a permis de couvrir une large gamme de conditions et d'en extraire les effets de l'historique. Ceci est relativement rare et ne peut se réaliser qu'à un seul site à la fois. Aussi, la conception du protocole d'échantillonnage a permis de baser les analyses sur des modèles théoriques et conceptuels puisque nous avons pu mesurer en continu des processus génériques qui ont cours dans un grand nombre de systèmes fluviaux. La plupart des découvertes sont fort probablement généralisables à d'autres cours d'eau à lit de graviers similaires au ruisseau Béard et peut-être à tous les cours d'eau à lit de graviers. Dans le cas de la dynamique de contraction-dilatation du lit, il se peut qu'elle soit spécifique au ruisseau Béard puisqu'elle n'a jamais été observée ailleurs, à notre connaissance à tout le moins. Les décisions quant aux choix des méthodes et analyses ont été prises avec précaution en optant toujours pour le choix qui minimisait la propagation des erreurs et les impacts sur les conclusions. La plupart des décisions ont été basées sur des critères sévères afin de ne pas arriver à des conclusions erronées. Dans cette optique, certaines relations et phénomènes décrits tout au long de la thèse sont probablement sous-estimés ou sont passés inaperçus. Globalement, nous estimons que les choix du site, du protocole d'échantillonnage, des méthodes de mesures et des analyses imposent des contraintes aux conclusions qui sont minimes par rapport à l'avancement substantiel des connaissances.

Chacune des portions de cette recherche peut servir de point de départ pour l’élaboration de nouveaux programmes de recherche sur le terrain et en laboratoire. Par exemple, les découvertes spécifiques des chapitres 2 à 4 soulèvent déjà plusieurs questions sur leurs implications réelles dans les systèmes fluviaux. Ces trois découvertes (les pulsations, le rôle de l’accélération de l’écoulement sur le transport en charge de fond et la dilatation-contraction du lit) peuvent être testées et développées rapidement dans de nouvelles études. Certaines méthodes et analyses employées aux chapitres 5 et 6 peuvent aussi être explorées à court terme. Au chapitre 5, ce sont principalement les directions de changement des indicateurs morphologiques qui sont analysées et non la valeur absolue de l’indicateur suite au passage de la crue. Par exemple, l’analyse se concentre sur la différence entre la pente du lit avant et après une crue qui a mobilisé les sédiments du lit. Il nous apparaît que cette approche est plus représentative et informative pour comprendre les tendances dans l’évolution des systèmes puisqu’elle permet de tenir compte de la trajectoire morphologique du cours d’eau. La notion de changement a aussi été considérée explicitement au chapitre 3, en utilisant l’accélération comme facteur plutôt qu’uniquement le débit ou une mesure globale de l’intensité de l’écoulement. La notion de taux de changements devrait être développée plus avant et ce, pour tous les aspects de la dynamique fluviale. Au chapitre 6, la prise en compte de la complexité par des analyses multivariées, jointes à des mesures simultanées à l’échelle de la crue a permis d’intégrer explicitement la notion d’histoire, ou de trajectoire morphologique. Cette notion avait été globalement évacuée par l’approche réductionniste puisqu’on était à la recherche de lois générales et non de cas spécifiques. L’historique du système doit absolument être réintégrée dans les études puisque son rôle est aussi important sinon plus que celui de l’écoulement dans la détermination de la réponse des rivières (Roy et Lane, 2003; Church, 2010). En plus de ces propositions, les chapitres 5 et 6 proposent un message qui dépasse les résultats spécifiques des études de cas et sont réellement les bases possibles d’une nouvelle façon d’approcher la complexité de la dynamique fluviale à moyen et long terme.



## BIBLIOGRAPHIE

---

- Adrian, R. J. (2007) Hairpin vortex organization in wall turbulence. *Physics of Fluids*, 19: 041301, doi: 10.1063/1.2717527.
- Allan, A. F. & Frostick, L. (1999) Framework Dilation, Winnowing, and Matrix Particle Size: the Behavior of Some Sand-Gravel Mixtures in a Laboratory Flume. *Journal of Sedimentary Research*, 69: 21-26.
- Alvera, B. & Garcia-Ruiz, J. M. (2000) Variability of sediment yield from a high mountain catchment, control Spanish Pyrenees. *Arctic Antarctic and Alpine Research*, 32: 478-484.
- Ashmore, P. E. (1991) How do gravel-bed rivers braid. *Canadian Journal of Earth Sciences*, 28: 326-341.
- Ashmore, P. E. & Church, M. (1998) Sediment transport and river morphology: a paradigm for study. In: Klingeman, P. C., Beschta, R. L., Komar, P. D. & Bradley, J. B. (eds), *Gravel-bed Rivers in the Environment*, Water Resources Publications: Highlands Ranch, Colorado, pp. 115–148.
- Ashworth, P. J. & Ferguson, R. I. (1986) Interrelationships of channel processes, changes and sediments in a proglacial braided river. *Geografiska Annaler Series a-Physical Geography*, 68: 361-371.
- Ashworth, P. J. & Ferguson, R. I. (1989) Size-Selective Entrainment of Bed-Load in Gravel Bed Streams. *Water Resources Research*, 25: 627-634.
- Ashworth, P. J., Ferguson, R. I., Ashmore, P. E., Paola, C., Powell, D. M., et al. (1992) Measurements in a Braided River Chute and Lobe .2. Sorting of Bed-Load During Entrainment, Transport, and Deposition. *Water Resources Research*, 28: 1887-1896.
- Bagnold, R. A. (1941) *The physics of blown sand and desert dunes*, Methuen & Co. Ltd, London.
- Bagnold, R. A. (1954) Experiments on a Gravity-Free Dispersion of Large Solid Spheres in a Newtonian Fluid under Shear. *Proceedings of the Royal Society of London. Series A. Mathematical and Physical Sciences*, 225: 49-63.
- Bak, P. & Chen, K. (1991) Self-Organized Criticality. *Scientific American*, 264: 46-53.
- Baker, V. R. & Pyne, S. (1978) G. K. Gilbert and modern geomorphology. *American Journal of Science*, 278: 97-123.
- Bennett, S. J. & Bridge, J. S. (1995a) An Experimental-Study of Flow, Bedload Transport and Bed Topography Under Conditions of Erosion and Deposition and Comparison With Theoretical-Models. *Sedimentology*, 42: 117-146.

- Bennett, S. J. & Bridge, J. S. (1995b) The Geometry and Dynamics of Low-Relief Bed Forms in Heterogeneous Sediment in a Laboratory Channel, and Their Relationship to Water-Flow and Sediment Transport. *Journal of Sedimentary Research Section a-Sedimentary Petrology and Processes*, 65: 29-39.
- Bergman, N., Laronne, J. B. & Reid, I. (2007) Benefits of Design Modifications to the Birkbeck Bedload Sampler Illustrated by Flash-Floods in an Ephemeral Gravel-Bed Channel. *Earth Surface Processes and Landforms*, 32: 317-328.
- Best, J. (2005) The fluid dynamics of river dunes: A review and some future research directions. *Journal of Geophysical Research*, 110: F04S02, doi: 10.1029/2004jf000218.
- Best, J. L. (1993) On the Interactions Between Turbulent Flow Structure, Sediment Transport and Bedform Development: Some Considerations From Recent Experimental Research. In: Clifford, N. J., French, J. R. & Hardisty, J. (eds), *Turbulence: Perspectives on Flow and Sediment Transport*, John Wiley & Sons, Chichester, pp. 61-92.
- Best, J. L. (1996) The fluid dynamics of small-scale alluvial bedforms. In: Carling & Dawson (eds), *Advances in fluvial dynamics and stratigraphy*, John Wiley & Sons, Chichester, pp. 67-125.
- Biggs, B. J. F., Nikora, V. I. & Snelder, T. H. (2005) Linking scales of flow variability to lotic ecosystem structure and function. *River Research and Applications*, 21: 283-298.
- Boyer, C., Roy, A. G. & Best, J. L. (2006) Dynamics of a River Channel Confluence With Discordant Beds: Flow Turbulence, Bed Load Sediment Transport, and Bed Morphology. *Journal of Geophysical Research-Earth Surface*, 111: F04007, doi: 10.1029/2005JF000458.
- Bracken, L. J. & Wainwright, J. (2006) Geomorphological equilibrium: myth and metaphor? *Transactions of the Institute of British Geographers*, 31: 167-178.
- Brasington, J., Middleton, R., Frostick, L. E. & Murphy, B. J. (2000) Detecting Significant Sediment Motion in a Laboratory Flume Using Digital Video Image Analysis. *Earth Surface Processes and Landforms*, 25: 191-196.
- Brasington, J. & Smart, R. M. A. (2003) Close range digital photogrammetric analysis of experimental drainage basin evolution. *Earth Surface Processes and Landforms*, 28: 231-247.
- Bravard, J. P. & Petit, F. (1997) *Les cours d'eau: Dynamique du système fluvial*, Armand Collin, Paris.
- Brayshaw, A. C., Frostick, L. E. & Reid, I. (1983) The Hydrodynamics of Particle Clusters and Sediment Entrainment in Coarse Alluvial Channels. *Sedimentology*, 30: 137-143.
- Breiman, L., Friedman, J., Stone, C. J. & Olshen, R. A. (1993) *Classification and regression trees*, Chapman & Hall, Boca Raton.

- Bridge, J. S. & Jarvis, J. (1982) The dynamics of a river bend: a study in flow and sedimentary processes. *Sedimentology*, 29: 499-541.
- Buffin-Belanger, T. & Roy, A. G. (1998) Effects of a Pebble Cluster on the Turbulent Structure of a Depth-Limited Flow in a Gravel-Bed River. *Geomorphology*, 25: 249-267.
- Buffin-Belanger, T. & Roy, A. G. (2005) 1 Min in the Life of a River: Selecting the Optimal Record Length for the Measurement of Turbulence in Fluvial Boundary Layers. *Geomorphology*, 68: 77-94.
- Buffin-Belanger, T., Roy, A. G. & Kirkbride, A. D. (2000) On Large-Scale Flow Structures in a Gravel-Bed River. *Geomorphology*, 32: 417-435.
- Buffington, J. M. (2012) Changes in Channel Morphology Over Human Time Scales. In: Church, M., Biron, P. & Roy, A. G. (eds), *Gravel Bed Rivers: Processes, Tools, Environments*, John Wiley & Sons, Chichester, pp. 435-463.
- Buffington, J. M., Dietrich, W. E. & Kirchner, J. W. (1992) Friction Angle Measurements on a Naturally Formed Gravel Streambed - Implications for Critical Boundary Shear-Stress. *Water Resources Research*, 28: 411-425.
- Buffington, J. M. & Montgomery, D. R. (1997) A Systematic Analysis of Eight Decades of Incipient Motion Studies, With Special Reference to Gravel-Bedded Rivers. *Water Resources Research*, 33: 1993-2029.
- Calantoni, J. & Puleo, J. A. (2006) Role of pressure gradients in sheet flow of coarse sediments under sawtooth waves. *Journal of Geophysical Research-Oceans*, 111: C01010, doi: 10.1029/2005JC002875.
- Cao, Z., Hu, P. & Pender, G. (2010) Reconciled bedload sediment transport rates in ephemeral and perennial rivers. *Earth Surface Processes and Landforms*, 35: 1655-1665.
- Carling, P. A. & Reader, N. A. (1982) Structure, composition and bulk properties of upland stream gravels. *Earth Surface Processes and Landforms*, 7: 349-365.
- Carson, M. A. & Griffiths, G. A. (1989) Gravel transport in the braided Waimakariri river - mechanisms, measurements and predictions. *Journal of Hydrology*, 109: 201-220.
- Charru, F., Mouilleron, H. & Eiff, O. (2004) Erosion and deposition of particles on a bed sheared by a viscous flow. *Journal of Fluid Mechanics*, 519: 55-80.
- Chen, L. & Stone, M. C. (2008) Influence of bed material size heterogeneity on bedload transport uncertainty. *Water Resources Research*, 44: W01405, doi: 10.1029/2006wr005483.
- Chorley, R. J. & Kennedy, B. A. (1971) *Physical geography : a systems approach*, Prentice-Hall International, London.
- Church, M. (2002) Geomorphic Thresholds in Riverine Landscapes. *Freshwater Biology*, 47: 541-557.

- Church, M. (2006a) Bed Material Transport and the Morphology of Alluvial River Channels. *Annual Review of Earth and Planetary Sciences*, 34: 325-354.
- Church, M. (2006b) Multiple scales in rivers. In: Habersack, H., Piégay, H., Hoey, T., Rinaldi, M. & Ergenziinger, P. (eds), *Gravel-Bed Rivers 6 – From process understanding to the restoration of mountain rivers*, Elsevier, London, pp. 3-32.
- Church, M. (2010) The trajectory of geomorphology. *Progress in Physical Geography*, 34: 265-286.
- Church, M., Hassan, M. A. & Wolcott, J. F. (1998) Stabilizing Self-Organized Structures in Gravel-Bed Stream Channels: Field and Experimental Observations. *Water Resources Research*, 34: 3169-3179.
- Clifford, N. J. & J.R., F. (1993) Monitoring and analysis of turbulence in geophysical boundaries: some analytical and conceptual issues. In: Clifford, N. J., French, J. R. & Hardisty, J. (eds), *Turbulence: Perspectives on Flow and Sediment Transport*, John Wiley & Sons, Chichester, pp. 93-120.
- Clifford, N. J., Richards, K. S. & Robert, A. (1992) The Influence of Microform Bed Roughness Elements on Flow and Sediment Transport in Gravel Bed Rivers - Comment. *Earth Surface Processes and Landforms*, 17: 529-534.
- Cohen, H. & Laronne, J. B. (2005) High rates of sediment transport by flashfloods in the Southern Judean Desert, Israel. *Hydrological Processes*, 19: 1687-1702.
- Cui, Y. T., Parker, G., Lisle, T. E., Gott, J., Hansler-Ball, M. E., et al. (2003) Sediment Pulses in Mountain Rivers: 1. Experiments. *Water Resources Research*, 39: 1239, doi: doi:10.1029/2002WR001803.
- Curran, J. C. & Wilcock, P. R. (2005) Effect of Sand Supply on Transport Rates in a Gravel-Bed Channel. *Journal of Hydraulic Engineering-Asce*, 131: 961-967.
- Dennis, D. J. C. & Nickels, T. B. (2011) Experimental measurement of large-scale three-dimensional structures in a turbulent boundary layer. Part 2. Long structures. *Journal of Fluid Mechanics*, 673: 218-244.
- Devries, P. (2002) Bedload Layer Thickness and Disturbance Depth in Gravel Bed Streams. *Journal of Hydraulic Engineering-Asce*, 128: 983-991.
- Dietrich, W. E., Bellugi, D. G., Sklar, L. S. & Stock, J. D. (2003) Geomorphic transport laws for predicting landscape form and dynamics. In: Wilcock, P. R. & Iverson, R. M. (eds), *Prediction in geomorphology*, American Geophysical Union, Washington, pp. 103-132.
- Dietrich, W. E., Kirchner, J. W., Ikeda, H. & Iseya, F. (1989) Sediment Supply and the Development of the Coarse Surface-Layer in Gravel-Bedded Rivers. *Nature*, 340: 215-217.

- Dinehart, R. L. (1992) Evolution of Coarse Gravel Bed Forms - Field-Measurements at Flood Stage. *Water Resources Research*, 28: 2667-2689.
- Dinehart, R. L. (1999) Correlative Velocity Fluctuations Over a Gravel River Bed. *Water Resources Research*, 35: 569-582.
- Diplas, P., Dancey, C. L., Celik, A. O., Valyrakis, M., Greer, K., et al. (2008) The Role of Impulse on the Initiation of Particle Movement Under Turbulent Flow Conditions. *Science*, 322: 717-720.
- Downs, P. W. & Gregory, K. J. (2004) *River channel management : towards sustainable catchment hydrosystems*, Arnold, London.
- Doyle, M. W. & Julian, J. P. (2005) The most-cited works in Geomorphology. *Geomorphology*, 72: 238-249.
- Drake, T. G. & Calantoni, J. (2001) Discrete particle model for sheet flow sediment transport in the nearshore. *Journal of Geophysical Research*, 106: 859-868.
- Drake, T. G., Shreve, R. L., Dietrich, W. E., Whiting, P. J. & Leopold, L. B. (1988) Bedload Transport of Fine Gravel Observed by Motion-Picture Photography. *Journal of Fluid Mechanics*, 192: 193-217.
- Dunbar, K. & Fugelsang, J. (2005a) Scientific Thinking and Reasoning. In: Holyoak, K. J. & Morrison, R. G. (eds), *The Cambridge handbook of thinking and reasoning*, Cambridge University Press, New York, pp. 705-725.
- Dunbar, K. N. & Fugelsang, J. A. (2005b) Causal thinking in science: How scientists and students interpret the unexpected. In: Gorman, M. E., Tweney, R. D., Gooding, D. C. & Kincannon, A. P. (eds), *Scientific and Technological Thinking*, Psychology Press, Taylor & Francis, London, pp. 57-79.
- Eaton, B. C., Church, M. & Millar, R. G. (2004) Rational regime model of alluvial channel morphology and response. *Earth Surface Processes and Landforms*, 29: 511-529.
- Enders, E. C., Boisclair, D. & Roy, A. G. (2003) The Effect of Turbulence on the Cost of Swimming for Juvenile Atlantic Salmon (*Salmo Salar*). *Canadian Journal of Fisheries and Aquatic Sciences*, 60: 1149-1160.
- Falco, R. E. (1977) Coherent motion in the outer region of turbulent boundary layers. *Physics of Fluids*, 20: s124-s132.
- Feder, J. (1988) *Fractals*, Plenum, New York.
- Ferguson, R. I., Kirkbride, A. D. & Roy, A. G. (1996) Markov analysis of velocity fluctuations in gravel-bed rivers. In: Ashworth, D. G., Bennett, S., Best, J. L. & Mclelland, S. J. (eds), *Coherent Flow Structure in Open Channels*, John Wiley & Sons, Chichester, pp. 165-183.

- Ferguson, R. I., Prestegaard, K. L. & Ashworth, P. J. (1989) Influence of Sand on Hydraulics and Gravel Transport in a Braided Gravel Bed River. *Water Resources Research*, 25: 635-643.
- Frey, P. & Church, M. (2009) How River Beds Move. *Science*, 325: 1509-1510.
- Frey, P. & Church, M. (2011) Bedload: a granular phenomenon. *Earth Surface Processes and Landforms*, 36: 58-69.
- Frostick, L. E., Lucas, P. M. & Reid, I. (1984) The Infiltration of Fine Matrices Into Coarse-Grained Alluvial Sediments and Its Implications for Stratigraphical Interpretation. *Journal of the Geological Society*, 141: 955-965.
- Fuller, I. C. & Hutchinson, E. L. (2007) Sediment flux in a small gravel-bed stream: Response to channel remediation works. *New Zealand Geographer*, 63: 169-180.
- Fuller, I. C., Large, A. R. G., Charlton, M. E., Heritage, G. L. & Milan, D. J. (2003) Reach-scale sediment transfers: An evaluation of two morphological budgeting approaches. *Earth Surface Processes and Landforms*, 28: 889-903.
- Gaeuman, D., Schmidt, J. C. & Wilcock, P. R. (2005) Complex Channel Responses to Changes in Stream Flow and Sediment Supply on the Lower Duchesne River, Utah. *Geomorphology*, 64: 185-206.
- Ganapathisubramani, B., Longmire, E. K. & I, M. (2003) Characteristics of vortex packets in turbulent boundary layers. *Journal of Fluid Mechanics*, 478: 35-46.
- Garcia, C., Cohen, H., Reid, I., Rovira, A., Ubeda, X., et al. (2007) Processes of initiation of motion leading to bedload transport in gravel-bed rivers. *Geophysical Research Letters*, 34: L06403, doi: 10.1029/2006GL028865.
- Garcia, C., Laronne, J. B. & Sala, M. (2000) Continuous monitoring of bedload flux in a mountain gravel-bed river. *Geomorphology*, 34: 23-31.
- Gibson, S., Abraham, D., Heath, R. & Schoellhamer, D. (2009) Vertical gradational variability of fines deposited in a gravel framework. *Sedimentology*, 56: 661-676.
- Gilbert, G. K. (1877) *Report on the geology of the Henry mountains*, Dept. of the interior, U.S. Geogr. and geol. survey of the Rocky mountain region, Washington.
- Gintz, D., Hassan, M. A. & Schmidt, K.-H. (1996) Frequency and magnitude of bedload transport in a mountain river. *Earth Surface Processes and Landforms*, 21: 433-445.
- Goff, J. R. & Ashmore, P. (1994) Gravel transport and morphological change in braided Sunwapta river, Alberta, Canada. *Earth Surface Processes and Landforms*, 19: 195-212.
- Gomez, B. (1991) Bedload Transport. *Earth-Science Reviews*, 31: 89-132.
- Gomez, B., Naff, R. L. & Hubbell, D. W. (1989) Temporal Variations in Bedload Transport Rates Associated With the Migration of Bedforms. *Earth Surface Processes and Landforms*, 14: 135-156.

- Gomez, B. & Phillips, J. D. (1999) Deterministic Uncertainty in Bed Load Transport. *Journal of Hydraulic Engineering-Asce*, 125: 305-308.
- Goring, D. G. & Nikora, V. I. (2002) Despiking Acoustic Doppler Velocimeter Data. *Journal of Hydraulic Engineering-Asce*, 128: 117-126.
- Grass, A. J. (1971) Structural features of turbulent flow over smooth and rough boundaries. *Journal of Fluid Mechanics*, 50: 233-255.
- Grass, A. J., Stuart, R. J. & Mansourtehrani, M. (1991) Vortical Structures and Coherent Motion in Turbulent-Flow Over Smooth and Rough Boundaries. *Philosophical Transactions of the Royal Society of London Series a-Mathematical Physical and Engineering Sciences*, 336: 35-65.
- Gregory, K. J. (1982) Fluvial geomorphology. *Progress in Physical Geography*, 6: 427-438.
- Gregory, K. J. (2000) *The changing nature of physical geography*, Arnold, Co-published in the USA by Oxford University Press, London, New York.
- Griffiths, G. A. (1979) Recent sedimentation history of the Waimakariri river, New Zealand. *Journal of Hydrology*, 18: 6-28.
- Habersack, H. M., Nachtnebel, H. P. & Laronne, J. B. (2001) The Continuous Measurement of Bedload Discharge in a Large Alpine Gravel Bed River. *Journal of Hydraulic Research*, 39: 125-133.
- Ham, D. G. & Church, M. (2000) Bed-Material Transport Estimated From Channel Morphodynamics: Chilliwack River, British Columbia. *Earth Surface Processes and Landforms*, 25: 1123-1142.
- Hardy, R. J., Best, J. L., Lane, S. N. & Carboneau, P. E. (2009) Coherent flow structures in a depth-limited flow over a gravel surface: The role of near-bed turbulence and influence of Reynolds number. *Journal of Geophysical Research-Earth Surface*, 114: F01003, doi: 10.1029/2007jf000970.
- Harris, T. & Richards, K. S. (1995) Design and calibration of a recording bedload trap. *Earth Surface Processes and Landforms*, 20: 711-720.
- Harrison, S. (2001) On Reductionism and Emergence in Geomorphology. *Transactions of the Institute of British Geographers*, 26: 327-339.
- Haschenburger, J. K. (2006) Observations of event-based streambed deformation in a gravel bed channel. *Water Resources Research*, 42: W11412, doi: 10.1029/2006wr004985.
- Hassan, M. A. & Church, M. (2000) Experiments on Surface Structure and Partial Sediment Transport on a Gravel Bed. *Water Resources Research*, 36: 1885-1895.

- Hassan, M. A. & Church, M. (2001) Sensitivity of Bed Load Transport in Harris Creek: Seasonal and Spatial Variation Over a Cobble-Gravel Bar. *Water Resources Research*, 37: 813-825.
- Hassan, M. A., Egozi, R. & Parker, G. (2006) Experiments on the effect of hydrograph characteristics on vertical grain sorting in gravel bed rivers. *Water Resources Research*, 42: W09408, doi: 10.1029/2005wr004707.
- Hassan, M. A. & Reid, I. (1990) The Influence of Microform Bed Roughness Elements on Flow and Sediment Transport in Gravel Bed Rivers. *Earth Surface Processes and Landforms*, 15: 739-750.
- Haynes, H. & Pender, G. (2007) Stress history effects on graded bed stability. *Journal of Hydraulic Engineering-Asce*, 133: 343-349.
- Heritage, G. L., Milan, D. J., Large, A. R. G. & Fuller, I. C. (2009) Influence of survey strategy and interpolation model on DEM quality. *Geomorphology*, 112: 334-344.
- Hirpa, F. A., Gebremichael, M. & Over, T. M. (2010) River flow fluctuation analysis: Effect of watershed area. *Water Resources Research*, 46: W12529, doi: 10.1029/2009wr009000.
- Hoefel, F. & Elgar, S. (2003) Wave-Induced Sediment Transport and Sandbar Migration. *Science*, 299: 1885-1887.
- Hoey, T. B. (1992) Temporal Variations in Bedload Transport Rates and Sediment Storage in Gravel-Bed Rivers. *Progress in Physical Geography*, 16: 319-338.
- Hoey, T. B. & Sutherland, A. J. (1991) Channel morphology and bedload pulses in braided rivers - a laboratory study. *Earth Surface Processes and Landforms*, 16: 447-462.
- Hooke, R. L. (2000) On the history of humans as geomorphic agents. *Geology*, 28: 843-846.
- Horton, R. E. (1945) Erosional development of streams and their drainage basins; hydrophysical approach to quantitative morphology. *Geological Society of America Bulletin*, 56: 275-370.
- Hsu, L., Finnegan, N. J. & Brodsky, E. E. (2011) A seismic signature of river bedload transport during storm events. *Geophysical Research Letters*, 38: L13407, doi: 10.1029/2011gl047759.
- Huang, Y., Schmitt, F. G., Lu, Z. & Liu, Y. (2009) Analysis of daily river flow fluctuations using empirical mode decomposition and arbitrary order Hilbert spectral analysis. *Journal of Hydrology*, 373: 103-111.
- Huggett, R. (2007) A history of the systems approach in geomorphology. *Geomorphologie-Relief Processus Environnement*, 2007: 145-157.
- Hutchins, N. & Marusic, I. (2007) Evidence of very long meandering features in the logarithmic region of turbulent boundary layers. *Journal of Fluid Mechanics*, 579: 1-28.

- Jackson, R. G. (1976) Sedimentological and fluid-dynamic implications of the turbulent bursting phenomenon in geophysical flows. *Journal of Fluid Mechanics*, 77: 531-560.
- Jaeger, H. M., Nagel, S. R. & Behringer, R. P. (1996) Granular solids, liquids, and gases. *Reviews of Modern Physics*, 68: 1259-1273.
- Jerolmack, D. J. (2011) Causes and effects of noise in landscape dynamics. *Eos Trans. AGU*, 92: 385-386.
- Johnson, M. F., Rice, S. P. & Reid, I. (2011) Increase in coarse sediment transport associated with disturbance of gravel river beds by signal crayfish (*Pacifastacus leniusculus*). *Earth Surface Processes and Landforms*, 36: 1680-1692.
- Johnson, R. M. & Warburton, J. (2002) Annual sediment budget of a UK mountain torrent. *Geografiska Annaler Series a-Physical Geography*, 84A: 73-88.
- Keiler, M. (2011) Geomorphology and Complexity - inseparably connected? *Zeitschrift Fur Geomorphologie*, 55: 233-257.
- Kim, K. C. & Adrian, R. J. (1999) Very large-scale motion in the outer layer. *Physics of Fluids*, 11: 417-422.
- Kirchner, J. W., Dietrich, W. E., Iseya, F. & Ikeda, H. (1990) The Variability of Critical Shear-Stress, Friction Angle, and Grain Protrusion in Water-Worked Sediments. *Sedimentology*, 37: 647-672.
- Kirkbride, A. D. & Ferguson, R. (1995) Turbulent Flow Structure in a Gravel-Bed River: Markov Chain Analysis of the Fluctuating Velocity Profile. *Earth Surface Processes and Landforms*, 20: 721-733.
- Kline, S. J., Reynolds, W. C., Schraub, F. A. & Runstadler, P. W. (1967) The structure of turbulent boundary layers. *Journal of Fluid Mechanics*, 30: 741-773.
- Kocurek, G., Ewing, R. C. & Mohrig, D. (2010) How do bedform patterns arise? New views on the role of bedform interactions within a set of boundary conditions. *Earth Surface Processes and Landforms*, 35: 51-63.
- Konrad, C. P., Booth, D. B., Burges, S. J. & Montgomery, D. R. (2002) Partial Entrainment of Gravel Bars During Floods. *Water Resources Research*, 38: 1104, doi: 10.1029/2001WR000828.
- Kuhnle, R. A. (1989) Bed-Surface Size Changes in Gravel-Bed Channel. *Journal of Hydraulic Engineering*, 115: 731-743.
- Kuhnle, R. A. (1992) Bed-Load Transport During Rising and Falling Stages on 2 Small Streams. *Earth Surface Processes and Landforms*, 17: 191-197.
- Kuhnle, R. A. & Southard, J. B. (1988) Bed-load transport fluctuations in a gravel bed laboratory channel. *Water Resources Research*, 24: 247-260.

- Lacey, R. W. J. & Roy, A. G. (2007) A comparative study of the turbulent flow field with and without a pebble cluster in a gravel bed river. *Water Resources Research*, 43: W05502, doi: 10.1029/2006WR005027.
- Lamarre, H. & Roy, A. G. (2005) Reach Scale Variability of Turbulent Flow Characteristics in a Gravel-Bed River. *Geomorphology*, 68: 95-113.
- Lane, S. N. (1998) The use of digital terrain modelling in the understanding of dynamic river channel systems. In: Lane, S. N., K.S., R. & Chandler, J. H. (eds), *Landform Monitoring, Modelling and Analysis*, John Wiley & Sons, Chichester, pp. 311-342.
- Lane, S. N., Chandler, J. H. & Richards, K. S. (1994) Developments in Monitoring and Modeling Small-Scale River Bed Topography. *Earth Surface Processes and Landforms*, 19: 349-368.
- Lane, S. N. & Richards, K. S. (1997) Linking River Channel Form and Process: Time, Space and Causality Revisited. *Earth Surface Processes and Landforms*, 22: 249-260.
- Lane, S. N. & Richards, K. S. (1998) High Resolution, Two-Dimensional Spatial Modelling of Flow Processes in a Multi-Thread Channel. *Hydrological Processes*, 12: 1279-1298.
- Lane, S. N., Richards, K. S. & Chandler, J. H. (1995) Morphological Estimation of the Time-Integrated Bed-Load Transport Rate. *Water Resources Research*, 31: 761-772.
- Lane, S. N., Richards, K. S. & Chandler, J. H. (1996) Discharge and Sediment Supply Controls on Erosion and Deposition in a Dynamic Alluvial Channel. *Geomorphology*, 15: 1-15.
- Lane, S. N., Westaway, R. M. & Hicks, D. M. (2003) Estimation of Erosion and Deposition Volumes in a Large, Gravel-Bed, Braided River Using Synoptic Remote Sensing. *Earth Surface Processes and Landforms*, 28: 249-271.
- Lapointe, M. (1992) Burst-Like Sediment Suspension Events in a Sand Bed River. *Earth Surface Processes and Landforms*, 17: 253-270.
- Laronne, J. B., Alexandrov, Y., Bergman, N., Cohen, H., Garcia, C., et al. (2003) The continuous monitoring of bed load flux in various fluvial environments. In: Bogen, J., Fergus, T. & Walling, D. (eds), *Erosion and Sediment Transport Measurement in Rivers: Technological and Methodological Advances*, IAHS Publication, The Netherlands, pp. 134-145.
- Laronne, J. B. & Reid, I. (1993) Very high-rates of bedload sediment transport by ephemeral desert rivers. *Nature*, 366: 148-150.
- Lawler, D. M. & Fairchild, I. J. (2010) New developments in process understanding and modelling in geomorphology: introduction and overview. *Earth Surface Processes and Landforms*, 35: 1247-1250.

- Lawless, M. & Robert, A. (2001a) Scales of Boundary Resistance in Coarse-Grained Channels: Turbulent Velocity Profiles and Implications. *Geomorphology*, 39: 221-238.
- Lawless, M. & Robert, A. (2001b) Three-Dimensional Flow Structure Around Small-Scale Bedforms in a Simulated Gravel-Bed Environment. *Earth Surface Processes and Landforms*, 26: 507-522.
- Leeder, M. R. (1983) On the interactions between turbulent flow, sediment transport and bedform mechanics in channelized flows. In: Collinson, J. D. & Lewin, J. (eds), *Modern and Ancient Fluvial Systems*, Blackwell Scientific, London, pp. 5-18.
- Legendre, P. & Legendre, L. (1998) *Numerical ecology*, Elsevier, The Netherlands.
- Legleiter, C. J., Phelps, T. L. & Wohl, E. E. (2007) Geostatistical analysis of the effects of stage and roughness on reach-scale spatial patterns of velocity and turbulence intensity. *Geomorphology*, 83: 322-345.
- Leighly, J. (1934) Turbulence and the Transportation of Rock Debris by Streams. *Geographical Review*, 24: 453-464.
- Lenzi, M. A., Mao, L. & Comiti, F. (2004) Magnitude-frequency analysis of bed load data in an Alpine boulder bed stream. *Water Resources Research*, 40: W07201, doi: 10.1029/2003wr002961.
- Leopold, L. B. & Maddock, T. J. 1953. The hydraulic geometry of stream channels and some physiographic implications. *Geological Survey Professional Paper 252*. Washington..
- Leopold, L. B., Wolman, M. G. & Miller, J. R. (1964) *Fluvial processes in geomorphology*, W.H. Freeman, San Francisco.
- Levi, E. (1983) Oscillatory Model for Wall-Bounded Turbulence. *Journal of Engineering Mechanics-Asce*, 109: 728-740.
- Lewis, J. (1991) An improved bedload sampler. In: Fan & Kuo (eds), *Proceedings of the Fifth Federal Interagency Sedimentation Conference*, United States Geological Survey, Washington, pp. 1-8.
- Liao, J. C. (2007) A review of fish swimming mechanics and behaviour in altered flows. *Philosophical Transactions of the Royal Society B: Biological Sciences*, 362: 1973-1993.
- Liao, J. C., Beal, D. N., Lauder, G. V. & Triantafyllou, M. S. (2003) Fish Exploiting Vortices Decrease Muscle Activity. *Science*, 302: 1566-1569.
- Lilliefors, H. W. (1967) On the Kolmogorov-Smirnov test for normality with mean and variance unknown. *Journal of the American Statistical Association*, 62: 399-402.
- Lindsay, J. B. & Ashmore, P. E. (2002) The effects of survey frequency on estimates of scour and fill in a braided river model. *Earth Surface Processes and Landforms*, 27: 27-43.

- Lisle, T. E. (1995) Particle-size variations between bed-load and bed material in natural gravel-bed channels. *Water Resources Research*, 31: 1107-1118.
- Liu, Z., Adrian, R. J. & Hanratty, T. J. (2001) Large-Scale Modes of Turbulent Channel Flow: Transport and Structure. *Journal of Fluid Mechanics*, 448: 53-80.
- Lu, S. S. & Willmarth, W. W. (1973) Measurements of the structure of the Reynolds stress in a turbulent boundary layer. *Journal of Fluid Mechanics*, 60: 481-511.
- Luchik, T. S. & Tiederman, W. G. (1987) Timescale and Structure of Ejections and Bursts in Turbulent Channel Flows. *Journal of Fluid Mechanics*, 174: 529-552.
- Macvicar, B. J. & Roy, A. G. (2007) Hydrodynamics of a forced riffle pool in a gravel bed river: 2. Scale and structure of coherent turbulent events. *Water Resources Research*, 43: W12402, doi: 10.1029/2006wr005274.
- Macvicar, B. J. & Roy, A. G. (2011) Sediment mobility in a forced riffle-pool. *Geomorphology*, 125: 445-456.
- Marquis, G. A. & Roy, A. G. (2006) Effect of flow depth and velocity on the scales of macroturbulent structures in gravel-bed rivers. *Geophysical Research Letters*, 33: L24406, doi: 10.1029/2006GL028420.
- Marquis, G. A. & Roy, A. G. (2011) Bridging the gap between turbulence and larger scales of flow motions in rivers. *Earth Surface Processes and Landforms*, 36: 563-568.
- Marquis, G. A. & Roy, A. G. (2012) Using multiple bedload measurements: Towards the identification of bed dilation and contraction in gravel-bed rivers. *Journal of Geophysical Research*, 117: F01014, doi: doi:10.1029/2011JF002120.
- Martin, Y. (2003) Evaluation of bed load transport formulae using field evidence from the Vedder River, British Columbia. *Geomorphology*, 53: 75-95.
- Martin, Y. & Church, M. (1995) Bed-Material Transport Estimated From Channel Surveys - Vedder River, British-Columbia. *Earth Surface Processes and Landforms*, 20: 347-361.
- Mayer, L. (1992) Some Comments on Equilibrium Concepts and Geomorphic Systems. *Geomorphology*, 5: 277-295.
- Mehta, A., Barker, G. C. & Luck, J. M. (2009) Heterogeneities in granular materials. *Physics today*, 62: 40-45.
- Middleton, R., Brasington, J., Murphy, B. J. & Frostick, L. E. (2000) Monitoring Gravel Framework Dilation Using a New Digital Particle Tracking Method. *Computers & Geosciences*, 26: 329-340.
- Milan, D. J., Heritage, G. L., Large, A. R. G. & Fuller, I. C. (2011) Filtering spatial error from DEMs: Implications for morphological change estimation. *Geomorphology*, 125: 160-171.
- Mitarai, N. & Nori, F. (2006) Wet granular materials. *Advances in Physics*, 55: 1-45.

- Monteith, H. & Pender, G. (2005) Flume Investigations Into the Influence of Shear Stress History on a Graded Sediment Bed. *Water Resources Research*, 41: W12401, doi: 10.1029/2005WR004297.
- Montgomery, D. R. & Buffington, J. M. (1997) Channel-Reach Morphology in Mountain Drainage Basins. *Geological Society of America Bulletin*, 109: 596-611.
- Moog, D. B. & Whiting, P. J. (1998) Annual Hysteresis in Bed Load Rating Curves. *Water Resources Research*, 34: 2393-2399.
- Murray, A. B., Lazarus, E., Ashton, A., Baas, A., Coco, G., et al. (2009) Geomorphology, complexity, and the emerging science of the Earth's surface. *Geomorphology*, 103: 496-505.
- Naden, P. (1987) modeling gravel-bed topography from sediment transport. *Earth Surface Processes and Landforms*, 12: 353-367.
- Nakagawa, H. & Nezu, I. (1981) Structure of Space-Time Correlations of Bursting Phenomena in an Open-Channel Flow. *Journal of Fluid Mechanics*, 104: 1-43.
- Nelson, J. M., Schmeeckle, M. W. & Shreve, R. L. (2001) Turbulence and particle entrainment. In: Mosley, M. P. (ed.) *Gravel Bed Rivers V*, New Zealand Hydrological Society, Christchurch, pp. 221-248.
- Nelson, P. A., Venditti, J. G., Dietrich, W. E., Kirchner, J. W., Ikeda, H., et al. (2009) Response of bed surface patchiness to reductions in sediment supply. *Journal of Geophysical Research-Earth Surface*, 114: F02005, doi: 10.1029/2008jf001144.
- Nezu, I. & Nakagawa, H. (1993) *Turbulence in Open-Channel Flows*, Balkema, Rotterdam.
- Nicholas, A. P., Ashworth, P. J., Kirkby, M. J., Macklin, M. G. & Murray, T. (1995) Sediment Slugs: Large-Scale Fluctuations in Fluvial Sediment Transport Rates and Storage Volumes. *Progress in Physical Geography*, 19: 500-519.
- Nicholas, A. P. & Quine, T. A. (2007) Crossing the divide: Representation of channels and processes in reduced-complexity river models at reach and landscape scales. *Geomorphology*, 90: 318-339.
- Nicholas, A. P. & Smith, G. H. S. (1998) Relationships between flow hydraulics, sediment supply, bedload transport and channel stability in the proglacial Virkisa River, Iceland. *Geografiska Annaler Series a-Physical Geography*, 80A: 111-122.
- Nikora, V. (2007) Hydrodynamics of gravel-bed rivers: scale issues. In: Habersack, H., Piégay, H. & Rinaldi, M. (eds), *Gravel-Bed Rivers VI: From Process Understanding to River Restoration*, Elsevier, Amsterdam, pp. 61-81.
- Nikora, V. (2010) Hydrodynamics of aquatic ecosystems: An interface between ecology, biomechanics and environmental fluid mechanics. *River Research and Applications*, 26: 367-384.

- Nino, Y. & Garcia, M. H. (1996) Experiments on Particle-Turbulence Interactions in the Near-Wall Region of an Open Channel Flow: Implications for Sediment Transport. *Journal of Fluid Mechanics*, 326: 285-319.
- Nowak, E. R., Knight, J. B., Ben-Naim, E., Jaeger, H. M. & Nagel, S. R. (1998) Density fluctuations in vibrated granular materials. *Physical Review E*, 57: 1971-1982.
- Orme, A. R. (2002) Shifting paradigms in geomorphology: the fate of research ideas in an educational context. *Geomorphology*, 47: 325-342.
- Packman, A. I. & Brooks, N. H. (1995) Colloidal Particle Exchange Between Stream and Stream Bed in a Laboratory Flume. *Marine and Freshwater Research*, 46: 233-236.
- Packman, A. I. & Brooks, N. H. (2001) Hyporheic Exchange of Solutes and Colloids With Moving Bed Forms. *Water Resources Research*, 37: 2591-2605.
- Packman, A. I., Brooks, N. H. & Morgan, J. J. (2000) Kaolinite Exchange Between a Stream and Streambed: Laboratory Experiments and Validation of a Colloid Transport Model. *Water Resources Research*, 36: 2363-2372.
- Packman, A. I. & Mackay, J. S. (2003) Interplay of Stream-Subsurface Exchange, Clay Particle Deposition, and Streambed Evolution. *Water Resources Research*, 39: 1097, doi: 10.1029/2002WR001432.
- Paiement-Paradis, G., Buffin-Belanger, T. & Roy, A. G. (2003) Scalings for Large Turbulent Flow Structures in Gravel-Bed Rivers. *Geophysical Research Letters*, 30: 1773, doi: 10.1029/2003GL017553.
- Paiement-Paradis, G., Marquis, G. & Roy, A. (2011) Effects of turbulence on the transport of individual particles as bedload in a gravel-bed river. *Earth Surface Processes and Landforms*, 36: 107-116.
- Paola, C., Foufoula-Georgiou, E., Dietrich, W. E., Hondzo, M., Mohrig, D., et al. (2006) Toward a unified science of the Earth's surface: Opportunities for synthesis among hydrology, geomorphology, geochemistry, and ecology. *Water Resources Research*, 42: W03s10, doi: 10.1029/2005wr004336.
- Paphitis, D. & Collins, M. B. (2005) Sand Grain Threshold, in Relation to Bed 'stress History': an Experimental Study. *Sedimentology*, 52: 827-838.
- Parker, G., Dhamotharan, S. & Stefan, H. (1982a) Model Experiments on Mobile, Paved Gravel Bed Streams. *Water Resources Research*, 18: 1395-1408.
- Parker, G. & Klingeman, P. C. (1982) On Why Gravel Bed Streams Are Paved. *Water Resources Research*, 18: 1409-1423.
- Parker, G., Klingeman, P. C. & Mclean, D. G. (1982b) Bedload and Size Distribution in Paved Gravel-Bed Streams. *Journal of the Hydraulics Division-Asce*, 108: 544-571.
- Parker, G. & Sutherland, A. J. (1990) Fluvial Armor. *Journal of Hydraulic Research*, 28: 529-544.

- Phillips, J. D. (1992) The end of equilibrium? *Geomorphology*, 5: 195-201.
- Phillips, J. D. (2003) Sources of Nonlinearity and Complexity in Geomorphic Systems. *Progress in Physical Geography*, 27: 1-23.
- Phillips, J. D. (2006) Deterministic chaos and historical geomorphology: A review and look forward. *Geomorphology*, 76: 109-121.
- Phillips, J. D. (2009) Changes, perturbations, and responses in geomorphic systems. *Progress in Physical Geography*, 33: 17-30.
- Phillips, J. D. (2010) The job of the river. *Earth Surface Processes and Landforms*, 35: 305-313.
- Powell, D. M., Reid, I. & Laronne, J. B. (1999) Hydraulic Interpretation of Cross-Stream Variations in Bed-Load Transport. *Journal of Hydraulic Engineering-Asce*, 125: 1243-1252.
- Powell, D. M., Reid, I. & Laronne, J. B. (2001) Evolution of Bed Load Grain Size Distribution With Increasing Flow Strength and the Effect of Flow Duration on the Caliber of Bed Load Sediment Yield in Ephemeral Gravel Bed Rivers. *Water Resources Research*, 37: 1463-1474.
- Proffitt, G. T. & Sutherland, A. J. (1983) Transport of Non-Uniform Sediments. *Journal of Hydraulic Research*, 21: 33-43.
- Puleo, J. A., Holland, K. T., Plant, N. G., Slinn, D. N. & Hanes, D. M. (2003) Fluid acceleration effects on suspended sediment transport in the swash zone. *Journal of Geophysical Research-Oceans*, 108: 3350, doi: 10.1029/2003JC001943.
- Pyne, S. J. (1980) *Grove Karl Gilbert : a great engine of research*, University of Texas Press, Austin.
- Raven, E. K., Lane, S. N. & Bracken, L. J. (2010) Understanding sediment transfer and morphological change for managing upland gravel-bed rivers. *Progress in Physical Geography*, 34: 23-45.
- Recking, A. (2010) A comparison between flume and field bed load transport data and consequences for surface-based bed load transport prediction. *Water Resources Research*, 46: W03518, doi: 10.1029/2009wr008007.
- Recking, A., Frey, P., Paquier, A. & Belleudy, P. (2009) An experimental investigation of mechanisms involved in bed load sheet production and migration. *Journal of Geophysical Research-Earth Surface*, 114: F03010, doi: 10.1029/2008jf000990.
- Reid, I., Frostick, L. E. & Layman, J. T. (1985) The Incidence and Nature of Bedload Transport During Flood Flows in Coarse-Grained Alluvial Channels. *Earth Surface Processes and Landforms*, 10: 33-44.

- Reid, I. & Laronne, J. B. (1995) Bed-Load Sediment Transport in an Ephemeral Stream and a Comparison With Seasonal and Perennial Counterparts. *Water Resources Research*, 31: 773-781.
- Reid, I., Layman, J. T. & Frostick, L. E. (1980) The Continuous Measurement of Bedload Discharge. *Journal of Hydraulic Research*, 18: 243-249.
- Reid, S. C., Lane, S. N., Berney, J. M. & Holden, J. (2007) The Timing and Magnitude of Coarse Sediment Transport Events Within an Upland, Temperate Gravel-Bed River. *Geomorphology*, 83: 152-182.
- Reynolds, O. (1885) On the dilatancy of media composed of rigid particles in contact, with experimental illustrations. *Philosophical Magazine*, Series 5: 469-281.
- Rhoads, B. L. (1999) Beyond pragmatism: The value of philosophical discourse for physical geography. *Annals of the Association of American Geographers*, 89: 760-771.
- Richards, K. (1996) Samples and cases: Generalisation and explanation in geomorphology. In: Rhoads, B. L. & Thorn, C. E. (eds), *Scientific Nature of Geomorphology*, John Wiley & Sons, Chichester, pp. 171-190.
- Richards, K. & Clifford, N. (1991) Fluvial Geomorphology - Structured Beds in Gravelly Rivers. *Progress in Physical Geography*, 15: 407-422.
- Richards, K. & Clifford, N. (2008) Science, systems and geomorphologies: why LESS may be more. *Earth Surface Processes and Landforms*, 33: 1323-1340.
- Robert, A. (1990) Boundary Roughness in Coarse-Grained Channels. *Progress in Physical Geography*, 14: 42-70.
- Robert, A. (2003) *River processes : an introduction to fluvial dynamics*, Arnold, London.
- Roy, A. G., Biron, P. M. & Lapointe, M. F. (1997) Implications of Low-Pass Filtering on Power Spectra and Autocorrelation Functions of Turbulent Velocity Signals. *Mathematical Geology*, 29: 653-668.
- Roy, A. G., Buffin-Belanger, T., Lamarre, H. & Kirkbride, A. D. (2004) Size, Shape and Dynamics of Large-Scale Turbulent Flow Structures in a Gravel-Bed River. *Journal of Fluid Mechanics*, 500: 1-27.
- Roy, A. G. & Lane, S. N. (2003) Putting morphology back into geomorphology: the case of river meanders and tributary junctions. In: Trudgill, S. & Roy, A. G. (eds), *Contemporary meanings in physical geography*, Arnold, London, pp. 103-125.
- Rudwick, M. J. S. (2008) *Worlds before Adam : the reconstruction of geohistory in the age of reform*, University of Chicago Press, Chicago.
- Ryan, S. E., Porth, L. S. & Troendle, C. A. (2005) Coarse Sediment Transport in Mountain Streams in Colorado and Wyoming, Usa. *Earth Surface Processes and Landforms*, 30: 269-288.

- Schmeeckle, M. W., Nelson, J. M. & Shreve, R. L. (2007) Forces on Stationary Particles in Near-Bed Turbulent Flows. *Journal of Geophysical Research-Earth Surface*, 112: F02003, doi: 10.1029/2006JF000536.
- Schumm, S. A. & Lichty, R. W. (1965) Time, Space and Causality in geomorphology. *American Journal of Science*, 263: 110-119.
- Sear, D. A. (2003) Event bed load yield measurement with load cell bed load traps and prediction of bed load yield from hydrograph shape. In: Bogen, J., Fergus, T. & Walling, D. E. (eds), *Erosion and Sediment Transport Measurements in Rivers: Technological and Methodological Advances*, IAHS Press, The Netherlands, pp. 146-153.
- Sear, D. A., Damon, W., Booker, D. J. & Anderson, D. G. (2000) A Load Cell Based Continuous Recording Bedload Trap. *Earth Surface Processes and Landforms*, 25: 659-672.
- Shvidchenko, A. B. & Pender, G. (2001) Macroturbulent Structure of Open-Channel Flow Over Gravel Beds. *Water Resources Research*, 37: 709-719.
- Singh, A., Fienberg, K., Jerolmack, D. J., Marr, J. & Foufoula-Georgiou, E. (2009) Experimental evidence for statistical scaling and intermittency in sediment transport rates. *Journal of Geophysical Research-Earth Surface*, 114: F01025, doi: 10.1029/2007jf000963.
- Singh, A., Porté-Agel, F. & Foufoula-Georgiou, E. (2010) On the influence of gravel bed dynamics on velocity power spectra. *Water Resources Research*, 46: W04509, doi: 10.1029/2009wr008190.
- Smart, G. M. & Habersack, H. M. (2007) Pressure fluctuations and gravel entrainment in rivers. *Journal of Hydraulic Research*, 45: 661-673.
- Smith, B. J., Warke, P. A. & Whalley, W. B. (2002) Landscape development, collective amnesia and the need for integration in geomorphological research. *Area*, 34: 409-418.
- Song, T. & Graf, W. H. (1996) Velocity and turbulence distribution in unsteady open-channel flows. *Journal of Hydraulic Engineering-Asce*, 122: 141-154.
- Sreenivasan, K. R. & Meneveau, C. (1986) The Fractal Facets of Turbulence. *Journal of Fluid Mechanics*, 173: 357-386.
- Stott, T. (2011) Fluvial geomorphology 2008-2009. *Progress in Physical Geography*, 35: 810-830.
- Strahler, A. N. (1952) Dynamic basis of geomorphology. *Geological Society of America Bulletin*, 63: 923-938.
- Strom, K., Papanicolaou, A. N., Evangelopoulos, N. & Odeh, M. (2004) Microforms in Gravel Bed Rivers: Formation, Disintegration, and Effects on Bedload Transport. *Journal of Hydraulic Engineering-Asce*, 130: 554-567.

- Thorndycraft, V. R., Benito, G. & Gregory, K. J. (2008) Fluvial geomorphology: A perspective on current status and methods. *Geomorphology*, 98: 2-12.
- Thorne, P. D., Williams, J. J. & Heathershaw, A. D. (1989) Insitu Acoustic Measurements of Marine Gravel Threshold and Transport. *Sedimentology*, 36: 61-74.
- Tomkins, C. D. & Adrian, R. J. (2003) Spanwise structure and scale growth in turbulent boundary layers. *Journal of Fluid Mechanics*, 490: 37-74.
- Turowski, J. M., Badoux, A. & Rickenmann, D. (2011) Start and end of bedload transport in gravel-bed streams. *Geophysical Research Letters*, 38: L04401, doi: 10.1029/2010gl046558.
- Turowski, J. M., Yager, E. M., Badoux, A., Rickenmann, D. & Molnar, P. (2009) The impact of exceptional events on erosion, bedload transport and channel stability in a step-pool channel. *Earth Surface Processes and Landforms*, 34: 1661-1673.
- Venditti, J. G., Dietrich, W. E., Nelson, P. A., Wydzga, M. A., Fadde, J., et al. (2010) Mobilization of coarse surface layers in gravel-bedded rivers by finer gravel bed load. *Water Resources Research*, 46: W07506, doi: 10.1029/2009wr008329.
- Vericat, D. & Batalla, R. J. (2010) Sediment transport from continuous monitoring in a perennial Mediterranean stream. *Catena*, 82: 77-86.
- Von Engeln, O. D. (1940) Symposium: Walther Penck's Contribution to Geomorphology. *Annals of the Association of American Geographers*, 30: 219-236.
- Warburton, J. (1992) Observations of Bed-Load Transport and Channel Bed Changes in a Proglacial Mountain Stream. *Arctic and Alpine Research*, 24: 195-203.
- Wathen, S. J., Ferguson, R. I., Hoey, T. B. & Werritty, A. (1995) Unequal Mobility of Gravel and Sand in Weakly Bimodal River Sediments. *Water Resources Research*, 31: 2087-2096.
- Wathen, S. J. & Hoey, T. B. (1998) Morphological Controls on the Downstream Passage of a Sediment Wave in a Gravel-Bed Stream. *Earth Surface Processes and Landforms*, 23: 715-730.
- Werner, B. T. (1999) Complexity in Natural Landform Patterns. *Science*, 284: 102-104.
- Wheaton, J. M., Brasington, J., Darby, S. E. & Sear, D. A. (2010) Accounting for uncertainty in DEMs from repeat topographic surveys: improved sediment budgets. *Earth Surface Processes and Landforms*, 35: 136-156.
- Whiting, P. J., Dietrich, W. E., Leopold, L. B., Drake, T. G. & Shreve, R. L. (1988) Bedload Sheets in Heterogeneous Sediment. *Geology*, 16: 105-108.
- Wilcock, P. R. (1992) Experimental investigation of the effect of mixture properties on transport dynamics. In: Billi, P., Hey, R. D., Thorne, C. R. & Tacconi, P. (eds), *Dynamics of Gravel-bed Rivers*, John Wiley & Sons, Chichester, pp. 109-139.

- Wilcock, P. R. (1997) The Components of Fractional Transport Rate. *Water Resources Research*, 33: 247-258.
- Wilcock, P. R. & Detemple, B. T. (2005) Persistence of Armor Layers in Gravel-Bed Streams. *Geophysical Research Letters*, 32: L08402, doi: 10.1029/2004GL021772.
- Wilcock, P. R. & Kenworthy, S. T. (2002) A Two-Fraction Model for the Transport of Sand/Gravel Mixtures. *Water Resources Research*, 38: 1194, doi: 10.1029/2001WR000684.
- Wilcock, P. R., Kenworthy, S. T. & Crowe, J. C. (2001) Experimental Study of the Transport of Mixed Sand and Gravel. *Water Resources Research*, 37: 3349-3358.
- Wilcock, P. R. & Mcardell, B. W. (1993) Surface-Based Fractional Transport Rates - Mobilization Thresholds and Partial Transport of a Sand-Gravel Sediment. *Water Resources Research*, 29: 1297-1312.
- Wilcock, P. R. & Mcardell, B. W. (1997) Partial Transport of a Sand/Gravel Sediment. *Water Resources Research*, 33: 235-245.
- Wilcock, P. R. & Southard, J. B. (1989) Bed-load transport of mixed size sediment - fractional transport rates, bed forms, and the development of a coarse bed surface-layer. *Water Resources Research*, 25: 1629-1641.
- Wong, M. & Parker, G. (2006) One-dimensional modeling of bed evolution in a gravel bed river subject to a cycled flood hydrograph. *Journal of Geophysical Research-Earth Surface*, 111: F03018, doi: 10.1029/2006jf000478.
- Yang, S. Q. & Chow, A. T. (2008) Turbulence structures in non-uniform flows. *Advances in Water Resources*, 31: 1344-1351.
- Yu, A. B. & Standish, N. (1988) An analytical-parametric theory of the random packing of particles. *Powder Technology*, 55: 171-186.
- Yu, A. B. & Standish, N. (1991) Estimation of the porosity of particle mixtures by a linear-mixture packing model. *Industrial & Engineering Chemistry Research*, 30: 1372-1385.
- Zhou, J., Adrian, R. J., Balachandar, S. & Kendall, T. M. (1999) Mechanisms for generating coherent packets of hairpin vortices in channel flow. *Journal of Fluid Mechanics*, 387: 353-396.